ВЕСТНИК ТРАНСПЛАНТОЛОГИИ И ИСКУССТВЕННЫХ ОРГАНОВ

VESTNIK TRANSPLANTOLOGII I ISKUSSTVENNYKH ORGANOV

RUSSIAN JOURNAL OF TRANSPLANTOLOGY AND ARTIFICIAL ORGANS

УЧРЕДИТЕЛЬ: ОБЩЕРОССИЙСКАЯ ОБЩЕСТВЕННАЯ ОРГАНИЗАЦИЯ ТРАНСПЛАНТОЛОГОВ «РОССИЙСКОЕ ТРАНСПЛАНТОЛОГИЧЕСКОЕ ОБЩЕСТВО»

THE OFFICIAL JOURNAL OF ALL-RUSSIAN PUBLIC ORGANIZATION OF TRANSPLANTOLOGISTS "RUSSIAN TRANSPLANT SOCIETY"

2025. Том XXVII. № 4

2025. Vol. XXVII. № 4

Научно-практический журнал основан в 1999 г.
Регистр. № 018616

Scientific and Practical Journal was founded in 1999
Reg. № 018616

Журнал «Вестник трансплантологии и искусственных органов» включен ВАК РФ в перечень российских рецензируемых научных изданий, в которых должны быть опубликованы результаты диссертационных работ

Журнал «Вестник трансплантологии и искусственных органов» включен ФГБУ «НМИЦ ТИО им. ак. В.И. Шумакова» Минздрава России в перечень российских рецензируемых научных изданий, в которых должны быть опубликованы основные результаты исследований в рамках диссертаций, представляемых к защите в диссертационный совет ФГБУ «НМИЦ ТИО им. ак. В.И. Шумакова» Минздрава России

Журнал «Вестник трансплантологии и искусственных органов» индексируется в Scopus и размещен на платформе Web of Science Core Collection: Emerging Science Citation Index

"Russian Journal of Transplantology and Artificial Organs" is included in the list of leading peer-reviewed scientific publication editions, produced in the Russian Federation and is recommended for publication of primary results of dissertation research

"Russian Journal of transplantology and artificial organs" is included by the Federal State Budgetary Institution "Shumakov National Medical Research Center of Transplantology and Artificial Organs" of the Ministry of Health of Russia in the list of Russian peer-reviewed scientific publications in which the main results of research should be published within the framework of dissertations submitted for defense to the dissertation council of Shumakov National Medical Research Center of Transplantology and Artificial Organs

"Russian Journal of Transplantology and Artificial Organs" is indexed in Scopus and in the Emerging Science Citation Index of the Web of Science Core Collection

ISSN 1995-1191

Адрес для корреспонденции:

Россия, 123182, Москва, ул. Щукинская, 1
Тел./факс +7 (499) 193 87 62
E-mail: vestniktranspl@gmail.com
Интернет-сайт журнала: https://journal.transpl.ru
Научная электронная библиотека: https://elibrary.ru

Address for correspondence:

1, Shchukinskaya st., Moscow 123182, Russia
Tel./Fax +7 (499) 193 87 62
E-mail: vestniktranspl@gmail.com
Journal's web site: https://journal.transpl.ru
Scientific eLibrary: https://elibrary.ru

СОДЕРЖАНИЕ

СТРАНИЦА ГЛАВНОГО РЕДАКТОРА

Векторы научного поиска и прорывные технологии в области трансплантологии обсуждали на заседании президиума РАН
С.В. Готье

КЛИНИЧЕСКАЯ ТРАНСПЛАНТОЛОГИЯ

Комбинированная машинная перфузия и безышемическая имплантация печени от доноров высокого риска: первый опыт применения в России
М.А. Болдырев, А.Р. Монахов, Н.В. Грудинин, В.К. Богданов, С.И. Зубенко, В.Р. Салимов, Д.М. Бондаренко, Н.П. Можейко, Н.М. Юсуф, М.Г. Минина, О.М. Цирульникова, С.В. Готье

Рациональный выбор поддерживающей иммуносупрессивной терапии после трансплантации печени
О.А. Герасимова, Н.В. Марченко, И.И. Тилеубергенов, В.Н. Жуйков

Влияние вида диализной терапии перед трансплантацией почки на первые два года посттрансплантационного периода
В.А. Бердинский, Е.С. Иванова, В.Е. Виноградов, Н.Ф. Фролова, О.Н. Котенко, Л.Ю. Артюхина, И.В. Дмитриев, П.А. Дроздов

Клинический случай успешного эндоскопического лечения синдрома Суайра–Джеймса–Маклеода
М.Т. Беков, И.В. Пашков, Е.Ф. Шигаев, К.С. Смирнов, Р.А. Латыпов, Д.О. Олешкевич

Риск утраты трансплантата: однофакторный и многофакторный анализ при трансплантации почек от доноров с расширенными критериями
М.Г. Минина, Д.А. Банкеев, А.Б. Зулькарнаев, В.С. Богданов, Э.А. Тенчурина, В.М. Севостьянов

Клиническое течение эректильной дисфункции и репродуктивное здоровье у пациентов после трансплантации почки
С.С. Кариев, Ф.Р. Насыров, Ш.Ш. Шавахабов, С.Х. Ибрагимов, З.Т. Маткаримов, Э.Р. Ибадов

Педиатрическая трансплантация печени в Узбекистане: первый клинический случай и анализ результатов
К.О. Семаш, Т.А. Джанбеков, М.М. Насыров, А.Р. Монахов, П.М. Гаджиева, С.А. Масютин

ТРАНСПЛАНТАЦИЯ СЕРДЦА И ВСПОМОГАТЕЛЬНОЕ КРОВООБРАЩЕНИЕ

Неотложная имплантация левожелудочкового обхода у детей с дооперационной краткосрочной механической поддержкой кровообращения методом периферической вено-артериальной экстракорпоральной мембранной оксигенации
В.Н. Попцов, Д.В. Рябцев, Е.А. Спирина, А.А. Кузнецова, В.В. Колядина, А.Ч. Чартаев, А.С. Епремян, А.К. Солодовникова, А.С. Игнаткина, Я.С. Карина

CONTENTS

EDITORIAL

6 Frontiers of transplantation science and breakthrough innovations: discussion at the Presidium of the Russian Academy of Sciences
S.V. Gautier

CLINICAL TRANSPLANTOLOGY

8 Combined machine perfusion and ischemia-free implantation of livers from high-risk donors: first experience in Russia
M.A. Boldyrev, A.R. Monakhov, N.V. Grudinin, V.K. Bogdanov, S.I. Zubenko, V.R. Salimov, D.M. Bondarenko, N.P. Mozheiko, N.M. Yusuf, M.G. Minina, O.M. Tsirulnikova, S.V. Gautier

22 Optimizing maintenance immunosuppressive therapy after liver transplantation
O.A. Gerasimova, N.V. Marchenko, I.I. Tileubergenov, V.N. Zhuykov

27 Effect of pre-transplant dialysis modality on outcomes in the first two years after kidney transplantation
V.A. Berdinsky, E.S. Ivanova, V.E. Vinogradov, N.F. Frolova, O.N. Kotenko, L.Yu. Artyukhina, I.V. Dmitriev, P.A. Drozdov

35 Successful endoscopic management of Swyer–James–MacLeod syndrome: a case report
M.T. Bekov, I.V. Pashkov, E.F. Shigaev, K.S. Smirnov, R.A. Latypov, D.O. Oleshkevich

41 Risk of graft loss: single-factor and multifactor analysis in kidney transplantation from expanded criteria donors
M.G. Minina, D.A. Bankeev, A.B. Zulkarnaev, V.S. Bogdanov, E.A. Tenchurina, V.M. Sevostyanov

49 Impact of kidney transplantation on erectile function and reproductive health in men with chronic kidney disease
S.S. Kariev, F.R. Nasyrov, Sh.Sh. Shavakhabov, S.Kh. Ibragimov, Z.T. Matkarimov, E.R. Ibadov

58 Pediatric liver transplantation in Uzbekistan: first clinical case and outcome analysis
K.O. Semash, T.A. Dzhanbekov, M.M. Nasyrov, A.R. Monakhov, P.M. Gadzhieva, S.A. Masyutin

HEART TRANSPLANTATION AND ASSISTED CIRCULATION

63 Urgent LVAD implantation in children on peripheral VA-ECMO support
V.N. Poptsov, D.V. Ryabtsev, E.A. Spirina, A.A. Kuznetsova, V.V. Kolyadina, A.Ch. Chartaev, A.S. Epremian, A.K. Solodovnikova, A.S. Ignatkina, Ya.S. Karina

Оценка эффективности новой полипропиленовой мембраны для мембранной оксигенации крови
В.К. Богданов, Ц. Лян, Ч. Лонг, Д.М. Бондаренко, В.А. Еленкин, А.П. Кулешов, Н.В. Васильев, Н.В. Грудинин
74

Evaluation of the effectiveness of novel polypropylene membranes for extracorporeal membrane oxygenation
V.K. Bogdanov, Ts. Liang, Ch. Long, D.M. Bondarenko, V.A. Elenkin, A.P. Kuleshov, N.V. Vasiliev, N.V. Grudinin

Клинический случай тотального эндопротезирования тазобедренного сустава пациенту с трансплантированным сердцем и высокой коморбидностью
В.Ю. Мурылев, П.М. Елизаров, П.А. Дроздов, Г.А. Куковенко, М.П. Елизаров, А.В. Музыченков, Г.С. Михайлянц, С.С. Алексеев, А.И. Руднев, К.Г. Яковлев, Д.О. Голубкин
80

Total hip replacement in a heart transplant recipient with multiple comorbidities: a case report
V.Yu. Murylev, P.M. Elizarov, P.A. Drozdov, G.A. Kukovenko, M.P. Elizarov, A.V. Muzychenkov, G.S. Michailyants, S.S. Alekseev, A.I. Rudnev, K.G. Yakovlev, D.O. Golubkin

Развитие гибридных моделирующих комплексов с учетом результатов математического моделирования и оптимизации систем вспомогательного кровообращения
А.И. Сырбу, А.О. Шевченко, Н.В. Грудинин, А.С. Бучнев
87

Hybrid hemodynamic modeling for optimization of mechanical circulatory support systems
A.I. Syrbu, A.O. Shevchenko, N.V. Grudinin, A.S. Buchnev

РЕГЕНЕРАТИВНАЯ МЕДИЦИНА И КЛЕТОЧНЫЕ ТЕХНОЛОГИИ

REGENERATIVE MEDICINE AND CELL TECHNOLOGIES

Мезенхимальные стромальные клетки при хронических фиброзирующих заболеваниях печени: роль в патогенезе и при терапевтическом применении
Н.А. Онищенко, М.Ю. Шагидулин, А.А. Ванюкова, А.В. Кузьмина, А.О. Никольская, Е.А. Волкова, А.И. Костышева, И.А. Лычагин, К.А. Казанцева, М.Р. Ибрагимова, А.М. Григорьев, А.С. Пономарева, Ю.Б. Басок
92

Pathogenic and therapeutic roles of mesenchymal stem cells in liver fibrosis
N.A. Onishchenko, M.Yu. Shagidulin, A.A. Vaniukova, A.V. Kuzmina, A.O. Nikolskaya, E.A. Volkova, A.I. Kostysheva, I.A. Lychagin, K.A. Kazantseva, M.R. Ibragimova, A.M. Grigoriev, A.S. Ponomareva, Yu.B. Basok

Исследование механических и структурных свойств шелковых скаффолдов для тканевой инженерии и реконструктивной хирургии
Е.И. Подболотова, А.Р. Пашутин, Н.В. Грудинин, Е.А. Волкова, О.И. Агапова, А.Е. Ефимов, И.И. Агапов
105

Silk-based scaffolds for tissue engineering and reconstructive surgery: mechanical and structural properties
E.I. Podbolotova, A.R. Pashutin, N.V. Grudinin, E.A. Volkova, O.I. Agapova, A.E. Efimov, I.I. Agapov

ТРАНСПЛАНТОМИКА

TRANSPLANTOMICS

Перспективные подходы к преодолению иммунологических и физиологических барьеров в трансплантологии. Ксенотрансплантация
Д.А. Великий, Ю.Б. Басок, Н.В. Грудинин, О.Е. Гичкун, А.П. Трашков, А.В. Варлачев, О.П. Шевченко
112

Advances in overcoming immunological and physiological barriers in xenotransplantation
D.A. Velikiy, Yu.B. Basok, N.V. Grudinin, O.E. Gichkun, A.P. Trashkov, A.V. Varlachev, O.P. Shevchenko

Связь развития посттрансплантационных осложнений с носительством полиморфного локуса rs1800469 гена *TGFB1* у детей – реципиентов печени
Р.М. Курабекова, О.Е. Гичкун, О.М. Цирульникова, И.Е. Пашкова, М.С. Власов, С.В. Мещеряков, О.П. Шевченко, С.В. Готье
116

Association between *TGFB1* rs1800469 polymorphism and post-transplant complications in pediatric liver recipients
R.M. Kourabekova, O.E. Gichkun, O.M. Tsirulnikova, I.E. Pashkova, M.S. Vlasov, S.V. Meshcheryakov, O.P. Shevchenko, S.V. Gautier

ДОНОРСТВО ОРГАНОВ

ORGAN DONATION

Трансплантация почек, полученных от доноров с расширенными критериями. Первое в РФ когортное многоцентровое исследование
Д.А. Банкеев, А.Б. Зулькарнаев, М.Г. Минина, В.С. Богданов, Э.А. Тенчурина, В.М. Севостьянов
122

Kidney transplantation from expanded criteria donors. The first multicenter cohort study in the Russian Federation
D.A. Bankeev, A.B. Zulkarnaev, M.G. Minina, V.S. Bogdanov, E.A. Tenchurina, V.M. Sevostyanov

ЗАМЕСТИТЕЛЬНАЯ ПОЧЕЧНАЯ ТЕРАПИЯ

Дислипидемия и стратегии медикаментозной гиполипидемической терапии у пациентов, получающих заместительную почечную терапию: обзор литературы
А.В. Самбуров, Н.А. Хайбулина, Т.Л. Кулик, Ш.Р. Галеев

ЭКСПЕРИМЕНТАЛЬНЫЕ ИССЛЕДОВАНИЯ

Исследование эффективности протоколов прекондиционирования трансплантата легких при донорстве после остановки эффективного кровообращения на экспериментальной модели кроликов
И.В. Пашков, Я.С. Якунин, К.С. Смирнов, В.К. Богданов, Н.П. Можейко, Л.А. Кирсанова, М.В. Ольховская, Н.В. Грудинин

СМЕЖНЫЕ ДИСЦИПЛИНЫ

Паттерны кальцификации биологических протезов клапанов сердца: кластеризация графических данных
Е.А. Овчаренко, К.Ю. Клышников, П.С. Онищенко, А.Е. Костюнин, А.А. Хромов, А.Н. Стасев, Т.Н. Акентьева, М.П. Фокеева, О.Л. Барбараш, Т.В. Глушкова

Случай успешной коррекции тотальной недостаточности трикуспидального клапана и клапана легочной артерии с использованием гомографтов у пациентки после ранее выполненной радикальной коррекции двойного отхождения сосудов от правого желудочка
К.В. Шаталов, И.В. Арнаутова, С.В. Пацера, К.М. Джиджихия, Р.Р. Ахтямов, В.А. Болсуновский, Д.В. Зотов, Ю.В. Гусарова

ИНФОРМАЦИЯ

Требования к публикациям

RENAL REPLACEMENT THERAPY

132 Dyslipidemia and lipid-lowering therapy in patients on renal replacement therapy: A literature review
A.V. Samburov, N.A. Khaibulina, T.L. Kulik, Sh.R. Galeev

EXPERIMENTAL RESEARCH

145 Comparative study of lung preconditioning protocols in donors after circulatory arrest: an experimental rabbit model
I.V. Pashkov, Ya.S. Yakunin, K.S. Smirnov, V.K. Bogdanov, N.P. Mozheiko, L.A. Kirsanova, M.V. Olkhovskaya, N.V. Grudinin

RELATED DISCIPLINES

153 Image-based clustering analysis of calcification patterns in bioprosthetic heart valves
E.A. Ovcharenko, K.Yu. Klyshnikov, P.S. Onishchenko, A.E. Kostyunin, A.A. Khromov, A.N. Stasev, T.N. Akentyeva, M.P. Fokeeva, O.L. Barbarash, T.V. Glushkova

163 Successful reoperation using homografts for tricuspid and pulmonary valve regurgitation after radical double outlet right ventricle correction
K.V. Shatalov, I.V. Arnautova, S.V. Patsera, K.M. Dzhidzhikhiya, R.R. Akhtiamov, V.A. Bolsunovskii, D.V. Zotov, Yu.V. Gusarova

INFORMATION

167 Instructions to authors

ВЕКТОРЫ НАУЧНОГО ПОИСКА И ПРОРЫВНЫЕ ТЕХНОЛОГИИ В ОБЛАСТИ ТРАНСПЛАНТОЛОГИИ ОБСУЖДАЛИ НА ЗАСЕДАНИИ ПРЕЗИДИУМА РАН

FRONTIERS OF TRANSPLANTATION SCIENCE AND BREAKTHROUGH INNOVATIONS: DISCUSSION AT THE PRESIDIUM OF THE RUSSIAN ACADEMY OF SCIENCES

Глубокоуважаемые коллеги!

30 сентября 2025 года состоялось заседание президиума Российской академии наук, основной темой которого стало обсуждение развития трансплантологии и донорства органов в Российской Федерации. Со вступительным словом на секции «Трансплантация солидных органов: векторы научного поиска, прорывные технологии, перспективы развития» выступил вице-президент РАН академик РАН Михаил Александрович Пирадов.

В докладе «Трансплантация солидных органов: разработка, научное обоснование и реализация в практике здравоохранения» был представлен анализ новейших направлений, уже доказавших свою эффективность. В их числе разработка и внедрение в клиническую практику новых методов малоинвазивной диагностики и прогноза осложнений, а также персонализации иммуносупрессивной терапии, основанных на молекулярно-генетических, эпигенетических и клинических критериях, позволяющих улучшить индивидуальный прогноз у реципиентов сердца, легкого, почки, печени.

В последние годы успехи, достигнутые в использовании специфических протеомных биомаркеров, дополнены изучением транскриптомных биомаркеров, среди которых выделяют особую группу малых некодирующих молекул микроРНК, принимающих участие в регуляции экспрессии генов.

В Национальном медицинском исследовательском центре трансплантологии и искусственных органов имени академика В.И. Шумакова разработаны диагностические и прогностические панели микроРНК, высокоэффективные при развитии отторжения,

Dear colleagues,

On September 30, 2025, the Presidium of the Russian Academy of Sciences (RAS) convened a meeting dedicated to transplant medicine and organ donation in the Russian Federation. The keynote speech was delivered by RAS Vice President and Fellow Prof. Mikhail Piradov, at the section titled "Solid Organ Transplantation: Frontiers of Transplantation Science, Breakthrough Innovations, and Future Outlook".

A report titled "Solid Organ Transplantation: Development, Scientific Rationale, and Implementation in Healthcare Practice" presented an analysis of latest, evidence-based advances in the field. These include development and clinical adoption of new minimally invasive methods for diagnosing and predicting complications, as well as introduction of personalized immunosuppressive strategies grounded in molecular, genetic, epigenetic, and clinical data. These approaches enhance individualized prognostic accuracy for recipients of heart, lung, kidney, and liver transplants.

In recent years, successes achieved in the use of specific proteomic biomarkers have been complemented by studies on transcriptomic biomarkers, particularly small non-coding miRNAs that play key roles in regulating gene expression.

The Shumakov National Medical Research Center of Transplantology and Artificial Organs has developed diagnostic and prognostic miRNA panels that are highly effective in detecting graft rejection, fibrosis, and infectious complications in heart and lung transplant recipients. A comprehensive assessment combining transcriptomic (miRNA) and proteomic (e.g., galectin-3, ST2, etc.) biomarkers significantly improves the diagnostic

фиброза и инфекционных осложнений у реципиентов сердца, легких. Комплексный анализ транскриптомных (микроРНК) и протеомных (галектин-3, ST2 и др.) биомаркеров значительно повышает диагностическую эффективность отдельных тестов при патологии трансплантата.

Выполнение молекулярно-генетических и иммунологических исследований биомаркеров позволяет не только диагностировать отторжение, фиброз трансплантированных почки, печени, сердца, легкого на ранних стадиях и провести коррекцию иммуносупрессивной терапии, но и улучшить понимание фундаментальных основ иммунной толерантности, иммуносупрессии, тонких механизмов взаимоотношения трансплантата с организмом реципиента.

На заседании Президиума РАН с докладами также выступили академик РАН М.Ш. Хубутия: «Исторические аспекты развития трансплантации органов»; член-корреспондент РАН А.О. Шевченко: «Активное долголетие реципиентов сердца»; академик РАН А.В. Шабунин и профессор РАН М.Г. Минина: «Инновационные технологии повышения эффективности донорства органов».

С уважением,
главный редактор
академик РАН С.В. Готье

accuracy of individual tests used to detect transplant-related pathologies.

Molecular genetic and immunological studies of biomarkers make it possible not only to diagnose rejection and fibrosis of transplanted kidneys, livers, hearts, and lungs at early stages and to adjust immunosuppressive therapy accordingly, but also to deepen our understanding of the fundamental principles of immune tolerance, immunosuppression, and the intricate interactions between the transplant and the recipient's body.

During the meeting of the Presidium of RAS, reports were also presented by RAS fellows Prof. Mogeli Khubutia ("Historical Aspects of the Development of Organ Transplantation"), Prof. Alexey Shevchenko ("Active Longevity of Heart Recipients"), and Prof. Alexey Shabunin together with Prof. Marina Minina ("Innovative Technologies for Enhancing the Effectiveness of Organ Donation").

Sincerely,
Sergey Gautier,
Fellow, Russian Academy of Sciences
Editor-in-chief, Russian Journal of Transplantology and Artificial Organs

DOI: 10.15825/1995-1191-2025-4-8-23

COMBINED MACHINE PERFUSION AND ISCHEMIA-FREE IMPLANTATION OF LIVERS FROM HIGH-RISK DONORS: FIRST EXPERIENCE IN RUSSIA

M.A. Boldyrev[1], A.R. Monakhov[1, 2], N.V. Grudinin[1], V.K. Bogdanov[1], S.I. Zubenko[1], V.R. Salimov[1], D.M. Bondarenko[1], N.P. Mozheiko[1], N.M. Yusuf[1], M.G. Minina[1, 3], O.M. Tsirulnikova[1, 2], S.V. Gautier[1, 2]

[1] Shumakov National Medical Research Center of Transplantology and Artificial Organs, Moscow, Russian Federation
[2] Sechenov University, Moscow, Russian Federation
[3] Botkin Hospital, Moscow, Russian Federation

Objective: to assess the efficacy and safety of combining sequential dual hypothermic oxygenated machine perfusion (DHOPE), controlled oxygenated rewarming (COR), and normothermic machine perfusion (NMP) with ischemia-free liver implantation (IFLI) for transplants obtained from high-risk expanded criteria donors (ECDs). **Materials and methods.** The study presents two cases of liver transplantation performed using the combined DHOPE-COR-NMP-IFLI protocol in May and June 2025 at the Shumakov National Medical Research Center of Transplantology and Artificial Organs. Liver allografts were procured from brain-dead ECDs. Perfusion was carried out using a cardiopulmonary bypass (CPB) machine following a period of static cold storage (SCS). The allografts were subsequently transplanted into recipients under continuous NMP after meeting viability criteria. The reproducibility and safety of the IFLI approach within the combined protocol were evaluated through descriptive analysis of donor characteristics, perfusion parameters, and intra- and postoperative outcomes in the recipients. **Results.** In both cases, the grafts met the established viability criteria despite pronounced macrovesicular steatosis (95% and 80%, respectively). In Case No. 1, all viability parameters were achieved after 4 hours of NMP. In Case No. 2, lactate clearance was suboptimal, reaching the acceptable threshold of 4.1 mmol/L only after 6 hours of perfusion. No post-perfusion syndrome or hemodynamic instability occurred in either recipient during graft reperfusion. Both recipients met the criteria for early allograft dysfunction, with cytolysis levels of 6562.9 and 1610.4 U/L, and 3822 and 2662 U/L, respectively. The recipients were discharged on postoperative days 17 and 34 without serious complications (Clavien–Dindo ≥IIIb). At 4- and 5-month follow-up, no transplant- or preservation-related complications were observed. **Conclusion.** The combined application of sequential machine perfusion (DHOPE-COR and NMP) with IFLI is a safe and effective dynamic preservation strategy. This approach enables the successful use of liver grafts from ECDs by minimizing ischemia–reperfusion injury.

Keywords: liver transplantation, machine perfusion, early graft dysfunction, expanded criteria donors.

INTRODUCTION

Expanding donor criteria is an effective strategy to address the growing gap between the number of organs available for transplantation and the number of patients in need [1, 2]. While broadening allograft eligibility helps reduce waiting-list mortality and partially mitigates organ shortages, it is also associated with less favorable transplant outcomes [3–5]. In this context, machine perfusion has emerged as a valuable tool, enabling the "resuscitation" of suboptimal organs affected by ischemia-reperfusion injury (IRI) and providing an opportunity to assess organ viability prior to transplantation [6–8].

Combined machine perfusion protocols, designed to compensate for the weaknesses of each individual technique, still leave one important challenge unresolved: the need for repeated static cold storage (SCS) after a normothermic machine perfusion (NMP) session, immediately before implantation [12]. The resulting "re-cooling" injury is becoming increasingly significant, especially as donor organs become more marginal. This sequence of repeated temperature fluctuations – re-cooling, brief cold ischemia, subsequent warm ischemia, and final reperfusion – creates additional stress on an already vulnerable graft [9–11].

Cirelli et al. describe two cases of liver transplantation from non-heart-beating donors with severe macrovesicular steatosis (>60% and >30%) after combined perfusion. Although both organs met the center's stringent viability criteria, one recipient required retransplantation

Corresponding author: Mikhail Boldyrev. Address: 1, Shchukinskaya str., Moscow, 123182, Russian Federation. Phone: (961) 974-59-55. E-mail: comex.ksb@gmail.com

on postoperative day 17, and the other developed acute kidney injury and acute respiratory failure. The authors emphasize that transplantation of severely steatotic livers remains a "risky endeavor", as their post-implantation behavior may be unpredictable even when NMP viability parameters appear acceptable [13].

Similarly, Patrono et al. report two cases of primary graft dysfunction (PGD) in allografts with 30% and 50% macrovesicular steatosis following NMP. Both grafts exhibited insufficient lactate clearance despite meeting other viability thresholds. The authors conclude that although transplantation of liver allografts with >30% steatosis may be feasible, viability assessment remains challenging, and liberalization of criteria can result in primary non-function [14, 15].

Based on studies on ischemia-free liver transplantation (IFLT), it can be assumed that complete elimination of ischemia enables the safe use of allografts with even 80–90% steatosis, with minimal injury to the graft. For centers where a full IFLT protocol is not technically feasible, reducing the procedure to ischemia-free liver implantation – i.e., omitting the donor-side perfusion stage – may represent a promising but insufficiently investigated compromise [16].

However, the studies published to date have employed isolated NMP after a preceding period of cold ischemia (an end-ischemic approach). This strategy inherently exposes the liver to IRI and does not provide adequate protection against the cumulative effects of SCS and subsequent reperfusion [17, 18].

In contrast, the use of a combined perfusion protocol incorporating dual hypothermic oxygenated perfusion (DHOPE) as a post–cold storage "resuscitation" stage, controlled oxygenated rewarming (COR) as a transitional phase between two temperature regimes, and NMP for comprehensive viability assessment, enables the relatively safe transplantation of high-risk allografts – including those from non-heart-beating donors – without compromising clinical outcomes [12].

Integrating the strengths of both approaches, namely DHOPE–COR–NMP sequence and the IFLI principles, would allow us to get the most out of each technique and ensure the safe transplantation of high-risk liver allografts. To date, however, we have not identified any studies investigating the combined application of these techniques.

DESCRIPTION OF CLINICAL OBSERVATIONS

In all reported cases, the liver allografts were referred to Shumakov National Medical Research Center of Transplantology and Artificial Organs (Shumakov Center) after being rejected by other transplant centers in accordance with the national allocation algorithm. The preservation protocol included the initial DHOPE, followed by COR, and concluded with NMP for viability assessment (the DHOPE–COR–NMP protocol). All grafts fulfilled the modified viability criteria established at Shumakov Center (Table 1), and were therefore deemed suitable for transplantation. Given the high-risk nature of these allografts and their individual characteristics, IFLI was selected as the optimal approach, instead of the conventional transition to SCS prior to implantation.

Combined sequential perfusion was carried out using the method we described earlier, which employs a cardiopulmonary bypass (CPB) machine and a custom perfusion circuit developed at Shumakov Center to ensure seamless perfusion, assembled from a standard CPB pump tubing set [19]. A modified histidine–tryptophan–ketoglutarate (HTK) solution served as the perfusate during the hypothermic phase (DHOPE + COR), while an erythrocyte-based perfusate was used during the NMP phase.

For perfusate drainage during IFLI, additional cannulation of the inferior vena cava (IVC) was performed via the subhepatic segment using 32–34 Fr cannulas.

Table 1

Criteria for liver graft viability during normothermic machine perfusion

Criteria for liver graft viability (assessment after 4–6 hours of normothermic perfusion)
Perfusate lactate <**4.5 mmol/L** after 4 hours of perfusion **OR**: **Stable decrease in lactate** with lactate **<4.5 mmol/L** after 6 hours
Presence of bile production AND: – pH difference (bile – perfusate) >**0.05, with bile pH ≥7.48**; – HCO_3^- difference (bile – perfusate) >**3.0 mmol/L, with bile HCO_3^- >18 mmol/L** – **(**Glucose difference (bile – perfusate) **<3.0 mmol/L** OR bile/perfusate glucose ratio **<0.67**) AND bile glucose **<16 mmol/L**
At least two of the following criteria:
Perfusate **pH >7.3** without continuous $NaHCO_3$ infusion;
Active **perfusate glucose metabolism** (reduction of high glucose levels and stabilization)
Stable hemodynamics: portal flow >**500 mL/min**, arterial flow >**150 mL/min**;
Homogeneous graft perfusion and soft parenchymal consistency

The suprahepatic segment of the vena cava was occluded with a Bulldog vascular clamp, leaving an adequate cuff to facilitate subsequent formation of caval anastomosis.

Ischemia-free liver implantation

Liver implantation during ongoing normothermic perfusion has been previously described by several authors and has remained largely unchanged since its introduction into clinical practice at Shumakov Center [10, 11]. At present, IFLI can be performed only with either the classical caval reconstruction involving replacement of the IVC or the standard technique with IVC preservation as described by A. Tzakis.

Before implantation, complete vascular integrity and hemostasis of the liver allograft parenchyma were confirmed. This step is essential, as any perfusate leakage could necessitate urgent volume replacement and potentially require temporary cessation of perfusion due to insufficient perfusate levels in the cardiotomy reservoir.

Following hepatectomy and preparation of the recipient's IVC cuff, the allograft was transferred into the abdominal cavity under continuous perfusion (Fig. 1).

Particular attention was given to the precise positioning of the Bulldog vascular clamp prior to initiating anastomosis formation, as improper placement could significantly complicate this stage of the procedure. The suprahepatic vena cava (or hepatico-caval) anastomosis was then constructed using the standard technique (Fig. 2).

Upon completion of the suprahepatic vena cava anastomosis, the Bulldog clamp was removed from the donor segment of the IVC to assess the integrity and hemostasis of the anastomosis.

Next, the portal vein was occluded with a vascular clamp, and portal perfusion was discontinued. From this point onward, perfusion of the allograft proceeded exclusively through the hepatic arterial system. A standard portal vein anastomosis was then performed (Fig. 3).

Next, following the same approach used for the caval anastomosis, the clamp was removed from the donor segment of the portal vein to verify the integrity and tightness of the anastomosis prior to reperfusion.

IVC decannulation was performed before initiating reperfusion, as this ensured a safe procedure without blood loss. To expose the retrohepatic portion of the IVC

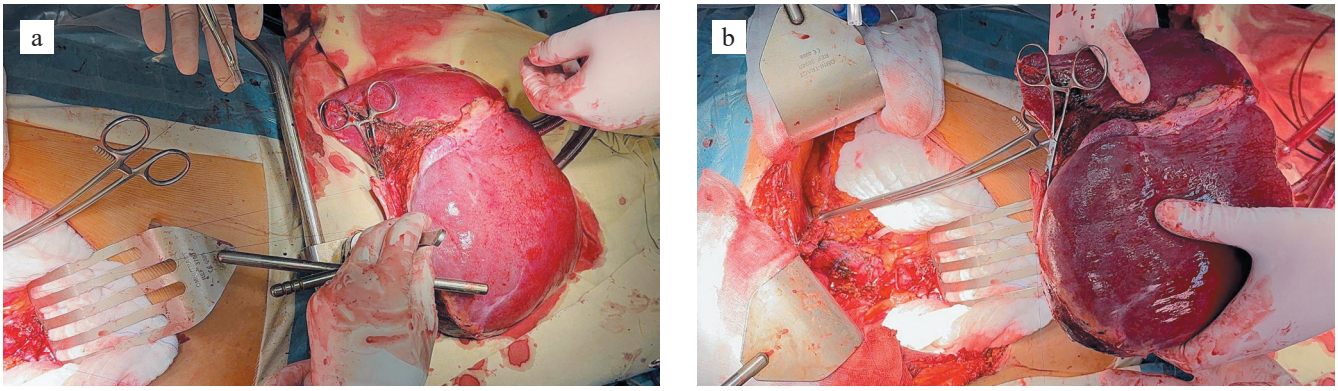

Fig. 1. (a) Liver allograft during ongoing normothermic machine perfusion; (b) preparation for ischemia-free liver implantation

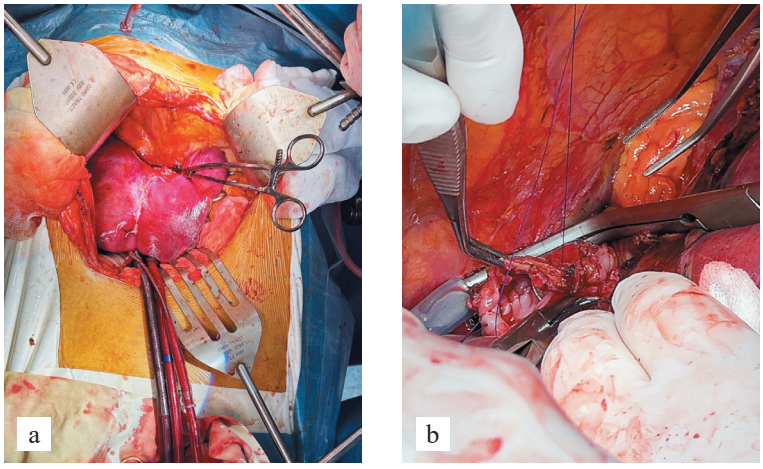

Fig. 2. (a) Beginning of the IFLI procedure; (b) caval anastomosis phase

and the cannula positioned in its subhepatic segment, the right lobe of the liver was gently rotated to the left. The opposing edges of the vein were then secured using mosquito clamps or other appropriate instruments; ligature holders could also be used. A stapling device or vascular clamp was pre-positioned on the subhepatic stump of the IVC, depending on the selected method for closing the stump or completing the caval reconstruction (Fig. 4).

In the observations described, a stapling device was used, as it minimized the duration of warm ischemia that would otherwise occur during manual suturing of the subhepatic portion of the IVC. Typically, due to tissue adhesion to the cannula, a small amount of traction was required to achieve IVC decannulation. Immediately after removal of the cannula, the IVC stump was either sutured or secured with a vascular clamp, and arterial perfusion was discontinued. The right lobe of the liver was then repositioned anatomically, followed by graft reperfusion and decannulation of the hepatic artery. From this point onward, liver transplantation proceeded according to the standard surgical technique.

Post-transplant period

The postoperative management included an initial stay in the intensive care unit for up to 12 hours, after which patients were transferred to a specialized transplant unit for early rehabilitation in accordance with the local protocol. All recipients received standardized medical care based on the center's established guidelines, which included:

– Administration of a pulse dose of methylprednisolone with subsequent rapid withdrawal or transition to oral therapy in patients with high immunological risk. In such cases, therapy was supplemented with basiliximab or thymoglobulin depending on the patient's immunological risk profile.
– Early initiation of calcineurin inhibitors with targeted trough levels of 6–8 ng/mL, along with mycophenolic acid, provided that complete blood count parameters were within acceptable limits.
– Routine ultrasound examination of the liver graft with Doppler flowmetry, as well as biochemical tests, complete blood count, coagulation profile, and calcineurin

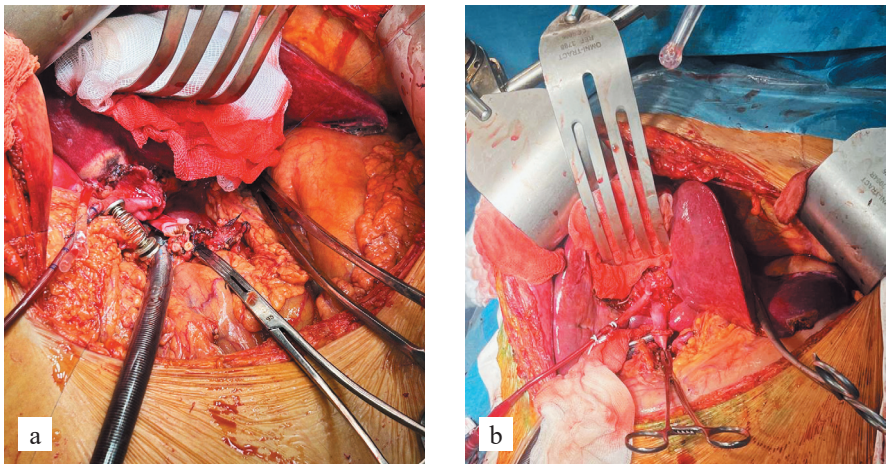

Fig. 3. IFLI procedure: (a) formation of (a) and formed (b) portal vein anastomosis

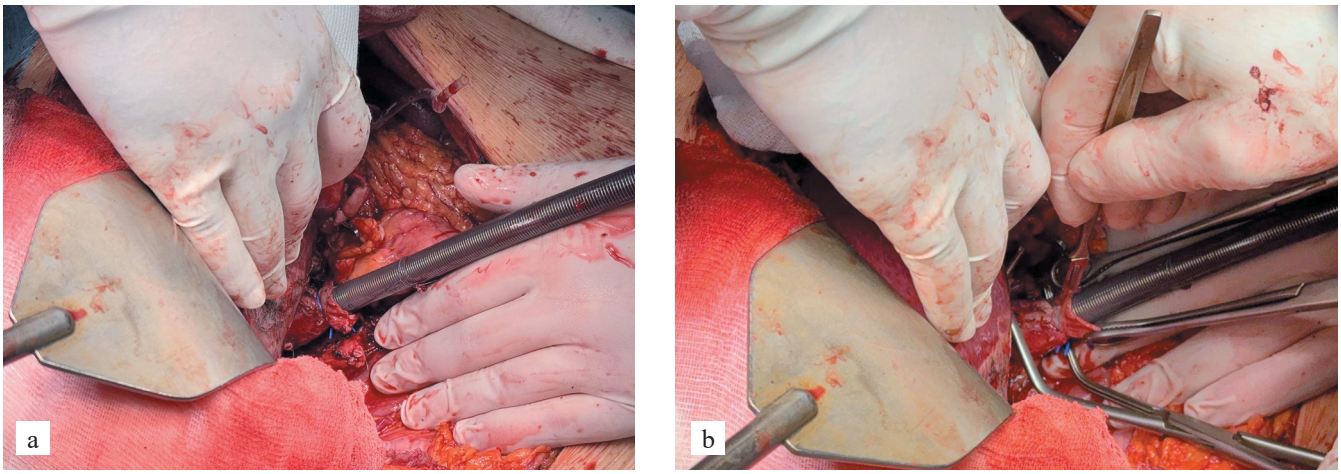

Fig. 4. (a) Visualization of the subhepatic section of the inferior vena cava with a return cannula and (b) its subsequent decannulation

inhibitor level measurement. These evaluations were performed daily during the first postoperative week, three times per week during the second week, and subsequently as clinically indicated.

An important component of postoperative management was intensive perioperative and postoperative monitoring. The following definitions were used as the primary criteria for identifying potential post-transplant complications:

– Acute graft rejection was suspected based on laboratory signs of increased cytolysis and cholestasis after excluding other potential problems, including vascular complications. The diagnosis was confirmed by percutaneous biopsy.
– Early liver graft dysfunction was determined according to the criteria proposed by K. Olthoff [20], defined as the presence of at least one of the following:
  - Serum bilirubin >171 μmol/L on postoperative day (POD) 7;
  - International normalized ratio (INR)> 1.6 on POD 7;
  - Aspartate aminotransferase (AST) or alanine aminotransferase (ALT) >2000 IU/L within the first 7 postoperative days.
– Primary graft failure was diagnosed in accordance with UNOS criteria [22], acute kidney injury was defined using KDIGO criteria [21].
– Ischemic cholangiopathy (IC) was diagnosed based on a combination of clinical symptoms (pruritus, jaundice), laboratory indicators of cholestasis (elevated gamma-glutamyl transferase and alkaline phosphatase), and instrumental findings (magnetic resonance cholangiopancreatography, MRCP). If clinical or laboratory abnormalities were present, instrumental examination was performed to confirm or exclude IC. In cases where instrumental signs of IC were present without accompanying clinical or laboratory abnormalities, the condition was classified as asymptomatic IC.
– Post-reperfusion syndrome was defined according to Aggarwal et al. [32] and Hilmi et al. [33] as a ≥30% decrease in mean arterial pressure lasting more than 1 minute within the first 5 minutes after reperfusion, the occurrence of asystole or hemodynamically significant arrhythmias (such as ventricular fibrillation), or the need to initiate vasopressor therapy during or immediately after reperfusion.

Characteristics of donors and liver allografts

Characteristics of donors and liver allografts are summarized in Table 2.

Macroscopic appearance of the liver before perfusion is shown in Fig. 5 (a – case No. 1, b – case No. 2).

Recipient characteristics

Transplants were performed in recipients who were compatible with donors according to the ABO blood group system and anthropometric parameters. Patients with high surgical or anesthesiological risk, those requiring emergency or urgent transplantation, and individuals with a high MELD score of 3.0 (>20 points) were excluded from consideration.

Case 1. Patient G., female, 34 years old, with liver cirrhosis secondary to autoimmune hepatitis and primary sclerosing cholangitis. BMI: 20.1; MELD 3.0: 16 points.

Case 2. Patient B., male, 51 years old, with liver cirrhosis due to HBV infection. BMI: 24.7; MELD 3.0: 13 points.

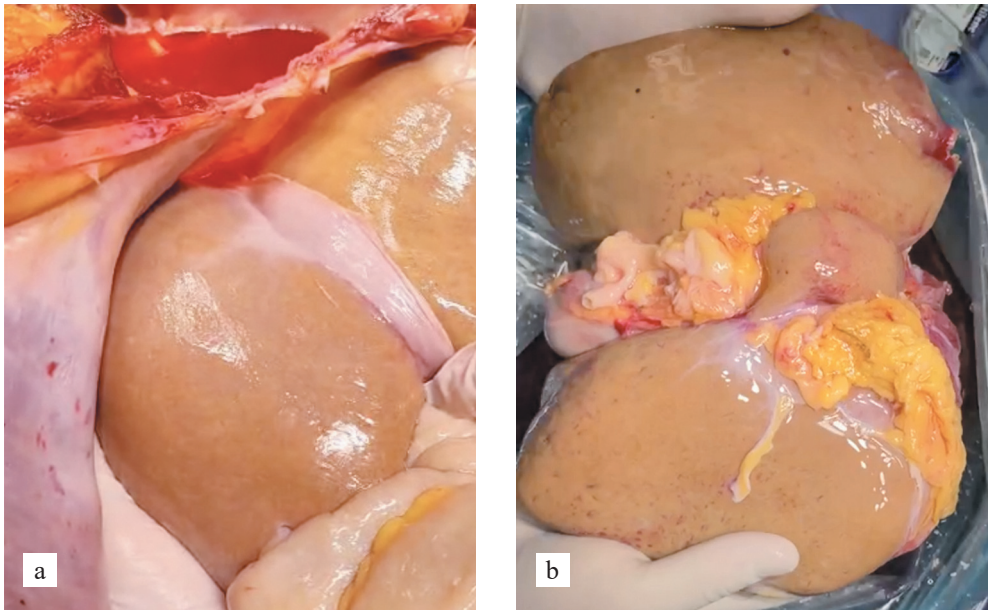

Fig. 5. Liver allografts before initiation of perfusion: (a) case No. 1 and (b) case No. 2

Perfusion parameters and viability assessment

The dynamics of the perfusate and bile parameters during NMP are presented in Fig. 6.

Combined perfusion was performed using a previously described technique [12], consisting of at least 90 minutes of DHOPE followed by a minimum of 60 minutes of COR, during which the liver allograft was gradually

Table 2

Main characteristics of recipients, donors, and perfusion

	Case 1	Case 2
	Donor	
Age	55	63
Gender	Male	Male
BMI	44.2	32.1
Donor type	DBD	DBD
Time in ICU	3 days	1 day
Donor Risk Index (DRI)	1.636	1.6
AST, U/L	143	38
ALT, U/L	86.2	31
Sodium, mmol/L	138	140
Total bilirubin, mmol/L	14.2	6.3
Creatinine, mmol/L	92.9	142
Macroscopic findings	Dense consistency, marked steatosis and fibrosis	Extremely soft consistency, marked steatosis
Microscopic findings	Macrovesicular steatosis 95%, liver fibrosis F-1 (METAVIR)	Macrovesicular steatosis 80%
	Transplant	
SCS, min	152	230
Weight before perfusion, g	1700	1930
Weight at the end of perfusion	1750	2300
	Perfusion	
DHOPE time, min	111	105
COR time, min	80	79
NMP time, min	707	595
IFLI time, min	70 *(as part of NMP)*	30 *(as part of NMP)*
Total perfusion time, min	898	779
Total storage time, min	1101	1009
Lactate at 4 hours, mmol/L	2.5	7.6
Lactate at 6 hours, mmol/L	3.6	4.1
	Indicators at 4 hours of perfusion and viability assessment	
ΔpH (bile–perfusate)	0.077	0.186
Bile pH	7.729	7.646
ΔHCO_3^- (bile–perfusate)	9.8	14.9
Bile HCO_3^-	43.5	36.5
Δ / ratio of glucose (bile–perfusate)	–2.5 / 0.42	–10.2 / 0.47
Bile glucose, mmol/L	1.8	9
Perfusate pH	7.652 *(without bicarbonate supplementation)*	7.46 *(without bicarbonate supplementation)*
Glucose metabolism	Yes (4.3 mmol/L)	No (19.2 mmol/L)
HA flow (mL/min)	610	420
PV flow (mL/min)	690	650
HA pressure (mmHg)	72	70
PV pressure (mmHg)	11	10
Transplanted	Yes	Yes

Abbreviations: ALT, alanine aminotransferase; AST, aspartate aminotransferase; SCS, static cold storage; DHOPE, dual hypothermic oxygenated machine perfusion; COR, controlled oxygenated rewarming; NMP, normothermic machine perfusion; IFLI, ischemia-free liver implantation; HA, hepatic artery; PV, portal vein.

Fig. 6. Liver transplant perfusion parameters in case No. 1 and case No. 2

warmed to 16 °C. Viability and injury markers were not assessed during the DHOPE and COR phases.

After completing the hypothermic perfusion stages and replacing the perfusate with a red blood cell–based solution, NMP was initiated. During the first hour of NMP, the temperature was gradually increased from 20 °C to 34–36 °C, accompanied by a controlled rise in hepatic arterial and portal venous flow while maintaining target perfusion pressures [12].

Viability assessment was carried out using criteria developed and modified at the Shumakov National Medical Research Center of Transplantology and Artificial Organs, as summarized in Table 1.

Characteristics of the perfusate and key perfusion parameters are presented in Table 2.

Case 1 (Fig. 7). Despite the need for sodium bicarbonate infusion during the first hour of perfusion (a total of 250 ml) to stabilize pH, the pH showed a trend toward normalization and remained within the physiological range. The initial perfusate lactate level was 13 mmol/L, rising to a peak of 17 mmol/L at 90 minutes, followed by a gradual fall to 2.5 mmol/L by the 4-hour mark. A steady decrease in perfusate glucose levels was also observed, reaching a minimum of 4.3 mmol/L at 4 hours, which necessitated supplementation with 40% dextrose. Perfusion flows and pressures were maintained in accordance with protocol and fulfilled the center's established viability criteria.

During perfusion, bile production showed a steady increase: less than 2 ml during the first 2 hours, 4 ml in the third hour, and subsequently 6–9 ml per hour.

Throughout perfusion, bile parameters remained within the thresholds indicative of cholangiocellular viability. Cytolysis markers during DHOPE were elevated but stable, with AST levels of 2008 and 2259 U/L and ALT levels of 2776.6 and 3016.4 U/L at 60 and 90 minutes, respectively. Overall, the liver allograft satisfied all established viability criteria and was considered suitable for transplantation.

Case 2 (Fig. 8).

Stabilization of pH was achieved only by the third hour of perfusion, with a total sodium bicarbonate infusion volume of 200 ml. Initial lactate level was 11.5 mmol/L, showing two peaks – 15 mmol/L at 30 minutes and 13.5 mmol/L at 2 hours – followed by a gradual decline to 7.6 mmol/L at 4 hours and 4.1 mmol/L at 6 hours. Despite continuous insulin infusion, glucose levels progressively increased and remained at 18–19 mmol/L until the end of perfusion. Bile secretion remained minimal throughout the procedure (2–2.5 ml/hour). Cytolysis markers at 60 and 90 minutes of DHOPE were 1829.7 and 2613.9 U/L (AST) and 504.5 and 824.8 U/L (ALT), respectively. The allograft fulfilled all established viability criteria except for glucose metabolism and was deemed suitable for transplantation.

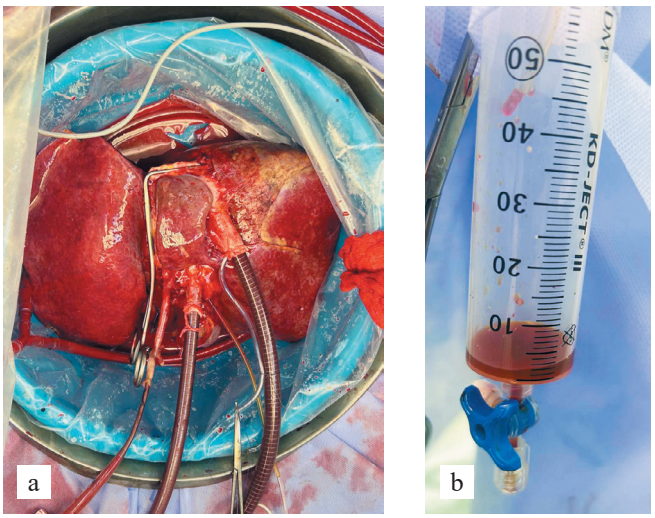

Fig. 7. (a) Liver allograft No. 1 and (b) bile secretion during NMP

Intraoperative liver transplantation characteristics

Case 1. Orthotopic liver transplantation was performed using the standard technique with IVC preservation according to A. Tzakis. Total operative time was 475 minutes, and biliary ischemia time was 70 minutes. Intraoperative blood loss was 700 ml, requiring transfusion of 2 units of red blood cells (RBCs) and 5 units of fresh frozen plasma (FFP). No postreperfusion syndrome or adverse hemodynamic response to reperfusion was observed. Arterial lactate level at the end of surgery was 2.4 mmol/L. Vasopressor therapy consisted of norepinephrine at 100 ng/kg/min.

Case 2. Orthotopic liver transplantation was also performed using the standard technique with IVC preservation according to A. Tzakis. Total operative time was 240 minutes, with a biliary ischemia time of 15 minutes. Blood loss was 1000 ml, and the patient received 2 units of RBCs and 2 units of FFP. No postreperfusion syndrome or hemodynamic instability during reperfusion was noted. Arterial lactate level at the conclusion of the procedure was 3.6 mmol/L, and vasopressor therapy consisted of norepinephrine at 90 ng/kg/min.

Postoperative period

The laboratory dynamics of the postoperative period in recipients are shown in Fig. 9.

Case 1. Peak AST and ALT levels reached 6562.9 U/L and 1610.4 U/L, respectively – meeting only one criterion for early allograft dysfunction. A rapid decline in

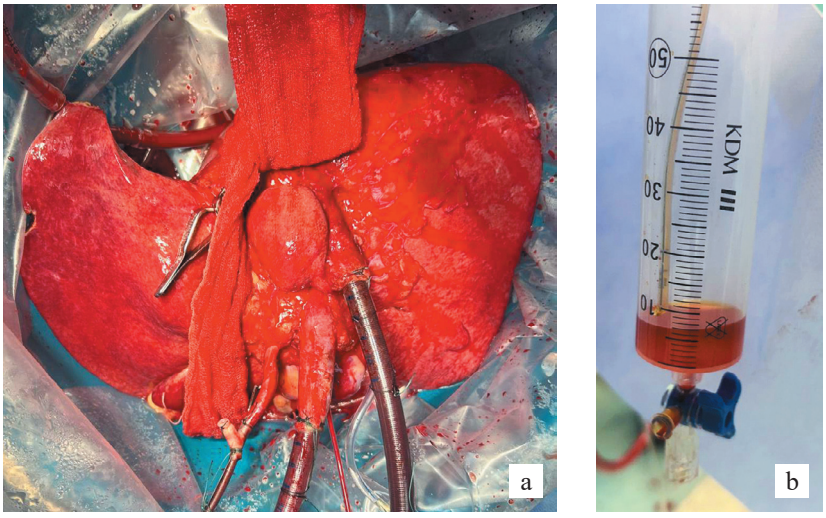

Fig. 8. (a) Liver allograft No. 2 and (b) bile secretion during NMP

transaminases was observed by postoperative day (POD) 2, with AST at 1267 U/L and ALT at 1212 U/L. The area under the curve (AUC) for AST was 5609.6 and for ALT 4353. Maximum total bilirubin level was 166 μmol/L on POD 6, followed by a steady decrease to normal values. Peak INR was 2.36 on POD 1. The postoperative course was uneventful, the patient was discharged on POD 17 without surgical or immunological complications. Two months after transplantation, the patient was readmitted due to Doppler-based findings suggestive of splenic artery steal syndrome. Splenic artery embolization was performed successfully. At the time of reporting, the follow-up period was four months.

Case 2. Peak AST and ALT levels were 3822 U/L and 2662 U/L, respectively, and constituted the only criterion fulfilled for early liver graft dysfunction. Similar to Case 1, AST and ALT values decreased rapidly by POD 2 (1429 and 2207 U/L, respectively), continuing to fall thereafter. The calculated AUC values were 4645 for AST and 8327 for ALT. The maximum total bilirubin level was 65.8 mmol/L on POD 1, followed by a steady decline to normal values. Peak INR was 3.11, also observed on POD 1. A postoperative hematoma in the subcutaneous tissue required evacuation, after which a vacuum-assisted wound system was applied on POD 3 and maintained for 7 days. The remaining postoperative course was uneventful. The patient was discharged on POD 34 without major complications. At the time of reporting, the follow-up period was 5 months.

Characteristics of the pathomorphological examination of the transplant

In all cases, microscopic (light microscopy) examination of the allograft was performed at three stages: before the start of perfusion, after completion of normothermic machine perfusion, and before suturing of the recipient's postoperative wound. A section of the bile duct was examined to assess conservation–ischemic injury both prior to perfusion and at the end of the surgery. Biopsies were obtained using an incisional technique from the edges of two liver lobes and from the distal portion of the common bile duct. Samples were fixed in 10% formalin and submitted for full pathomorphological examination.

An important observation is the *discordance* between the pathomorphological findings – including diffuse-focal and subtotal hepatocyte necrosis – and the clinically smooth postoperative course observed in both recipients. This discrepancy will be analyzed further in the *Discussion* section.

Case 1 (Fig. 10). *Preperfusion* biopsy showed moderate capsule sclerosis, diffuse-focal fatty degeneration (90–95%), involving medium and large-droplet degeneration of hepatocytes, fibrosis of the portal tracts and central vein walls, stage F1 fibrosis according to METAVIR.

Postperfusion biopsy, in addition to previously noted features, showed subcapsular and capsular hemorrhages, parenchymal edema, ruptured fat vacuoles in some areas, diffuse focal hepatocyte necrosis, and microhemorrhages within the parenchyma. The *postreperfusion* biopsy revealed subcapsular hepatocyte necrosis extending deep

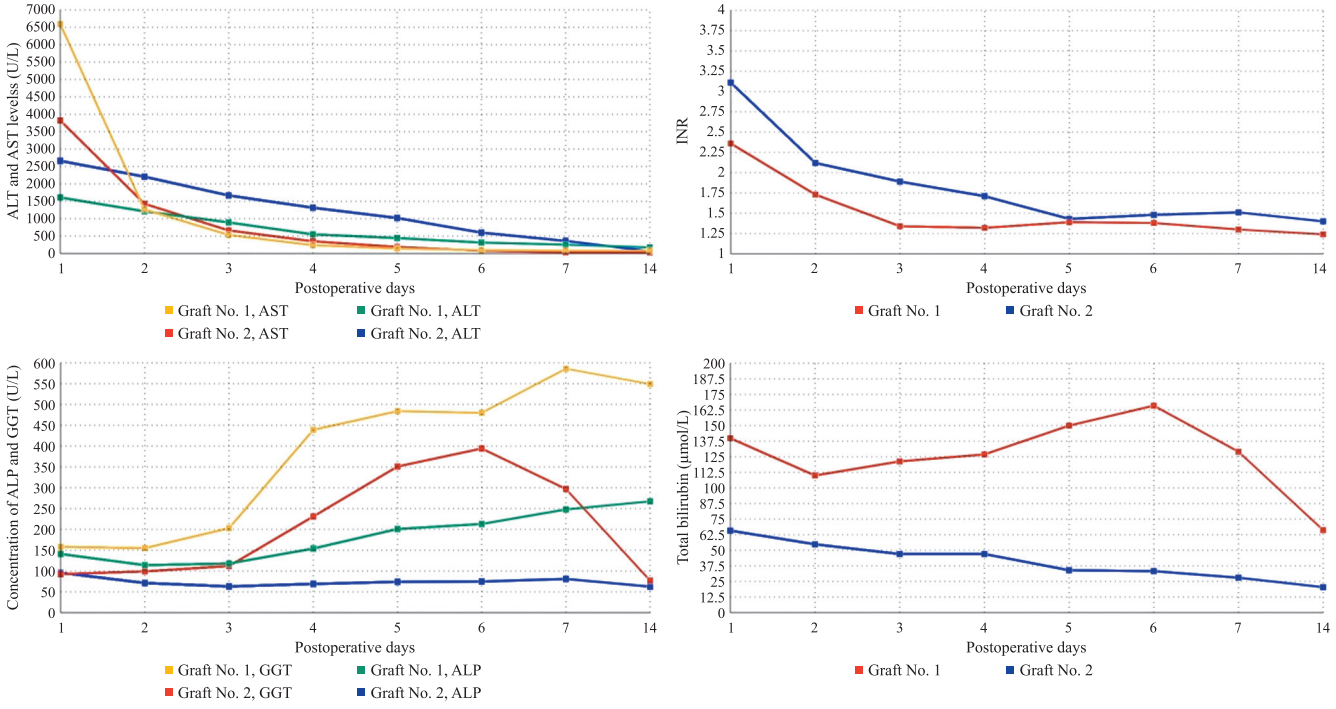

Fig. 9. Postoperative recipient parameters (case No. 1 and case No. 2.). Abbreviations: ALT, alanine aminotransferase; AST, aspartate aminotransferase; INR, international normalized ratio; ALP, alkaline phosphatase; GGT, gamma-glutamyl transferase

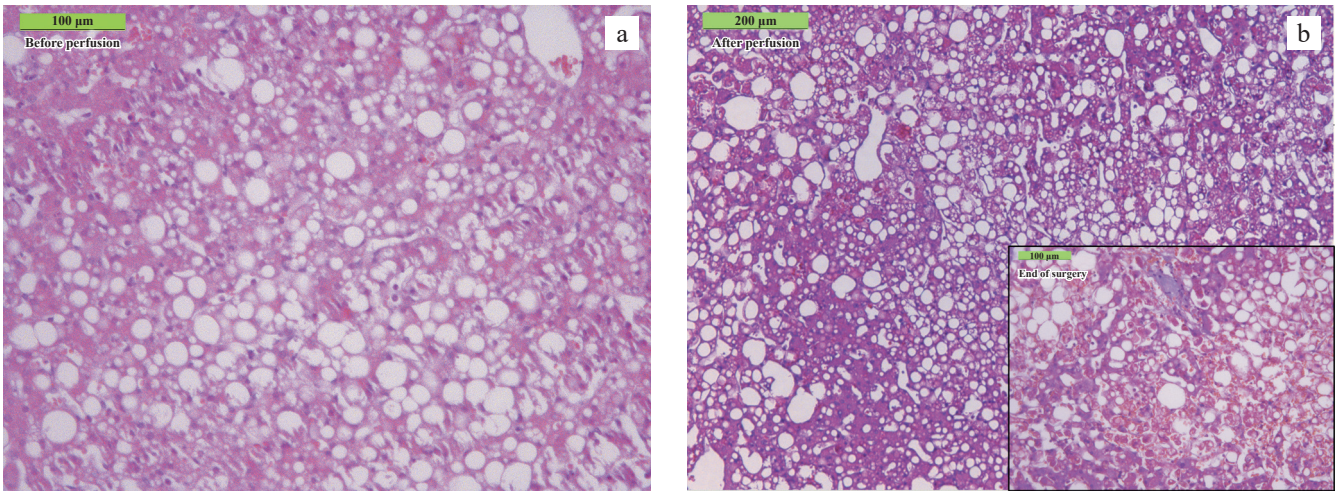

Fig. 10. Micrographs of a liver allograft biopsy in case No. 1 before and after machine perfusion. (a) Before perfusion (magnification 20×, H&E stain); (b) After perfusion (magnification 10×, H&E stain) and at the end of surgery (magnification 20×, Masson's trichrome stain). Detailed histological description is provided in the text

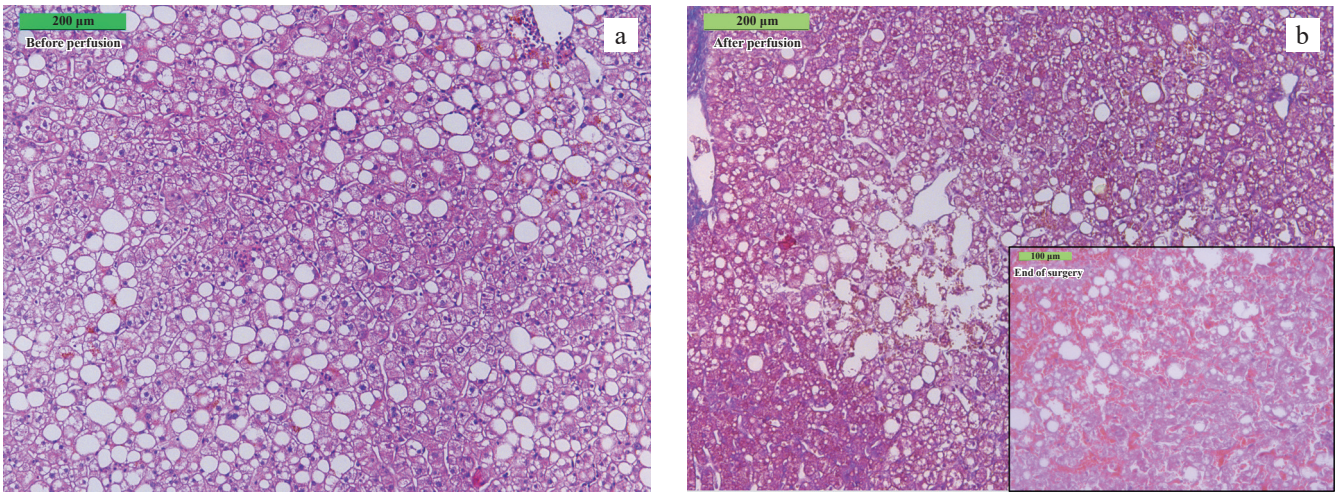

Fig. 11. Micrographs of a liver allograft biopsy in case No. 2 before and after machine perfusion. (a) Before perfusion (magnification 10×, H&E stain); (b) After perfusion (magnification 10×, Masson's trichrome stain) and at the end of surgery (magnification 20×, H&E stain). Detailed histological description is provided in the text

into the parenchyma with associated hemorrhages – most likely of compressive origin – as well as diffuse focal hepatocyte necrosis with hemorrhage. Bile duct biopsy revealed preserved peribiliary glands and biliary epithelium, with focal areas of epithelial desquamation.

Case 2 (Fig. 11). *Preperfusion* biopsy confirmed diffuse focal large-droplet fatty degeneration of hepatocytes involving up to 80%. Postperfusion biopsy showed subtotal hepatocyte necrosis and diffuse parenchymal hemorrhages.

Post-reperfusion biopsy also revealed diffuse focal hepatocyte necrosis accompanied by subcapsular and intraparenchymal hemorrhages, fibrosis of the central vein walls and portal tracts, and loose inflammatory infiltration within the portal areas. The bile duct biopsy showed no abnormalities and confirmed preservation of the peribiliary glands and biliary epithelium.

DISCUSSION

Minimizing or eliminating IRI is fundamental to expanding donor criteria, as IRI remains a major limitation to the maximal utilization of allografts from deceased donors [24, 25]. The concept of IFLT directly supports this principle. In a randomized controlled trial, Guo et al. compared outcomes in recipients of allografts preserved with IFLT (n = 32) versus SCS (n = 33). Early liver graft dysfunction, a key indicator of IRI, occurred in only 6% (n = 2) of patients in the IFLT group compared with 24% (n = 8) in the SCS group (p = 0.044). Post-reperfusion syndrome – another marker of preservation-related injury – developed in 9% (n = 3) of IFLT recipients versus 64% (n = 21) in the SCS group (p < 0.001) [16].

Further supporting these findings, He et al. reported the successful transplantation of a liver allograft with 85–95% macrovesicular steatosis using the IFLT technique,

reporting peak AST and ALT levels of only 375 and 123 U/L, and gamma-glutamyl transferase and alkaline phosphatase levels of 86 and 79 U/L, respectively [26].

Collectively, these results suggest that the complete avoidance of IRI enables the safe transplantation of virtually any organ – regardless of its suboptimal baseline condition – as long as it maintains adequate function in the donor prior to procurement.

However, despite its remarkable effectiveness in preventing IRI, IFLT has several technical drawbacks. Perfusion must begin at the donor hospital, and procurement procedure requires highly advanced surgical expertise, as it involves complete mobilization of the liver and inferior vena cava, along with meticulous dissection of the hepatoduodenal ligament. Furthermore, transporting the perfusion device with the organ continuously perfused to the recipient's hospital is logistically complex and labor-intensive [26]. To address these challenges, a simplified modification of IFLT – IFLI – which excludes the donor stage of machine perfusion has been proposed. IFLI prevents the recooling injury that occurs when an organ is re-cooled after completion of NMP but before implantation [10, 11, 27].

Chen et al. reported a significantly lower incidence of post-reperfusion syndrome in the IFLI group compared with the NMP group (8% vs. 58.8%, $p < 0.001$) and a higher frequency of primary graft dysfunction in recipients who did not undergo IFLI ($p = 0.041$). In a comparative study of IFLI ($n = 7$), NMP ($n = 7$), and SCS ($n = 14$), the same authors demonstrated reduced cytolysis in both perfusion groups relative to SCS ($p = 0.0015$ and $p = 0.016$ for AST and ALT, respectively), as well as a lower incidence of early dysfunction in the IFLI group compared with SCS ($p = 0.022$) and NMP ($p = 0.462$) [11]. Their use of fairly broad criteria for extended liver donation (Eurotransplant [29] and Vodkin et al. [28]) may partially explain the less pronounced results of IFLI in that cohort.

Notably, the avoidance of secondary warm ischemia may itself offer clinical benefits. In a study of 1,256 liver transplant recipients from brain-dead donors, Al-Kurd et al. reported a significantly lower risk of graft loss at both 1 and 5 years when secondary warm ischemia time was kept below 30 minutes [30]. Similarly, Sakamoto et al., analyzing outcomes in 67 living donor liver transplant recipients, found that secondary warm ischemia exceeding 48 minutes was a significant risk factor for the development of post-transplant biliary strictures ($p = 0.008$) [31].

Minimization of IRI and mitigation of its consequences can, as previously noted, be achieved through isolated or combined machine perfusion protocols. In our view, the DHOPE-COR-NMP protocol developed by the team at the University Medical Center Groningen represents the most effective strategy currently available [12]. Despite its strong potential – particularly for the utilization of high-risk organs from non-heart-beating (NHB) donors – its effectiveness remains limited when applied to allografts with significant macrovesicular steatosis (>30%).

Cirelli et al. reported two cases of liver transplantation using allografts from NHB donors with severe macrovesicular steatosis (>60% and >30%) following combined DHOPE-COR-NMP perfusion [13]. Although both grafts satisfied the center's stringent viability criteria (Groningen criteria), the clinical outcomes were suboptimal. In the first case, retransplantation was required on POD 17 due to persistent high-volume ascites (>10 L/day) and sustained vasopressor dependence. The authors attributed this to a 30% reduction in graft volume caused by rapid resolution of steatosis, which led to excessive length and subsequent kinking of the suprahepatic vena cava. The patient also experienced pronounced post-perfusion syndrome requiring norepinephrine therapy, acute kidney injury necessitating dialysis, and later kidney transplantation.

In the second case, the presence of lipopeliosis in the graft biopsy raised suspicion of "fat embolism" syndrome, which may have contributed to acute hypoxic respiratory failure and acute kidney injury. Based on these observations, the authors concluded that transplantation of organs with severe steatosis remains a risky endeavor, as graft behavior can remain unpredictable even when viability criteria are met during NMP.

In our study, we presented the outcomes of applying the combined DHOPE–COR–NMP–IFLI protocol, which by the time of reporting had become a routine component of our practice for high-risk donors. The cases described demonstrate the high efficacy and safety of machine perfusion in the transplantation of allografts with macrovesicular steatosis exceeding 80%, with no serious postoperative complications observed.

In our view, the markedly elevated peak AST and ALT levels likely reflect not the extent of IRI but rather the systemic entry of a substantial volume of transaminase-rich perfusate (more than 500 ml). This interpretation is supported by the relatively low area under the curve (AUC) for transaminase levels and their rapid decline as early as POD 2. Notably, the only instance of early liver graft dysfunction was identified solely on the basis of conventional biochemical criteria (AST/ALT peaks), without any clinical correlate or adverse effect on the postoperative course. This observation aligns with a broader shift in the field toward revising early dysfunction criteria in the era of dynamic perfusion preservation.

Graft function has remained stable for more than three months following transplantation, underscoring the satisfactory short-term outcomes achievable in highly steatotic allografts using this combined perfusion protocol.

In our practice, we apply viability criteria that are considerably broader than the classical, generally accepted standards. We believe that the sustained downward trend in lactate levels – rather than the absolute value

at any given time – is a far more meaningful indicator of graft viability. Moreover, we consistently observe that livers with a high degree of steatosis demonstrate a delayed lactate peak.

The IFLI stage is particularly critical, as any disruption in allograft perfusion can immediately convert the preservation strategy into one involving warm ischemia. Nevertheless, when the standard protocol for implantation under continuous normothermic perfusion is strictly followed, IFLI becomes a routine and reproducible method. The prolonged implantation time in Case 1 (70 minutes) was attributable to the recipient's anatomical features and technical difficulties associated with forming the caval anastomosis.

In all cases, we used the caval reconstruction with preservation of the IVC, creating a hepato-caval anastomosis between the suprahepatic IVC of the graft and a common cuff of the recipient's hepatic veins, following the technique of A. Tzakis. The classical approach, which includes complete replacement of the recipient's IVC, necessitates formation of the lower caval anastomosis only after graft reperfusion, because a cannula remains positioned in the subhepatic IVC to drain perfusate into the cardiotomy reservoir. Similarly, a modified implantation technique using IVC preservation as proposed by J. Belghitti appears impractical in the context of continuous perfusion, as complete isolation of the cavotomy field would disrupt outflow of perfusate through the IVC of the graft into the cardiotomy reservoir.

When preparing the graft for implantation, it is essential to retain an adequate length of the suprahepatic segment of the IVC above the vascular clamp to ensure proper anastomotic construction. Insufficient tissue may result in suture breakage and inadequate alignment of the vascular edges, whereas excessive wall length may create an overly long venous segment, increasing the risk of kinking or bending.

An important observation in our series is the discrepancy between the pathomorphological findings from post-perfusion and post-reperfusion biopsies and the favorable postoperative clinical course in both recipients. Despite diffuse–focal and subtotal hepatocyte necrosis, intraparenchymal and subcapsular hemorrhages, and inflammatory infiltration, the only criterion for early allograft dysfunction that was met was the elevation of cytolytic enzymes (AST and ALT) on POD 1. Given the rapid decline in their levels on subsequent days – and therefore the relatively low AUC – we propose, as previously noted, that these early enzyme surges are more likely attributable to the rapid entry of a large volume (>500 mL) of aminotransferase-rich perfusate into the systemic circulation during reperfusion ("bolus effect") rather than to extensive IRI of the graft itself.

Notably, neither recipient developed graft-specific complications typically expected with such a pathomorphological profile – such as primary graft non-function or severe early allograft dysfunction [40, 41].

In all cases, we performed an incisional (marginal) biopsy of the liver allograft. Several studies have shown that this technique provides a larger volume of tissue and can better detect – or even overestimate – the extent of pathomorphological processes compared with puncture (fine-needle) biopsy [34, 35, 37]. The main limitation of incisional biopsy is that the obtained fragment is taken from a marginal subcapsular area, where fibrosis and other alterations may be more pronounced than in deeper regions of the graft. This may lead to overdiagnosis and inaccurate assessment of the true prevalence of pathological processes [34–37]. For example, histologic examination of zones where the graft comes into contact with the perfusion container may reveal changes consistent with diffuse compression necrosis of hepatocytes rather than representing a widespread process throughout the parenchyma. Importantly, compression necrosis itself does not appear to impair allograft function or influence immediate postoperative outcomes [38, 39].

The relationship between pathomorphological findings and clinical outcomes under conditions of dynamic perfusion preservation requires further research to determine the optimal biopsy technique and to clarify its role in predicting postoperative outcomes.

Overall, IFLI combined with the DHOPE-COR-NMP protocol appears to be a promising strategy for dynamic preservation and implantation of liver allografts from extended-criteria, high-risk donors. Larger studies are needed to better define the potential limitations of this technique and its place within the current landscape of perfusion technologies.

The authors declare no conflict of interest.

REFERENCES

1. *Langone AJ, Helderman JH*. Disparity between solid-organ supply and demand. *N Engl J Med*. 2003 Aug 14; 349 (7): 704–706. doi: 10.1056/NEJMe038117.
2. *Kwong AJ, Kim WR, Lake JR, Schladt DP, Schnellinger EM, Gauntt K et al.* OPTN/SRTR 2022 Annual Data Report: Liver. *Am J Transplant*. 2024 Feb; 24 (2S1): S176–S265. doi: 10.1016/j.ajt.2024.01.014. PMID: 38431359.
3. *Moein M, Bahreini A, Razavi A, Badie S, Coyle S, Abedini M et al.* A Review of Long-Term Outcomes of Liver Transplantation Using Extended Criteria Donors in the United States. *J Surg Res*. 2025 Feb; 306: 561–569. doi: 10.1016/j.jss.2024.12.055.
4. *Feng S, Goodrich NP, Bragg-Gresham JL, Dykstra DM, Punch JD, DebRoy MA et al.* Characteristics associated with liver graft failure: the concept of a donor risk index. *Am J Transplant*. 2006 Apr; 6 (4): 783–790. doi: 10.1111/j.1600-6143.2006.01242.x. Erratum in: *Am J Transplant*. 2018 Dec; 18 (12): 3085. doi: 10.1111/ajt.15155.

5. *Zhang T, Dunson J, Kanwal F, Galvan NTN, Vierling JM, O'Mahony C et al.* Trends in Outcomes for Marginal Allografts in Liver Transplant. *JAMA Surg*. 2020 Aug 5; 155 (10): 926–932. doi: 10.1001/jamasurg.2020.2484. Epub ahead of print. Erratum in: *JAMA Surg*. 2020 Oct 1; 155 (10): 1002. doi: 10.1001/jamasurg.2020.4315.
6. *Mergental H, Laing RW, Kirkham AJ, Clarke G, Boteon YL, Barton D et al.* Discarded livers tested by normothermic machine perfusion in the VITTAL trial: Secondary end points and 5-year outcomes. *Liver Transpl*. 2024 Jan 1; 30 (1): 30–45. doi: 10.1097/LVT.0000000000000270.
7. *Dutkowski P, Polak WG, Muiesan P, Schlegel A, Verhoeven CJ, Scalera I et al.* First Comparison of Hypothermic Oxygenated PErfusion Versus Static Cold Storage of Human Donation After Cardiac Death Liver Transplants: An International-matched Case Analysis. *Ann Surg*. 2015 Nov; 262 (5): 764–770; discussion 770–771. doi: 10.1097/SLA.0000000000001473.
8. *Van Rijn R, Schurink IJ, de Vries Y, van den Berg AP, Cortes Cerisuelo M, Darwish Murad S et al.* Hypothermic Machine Perfusion in Liver Transplantation – A Randomized Trial. *N Engl J Med*. 2021 Apr 15; 384 (15): 1391–1401. doi: 10.1056/NEJMoa2031532.
9. *Gruttadauria S, Vella I, Calamia S, Li Petri S, Accardo C, Pagano D, di Francesco F.* Liver Transplantation After *Ex-Vivo* Normothermic Machine Perfusion: A No-Recooling Technique With Room-Temperature Albumin Flush. *ASAIO J*. 2025 Jul 31. Online ahead of print. doi: 10.1097/MAT.0000000000002516.
10. *Chen Z, Hong X, Huang S, Wang T, Ma Y, Guo Y et al.* Continuous Normothermic Machine Perfusion for Renovation of Extended Criteria Donor Livers Without Recooling in Liver Transplantation: A Pilot Experience. *Front Surg*. 2021 May 24; 8: 638090. doi: 10.3389/fsurg.2021.638090.
11. *Chen Z, Wang T, Chen C, Zhao Q, Ma Y, Guo Y et al.* Transplantation of Extended Criteria Donor Livers Following Continuous Normothermic Machine Perfusion Without Recooling. *Transplantation*. 2022 Jun 1; 106 (6): 1193–1200. doi: 10.1097/TP.0000000000003945.
12. *Van Leeuwen OB, Bodewes SB, Lantinga VA, Haring MPD, Thorne AM, Brüggenwirth IMA et al*. Sequential hypothermic and normothermic machine perfusion enables safe transplantation of high-risk donor livers. *Am J Transplant*. 2022 Jun; 22 (6): 1658–1670. doi: 10.1111/ajt.17022.
13. *Cirelli R, Thorne AM, van Leeuwen OB, Lascaris B, Lantinga VA, Bodewes SB et al.* Transplantation of Severely Steatotic Liver Grafts After Machine Perfusion Remains a Risky Challenge. *Clin Transplant*. 2025 Aug; 39 (8): e70260. doi: 10.1111/ctr.70260.
14. *Patrono D, De Stefano N, Vissio E, Apostu AL, Petronio N, Vitelli G et al.* How to Preserve Steatotic Liver Grafts for Transplantation. *J Clin Med*. 2023 Jun 12; 12 (12): 3982. doi: 10.3390/jcm12123982.
15. *Patrono D, De Carlis R, Gambella A, Farnesi F, Podestà A, Lauterio A et al.* Viability assessment and transplantation of fatty liver grafts using end-ischemic normothermic machine perfusion. *Liver Transpl*. 2023 May 1; 29 (5): 508–520. doi: 10.1002/lt.26574.
16. *Guo Z, Zhao Q, Jia Z, Huang C, Wang D, Ju W et al.* A randomized-controlled trial of ischemia-free liver transplantation for end-stage liver disease. *J Hepatol*. 2023 Aug; 79 (2): 394–402. doi: 10.1016/j.jhep.2023.04.010.
17. *Bral M, Dajani K, Leon Izquierdo D, Bigam D, Kneteman N, Ceresa CDL et al.* A Back-to-Base Experience of Human Normothermic *Ex Situ* Liver Perfusion: Does the Chill Kill? *Liver Transpl*. 2019 Jun; 25 (6): 848–858. doi: 10.1002/lt.25464.
18. *Parente A, Tirotta F, Pini A, Eden J, Dondossola D, Manzia TM et al.* Machine perfusion techniques for liver transplantation – A meta-analysis of the first seven randomized-controlled trials. *J Hepatol*. 2023 Nov; 79 (5): 1201–1213. doi: 10.1016/j.jhep.2023.05.027.
19. *Gautier SV, Grudinin NV, Monakhov AR, Boldyrev MA, Bogdanov VK, Bondarenko DM et al*. Combined sequential hypothermic oxygenated and normothermic machine perfusion for liver transplant from an expanded criteria donor: first clinical application in Russia. Russian Journal of Transplantology and Artificial Organs. 2025; 27 (2): 8–22. https://doi.org/10.15825/1995-1191-2025-2-8-22.
20. *Olthoff KM, Kulik L, Samstein B, Kaminski M, Abecassis M, Emond J et al.* Validation of a current definition of early allograft dysfunction in liver transplant recipients and analysis of risk factors. *Liver Transpl*. 2010 Aug; 16 (8): 943–949. doi: 10.1002/lt.22091.
21. *Khwaja A.* KDIGO clinical practice guidelines for acute kidney injury. *Nephron Clin Pract*. 2012; 120 (4): c179–c184. doi: 10.1159/000339789.
22. *Al-Freah MAB, McPhail MJW, Dionigi E, Foxton MR, Auzinger G, Rela M et al.* Improving the Diagnostic Criteria for Primary Liver Graft Nonfunction in Adults Utilizing Standard and Transportable Laboratory Parameters: An Outcome-Based Analysis. *Am J Transplant*. 2017 May; 17 (5): 1255–1266. doi: 10.1111/ajt.14230.
23. *Clavien PA, Harvey PR, Strasberg SM.* Preservation and reperfusion injuries in liver allografts. An overview and synthesis of current studies. *Transplantation*. 1992 May; 53 (5): 957–978. doi: 10.1097/00007890-199205000-00001.
24. *Rampes S, Ma D*. Hepatic ischemia-reperfusion injury in liver transplant setting: mechanisms and protective strategies. *J Biomed Res*. 2019 Jul 28; 33 (4): 221–234. doi: 10.7555/JBR.32.20180087.
25. *Wang L, Li J, He S, Liu Y, Chen H, He S et al.* Resolving the graft ischemia-reperfusion injury during liver transplantation at the single cell resolution. *Cell Death Dis*. 2021 Jun 8; 12 (6): 589. doi: 10.1038/s41419-021-03878-3.
26. *He X, Guo Z, Zhao Q, Ju W, Wang D, Wu L et al.* The first case of ischemia-free organ transplantation in humans: A proof of concept. *Am J Transplant*. 2018 Mar; 18 (3): 737–744. doi: 10.1111/ajt.14583.
27. *Ju W, Chen Z, Zhao Q, Zhang Y, Huang C, Wang L et al.* Non-re-cooling implantation of marginal liver graft after machine perfusion: report of a case. *Ann Transl Med*. 2020 Nov; 8 (21): 1465. doi: 10.21037/atm-20-2774.

28. *Vodkin I, Kuo A.* Extended Criteria Donors in Liver Transplantation. *Clin Liver Dis*. 2017 May; 21 (2): 289–301. doi: 10.1016/j.cld.2016.12.004.
29. *Oosterlee A, Rahmel A*. Eurotransplant International Foundation Annual Report 2008. April 27, 2011.
30. *Al-Kurd A, Kitajima T, Delvecchio K, Tayseer Shamaa M, Ivanics T, Yeddula S et al*. Short recipient warm ischemia time improves outcomes in deceased donor liver transplantation. *Transpl Int*. 2021 Aug; 34 (8): 1422–1432. doi: 10.1111/tri.13962.
31. *Sakamoto A, Sakamoto K, Hikida T, Ito C, Iwata M, Shine M et al.* Prolonged warm ischemia time in the recipient is associated with post-transplant biliary stricture following living-donor liver transplantation. *Surg Today*. 2024 Oct; 54 (10): 1193–1200. doi: 10.1007/s00595-024-02823-z.
32. *Aggarwal S, Kang Y, Freeman JA, Fortunato FL, Pinsky MR.* Postreperfusion syndrome: cardiovascular collapse following hepatic reperfusion during liver transplantation. *Transplant Proc*. 1987 Aug; 19 (4 Suppl 3): 54–55.
33. *Hilmi I, Horton CN, Planinsic RM, Sakai T, Nicolau-Raducu R, Damian D et al.* The impact of postreperfusion syndrome on short-term patient and liver allograft outcome in patients undergoing orthotopic liver transplantation. *Liver Transpl*. 2008 Apr; 14 (4): 504–508. doi: 10.1002/lt.21381.
34. *Padoin AV, Mottin CC, Moretto M, Berleze D, Kupski C, Glock L et al*. A comparison of wedge and needle hepatic biopsy in open bariatric surgery. *Obes Surg*. 2006 Feb; 16 (2): 178–182. doi: 10.1381/096089206775565159.
35. *Rawlins SR, Mullen CM, Simon HM, Kim T, Landas SK, Walser MS, Levine RA.* Wedge and needle liver biopsies show discordant histopathology in morbidly obese patients undergoing Roux-en-Y gastric bypass surgery. *Gastroenterol Rep (Oxf)*. 2013 Jul; 1 (1): 51–57. doi: 10.1093/gastro/got006.
36. *Kimbrell TL, Milovancev M, Olsen R, Löhr CV*. Comparison of diagnostic accuracy of laparoscopic 3 mm and 5 mm cup biopsies to wedge biopsies of canine livers. *J Vet Intern Med*. 2018 Mar; 32 (2): 701–706. doi: 10.1111/jvim.15054.
37. *Neuberger J, Patel J, Caldwell H, Davies S, Hebditch V, Hollywood C et al.* Guidelines on the use of liver biopsy in clinical practice from the British Society of Gastroenterology, the Royal College of Radiologists and the Royal College of Pathology. *Gut*. 2020 Aug; 69 (8): 1382–1403. doi: 10.1136/gutjnl-2020-321299.
38. *Martin JL, Rhodes F, Upponi S, Udeaja Y, Swift L, Fear C et al.* Localized Liver Injury During Normothermic *Ex Situ* Liver Perfusion Has No Impact on Short-term Liver Transplant Outcomes. *Transplantation*. 2024 Jun 1; 108 (6): 1403–1409. doi: 10.1097/TP.0000000000004970.
39. *Eshmuminov D, Becker D, Bautista Borrego L, Hefti M, Schuler MJ, Hagedorn C et al.* An integrated perfusion machine preserves injured human livers for 1 week. *Nat Biotechnol*. 2020 Feb; 38 (2): 189–198. https://doi.org/10.1038/s41587-019-0374-x.
40. *Hartog H, Hann A, Perera MTPR*. Primary Nonfunction of the Liver Allograft. *Transplantation*. 2022 Jan 1; 106 (1): 117–128. doi: 10.1097/TP.0000000000003682.
41. *Limia ME, Liu XL, Yu J, Byrnes K.* Primary Non-Function of Hepatic Allograft With Preexisting Microvesicular Steatosis/Foamy Degeneration and Mild Large-Droplet Macrovesicular Steatosis. *Gastroenterology Res*. 2024 Feb; 17 (1): 37–40. doi: 10.14740/gr1687.

The article was submitted to the journal on 11.08.2025

DOI: 10.15825/1995-1191-2025-4-24-30

OPTIMIZING MAINTENANCE IMMUNOSUPPRESSIVE THERAPY AFTER LIVER TRANSPLANTATION

O.A. Gerasimova[1], N.V. Marchenko[1, 2], I.I. Tileubergenov[1], V.N. Zhuykov[1]

[1] Granov Russian Research Center of Radiology and Surgical Technologies, St. Petersburg, Russian Federation

[2] St. Petersburg State University, St. Petersburg, Russian Federation

Objective: to justify the rational selection of maintenance immunosuppressive therapy following liver transplantation (LT). **Materials and methods.** The study included 42 recipients of deceased donor liver grafts, observed for periods ranging from 1 month to 15 years LT. The mean age at transplantation was 49.4 ± 7.0 years. All patients received everolimus in combination with low-dose extended-release tacrolimus. Indications for everolimus therapy were tacrolimus-induced nephrotoxicity (n = 13), history of hepatocellular carcinoma (HCC, n = 21), and development of *de novo* malignancies at non-hepatic sites (n = 8). Target trough concentrations were 2–3 ng/mL for tacrolimus and 3–8 ng/mL for everolimus. Adverse events of everolimus and serum cholesterol dynamics were assessed at 12, 36, 60, and 120 months after conversion to this regimen, and compared with data from 20 randomly selected recipients maintained on tacrolimus monotherapy. Estimated glomerular filtration rate (eGFR) was calculated using the CKD-EPI equation at the same time points. Liver stiffness (kPa) was measured by transient elastography once at study completion. In patients with a history of HCC, baseline alpha-fetoprotein (AFP) levels were also taken into account. **Results.** Long-term use of everolimus with low-dose extended-release tacrolimus did not impair renal function (baseline GFR: 84.13 ± 16.70 mL/min/1.73 m^2; final GFR: 84.99 ± 21.30 mL/min/1.73 m^2). However, serum cholesterol levels were consistently higher compared with tacrolimus monotherapy (12 months: 5.7 ± 0.91 *vs* 4.01 ± 1.21 mmol/L; 120 months: 5.52 ± 1.51 *vs* 4.58 ± 0.72 mmol/L). Among 21 patients with a history of HCC, recurrence or progression occurred in 6 patients (30%), which was associated with elevated baseline AFP levels prior to LT (429.2 ± 306.9 U/mL; Z = 4.2, p = 0.0001). Liver stiffness, assessed once at the endpoint of the retrospective study, averaged 4.8 ± 1.8 kPa, corresponding to F0–1 by the METAVIR scale. **Conclusion.** Long-term maintenance therapy with everolimus combined with low-dose extended-release tacrolimus after LT is safe and helps mitigate calcineurin inhibitor (CNI) nephrotoxicity. Nevertheless, this regimen does not prevent recurrent HCC, which depends on the biological activity of the tumor.

Keywords: liver transplantation, everolimus, extended-release tacrolimus, glomerular filtration rate, hypercholesterolemia, liver stiffness, alpha-fetoprotein.

INTRODUCTION

For decades, progress in transplantation has been closely linked to the development of new immunosuppressive drugs, such as cyclosporine, tacrolimus, sirolimus, mycophenolate mofetil, thymoglobulin, and interleukin-2 receptor antagonists. In recent years, however, clinical trials of new molecules have faced setbacks, while the growth of the generic market has provided economic benefits but also introduced challenges in selecting and alternating between brands, some of which remain insufficiently studied [1]. This does not apply to everolimus and mycophenolic acid, which have undergone rigorous clinical trials and are recognized as fully effective immunosuppressants [2].

Calcineurin inhibitors (CNIs), particularly tacrolimus, remain the cornerstone of maintenance immunosuppression following liver transplantation (LT) [3, 4]. Nevertheless, the optimal regimen for long-term maintenance remains uncertain, as meta-analyses have not shown clear superiority of any single drug combination [5].

A major limitation of CNIs is the well-documented risk of chronic nephrotoxicity with prolonged use, which negatively affects long-term survival [3, 6]. One preventive strategy is minimizing tacrolimus exposure in combination with the mammalian target of rapamycin (mTOR) inhibitors [3, 7]. In addition, everolimus, due to its antiproliferative properties, is often prescribed for LT recipients with a history of hepatocellular carcinoma (HCC) or *de novo* extrahepatic malignancies [8]. As a result, a distinct cohort of patients is emerging for whom a maintenance regimen combining low-dose CNIs with mTOR inhibitors is preferred.

Based on these findings and previous studies confirming the efficacy of extended-release tacrolimus after LT, the authors analyzed their single-center experience with

Corresponding author: Olga Gerasimova. Address: 70, Leningradskaya str., Pesochnyy, St. Petersburg, 197758, Russian Federation. Phone: (812) 439-66-40. E-mail: ren321@mail.ru, oa_gerasimova@rrcrst.ru

the long-term use of low-dose extended-release tacrolimus in combination with everolimus. As such studies remain limited [9, 10], evaluating the effectiveness of this regimen may provide important evidence for improving long-term survival after LT. The aim of this study was to substantiate a rational approach to maintenance immunosuppression in the late post-transplant period.

MATERIALS AND METHODS

A retrospective analysis was conducted on 42 LT recipients under follow-up at an outpatient transplant center, with observation periods ranging from 1 to 15 years post-transplant. The cohort included 16 men and 26 women, with a mean age at LT of 49.4 ± 7.0 years. Data collection was completed by the end of 2023. Indications for everolimus initiation included early signs of nephrotoxicity in 13 patients, a history of HCC in 21 patients, and the presence of *de novo* extrahepatic malignancies in 8 patients (Fig. 1). Everolimus was introduced no earlier than 1 month after LT. The initial daily dose was 3 mg, titrated to maintain a target trough concentration of 3–8 ng/ml. Tacrolimus trough levels were maintained at approximately 2 ng/ml. Tacrolimus and everolimus concentrations were monitored using an automated biochemistry analyzer.

The effectiveness of immunosuppressive therapy was evaluated using key biochemical parameters: bilirubin, alanine transaminase (ALT), aspartate transaminase (AST), alkaline phosphatase, gamma-glutamyltransferase (GGT), creatinine, and urea. Proteinuria was assessed, and glomerular filtration rate (GFR) was calculated using the CKD-EPI formula (ml/min/1.73 m^2).

Total blood cholesterol levels were retrospectively analyzed and compared with a random sample of 20 LT recipients who received standard-dose extended-release tacrolimus monotherapy without evidence of graft dysfunction. Alpha-fetoprotein (AFP) levels were determined preoperatively in patients with HCC.

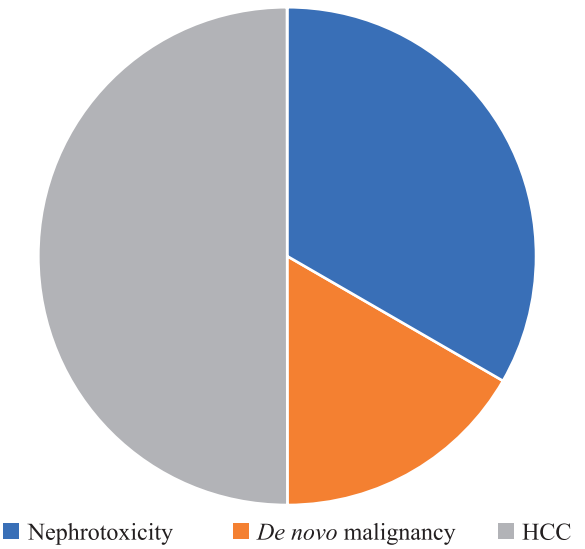

Fig. 1. Distribution of patients according to the indication for conversion to everolimus

At the end of follow-up, liver stiffness was measured in kilopascals (kPa) using a Fibroscan-430Mini transient elastography device.

Statistical analysis was performed using Statistica for Windows, version 14. Both descriptive and nonparametric methods were applied. Intergroup differences were evaluated using the Mann–Whitney U test, and correlations within the study group were assessed using Spearman's rank coefficient. Results were considered statistically significant at $p < 0.05$.

RESULTS

At target concentrations of everolimus (3–8 ng/mL) and tacrolimus (≤3 ng/mL), the mean maintenance doses at the end of the follow-up period were 2.75 ± 0.4 mg/day and 2.1 ± 0.9 mg/day, respectively (Table 1).

Long-term monitoring of liver graft function showed no significant deviations from normal values for bilirubin, ALT, or AST at 12, 36, 60, and 120 months of therapy with this immunosuppressive regimen. Recorded adverse events were not life-threatening for either the graft or recipients and were effectively managed with supportive measures, such as iron supplementation for anemia and dose adjustments of immunosuppressive agents (Fig. 2).

The most frequent complication was hypercholesterolemia, observed in 28.5% of patients. Mean total cholesterol did not significantly change over time, amounting to 5.69 ± 1.19 mmol/L at baseline and 5.52 ± 1.51 mmol/L after 10 years of combined therapy (Fig. 4). However, when compared with a random control group of 20 LT recipients maintained on long-term tacrolimus monotherapy with normal graft function, cholesterol levels were consistently and significantly higher in the study group throughout the entire follow-up (Table 2), thus confirming the negative effect of everolimus on blood cholesterol levels.

All patients with hypercholesterolemia were advised long-term statin therapy. Nevertheless, some declined treatment, which contributed to persistently unsatisfactory overall cholesterol levels. In contrast, in a subgroup of 10 patients who adhered to statin therapy, cholesterol remained within acceptable limits, averaging 4.73 ± 0.31 mmol/L after 10 years.

Table 1

Average maintenance doses and target immunosuppressant concentrations

Drug	Starting dose	Average maintenance dose	Target concentration
Everolimus	3 mg	2.75 ± 0.40 mg/day	3–8 ng/mL
Tacrolimus		2.10 ± 0.90 mg/day	2–3 ng/mL

Over a 12–120 month follow-up, mean creatinine levels and estimated GFR (eGFR) remained within acceptable limits (Fig. 3). After one year of combined everolimus and low-dose extended-release tacrolimus therapy, the mean eGFR was 84.13 ± 16.70 mL/min/1.73 m^2. At 3 and 5 years, values were 91.15 ± 14.17 and 84.92 ± 17.72 mL/min/1.73 m^2, respectively; among patients reaching the 10-year threshold, mean eGFR was 84.99 ± 21.30 mL/min/1.73 m^2.

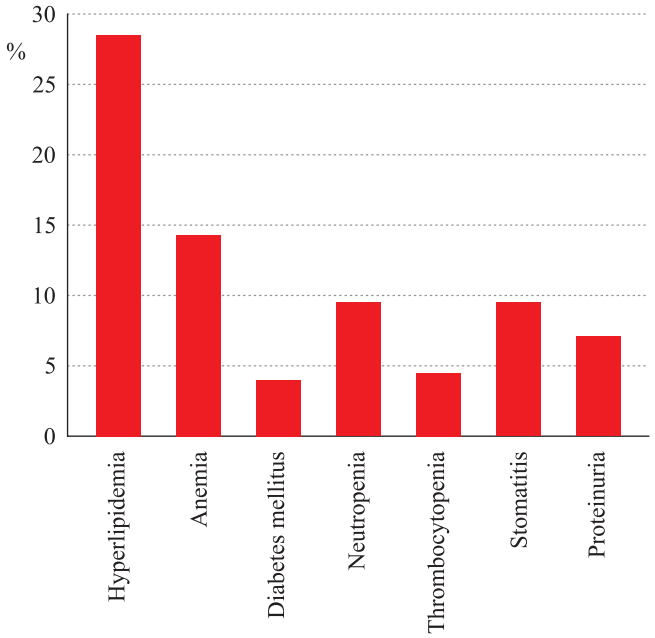

Fig. 2. Proportion of adverse events during long-term therapy with everolimus combined with low-dose extended-release tacrolimus

Among the 21 patients with a history of HCC treated with this regimen, recurrence or progression occurred in 6 patients (30%) at various time points post-LT. The mean pre-LT AFP level in this subgroup was 429.2 ± 306.9 IU/mL (range 3.6–1500 IU/mL). Recurrence was significantly associated with baseline AFP concentration (Z = 4.2, p = 0.0001).

Transient elastography performed at the end of follow-up provided indirect evidence of regimen effectiveness. The mean liver stiffness was 4.8 ± 1.8 kPa, corresponding to METAVIR stages F0–F1, indicating no significant fibrosis progression.

Table 2

Comparative dynamics of blood cholesterol levels in liver transplant recipients under different immunosuppressive regimens (p < 0.05*, p < 0.01)**

Regimen / Duration	12 months	36 months	60 months	120 months
Tacrolimus + Everolimus	5.7 ± 0.91*	5.52 ± 1.32**	5.4 ± 1.38*	5.52 ± 1.51**
Tacrolimus alone	4.01 ± 1.21	4.11 ± 0.82	4.34 ± 0.90	4.58 ± 0.72

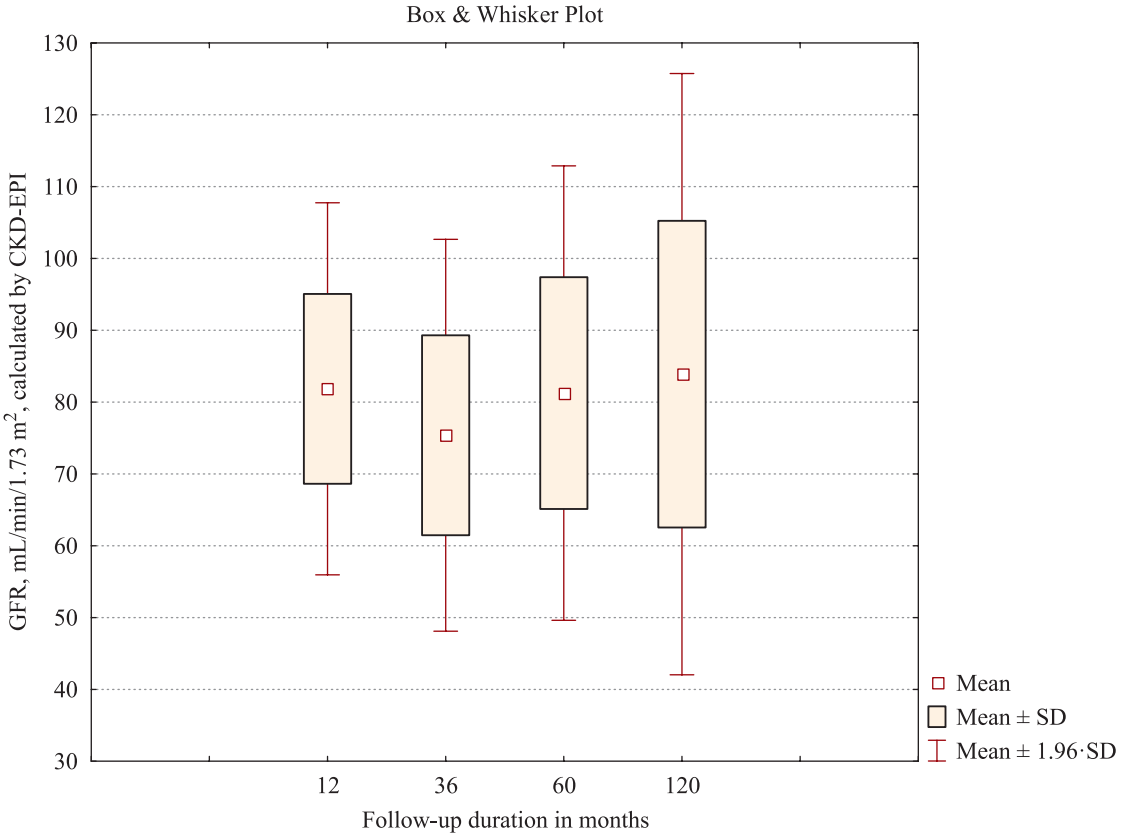

Fig. 3. Dynamics of renal function in patients receiving low-dose extended-release tacrolimus with everolimus

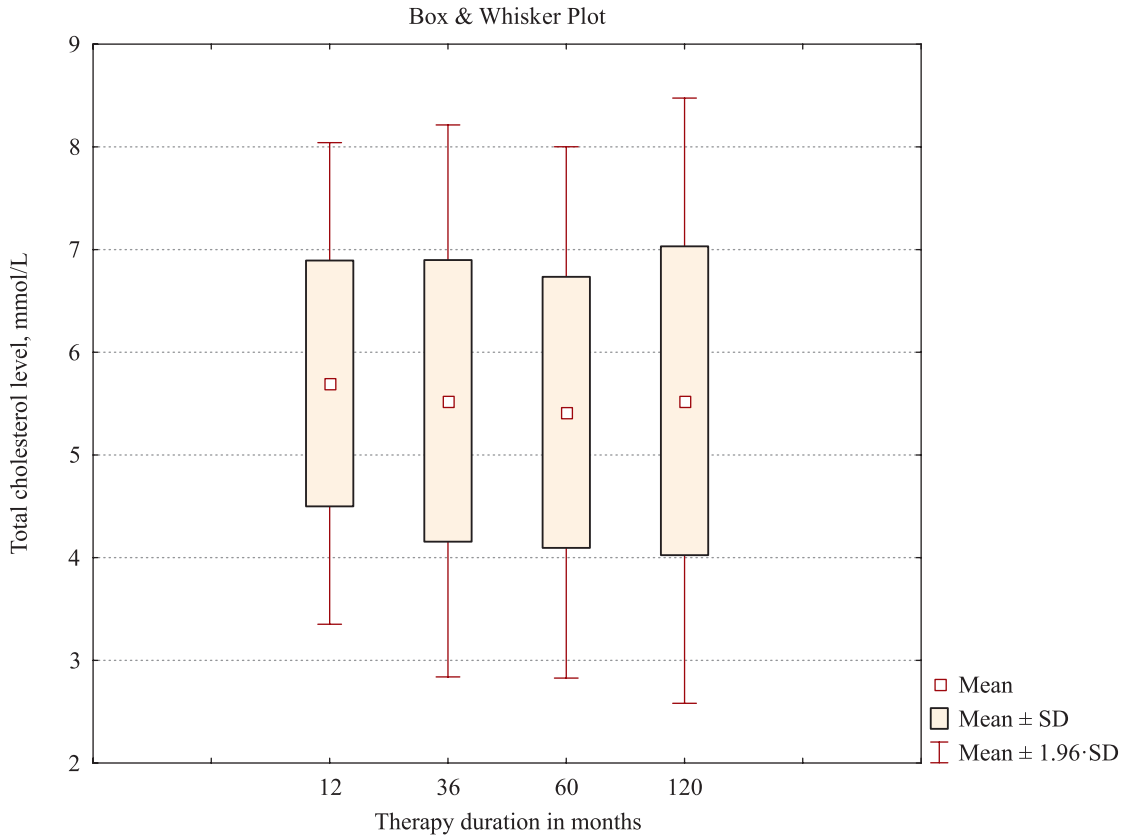

Fig. 4. Dynamics of total serum cholesterol in patients receiving long-term therapy with everolimus and low-dose extended-release tacrolimus

DISCUSSION

In a review study, Pavel Trunecka [2] analyzed publications addressing late conversion from twice-daily tacrolimus to its extended-release formulation. The findings showed that switching to extended-release tacrolimus is justified, as it improves dosing convenience, enhances adherence, and contributes to better patient survival. In the present cohort, however, everolimus was used as the second immunosuppressive component, necessitating twice-daily dosing, which diminished the compliance-related advantage of once-daily tacrolimus. Nevertheless, long-term use of the extended-release formulation contributed to more stable blood concentrations, consistent with observations reported by other investigators [11].

Based on data from two randomized trials [12] that included 772 liver transplant recipients – 488 from deceased donors (H2304) and 284 from living-related donors (H2307) – pooled analyses were conducted to evaluate the efficacy and safety of everolimus with low-dose tacrolimus versus standard-dose tacrolimus over 24 months of follow-up. The two regimens demonstrated comparable overall efficacy when assessed by the incidence of biopsy-confirmed rejection, graft loss, or death (9.8% vs. 10.8%; p = 0.641). Importantly, renal outcomes favored the everolimus regimen, with a smaller decline in eGFR at 24 months (–8.37 vs. –13.40 mL/min/1.73 m^2; p = 0.001).

In our study, which featured a considerably longer follow-up period but included a smaller cohort, no decline in renal function was observed. Twelve months after conversion, mean eGFR was 84.13 ± 16.70 mL/min/1.73 m^2, and after ≥120 months on reduced-dose extended-release tacrolimus plus everolimus, mean eGFR remained stable at 84.99 ± 21.30 mL/min/1.73 m^2. This favorable outcome is most likely attributable to the small patient sample and the benefit of close, individualized monitoring.

Regarding HCC recurrence, previous studies in patients outside the Milan criteria suggested a trend toward lower recurrence with everolimus (5.9% [1/17] vs. 23.1% [6/26], p = 0.215), though the difference did not reach statistical significance. For patients within the Milan criteria, recurrence rates were comparable, regardless of pre-transplant AFP levels [12]. The authors of this comparative study concluded that further long-term studies are needed.

In our cohort, recurrence was clearly influenced by AFP concentration prior to LT. While values ranged widely – from normal to 1500 IU/mL – the mean AFP was 429.2 ± 306.9 IU/mL. Importantly, AFP levels >400 IU/mL, a threshold generally recognized as conferring a high risk of HCC recurrence [13], were strongly associated with post-LT relapse (Z = 4.2, p = 0.0001).

A recent review by S. Poudel et al. [14] summarized current approaches to maintenance immunosuppression

after LT. To minimize toxicity, monotherapy with either CNIs or mTOR inhibitors is recommended in clinically stable patients. In the presence of renal dysfunction or proteinuria, modification of therapy is advised – most often by combining an mTOR inhibitor with a low-dose CNI. In the late post-transplant period, efforts are increasingly directed toward minimizing or even discontinuing immunosuppression, particularly to reduce the risk of HCC recurrence. However, this strategy carries a substantial risk of irreversible rejection and graft loss. Against this background, the regimen applied in our study can be regarded as a rational choice.

CONCLUSION

Our experience with a maintenance immunosuppressive regimen combining low-dose extended-release tacrolimus with everolimus suggests that this approach is safe and effective, supporting stable graft function and preserving renal function in long-term LT recipients. The most frequent complication associated with prolonged everolimus therapy was hypercholesterolemia, which can be successfully managed with modern lipid-lowering drugs.

However, this regimen does not reliably prevent HCC recurrence after LT. It is evident that the biological activity of the tumor and adherence to transplant center selection criteria are decisive prognostic factors. The possibility that higher prophylactic doses of everolimus may provide additional benefit remains an open question and warrants further investigation.

The authors declare no conflict of interest.

REFERENCES

1. *Van Gelder T*. ESOT Advisory Committee on Generic Substitution. European Society for Organ Transplantation Advisory Committee recommendations on generic substitution of immunosuppressive drugs. *Transpl Int*. 2011 Dec; 24 (12): 1135–1141. doi: 10.1111/j.1432-2277.2011.01378.x. PMID: 22032583.
2. *Trunečka P*. Once-daily tacrolimus in liver transplantation: a ‘me-too drug’, or a therapeutic advantage. *Curr Opin Organ Transplant*. 2017 Apr; 22 (2): 118–122. doi: 10.1097/MOT.0000000000000387. PMID: 28079558.
3. *Keating GM, Lyseng-Williamson KA*. Everolimus: a guide to its use in liver transplantation. *BioDrugs*. 2013 Aug; 27 (4): 407–411. doi: 10.1007/s40259-013-0041-6. PMID: 23696253.
4. *Abaalkhail FA, Al Sebayel MI, Shagrani MA, O’Hali WA, Almasri NM, Alalwan AA et al*. Clinical Practice Guidelines for Liver Transplantation in Saudi Arabia. *Saudi Med J*. 2021 Sep; 42 (9): 927–968. doi: 10.15537/smj.2021.42.9.20210126. PMID: 34470833; PMCID: PMC9280503.
5. *Rodríguez-Perálvarez M, Guerrero-Misas M, Thorburn D, Davidson BR, Tsochatzis E, Gurusamy KS*. Maintenance immunosuppression for adults undergoing liver transplantation: a network meta-analysis. *Cochrane Database Syst Rev*. 2017 Mar 31; 3 (3): CD011639. doi: 10.1002/14651858.CD011639.pub2.
6. *De Simone P, Fagiuoli S, Cescon M, De Carlis L, Tisone G, Volpes R, Cillo U*. Consensus Panel. Use of Everolimus in Liver Transplantation: Recommendations From a Working Group. *Transplantation*. 2017 Feb; 101 (2): 239–251. doi: 10.1097/TP.0000000000001438.
7. *Di Maira T, Little EC, Berenguer M.* Immunosuppression in liver transplant. *Best Pract Res Clin Gastroenterol*. 2020 Jun-Aug; 46–47: 101681. doi: 10.1016/j.bpg.2020.101681. Epub 2020 Sep 11. PMID: 33158467.
8. *Cillo U, De Carlis L, Del Gaudio M, De Simone P, Fagiuoli S, Lupo F et al.* Immunosuppressive regimens for adult liver transplant recipients in real-life practice: consensus recommendations from an Italian Working Group. *Hepatol Int*. 2020 Dec; 14 (6): 930–943. doi: 10.1007/s12072-020-10091-5. Erratum in: *Hepatol Int*. 2021 Jun; 15 (3): 831. PMID: 33099753; PMCID: PMC7803715.
9. *Mulder MB, van Hoek B, van den Berg AP, Polak WG, Alwayn IPJ, de Jong KP et al.* Three-year results of renal function in liver transplant recipients on low-dose sirolimus and tacrolimus: a multicenter, randomized, controlled trial. *Liver Transpl*. 2023 Feb 1; 29 (2): 184–195. doi: 10.1097/LVT.0000000000000003. Epub 2023 Jan 3. PMID: 36668691.
10. *Trunečka P, Klempnauer J, Bechstein WO, Pirenne J, Friman S, Zhao A et al.* DIAMOND† study group. Renal Function in *De Novo* Liver Transplant Recipients Receiving Different Prolonged-Release Tacrolimus Regimens – The DIAMOND Study. *Am J Transplant*. 2015 Jul; 15 (7): 1843–1854. doi: 10.1111/ajt.13182. PMID: 25707487; PMCID: PMC5024030.
11. *Dumortier J, Duvoux C, Dubel L, Bazin F, Houssel-Debry P*. A Multicenter, Prospective, Observational Study of Conversion from Twice-Daily Immediate-Release to Once-Daily Prolonged-Release Tacrolimus in Liver Transplant Recipients in France: The COBALT Study. *Ann Transplant*. 2019 Aug 27; 24: 506–516. doi: 10.12659/AOT.916041. PMID: 31451681; PMCID: PMC6728630.
12. *Lee SG, Jeng LB, Saliba F, Singh Soin A, Lee WC, De Simone P et al*. Efficacy and safety of everolimus with reduced tacrolimus in liver transplant recipients: 24-month results from the pooled analysis of 2 randomized controlled trials. *Transplantation*. 2021 Jul 1; 105 (7): 1564–1575. doi: 10.1097/TP.0000000000003394. PMID: 33741847; PMCID: PMC8221719.
13. *Reig M, Forner A, Rimola J, Ferrer-Fàbrega J, Burrel M, Garcia-Criado Á et al.* BCLC strategy for prognosis prediction and treatment recommendation: The 2022 update. *J Hepatol*. 2022 Mar; 76 (3): 681–693. doi: 10.1016/j.jhep.2021.11.018. PMID: 34801630; PMCID: PMC8866082.
14. *Poudel S, Gupta S, Saigal S*. Basics and Art of Immunosuppression in Liver Transplantation. *J Clin Exp Hepatol*. 2024 May-Jun; 14 (3): 101345. doi: 10.1016/j.jceh.2024.101345. PMID: 38450290; PMCID: PMC10912712.

The article was submitted to the journal on 21.02.2025

DOI: 10.15825/1995-1191-2025-4-31-40

EFFECT OF PRE-TRANSPLANT DIALYSIS MODALITY ON OUTCOMES IN THE FIRST TWO YEARS AFTER KIDNEY TRANSPLANTATION

V.A. Berdinsky[1], E.S. Ivanova[1], V.E. Vinogradov[1], N.F. Frolova[1], O.N. Kotenko[1], L.Yu. Artyukhina[1], I.V. Dmitriev[2], P.A. Drozdov[3]

[1] Municipal Clinical Hospital No. 52, Moscow, Russian Federation
[2] Sklifosovsky Research Institute of Emergency Care, Moscow, Russian Federation
[3] Botkin Hospital, Moscow, Russian Federation

Kidney transplantation (KT) is the treatment of choice for patients with end-stage renal disease (ESRD), offering superior survival and quality of life compared with dialysis. Several observational studies have investigated the influence of hemodialysis (HD) and peritoneal dialysis (PD) on post-transplant outcomes. **Objective:** to assess the effect of dialysis modality prior to KT on outcomes during the first two years after transplantation. **Materials and methods.** The study included 95 KT recipients, divided into two groups: (1) patients previously treated with PD (n = 45) and (2) patients previously treated with HD (n = 50). The groups were comparable in age, dialysis duration, and immunosuppressive therapy regimens. The mean follow-up period was 19.4 ± 6.4 months. **Results.** Delayed graft function (DGF) occurred less frequently in the PD group (17.8%) compared with the HD group (34%), although the difference did not reach statistical significance (p = 0.08). Patients in the HD group required significantly more rehospitalizations, with a median of 2.24 [1–3] compared to 1.9 [0–2.5] in the PD group (p = 0.01). Infectious complications were also more common among HD patients (62% *vs* 42%, p = 0.005). In particular, bacterial infections occurred significantly more often in the HD group (63% *vs* 43%, p = 0.0001), whereas viral and fungal infections were detected at similar frequencies in both groups (p > 0.2). The incidence of graft rejection was comparable between groups. Two-year graft survival (91% in PD *vs* 94% in HD, p = 0.8) and patient survival (94% in PD *vs* 96% in HD, p = 0.9) did not differ significantly. Likewise, serum creatinine and daily proteinuria at the end of follow-up showed no statistically significant differences (p = 0.7 and p = 0.3, respectively). **Conclusion.** In this study, patients who received PD prior to transplantation showed more favorable post-transplant outcomes, including a significantly lower frequency of rehospitalizations and infectious complications, as well as a trend toward reduced DGF. However, two-year graft and patient survival were similar between the PD and HD groups.

Keywords: kidney transplantation, peritoneal dialysis, hemodialysis.

INTRODUCTION

Over the past few decades, the number of patients with end-stage renal disease (ESRD) requiring renal replacement therapy (RRT) has increased substantially [1]. Kidney transplantation (KT) remains the preferred treatment option for patients with ESRD, as it offers significant benefits in terms of improved life expectancy, quality of life, and reduced healthcare costs [2].

However, most patients with ESRD do not undergo pre-dialysis KT due to donor organ shortages, delayed referral to nephrologists, and persistent medical and financial barriers. Consequently, initiation of dialysis therapy becomes necessary. Despite extensive research, the relative advantages and disadvantages of different dialysis modalities and their influence on post-transplant outcomes remain subjects of ongoing debate. Because randomized controlled trials comparing dialysis modalities are difficult to conduct, numerous observational studies have investigated the association between hemodialysis (HD) and peritoneal dialysis (PD) with post-transplant outcomes [3–9]. Yet, the results of these studies remain inconclusive.

The majority of published data suggest clinical equivalence between the two dialysis modalities with respect to both short-term outcomes (such as graft function and early complications) and long-term outcomes (including patient survival and cardiovascular events) following KT.

The present study aimed to evaluate the impact of dialysis modality on outcomes during the first two years of the post-transplant period. This paper reports the initial findings obtained within the framework of a new scientific and practical healthcare project, “Application of innovative approaches to extending the donor kidney waiting list, preparing patients for transplantation (including those with thrombotic microangiopathy [TMA]), and managing recipients in the early post-transplant period”.

Corresponding author: Ekaterina Ivanova. Address: 3, Pekhotnaya str., Moscow, 123182, Russian Federation.
Phone: (499) 196-17-94. E-mail: katerineiv@mail.ru

MATERIALS AND METHODS

The study included 95 kidney transplant recipients, 54 men and 41 women, aged 21 to 73 years (mean age: 45.2 ± 12.0 years), who underwent KT between January 2021 and June 2022 and were subsequently followed up at the Moscow Research and Clinical Center of Kidney Transplant Nephrology and Pathology, Municipal Clinical Hospital No. 52.

Exclusion criteria were: repeat kidney transplantation, combined organ transplantation (kidney plus another organ), RRT exceeding 5 years, and conversion between PD and HD.

All patients were stratified into two groups according to the type of RRT prior to transplantation: PD group (45 patients) and HD group (50 patients). In the HD group, the proportion of men was significantly higher than in the PD group (68% vs. 44%, p = 0.02). There were no significant differences between the groups regarding age at transplantation: 45.3 ± 11.9 years in the PD group versus 45.1 ± 12.2 years in the HD group (p = 0.9) (Table 1).

Similarly, the groups did not differ in the duration of RRT prior to KT or in induction and maintenance immunosuppressive therapy (IST). RRT lasted for 15.3 [5.7; 24.9] months in the PD group and 21.6 [9.3; 39.1] months in the HD group (p = 0.08).

Most patients received basiliximab as induction IST (PD – 93%, HD – 94%). All patients were treated with standard triple-drug maintenance IST consisting of a corticosteroid, a calcineurin inhibitor (CNI), and either mycophenolic acid or everolimus. Tacrolimus was the predominant CNI used (PD – 93%, HD – 92%, p = 0.8). Mycophenolic acid was prescribed to all patients in the PD group and to 98% of those in the HD group (p = 0.3), while 2% of HD patients received everolimus instead.

The average follow-up period for patients was 19.4 ± 6.4 months. The study evaluated the frequency of primary and delayed KT function, rehospitalizations, infectious complications, KT rejection, serum creatinine levels, and daily proteinuria (DPU) at the end of the follow-up period. Primary KT function was defined as the absence of a need for dialysis after transplantation, whereas delayed KT function was defined as the requirement for dialysis within 7 days post-transplant.

All patient readmissions following the initial hospitalization for KT were analyzed, excluding those associated with routine procedures such as removal of the PD catheter, removal of the tunneled central venous catheter, removal of the KT ureteral stent, ligation of the arteriovenous fistula, and routine ophthalmologic or gynecologic surgeries.

Infectious complications were included only when they required hospitalization for treatment. KT rejection was considered only in histologically confirmed cases. Kidney graft function was assessed by serum creatinine levels and DPU at the end of the follow-up period.

Statistical analysis was conducted using IBM SPSS Statistics, version 23. Quantitative data were expressed as mean ± standard deviation for normally distributed variables or as median and percentiles for non-normally distributed data. For frequency comparisons between two independent samples, Fisher's exact test was applied to nominal data, and the Mann–Whitney U test was used for quantitative data. Patient and graft survival were analyzed using the Kaplan–Meier method.

RESULTS

Analysis of the initial KT function revealed delayed graft function in 8 patients (17.8%) in the PD group and 17 patients (34%) in the HD group (p = 0.08). Patients in the HD group required significantly more frequent hospitalizations during the follow-up period. The median number of readmissions in this group was 2.24 [1; 3], compared to 1.9 [0; 2.5] in the PD group (p = 0.01). The complete spectrum of hospitalization causes is presented in Table 2.

Infections were the most common cause of hospitalization. These occurred significantly more often in the HD group than in the PD group – 69 hospitalizations (63%) versus 28 hospitalizations (46%), respectively

Table 1

Clinical and demographic characteristics of patients in the PD and HD groups

	PD group (n = 45)	HD group (n = 50)	p
Gender, male, n (%)	20 (44%)	34 (68%)	0.02*
Age at transplantation, years	45.3 ± 11.9	45.1 ± 12.2	0.9
Duration of RRT prior to KT, months	15.3 [5.7; 24.9]	21.6 [9.3; 39.1]	0.08
Induction IST: Methylprednisolone, n (%) Basiliximab, n (%) Antithymocyte globulin, n (%)	 3 (7%) 42 (93%) 0	 0 47 (94%) 3 (6%)	 >0.8 >0.8 >0.8
Baseline IST: Tacrolimus, n (%) Mycophenolate mofetil, n (%)	 42 (93%) 45 (100%)	 46 (92%) 49 (98%)	 0.8 0.3

*, statistically significant differences.

(p = 0.005). Bacterial infections were considerably more frequent in the HD group, with 43 episodes (63%) compared to 12 episodes (43%) in the PD group (p = 0.0001) (Fig. 1a). Viral infections were slightly more common among PD patients (14 cases, 50%) compared to HD patients (20 cases, 29%), though the difference was not statistically significant (p = 0.5). Fungal infections occurred with similar frequency in both groups: 2 cases (7%) in the PD group and 6 cases (8%) in the HD group (p = 0.2).

When analyzing the etiological structure of infectious complications, the most frequent conditions were KT pyelonephritis, pneumonia, COVID-19, and cytomegalovirus (CMV) infection (Fig. 1b). KT pyelonephritis occurred more often in the HD group – 31 cases (45%) versus 6 cases (21%) in the PD group – although this difference did not reach statistical significance (p = 0.058). Pneumonia was likewise more common among HD patients, with 12 episodes (17%) compared to 2 episodes (7%) in the PD group (p = 0.09). COVID-19-related hospitalizations occurred at similar frequencies in both groups: 7 cases (25%) in the PD group and 18 cases (26%) in the HD group (p = 0.9). The incidence of CMV infection was slightly higher in PD patients (5 cases, 18%) compared to HD patients (5 cases, 7%) (p = 0.8).

KT biopsy accounted for 17 hospitalizations (28%) in the PD group and 17 (15%) in the HD group (p = 0.9), with some patients requiring repeat biopsies. The spectrum of KT pathology identified is presented in Fig. 2. In some cases, multiple pathological findings were detected in a single biopsy specimen.

There were no significant differences between groups in the frequency of rejection episodes. Cellular rejection was diagnosed in 3 PD patients and 5 HD patients; antibody-mediated rejection occurred in 1 HD patient; and mixed rejection was identified in 2 PD patients and 2 HD patients. Interstitial fibrosis and tubular atrophy were the most common histological findings, observed in 8 PD patients and 7 HD patients. Acute tubular necrosis occurred with similar frequency in both groups (5 and 4 cases, respectively). Less frequent diagnoses included CNI toxicity, BK virus nephropathy, hypertensive arteriolar nephrosclerosis, and IgA nephropathy.

Surgical interventions were performed 8 times (13%) in patients from the PD group and 8 times (7%) in patients from the HD group (p = 0.8). Among the surgical causes of hospitalization, the most frequent procedu-

Table 2

Causes of hospitalization in the PD and HD groups

Cause of hospitalization	PD group (61 hospitalizations)	HD group (110 hospitalizations)	p
Infections, n (%)	28 (46%)	69 (63%)	0.005*
KT biopsy, n (%)	17 (28%)	17 (15%)	0.9
Surgery, n (%)	8 (13%)	8 (7%)	0.8
Cardiovascular disease (CVD), n (%)	3 (5%)	4 (4%)	0.9
Others, n (%)	5 (8%)	12 (11%)	0.1
Total, n (%)	61 (100%)	110 (100%)	0.01*

*, statistically significant differences.

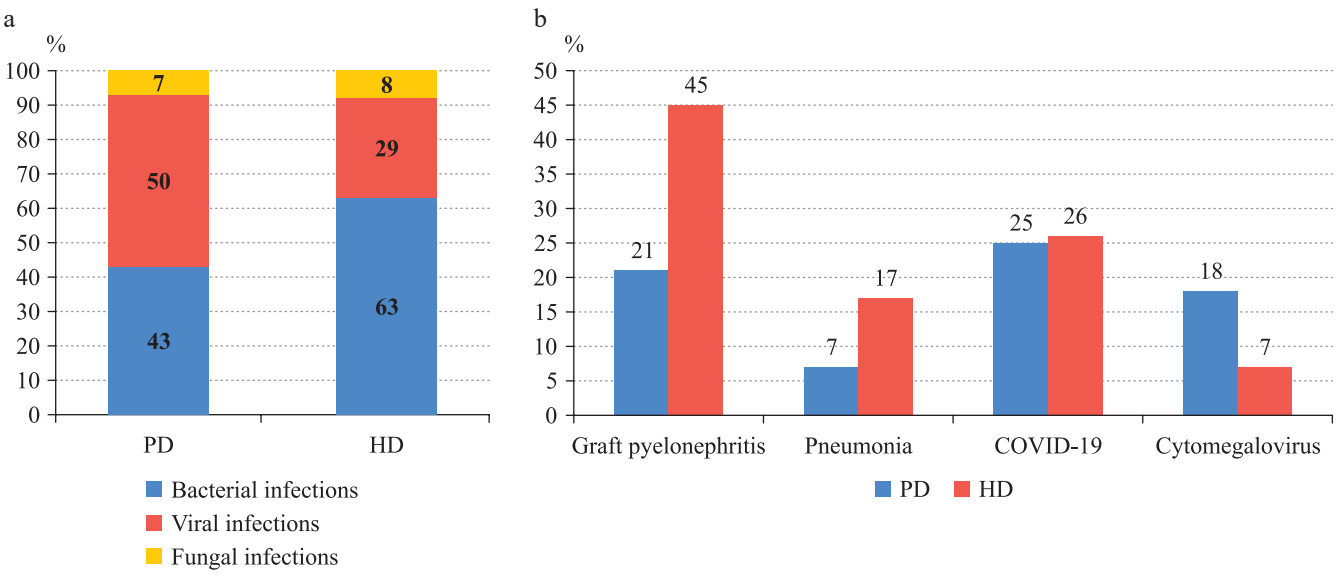

Fig. 1. Infectious complications in PD and HD patients: a, by etiological factor; b, by disease

res were balloon angioplasty (BA) and stenting of the transplant renal artery (TRA), performed in 4 patients from the PD group and 2 patients from the HD group. Percutaneous nephrostomy (PCN) of the transplant was required in 1 patient from the PD group and 3 patients from the HD group. Less common interventions included herniotomy for postoperative hernia, nephrectomy of the native kidneys, and excision of postoperative scar tissue (Fig. 3).

Hospitalizations due to cardiovascular diseases (CVD) occurred with comparable frequency in both the PD and HD groups (Fig. 4). In the HD group, there were two hospitalizations for stroke and its sequelae, one for acute myocardial infarction (AMI), and one for coronary artery disease (CAD) with atrial fibrillation (AF). In the PD group, three hospitalizations due to stroke associated with AMI, myocardial ischemia (MI), and AF.

The two-year KT survival rate was 91% in the PD group and 94% in the HD group (p = 0.8) (Fig. 5a). Causes of graft loss in the PD group included primary non-functioning graft, antibody-mediated rejection (AMR), and BK virus nephropathy. In the HD group, graft loss was primarily associated with primary non-functioning graft, AMR, and KT pyelonephritis complicated by urosepsis.

At the end of the follow-up period, no statistically significant differences were found between the groups in serum creatinine levels or daily proteinuria (DPU) (Fig. 6). The median serum creatinine level in the PD group was 144 [115; 190] μmol/L, compared with 138 [115; 171] μmol/L in the HD group (p = 0.7). Median DPU values were 0.09 [0.02; 0.1] g/day in the PD group and 0.1 [0.02; 0.2] g/day in the HD group (p = 0.3).

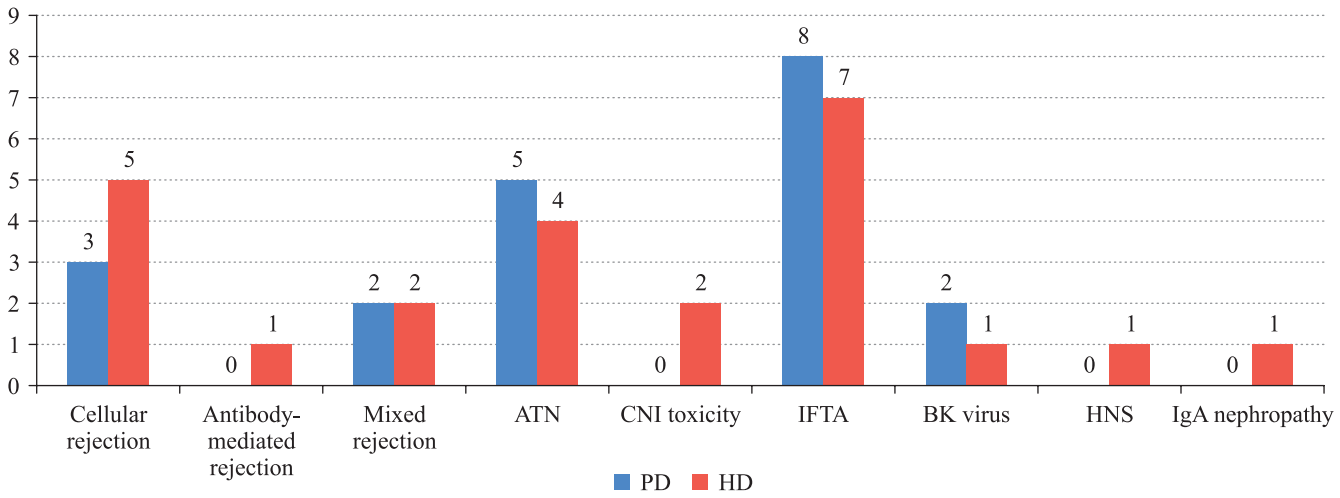

Fig. 2. Results of KT biopsy in the PD and HD groups. ATN, acute tubular necrosis; CNI toxicity, calcineurin inhibitor toxicity; IFTA, interstitial fibrosis and tubular atrophy; BK, BK viral infection; HNS, Hypertensive arteriolar nephrosclerosis

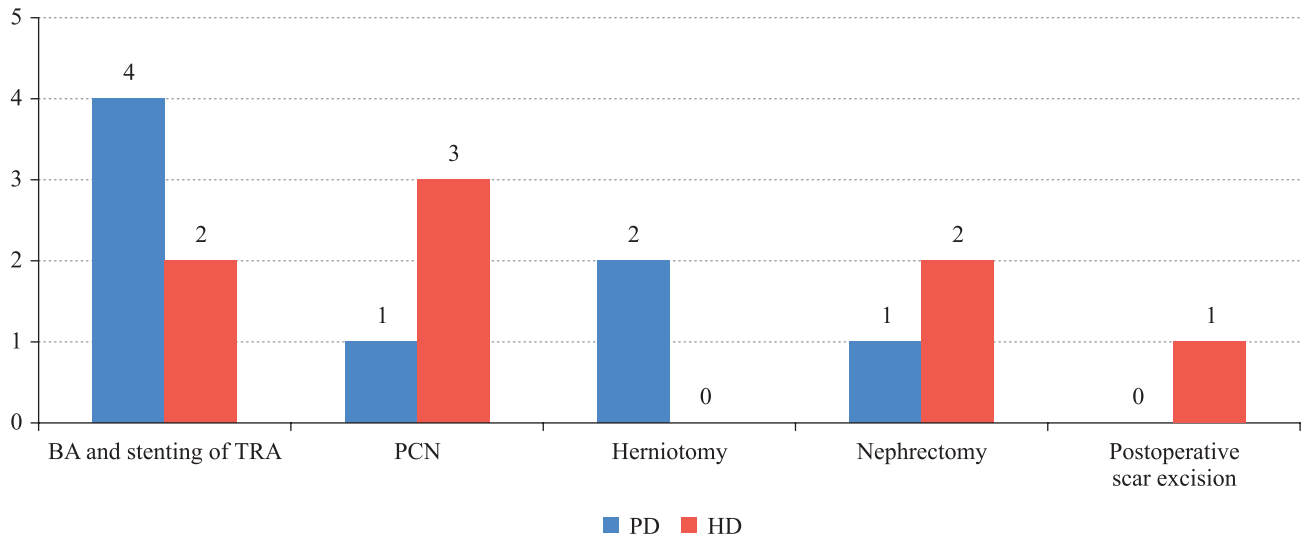

Fig. 3. Reason for surgical interventions in the PD and GD groups. Abbreviations: BA, balloon angioplasty; TRA, transplant renal artery; PCN, percutaneous nephrostomy; HD, hemodialysis; PD, peritoneal dialysis

The two-year patient survival rate did not differ significantly between the PD and HD groups, amounting to 94% and 96%, respectively (p = 0.9) (Fig. 5b). Mortality in the HD group was associated with infectious causes, while in the PD group it was related to CVD. Specifically, deaths in the PD group were due to stroke and AMI, whereas in the HD group they were caused by sepsis secondary to omentobursitis and urosepsis.

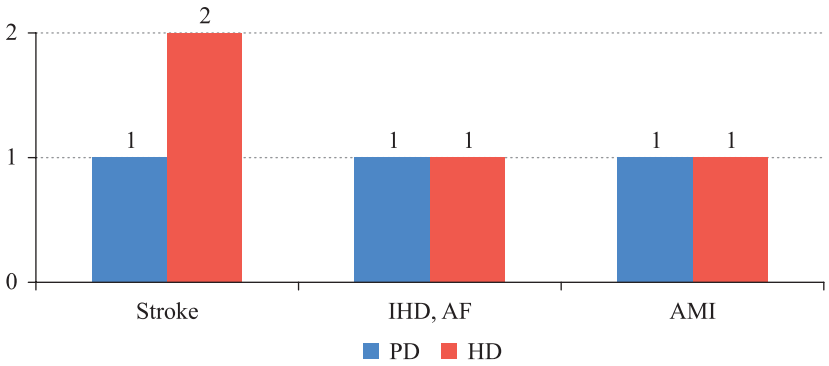

Fig. 4. Causes of hospitalization with cardiovascular disease in PD and HD patients

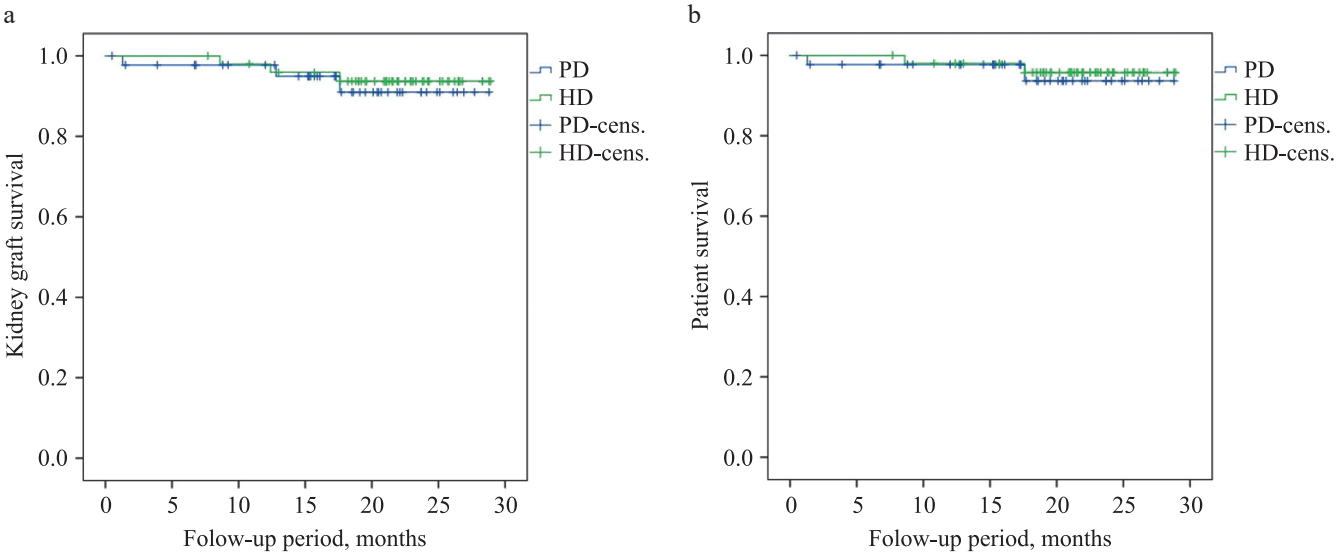

Fig. 5. Two-year survival in PD and HD groups: a, kidney graft survival; b, patient survival

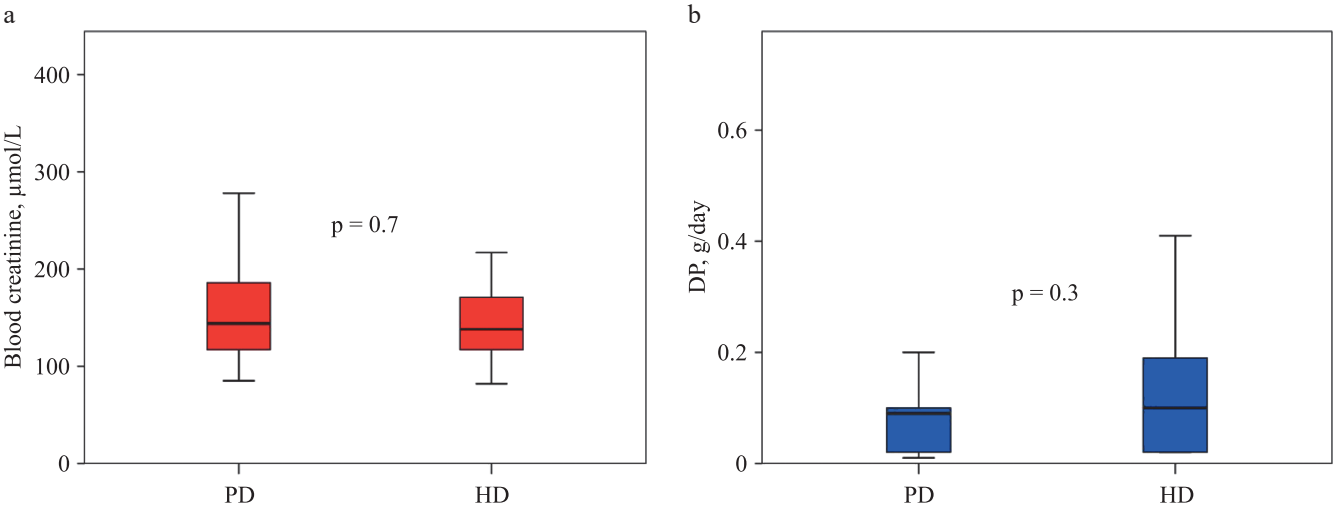

Fig. 6. Levels of (a) blood creatinine and (b) daily proteinuria at the end of follow-up

DISCUSSION

KT improves both quality of life and overall survival among patients with end-stage renal disease. This study assessed the impact of the type of pretransplant dialysis modality on early post-transplant outcomes, focusing on the first two years after KT, including graft function, postoperative complications, and patient survival.

It is well established that delayed graft function (DGF) is associated with an increased risk of acute rejection and mortality [10, 11]. Most small single-center studies have reported a lower incidence of DGF among patients previously treated with PD compared with HD [12–15], while others have found no significant difference between the two modalities [16–18]. In larger studies using national databases,, Snyder et al. [19] also showed a lower frequency of DGF in the PD group compared with the HD group. Consistent with these findings, our study showed that DGF occurred less frequently in the PD group than in the HD group (17.8% vs. 34%), although the difference did not reach statistical significance ($p = 0.08$).

The reduced risk of delayed KT function observed in PD patients may be down to several factors. One of the most significant is the likelihood of higher residual renal function in PD patients [20, 21]. Furthermore, PD patients are often relatively hypervolemic immediately prior to KT compared to HD patients, which may provide a degree of hemodynamic stability and protection against ischemic injury, thereby reducing the risk of DGF [22, 23]. Another proposed mechanism is less inflammation and oxidative stress due to the biocompatibility of the peritoneum as a kind of peritoneal membrane compared to dialyzer membranes [24, 25].

Most studies have reported no difference in the incidence of infectious complications between PD and HD patients prior to KT [18, 26]. Only one study [5] found that recipients with prior PD had a higher risk of developing peritonitis and urinary tract infections compared with those previously on HD. In contrast, our study demonstrated that infectious complications were more frequent among HD patients. Several factors may explain this finding. HD patients are regularly exposed to larger patient populations within dialysis units, increasing the risk of cross-infection compared to PD patients who perform dialysis at home. Following KT, immunosuppressive therapy further predisposes these patients to reactivation of latent infections. Additionally, HD is associated with greater oxidative stress, as artificial dialysis membranes used in HD can activate complement components and phagocytic leukocytes, leading to enhanced generation of free radicals and a persistent microinflammatory state [27]. The intensity of this oxidative stress tends to decrease gradually within the first year post-transplant.

Conversely, some studies have shown that complement activation capacity is diminished in HD patients relative to healthy controls. This acquired complement protein deficiency may partly account for the increased susceptibility to infection and sepsis observed in HD patients [28]. However, the use of immunosuppressive agents alongside prophylactic antimicrobial therapy during the early post-transplant period may mitigate these differences, resulting in comparable rates of acute rejection, graft survival, infection, and other complications among patients with different pre-transplant dialysis modalities [26].

Vanholder et al. [29] reported a higher rate of acute rejection in patients who received PD prior to KT. They attributed this finding to a potentially greater baseline immunodeficiency among HD patients compared with PD patients. However, several subsequent studies have found no significant difference in rejection rates between the two groups [13, 16, 17]. In a meta-analysis of six studies including 3,283 patients, Tang et al. [25] also found no difference in rejection incidence between PD and HD recipients. Consistent with these findings, our study likewise revealed no difference in the rate of acute rejection between the PD and HD groups.

In the 21st century, multiple large registry-based studies have examined the influence of pre-transplant dialysis modality on graft survival [3, 30, 31]. Initial unadjusted analyses in these studies suggested that pre-transplant PD was associated with a lower frequency of graft loss. However, after applying statistical adjustments for inflammatory and protein-energy malnutrition syndromes and other transplant-related variables using Cox multivariate regression and instrumental variable methods, these differences were no longer significant. The results indicate that the previously observed survival advantage of PD may have been due to baseline differences between patient populations, rather than the dialysis modality itself.

These conclusions are further supported by recent single-center studies, which have consistently demonstrated comparable graft survival between the two groups [4, 18, 32]. Similarly, in our study, two-year graft survival did not differ significantly between PD and HD recipients (91% vs. 94%, $p = 0.8$). In addition, serum creatinine and DPU levels at the end of follow-up were comparable between the two groups.

Several large registry-based studies have reported a survival advantage among patients who underwent PD pre-transplant, showing a reduction in post-transplant mortality compared with those previously treated with HD [3, 4, 30]. However, other studies have found no significant difference in patient survival between the two modalities [5, 19, 31].

Pre-transplant PD may confer certain physiological advantages that persist after KT and contribute to improved outcomes. These include more stable volume and blood pressure control, absence of myocardial stunning, and better preservation of residual renal function, all of which may translate into better cardiovascular outcomes with PD. Nonetheless, results across studies remain inconsistent [33, 34].

In a large registry analysis, Molnar et al. [3] observed lower overall mortality among patients treated with PD pre-transplant, largely attributable to reduced cardiovascular deaths. Similarly, Schwenger et al. [30] reported both lower overall and cardiovascular mortality in recipients with prior PD. In contrast, Kramer et al. [31], who analyzed data from 10,135 PD and 18,953 HD patients using multivariate regression and instrumental variable analysis, found that after statistical adjustment, mortality did not differ between the two groups.

Two meta-analyses published in 2016, combining data from most major studies conducted over the preceding two decades [24, 25], showed better post-transplant survival among patients on pre-transplant PD due to lower cardiovascular mortality, which in turn may be due to better overall health and other factors such as residual kidney function.

In our study, the two-year patient survival following KT did not differ significantly between recipients with prior PD and those with prior HD. Among HD patients, mortality was primarily infection-related, whereas in the PD group, deaths were attributed to CVD. Notably, both PD patients who died had a history of CVD prior to transplantation.

These findings align with results from large meta-analyses, which indicate that the first three months after KT represent a period of elevated mortality risk, predominantly due to cardiovascular events and infections. In the long term, CVD and malignancy remain the leading causes of death among KT recipients [35, 36].

Therefore, it is highly likely that the pre-transplant long-term survival outcomes among PD and HD patients may differ in terms of both causes of mortality and their distribution.

CONCLUSION

In our study, patients who underwent PD prior to KT had slightly better post-transplant outcomes. Specifically, the PD group showed a significant reduction in the frequency of rehospitalizations and infectious complications, as well as a trend toward a lower incidence of DGF, while no significant differences were observed in graft survival or patient mortality during the first two years following KT. With an increased number of patients and a longer follow-up period, these results may evolve; therefore, continued data collection and ongoing analysis are essential.

This study was conducted within the framework of the scientific and practical healthcare project of the Moscow Health Department (Application No. 2002-27/23), titled "Application of Innovative Approaches to Expanding the Waiting List for Donor Kidneys, Preparing Patients for Transplantation (Including Patients with Thrombotic Microangiopathy), and Managing Recipients in the Early Post-Transplant Period". The project was financially supported by a grant from the Moscow Center for Innovative Technologies in Healthcare.

The authors declare no conflict of interest.

REFERENCES

1. *Thurlow JS, Joshi M, Yan G, Norris KC, Agodoa LY, Yuan CM, Nee R.* Global Epidemiology of End-Stage Kidney Disease and Disparities in Kidney Replacement Therapy. *Am J Nephrol*. 2021; 52 (2): 98–107. doi: 10.1159/000514550.
2. *Amaral S, Sayed BA, Kutner N, Patzer RE.* Preemptive kidney transplantation is associated with survival benefits among pediatric patients with end-stage renal disease. *Kidney Int*. 2016 Nov; 90 (5): 1100–1108. doi: 10.1016/j.kint.2016.07.028.
3. *Molnar MZ, Mehrotra R, Duong U, Bunnapradist S, Lukowsky LR, Krishnan M et al.* Dialysis modality and outcomes in kidney transplant recipients. *Clin J Am Soc Nephrol*. 2012 Feb; 7 (2): 332–341. doi: 10.2215/CJN.07110711.
4. *López-Oliva MO, Rivas B, Pérez-Fernández E, Ossorio M, Ros S, Chica C et al.* Pretransplant peritoneal dialysis relative to hemodialysis improves long-term survival of kidney transplant patients: a single-center observational study. *Int Urol Nephrol*. 2014 Apr; 46 (4): 825–832. doi: 10.1007/s11255-013-0521-0.
5. *Lin HT, Liu FC, Lin JR, Pang ST, Yu HP*. Impact of the pretransplant dialysis modality on kidney transplantation outcomes: a nationwide cohort study. *BMJ Open*. 2018 Jun 4; 8 (6): e020558. doi: 10.1136/bmjopen-2017-020558.
6. *Lenihan CR, Liu S, Airy M, Walther C, Montez-Rath ME, Winkelmayer WC*. The association of pre-kidney transplant dialysis modality with *de novo* posttransplant heart failure. *Cardiorenal Med*. 2021; 11 (5–6): 209–217. doi: 10.1159/000518535.
7. *So S, Au EHK, Lim WH, Lee VWS, Wong G.* Factors influencing long-term patient and allograft outcomes in elderly kidney transplant recipients. *Kidney Int Rep*. 2020 Dec 13; 6 (3): 727–736. doi: 10.1016/j.ekir.2020.11.035.
8. *Gardezi AI, Aziz F, Parajuli S*. The Role of Peritoneal Dialysis in Different Phases of Kidney Transplantation. *Kidney360*. 2022 Feb 28; 3 (4): 779–787. doi: 10.34067/KID.0000482022.
9. *Morozov YuA, Marchenko TV, Goncharova AV, Doletskaya LG*. Function of the kidney transplant at children in the early and late postoperative periods. *Russian Journal of Pediatric Surgery, Anesthesia and Intensive Care*. 2016; 6 (1): 8–15.
10. *Bahl D, Haddad Z, Datoo A, Qazi YA*. Delayed graft function in kidney transplantation. *Curr Opin Organ Transplant*. 2019 Feb; 24 (1): 82–86. https://doi.org/10.1097/MOT.0000000000000604.
11. *Tapiawala SN, Tinckam KJ, Cardella CJ, Schiff J, Cattran DC, Cole EH, Kim SJ.* Delayed graft function and the risk for death with a functioning graft. *J Am Soc Nephrol*. 2010 Jan; 21 (1): 153–161. https://doi.org/10.1681/ASN.2009040412.
12. *Freitas C, Fructuoso M, Martins LS, Almeida M, Pedroso S, Dias L et al.* Posttransplant outcomes of peritoneal

dialysis versus hemodialysis patients. *Transplant Proc*. 2011 Jan-Feb; 43 (1): 113–116. https://doi.org/10.1016/j.transproceed.2010.12.008.
13. *Sezer S, Karakan S, Özdemir Acar FN, Haberal M*. Dialysis as a bridge therapy to renal transplantation: Comparison of graft outcomes according to mode of dialysis treatment. *Transplant Proc*. 2011 Mar; 43 (2): 485–487. https://doi.org/10.1016/j.transproceed.2011.01.027.
14. *Sharma A, Teigeler TL, Behnke M, Cotterell A, Fisher R, King A et al.* The mode of pretransplant dialysis does not affect postrenal transplant outcomes in African Americans. *J Transplant*. 2012; 2012: 303596. https://doi.org/10.1155/2012/303596.
15. *Song SH, Lee JG, Lee J, Huh KH, Kim MS, Kim SI, Kim YS.* Outcomes of kidney recipients according to mode of pretransplantation renal replacement therapy. *Transplant Proc*. 2016 Sep; 48 (7): 2461–2463. https://doi.org/10.1016/j.transproceed. 2016.02.096.
16. *Yang Q, Zhao S, Chen W, Mao H, Huang F, Zheng Z et al*. Influence of dialysis modality on renal transplant complications and outcomes. *Clin Nephrol.* 2009 Jul; 72 (1): 62–68. https://doi.org/10.5414/CNP72062.
17. *Caliskan Y, Yazici H, Gorgulu N, Yelken B, Emre T, Turkmen A et al*. Effect of pretransplant dialysis modality on kidney transplantation outcome. *Perit Dial Int*. 2009 Feb; 29 Suppl 2: S117–S122. https://doi.org/10.1177/089686080902902S23.
18. *Dipalma T, Fernandez-Ruiz M, Praga M, Polanco N, Gonzalez E, Gutierrez-Solis E et al.* Pretransplant dialysis modality does not influence short- or longterm outcome in kidney transplant recipients: Analysis of paired kidneys from the same deceased donor. *Clin Transplant.* 2016 Sep; 30 (9): 1097–1107. https://doi.org/10.1111/ctr.12793.
19. *Snyder JJ, Kasiske BL, Gilbertson DT, Collins AJ*. A comparison of transplant outcomes in peritoneal and hemodialysis patients. *Kidney Int*. 2002 Oct; 62 (4): 1423–1430. https://doi.org/10.1111/j.1523-1755.2002.kid563.x.
20. *Moist LM, Port FK, Orzol SM, Young EW, Ostbye T, Wolfe RA*. Predictors of loss of residual renal function among new dialysis patients. *J Am Soc Nephrol*. 2000 Mar; 11 (3): 556–564. https://doi.org/10.1681/ASN.V113556.
21. *Jansen MA, Hart AA, Korevaar JC, Dekker FW, Boeschoten EW, Krediet RT*. NECOSAD Study Group. Predictors of the rate of decline of residual renal function in incident dialysis patients. *Kidney Int*. 2002 Sep; 62 (3): 1046–1053. https://doi.org/10.1046/j.1523-1755.2002.00505.x.
22. *Jain D, Haddad DB, Goel N*. Choice of dialysis modality prior to kidney transplantation: Does it matter? *World J Nephrol*. 2019 Jan 21; 8 (1): 1–10. https://doi.org/10.5527/wjn.v8.i1.0000.
23. *Lobbedez T, Lecouf A, Abbadie O, Ficheux M, de Ligny BH, Ryckelynck JP.* Peritoneal dialysis and renal transplantation. *Contrib Nephrol*. 2009; 163: 250–256. https://doi.org/10.1159/000223806.
24. *Joachim E, Gardezi AI, Chan MR, Shin JI, Astor BC, Waheed S*. Association of pre-transplant dialysis modality and posttransplant outcomes: A meta-analysis. *Perit Dial Int.* 2017 May-Jun; 37 (3): 259–265. https://doi.org/10.3747/pdi.2016.00011.
25. *Tang M, Li T, Liu H*. A comparison of transplant outcomes in peritoneal and hemodialysis patients: A meta-analysis. *Blood Purif*. 2016; 42 (2): 170–176. https://doi.org/10.1159/000446272.
26. *Hou YF, Wang XX, Yang HJ, Zhong S*. Impact of pretransplant dialysis modality on kidney transplant outcomes: a systematic review and meta-analysis. *Eur Rev Med Pharmacol Sci*. 2022 Apr; 26 (7): 2292–2304. doi: 10.26355/eurrev_202204_28459.
27. *Liakopoulos V, Roumeliotis S, Gorny X, Dounousi E, Mertens PR*. Oxidative Stress in Hemodialysis Patients: A Review of the Literature. *Oxid Med Cell Longev*. 2017; 2017: 3081856.
28. *Poppelaars F, Faria B, Gaya da Costa M, Franssen CFM, van Son WJ, Berger SP et al.* The Complement System in Dialysis: A Forgotten Story? *Front Immunol*. 2018 Jan 25; 9: 71. doi: 10.3389/fimmu.2018.00071.
29. *Vanholder R, Heering P, Loo AV, Biesen WV, Lambert MC, Hesse U et al*. Reduced incidence of acute renal graft failure in patients treated with peritoneal dialysis compared with hemodialysis. *Am J Kidney Dis*. 1999 May; 33 (5): 934–940. https://doi.org/10.1016/S0272-6386(99)70429-4.
30. *Schwenger V, Dohler B, Morath C, Zeier M, Opelz G*. The role of pretransplant dialysis modality on renal allograft outcome. *Nephrol Dial Transplant*. 2011 Nov; 26 (11): 3761–3766. https://doi.org/10.1093/ndt/gfr132.
31. *Kramer A, Jager KJ, Fogarty DG, Ravani P, Finne P, Pérez-Panadés J et al.* Association between pre-transplant dialysis modality and patient and graft survival after kidney transplantation. *Nephrol Dial Transplant*. 2012 Dec; 27 (12): 4473–4480. https://doi.org/10.1093/ndt/gfs450.
32. *Che X, Yang X, Yan J, Yuan Y, Ma Q, Ying L et al*. Effects of pretransplant peritoneal vs hemodialysis modality on outcome of first kidney transplantation from donors after cardiac death. *BMC Nephrol*. 2018 Sep 17; 19 (1): 235. https://doi.org/10.1186/s12882-018-1013-3.
33. *Van Biesen W, Vanholder R, Verbeke F, Lameire N*. Is peritoneal dialysis associated with increased cardiovascular morbidity and mortality? *Perit Dial Int*. 2006 Jul-Aug; 26 (4): 429–434. https://doi.org/10.1177/089686080602600405.
34. *Albakr RB, Bargman JM*. A comparison of hemodialysis and peritoneal dialysis in patients with cardiovascular disease. *Cardiol Clin*. 2021 Aug; 39 (3): 447–453. https://doi.org/10.1016/j.ccl.2021.04.013.
35. *Awan AA, Niu J, Pan JS, Erickson KF, Mandayam S, Winkelmayer WC et al.* Trends in the Causes of Death among Kidney Transplant Recipients in the United States (1996–2014). *Am J Nephrol*. 2018; 48 (6): 472–481. doi: 10.1159/000495081. Epub 2018 Nov 23. PMID: 30472701; PMCID: PMC6347016.
36. *Ying T, Shi B, Kelly PJ, Pilmore H, Clayton PA, Chadban SJ*. Death after Kidney Transplantation: An Analysis by Era and Time Post-Transplant. *J Am Soc Nephrol*. 2020 Dec; 31 (12): 2887–2899. doi: 10.1681/ASN.2020050566.

The article was submitted to the journal on 27.04.2025

DOI: 10.15825/1995-1191-2025-4-41-47

SUCCESSFUL ENDOSCOPIC MANAGEMENT OF SWYER–JAMES–MACLEOD SYNDROME: A CASE REPORT

M.T. Bekov, I.V. Pashkov, E.F. Shigaev, K.S. Smirnov, R.A. Latypov, D.O. Oleshkevich

Shumakov National Medical Research Center of Transplantology and Artificial Organs, Moscow, Russian Federation

Swyer–James–MacLeod syndrome is a rare disease characterized by emphysematous transformation of an entire lung or lobe. Traditionally, the main treatment method has been surgical resection of the affected lung or lobe to reduce compression of adjacent healthy lung tissue and improve vital lung capacity. This article presents a clinical case of successful endoscopic treatment in a patient with emphysematous transformation of the entire lung, who was referred to the transplant center as a potential candidate for lung transplantation.

Keywords: interventional bronchoscopy, thoracic surgery, Swyer–James–MacLeod syndrome, panlobular emphysema, endoscopy, valve bronchoblockade.

INTRODUCTION

Swyer–James–MacLeod syndrome was first reported in 1953 by P.R. Swyer and G.S. James as "unilateral pulmonary emphysema". A year later, John MacLeod reported a similar case, describing it as "abnormal transparency of one lung" [1]. MacLeod suggested that the underlying cause was obliterative unilateral bronchiolitis, developing as a consequence of recurrent respiratory infections during childhood. However, current literature generally attributes the condition to a congenital or developmental defect, characterized by hypoplasia of the pulmonary artery and small bronchi [1, 2].

The disease may remain asymptomatic until adulthood or present with nonspecific respiratory symptoms, including productive cough, exertional dyspnea, hemoptysis, reduced exercise tolerance, and recurrent pulmonary infections. The disease can be unilateral or bilateral, but it typically affects a single lobe or lung. Despite these possible manifestations, most cases remain clinically silent for years and are often diagnosed incidentally in adulthood [3, 4].

Due to similar clinical manifestations, MacLeod syndrome is frequently misdiagnosed as chronic obstructive pulmonary disease, bronchial asthma, pneumothorax, or pulmonary embolism. The condition should be suspected in patients with presumed asthma who do not respond to conventional therapy [5, 6]. In childhood, the disease usually has minimal clinical impact, but in adulthood, it may progress and sometimes require surgical intervention [7, 8].

Diagnosis is most often suspected based on imaging studies. Chest radiography typically reveals hyperlucency and hyperinflation of one lobe or lung, accompanied by reduced volume of the contralateral lung (Fig. 1). Spirometry shows obstruction, while lung perfusion scintigraphy shows a noticeable reduction in perfusion of the affected lung, with normal or increased perfusion on the opposite side [9, 10].

The primary surgical approach involves resection of the affected lung or lobe to enhance ventilation of the remaining functional alveolar tissue. Despite decades of surgical experience in managing bullous emphysema of various etiologies, lung volume reduction remains the most commonly employed treatment strategy for this condition [10].

In 1990, a group of Russian surgeons successfully introduced an alternative technique – transthoracic occlusion of the bronchus supplying the affected lung, allowing preservation of pulmonary parenchyma. However, no subsequent reports describing its use have appeared in either Russian or international literature [11, 12].

CLINICAL CASE

A 24-year-old female patient (patient X) presented for the first time with respiratory failure during physical exertion. Chest X-ray initially suggested right-sided pneumothorax, and she was hospitalized locally; however, this diagnosis was not confirmed. Subsequent CT scan revealed total bullous emphysema of the right lung§ and mediastinal pulmonary hernia.

Her medical history was notable for frequent respiratory infections during childhood. Following additional investigations and exclusion of other pathologies, she was diagnosed with McLeod syndrome. After discharge, the patient continued to experience recurrent frequent colds, and from October 2019, she began to experience shortness of breath at rest.

Corresponding author: Maksat Bekov. Address: 1, Shchukinskaya str., Moscow, 123182, Russian Federation. Phone: (926) 399-49-75. E-mail: doctorbekov@gmail.com

A thoracic surgeon evaluated her and found that surgical intervention was contraindicated due to a significant decrease in external respiratory function, recommending consultation with a transplant specialist. In January 2020, she underwent remote consultation at Shumakov National Medical Research Center of Transplantology and Artificial Organs, where hospitalization at the transplant center was advised to determine further management.

At the Shumakov Center, examination findings were as follows: forced expiratory volume in 1 second (FEV_1): 1.03 L (25%), forced vital capacity (FVC): 0.82 L (23%), maximal inspiratory pressure (MIP): 79%, maximal mid-expiratory flow rate ($MMEF_{25–75}$): 0.69 L/s (17%), echocardiography: no signs of pulmonary hypertension, perfusion scintigraphy: normal perfusion volume in the left lung. CT findings revealed severe bullous emphysema of the right lung with mediastinal shift and compression of the left lung (Fig. 2).

Based on the results of a comprehensive examination, it was determined that, despite severe respiratory failure, the patient's overall physical condition remained satisfactory. Consequently, a decision was made to insert an endobronchial valve in the upper lobe of the affected lung with the aim of reducing hyperinflation and alleviating

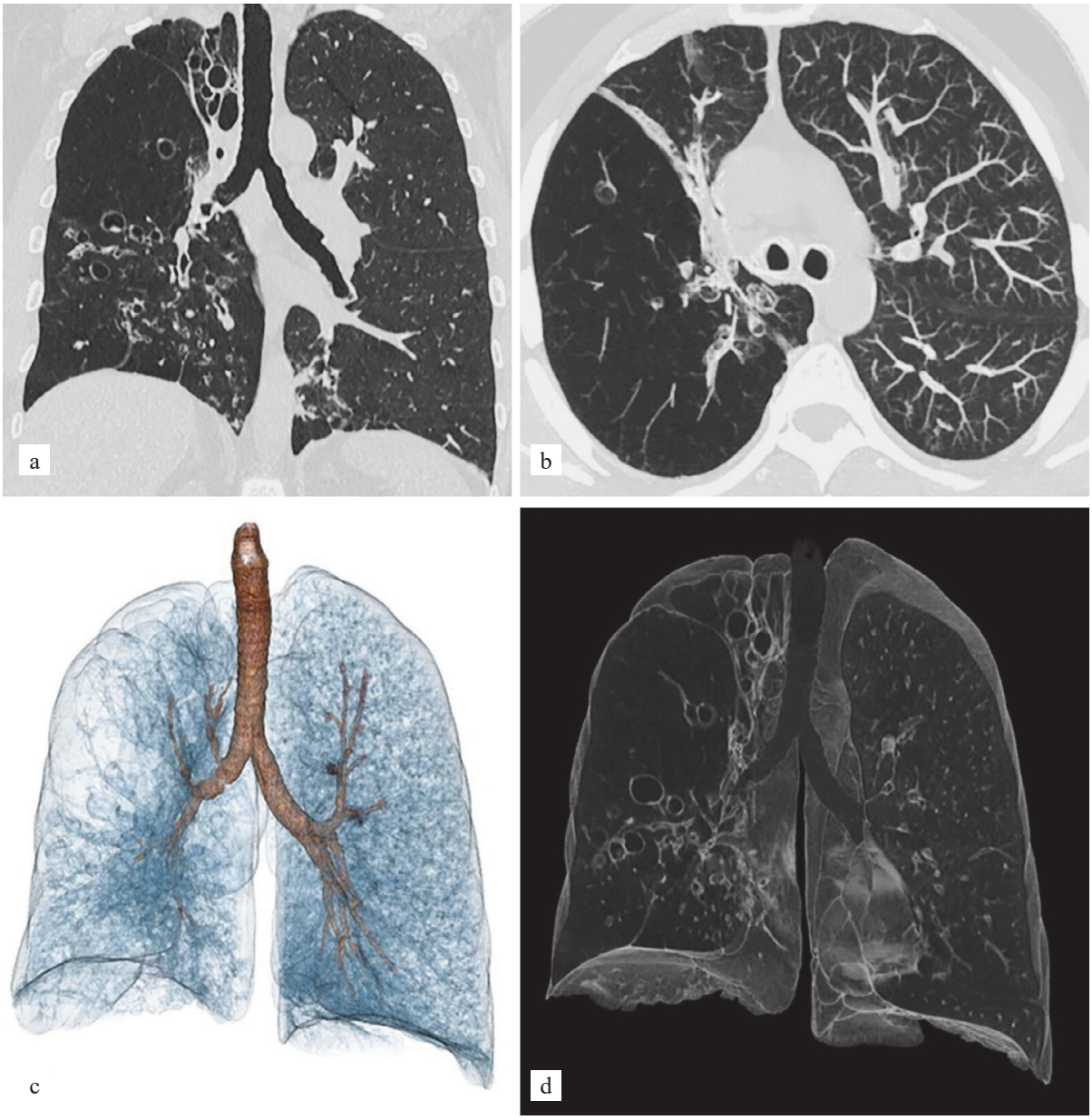

Fig. 1. Computed tomography findings in an adult patient with Swyer–James–MacLeod syndrome: a, frontal projection; b, axial maximum-intensity projection; c, d, volume-rendered chest CT images show diffusely decreased attenuation of the right lung with signs of marked hypoperfusion and bronchiectasis, some with mucous plugging. There is volume reduction of the right lung, mainly in its upper lobe, with asymmetry of the pulmonary arteries, which are preserved in the left lung. (Source: L.P. Gomes de Farias et al. Swyer–James–MacLeod Syndrome: The Hyperlucent Lung. Radiology: Cardiothoracic Imaging)

compression of the contralateral (healthy) left lung. The procedure was carried out under general anesthesia.

One month after the insertion, a positive clinical response was observed, characterized by improved exercise tolerance and reduced dyspnea. It was concluded that there were no current indications for lung transplantation, and outpatient follow-up was continued.

Four months after insertion of the endobronchial valve, the patient reported a deterioration of her condition, returning to the pre-intervention level. Computed tomography revealed proximal migration of the bronchial blocker, resulting in recurrent hyperinflation of the upper lobe of the right lung with secondary compression of the left lung. The displaced valve was removed, and a repeat endobronchial valve insertion was performed – this time targeting both the intermediate and upper lobes of the right lung (Fig. 3).

Five days after the second intervention, despite some reduction in respiratory insufficiency, the patient's condition remained unfavorable. A sharp displacement of the mediastinum secondary to subtotal atelectasis led to severe retrosternal pain, although there were no signs of cardiovascular compromise.

Given the ineffectiveness of repeated insertion of endobronchial valves, a decision was made to perform circumferential argon plasma coagulation to induce fibrotic stricture formation, thereby decreasing ventilation and reducing hyperinflation of the affected lung. The procedure was performed under high-frequency ventilation (HFV) using an electrosurgical coagulator (ERBE VIO3, PRESICE mode).

In the postoperative period, the patient experienced an exacerbation of chronic bronchitis, which was managed with antibiotic therapy.

Two weeks after the intervention, the patient showed a decrease in respiratory insufficiency. During outpatient follow-up at 3, 6, and 12 months, there was sustained improvement in respiratory function, with significant regression of respiratory failure, increased exercise tolerance, and no episodes of acute bronchitis from the third postoperative month onward.

Computed tomography performed one year after the procedure revealed complete atelectasis of the affected right lung, atresia of the intermediate and upper lobe bronchi, a mediastinal shift toward the right, and compensatory hyperinflation of the contralateral (left) lung. Despite occasional mild chest discomfort, the patient's

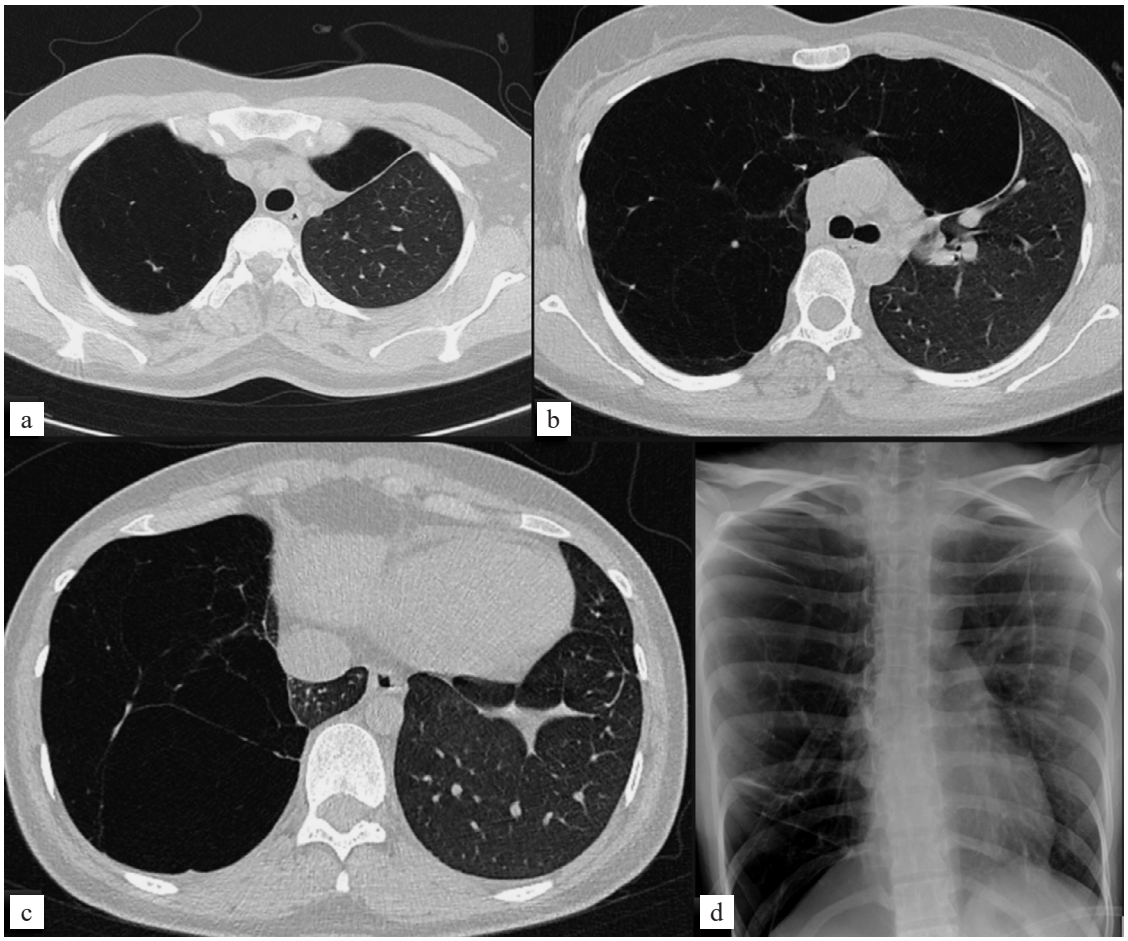

Fig. 2. Radiological findings prior to surgical intervention: a, 3rd thoracic vertebra; b, 5th thoracic vertebra (tracheal bifurcation); c, 7th thoracic vertebra (beginning of the diaphragm); d, frontal chest X-ray

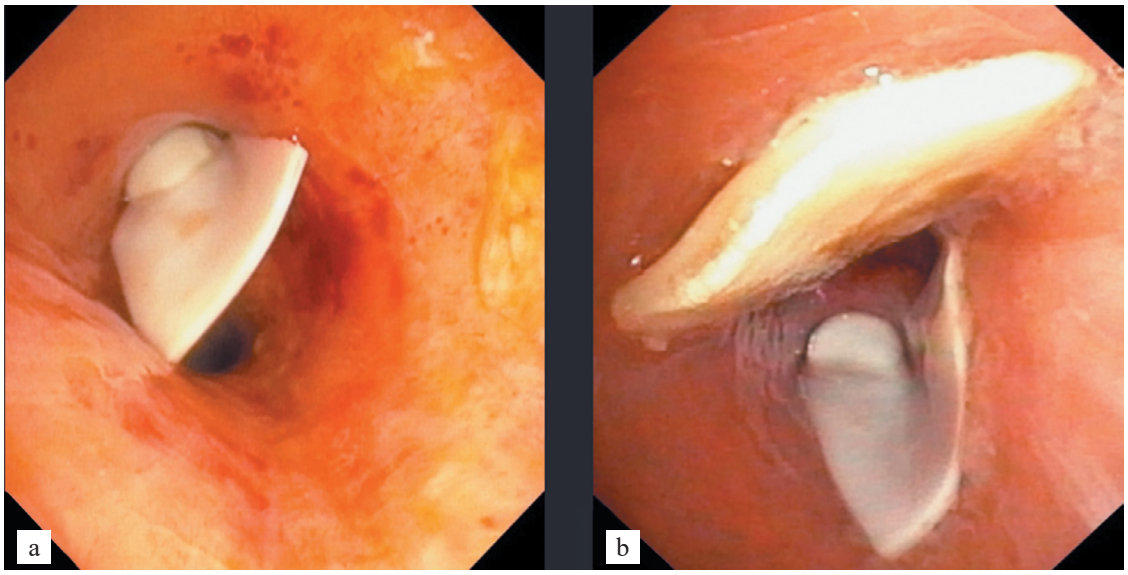

Fig. 3. Endoscopic valve bronchoblockade of the upper lobe of the affected right lung: a, upper lobe; b, intermediate and upper lobe bronchi

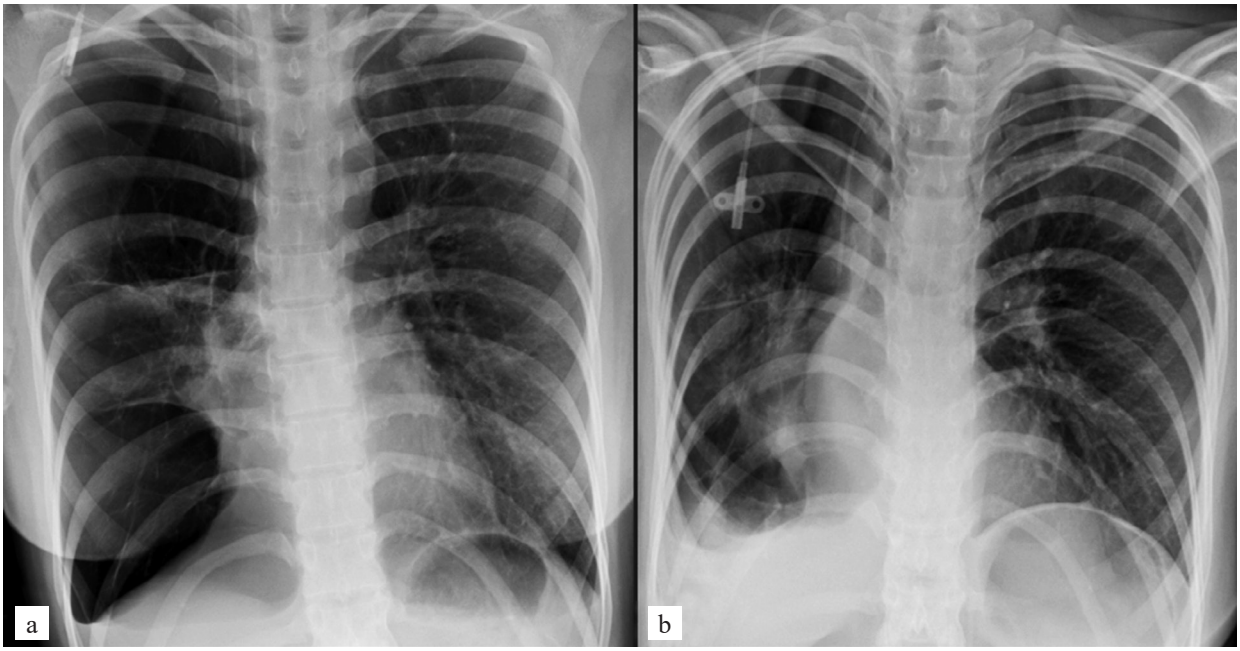

Fig. 4. Control chest X-rays following the insertion of an endobronchial valve into the right upper lobe and intermediate bronchi: a, 3 days post-procedure; b, 2 weeks post-procedure

pulmonary function parameters improved substantially, with FEV_1 2.15 L (56%), FVC 1.87 L (56%), MIP 87%, and $MMEF_{25–75}$ 1.74 L/s (43%). No evidence of heart failure was observed on echocardiography, ECG, or functional tests (Figs. 5 and 6).

CONCLUSION

Throughout the entire inpatient and outpatient observation period, spanning more than three years, no serious infectious or cardiovascular complications were recorded. This fact underscores the safety and effectiveness of the treatment approach applied. Moreover, the patient achieved not only a sustained, but also a significant improvement in respiratory function, which was accompanied by a notable increase in exercise tolerance.

The positive outcomes suggest that endobronchial valve therapy with subsequent argon plasma coagulation may represent a highly effective alternative to radical surgical procedures. This is particularly significant for patients with Swyer–James–MacLeod syndrome and other conditions associated with panlobular emphysema. Thus, implementation of this therapeutic approach has the potential to enhance clinical outcomes and signifi-

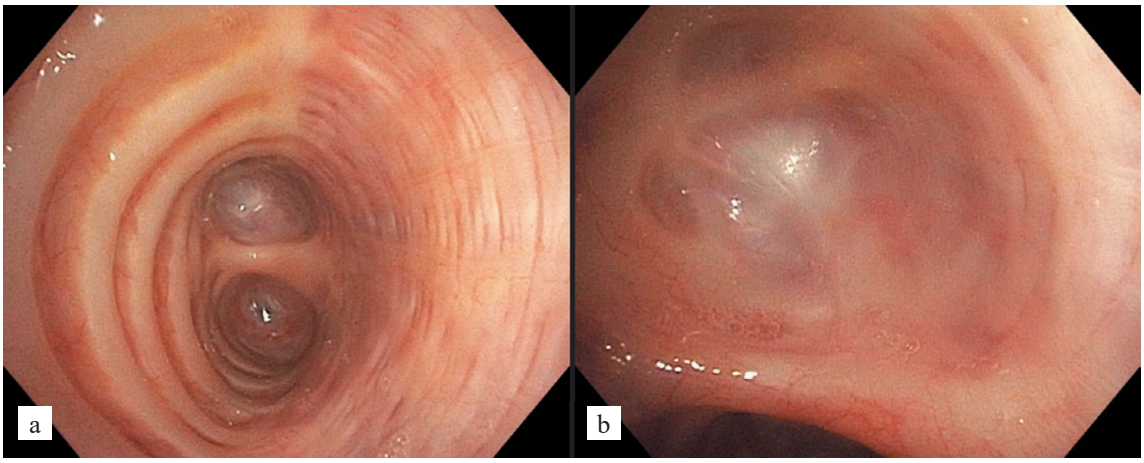

Fig. 5. Endoscopic views of complete atresia of the right upper lobe and intermediate bronchi: a, atresia of the intermediate and upper lobe bronchi on the right; b, atresia of the upper lobe bronchus on the right

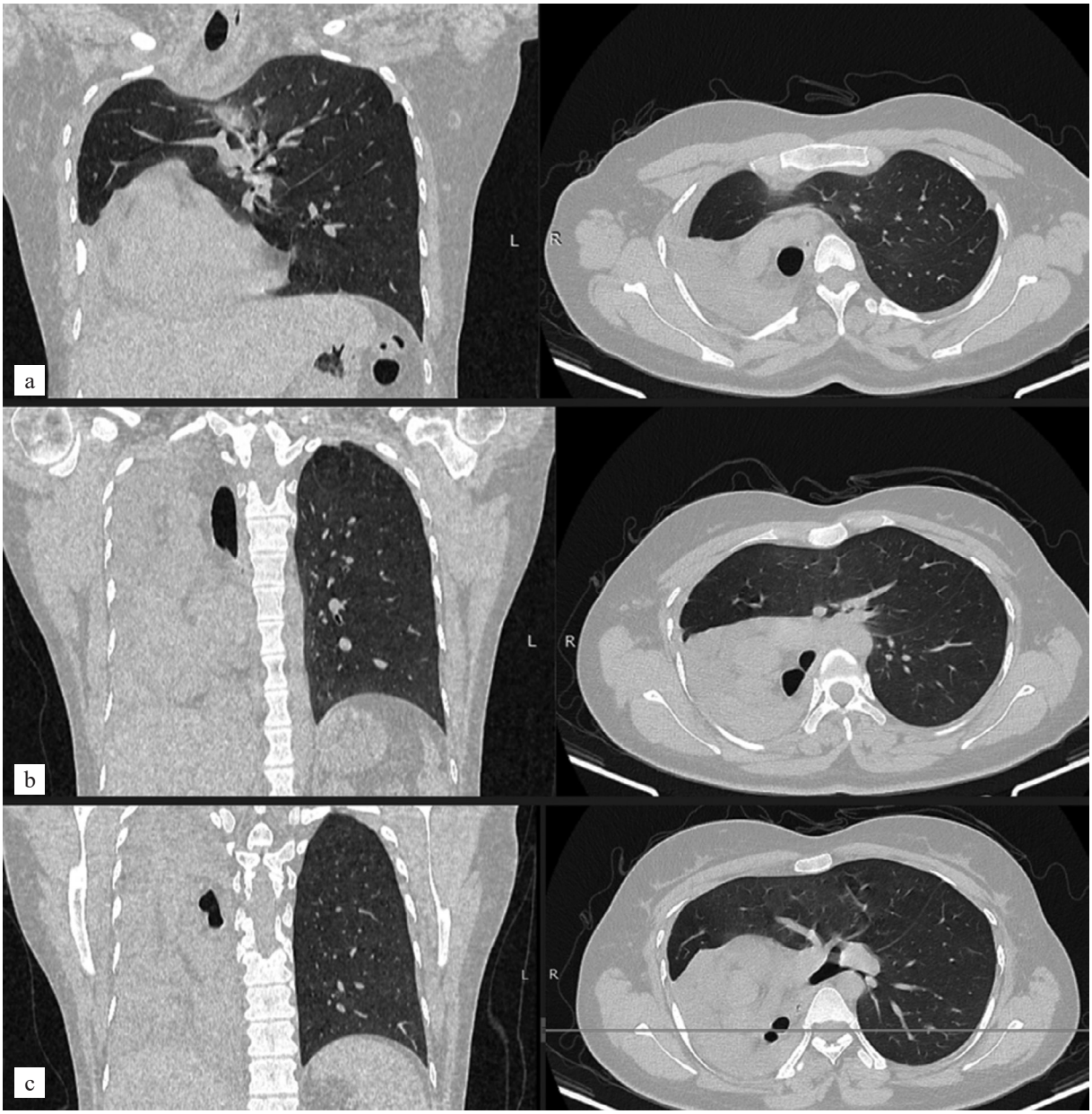

Fig. 6. Computed tomography findings 1 year after endoscopic treatment: a, 3rd thoracic vertebra; b, 5th thoracic vertebra (tracheal bifurcation); c, 7th thoracic vertebra (site of right main bronchus atresia)

cantly improve patients' quality of life, while avoiding the risks inherent in major surgical interventions.

The authors declare no conflict of interest.

REFERENCES

1. *Kent DC*. Physiologic aspects of idiopathic unilateral hyperlucent lung: With a review of the literature. *Am Rev Respir Dis*. 1964 Aug; 90: 202–212. doi: 10.1164/arrd.1964.90.2.202.
2. *Hekali P, Halttunen P, Korhola O, Korppi-Tommola T.* Chronic unilateral hyperlucent lung. A consecutive series of 40 patients. *Rofo*. 1982 Jan; 136 (1): 41–48. doi: 10.1055/s-2008-1055993.
3. *Dirweesh A, Alvarez C, Khan M, Shah N.* A unilateral hyperlucent lung – Swyer–James syndrome: A case report and literature review. *Respir Med Case Rep*. 2017 Jan 16; 20: 104–106. doi: 10.1016/j.rmcr.2017.01.004.
4. *Hamada S, Tsukino M*. Swyer–James–MacLeod syndrome: the differential diagnosis of unilateral hyperlucency. *Intern Med*. 2018 Apr 27; 57 (17): 2591–2592. doi: 10.2169/internalmedicine.0725-17.
5. *Fontes CP, de Sousa MR*. Swyer–James–MacLeod syndrome: an important differential diagnosis in adulthood. *BMJ Case Rep*. 2021 Sep 13; 14 (9): e246337. doi: 10.1136/bcr-2021-246337.
6. *Mehra S, Basnayake T, Falhammar H, Heraganahally S, Tripathi S*. Swyer–James–MacLeod syndrome – a rare diagnosis presented through two adult patients. *Respirol Case Rep*. 2017 Jun 16; 5 (5): e00245. doi: 10.1002/rcr2.245.
7. *Machado D, Lima F, Marques C, Monteiro R*. Swyer–James–MacLeod syndrome as a rare cause of unilateral hyperlucent lung: Three case reports. *Medicine (Baltimore)*. 2019 Feb; 98 (6): e14269. doi: 10.1097/MD.0000000000014269.
8. *Dâmaso S, Carreira NR, Gonçalves C, Aguiar P.* Congenital lobar emphysema in early adulthood. *Cureus*. 2021 Jan 9; 13 (1): e12590. doi: 10.7759/cureus.12590.
9. *Gomes de Farias LP, Kaiser Ururahy Nunes Fonseca E, Chate RC, Sawamura MVY.* Swyer–James–MacLeod Syndrome: The Hyperlucent Lung. *Radiol Cardiothorac Imaging*. 2020 Jun 18; 2 (3): e190246. doi: 10.1148/ryct.2020190246.
10. *Sen HS, Taylan M, Abakay O, Sezgi C, Cetincakmak MG.* Adult diagnosis of Swyer–James–MacLeod syndrome: retrospective analysis of four cases. *Respir Care*. 2014 Apr; 59 (4): e51–e54. doi: 10.4187/respcare.02552.
11. *Cruz MV, Trachiotis GD*. Pneumonectomy in a patient with Swyer–James–MacLeod syndrome. *Surgical Science*. 2015 Feb; 6 (2): 55–58. doi: 10.4236/ss.2015.62009.
12. *Vishnevsky AA, Nikoladze GD*. New approach to the surgical treatment of Swyer–James–MacLeod syndrome. *Ann Thorac Sur*g. 1990 Jul; 50 (1): 103–104. doi: 10.1016/0003-4975(90)90098-q.

The article was submitted to the journal on 22.07.2025

DOI: 10.15825/1995-1191-2025-4-48-56

RISK OF GRAFT LOSS: SINGLE-FACTOR AND MULTIFACTOR ANALYSIS IN KIDNEY TRANSPLANTATION FROM EXPANDED CRITERIA DONORS

M.G. Minina[1, 2], D.A. Bankeev[1], A.B. Zulkarnaev[1], V.S. Bogdanov[1], E.A. Tenchurina[1], V.M. Sevostyanov[1]

[1] Botkin Hospital, Moscow, Russian Federation

[2] Shumakov National Medical Research Center of Transplantology and Artificial Organs, Moscow, Russian Federation

Objective: to identify donor and recipient factors associated with the risk of loss of graft function in recipients of kidney grafts from expanded-criteria, brain-dead donors. **Materials and methods.** A retrospective multicenter cohort study included 254 donors who met the UNOS expanded-criteria definition and 444 corresponding recipients. Donor and recipient characteristics, perioperative parameters, and post-transplant outcomes were analyzed using single- and multivariable Cox regression models. **Results.** Mean donor age was 58.3 ± 4.8 years, and median cold ischemia time was 14.4 [12.3–17.0] hours. Mean recipient age was 51.6 ± 9.6 years. Class I anti-human leukocyte antigen (anti-HLA) antibodies (mean fluorescence intensity [MFI] >500) were detected in 40 (9.2%) recipients, and class II antibodies in 56 (12.8%). Delayed graft function occurred in 34.3% of recipients. Multivariate analysis revealed that lower donor minimum glomerular filtration rate (GFR) (HR = 0.98; 95% CI 0.965–0.997; p = 0.023) and higher combined donor ALT + AST levels (HR = 1.208; 95% CI 1.063–1.372; p = 0.004) were significantly associated with an increased risk of graft loss. Donor age was not a significant predictor. Among recipient factors, diabetes mellitus with target-organ damage (HR = 3.727; 95% CI 1.380–10.07; p = 0.009), nephropathy of unknown origin (HR = 3.816; 95% CI 1.212–12.02; p = 0.022), and elevated class II anti-HLA antibody levels (HR = 1.125 per 1000 MFI; 95% CI 1.039–1.218; p = 0.004) were the strongest predictors of graft loss. When recipient GFR at three months post-transplant was included in the model, the significance of donor-related factors (GFR, ALT, AST) was negated. **Conclusion.** Recipient-related predictors of graft loss are diabetes mellitus, unknown etiology of initial CKD, high class II anti-HLA antibody levels, and reduced GFR at three months post-transplant. Donor-related predictors of graft loss are minimum GFR during the entire period of donor hospitalization and elevated ALT/AST levels; however, these factors become statistically insignificant when recipient GFR three months after KT is included in the model.

Keywords: kidney transplantation; expanded criteria donors; brain death; graft survival.

INTRODUCTION

Expanding organ donation criteria remains one of the key strategies in addressing the persistent shortage of transplants [1–3]. The United Network for Organ Sharing (UNOS) defines expanded criteria donors (ECDs) as kidney donors aged 60 years or older, or those aged 50–59 years who meet at least two of the following conditions: a history of hypertension, death resulting from an acute cerebrovascular accident, or a serum creatinine level greater than 1.5 mg/dL [4].

According to the registry of the Russian Transplant Society, postmortem organ donation continues to develop actively in Russia [5]. However, the contribution of ECDs to the overall donor pool, as well as the outcomes of such transplants, remains insufficiently studied at the national level. Large-scale studies that not only report on immediate postoperative outcomes but also analyze factors associated with adverse transplant outcomes are particularly scarce.

It is well established that long-term transplant outcomes are influenced by a complex interplay of donor-related factors (such as age, cause of death, kidney function, and histological changes) and recipient-related factors (including age, sensitization status, and comorbidities) [6]. However, the relative impact of these risks may vary significantly depending on the population, donor conditioning practices, organ procurement and preservation techniques, and immunosuppressive strategies.

Objective: to identify donor and recipient factors associated with the risk of loss of graft function in recipients of kidney grafts from expanded criteria donors diagnosed with brain death.

Corresponding author: Dmitry Bankeev. Address: 5/17, Vtoroy Botkinsky Proezd, Moscow, 125284, Russian Federation. Phone: (912) 743-09-97. E-mail: 79127430997@ya.ru

MATERIALS AND METHODS

A retrospective multicenter cohort study was conducted using data from the Moscow Organ Donation Coordination Center, Botkin Hospital. The database included 254 donors who met the UNOS expanded criteria between 2021 and 2022; in some cases, only one kidney was procured. Donor data were supplemented with information on 444 kidney transplant recipients obtained from participating transplant centers.

Statistical analysis

Descriptive statistics for qualitative variables are presented as absolute frequencies and percentages. Quantitative variables are described as the mean and standard deviation for distributions close to normal, and as the median with first and third quartiles for non-normal distributions. Normality was assessed through visual analysis of frequency histograms and quantile–quantile (Q–Q) plots.

The association between factors and the risk of graft loss was evaluated using Cox proportional hazards regression models. Effect sizes were expressed as hazard ratios (HR) with corresponding 95% confidence intervals (CI). The proportional hazards assumption was tested using Schoenfeld residuals and log(-log) survival plots. The linearity of continuous predictors with respect to the log hazard function was assessed using martingale residuals.

Residual plots and DFBETA statistics were jointly examined to identify influential observations. Multicollinearity among predictors was evaluated using correlation matrix analysis and variance inflation factors. Model comparison and selection were based on the Akaike Information Criterion (AIC), with lower values indicating better balance between model fit and complexity. The discriminative ability of the final model was quantified using Harrell's concordance index (C-index), representing the probability that, for any two randomly selected patients, the model correctly predicts which patient experiences the event first.

The sample size was not calculated and was limited by available data, including all donors who met the expanded criteria during 2021–2022.

Statistical significance was evaluated using a two-tailed test, with a p-value <0.05 considered statistically significant. All analyses were performed using R, version 4.5.1.

RESULTS

Donor factors

The mean age of donors was 58.3 ± 4.8 years (range: 50–74 years), with 155 (61%) being male. Mean body mass index (BMI) was 30.8 ± 5.9 kg/m^2 (range: 18.4–54.7 kg/m^2). A total of 37 donors (14.6%) had confirmed diabetes mellitus, and 171 (67.3%) had systemic atherosclerosis.

During hospitalization prior to organ procurement, norepinephrine was administered in 252 donors (99.2%) and epinephrine in 7 donors (2.8%). The maximum norepinephrine dose was 525 [330; 800] ng/kg/min (range: 60–3700 ng/kg/min), and the maximum epinephrine dose was 150 [75.5; 340] ng/kg/min (range: 10–1200 ng/kg/min). Successful cardiopulmonary resuscitation (CPR) was performed in 18 donors (7.1%).

GFR (CKD-EPI) in donors upon admission, at the minimum recorded value during hospitalization, and immediately before organ retrieval was 79.5 ± 21.0 mL/min/1.73 m^2 (range: 22.7–134.7), 70.2 ± 24.4 mL/min/1.73 m^2 (range: 10.1–134.7), and 73.8 ± 23.8 mL/min/1.73 m^2 (range: 10.1–134.7), respectively. Enzyme activity was also assessed upon admission and prior to organ retrieval. Alanine aminotransferase (ALT) level was 28.0 [23; 43] U/L (range: 7–406) and 28 [21; 46] U/L (range: 7–866), while aspartate aminotransferase (AST) level was 25.0 [18; 36] U/L (range: 5–413) and 24.5 [17; 36] U/L (range: 5–1090), respectively.

Multi-organ procurement was performed in 182 donors (71.7%), with a cold ischemia time of 14.4 [12.3; 17.0] hours (range: 6.9–26.0 hours).

In univariate analysis, donor gender, age, BMI, diabetes, systemic atherosclerosis, and level of vasopressor therapy (norepinephrine and epinephrine) were not significantly associated with the risk of kidney graft loss (Fig. 1). However, CPR and decreased GFR upon admission were associated with an increased risk of graft loss from any cause, as well as with loss of graft function. Additionally, minimum GFR values, maximum ALT and AST levels, and enzyme levels immediately prior to organ retrieval were associated with an increased risk of death-censored graft loss.

Recipient factors

Recipient mean age was 51.6 ± 9.6 years (range: 19–72 years), with 271 (60.2%) being male. BMI was 25.8 ± 4.5 kg/m^2 (range: 13.6–38.4 kg/m^2). A total of 337 recipients (78.4%) were undergoing maintenance hemodialysis prior to transplantation. Median duration of renal replacement therapy was 24 [12; 48] months (range: 1–240 months).

The most frequent comorbid conditions included ischemic heart disease in 73 recipients (17.0%), with a history of coronary artery stenting in 47 (10.9%), diabetes in 44 (10.2%), atrial fibrillation in 26 (6.0%), and chronic heart failure in 63 (14.7%).

Chronic kidney disease (CKD) was most commonly caused by chronic glomerulonephritis, identified in 179 recipients (41.6%). Other etiologies were considerably less frequent: autosomal dominant polycystic kidney disease in 61 (14.2%), diabetic nephropathy in 49 (11.4%), hypertensive nephropathy in 44 (10.2%),

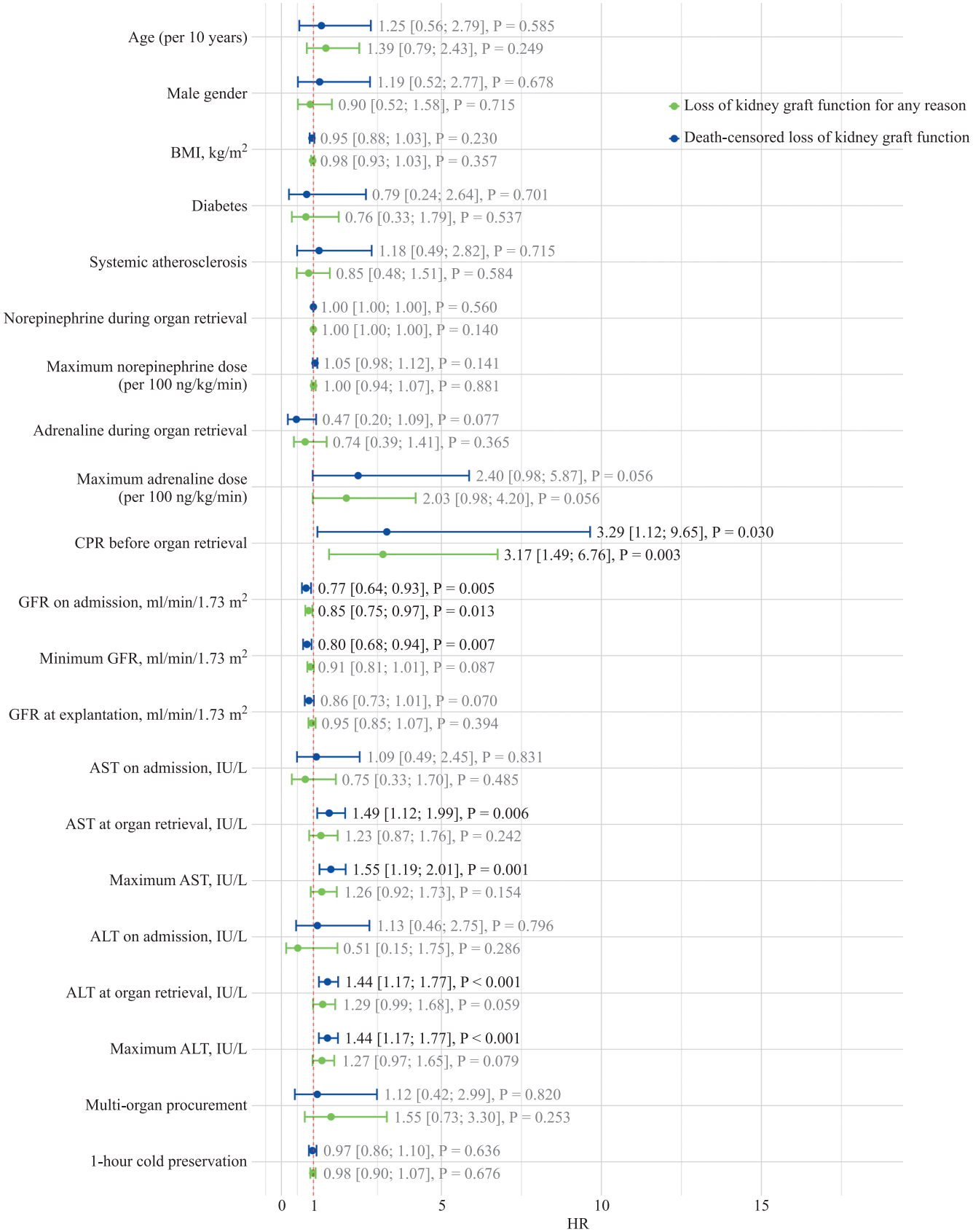

Fig. 1. Donor factors potentially associated with the risk of graft loss. BMI, body mass index; CPR, cardiopulmonary resuscitation; GFR, glomerular filtration rate (CKD-EPI); ALT, alanine aminotransferase; AST, aspartate aminotransferase. Hazard ratio (HR) estimates and 95% confidence intervals (CI) are shown. For GFR, estimates are presented per 10 mL/min/1.73 m^2; for ALT and AST – per 100 U/L

tubulointerstitial nephritis in 25 (5.6%), and secondary glomerulopathies in 22 (5.0%). Nephropathy of unknown origin was diagnosed in 55 recipients (12.2%), while other causes accounted for 15 cases (3.3%).

Class I anti- human leukocyte antigen (HLA) antibodies (mean fluorescence intensity [MFI] >500) were detected in 40 recipients (9.2%), with a median MFI of 2071.5 [1111.0; 3799.0] (range: 725–19,477 units). Class II with MFI >500 units were identified in 56 recipients (12.8%), with a median MFI of 2618 [1305.5; 7269.0] (range: 526–20,772 units).

Most patients (n = 362; 84.2%) received induction immunosuppression with basiliximab and methylprednisolone. Antithymocyte globulin combined with methylprednisolone was administered to 61 recipients (14.2%), while 4 (0.9%) received a triple combination of basiliximab, antithymocyte globulin, and methylprednisolone. Only 3 recipients (0.7%) received methylprednisolone alone.

The majority of recipients (n = 403; 93.9%) were maintained on standard triple immunosuppressive therapy, consisting of a calcineurin inhibitor, mycophenolate, and methylprednisolone.

Delayed graft function (DGF) occurred in approximately one-third of recipients (n = 147, 34.3%). Among these, the median number of hemodialysis sessions required before recovery of graft function was 3 [2; 6] (range: 1–26 sessions).

The mean eGFR (CKD-EPI) at discharge, and at 1, 3, 6, and 12 months post-transplant was 37.0 (17.9) mL/min/1.73 m^2 (range: 5.0–109.5), 40.0 (17.9) (range: 5.6–95.0), 44.8 (16.9) (range: 4.2–97.7), 46.4 (15.3) (range: 5.4–88.4), and 46.2 (15.8) mL/min/1.73 m^2 (range: 4.8–94.9), respectively.

In the univariate analysis, recipient age, ischemic heart disease, atrial fibrillation, chronic heart failure, and end-stage renal disease were associated with an increased risk of all-cause mortality but not with death-censored graft loss (Fig. 2). Nephropathy of unknown origin and elevated anti-HLA class I antibody levels were significantly associated with death-censored graft loss. In contrast, the presence of diabetes mellitus, higher anti-HLA class II antibody, DGF, a greater number of post-transplant hemodialysis sessions, and lower GFR were associated with an increased risk of both all-cause and death-censored graft loss.

In the multivariate analysis, we deliberately deviated from the commonly used but widely criticized stepwise predictor selection approach. Instead, predictors were grouped and included in the models based on the biological nature of the phenomena under study.

Tables 1–3 present the analysis of donor and recipient characteristics potentially associated with the risk of loss of graft function. Donor age, considered a key biological determinant, was not statistically significantly associated with graft function loss in any of the models (Models 1 and 2, Table 1). Successful CPR was associated with an increased risk of loss of graft function, but this association was observed only in the model that did not include donor GFR. Furthermore, ALT and AST levels, combined into a single composite variable using principal component analysis, demonstrated a significant association with the risk of loss of graft function. Among the three GFR indicators evaluated (upon admission, minimum recorded value, and before organ retrieval), the model incorporating the minimum GFR showed the best quality.

Among recipient-related factors, diabetes mellitus with target organ injury and nephropathy of unknown origin remained significantly associated with increased risk of loss of graft function, even after adjusting for MFI levels of both class I and class II anti-HLA antibodies. When evaluated separately, both class I and class II antibodies were significantly associated with the risk

Table 1

Multivariate analysis of factors potentially associated with the risk of loss of kidney graft function

Indicator	Model 1. AIC = 287.043, C-index = 0.574			Model 2. AIC = 283.788, C-index = 0.635			Model 3. AIC = 278.063, C-index = 0.630		
	HR	95% CI	P value	HR	95% CI	P value	HR	95% CI	P value
Donor age, per year	1.018	0.938; 1.105	0.668	1.011	0.931; 1.097	0.8			
Cardiopulmonary resuscitation (yes/no)	3.331	1.132; 9.800	**0.029**	2.287	0.753; 6.942	0.144			
Preservation time, per hour	0.966	0.853; 1.094	0.59	0.962	0.847; 1.093	0.554			
Minimum GFR, per mL/min/1.73 m^2				0.98	0.963; 0.997	**0.021**	0.981	0.965; 0.997	**0.023**
ALT, AST *							1.167	1.039; 1.311	**0.009**

* First principal component obtained from baseline AST and ALT values (principal component method). Reflects the total variation in AST and ALT levels. Abbreviations: GFR, glomerular filtration rate, estimated by creatinine clearance (CKD-EPI); AIC, Akaike information criterion.

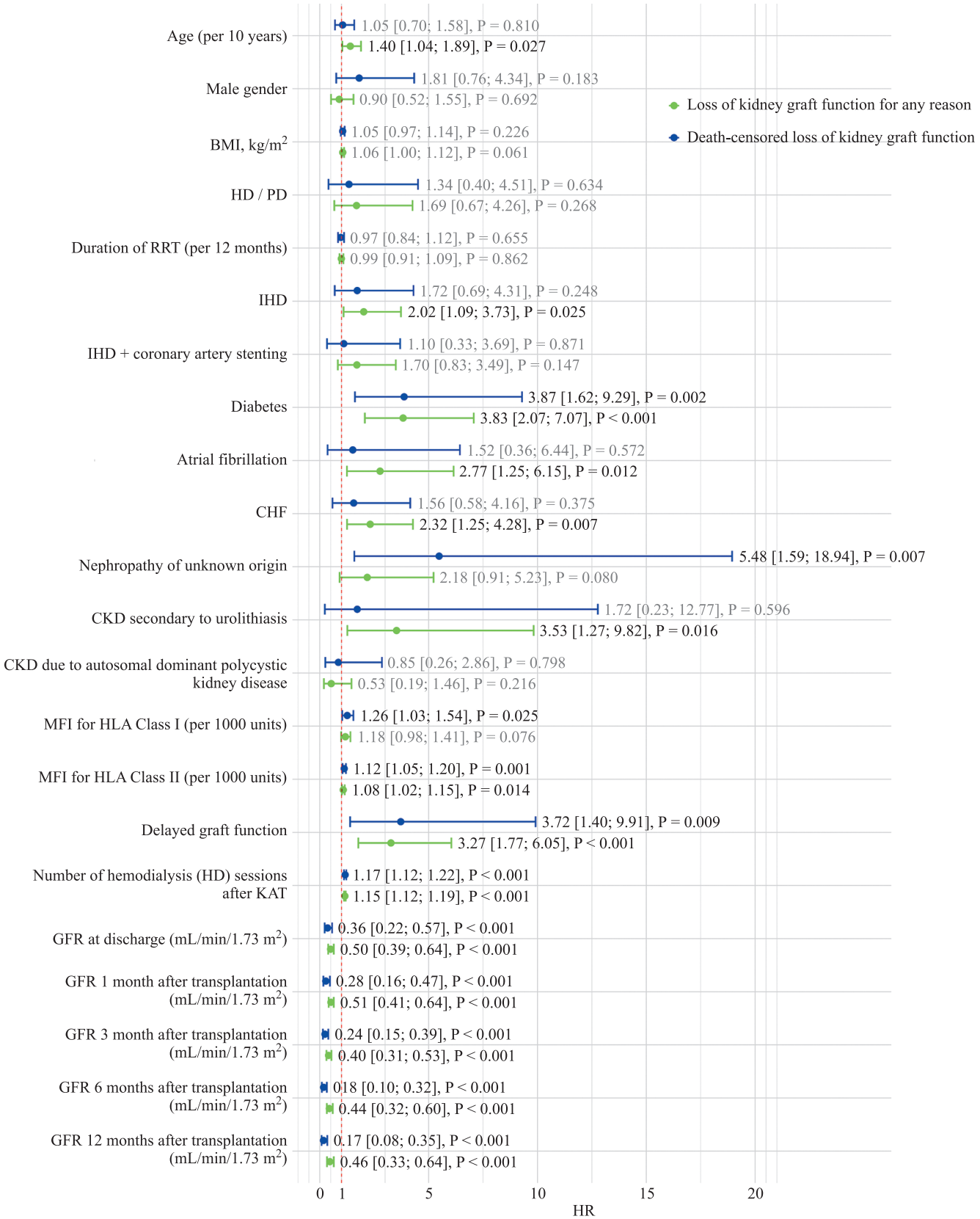

Fig. 2. Recipient factors potentially associated with the risk of kidney graft loss. HD, hemodialysis; PD, peritoneal dialysis; RRT, renal replacement therapy; IHD, ischemic heart disease; CKD, chronic kidney disease; CHF, chronic heart failure; KAT, kidney allotransplantation; GFR, glomerular filtration rate (CKD-EPI); MFI, mean fluorescence intensity; HLA, human leukocyte antigens. Hazard ratio (HR) estimates and 95% confidence intervals (CI) are presented. For GFR, estimates are provided per 10 mL/min/1.73 m^2

Table 2

Multivariate analysis of recipient characteristics potentially associated with the risk of loss of kidney graft function. Models 4 and 5

Indicator	Model 4. AIC = 279.880, C-index = 0.771			Model 5. AIC = 249.720, C-index = 0.801		
	HR	95% CI	P value	HR	95% CI	P value
Diabetes mellitus with damage to recipient's target organs (yes/no)	5.643	2.098; 15.18	**<0.001**	4.665	1.800; 12.09	**0.002**
Recipient nephropathy of unknown origin (yes/no)	4.218	1.412; 12.60	**0.01**	3.248	1.037; 10.18	**0.043**
ADPKD (yes/no)	1.601	0.433; 5.914	0.481			
Urolithiasis (yes/no)	3.134	0.395; 24.86	0.28			
MFI for HLA Class I (per 1000 units)				1.244	0.979; 1.581	0.073
MFI for HLA Class II (per 1000 units)				1.106	1.025; 1.193	**0.01**

Abbreviations: ADPKD, autosomal dominant polycystic kidney disease; MFI, mean fluorescence intensity; HLA, human leukocyte antigens; AIC, Akaike information criterion.

Table 3

Multivariate analysis of characteristics potentially associated with the risk of loss of kidney graft function (Models 6, 7, and 8)

Indicator	Model 6. AIC = 238.063, C-index = 0.830			Model 7, AIC = 147.515, C-index = 0.911			Model 8. AIC = 116.677, C-index = 0.952		
	HR	95% CI	P value	HR	95% CI	P value	HR	95% CI	P value
Minimum donor GFR, mL/min/1.73 m^2	0.982	0.965; 1.000	**0.045**	0.985	0.956; 1.016	0.344			
Donor ALT, AST*	1.208	1.063; 1.372	**0.004**	1.166	0.990; 1.373	0.066			
Diabetes mellitus with damage to recipient's target organs (yes/no)	3.727	1.380; 10.07	**0.009**	7.558	1.680; 33.99	**0.008**	6.833	2.053; 22.74	**0.002**
Recipient nephropathy of unknown origin (yes/no)	3.816	1.212; 12.02	**0.022**	7.162	1.587; 32.31	**0.01**	5.544	1.362; 22.56	**0.017**
MFI for HLA Class II (per 1000 units)	1.125	1.039; 1.218	**0.004**	1.424	1.208; 1.680	**<0.001**	1.129	1.030; 1.238	**0.01**
Delayed graft function (yes/no)				0.477	0.120; 1.895	0.293			
Recipient GFR three months after discharge, per mL/min/1.73 m^2				0.888	0.838; 0.940	**<0.001**	0.888	0.843; 0.935	**<0.001**

* First principal component obtained from baseline AST and ALT values (principal component method). Reflects the total variation in AST and ALT levels. Abbreviations: GFR, glomerular filtration rate (estimated by CKD-EPI creatinine equation); MFI, mean fluorescence intensity; HLA, human leukocyte antigens; AIC, Akaike information criterion.

of loss of graft function (data not shown in this study). However, when included in the same multivariate model, only the association with class II anti-HLA antibodies remained statistically significant (Table 2).

When the minimum donor GFR, donor ALT and AST levels, recipient diabetes mellitus with target organ damage, nephropathy of unknown origin, and class II anti-HLA antibody levels were simultaneously included in Model 6 (Table 3), all factors demonstrated a statistically significant association with the risk of off of graft function.

However, after incorporating post-transplant indicators, specifically DGF and recipient GFR at three months, the minimum donor GFR and ALT/AST levels were no longer significantly associated with risk. Moreover, simplifying the model by excluding these non-significant variables improved its overall performance

DISCUSSION

In none of the models was donor age found to be significantly associated with the risk of off of graft function. The donors in this study represented a broad age range (50–74 years). Although a decline in functional reserve is generally expected in older donors [7, 8], approximately half of the donors were between 55 and 62 years old. It is likely that the functional state of the kidneys is approximately the same in this age range [9].

One of the most important risk factors for graft loss identified in this study was minimum donor GFR, consistent with findings from previous research [10, 11].

ALT and AST levels also emerged as potentially important indicators. In multivariate models incorporating donor and recipient characteristics prior to transplantation or during the early postoperative period, elevated liver enzyme levels were associated with an increased risk of graft loss. The biological mechanisms underlying this association remain unclear. It is plausible that the relationship between enzyme levels and graft outcomes is indirect, mediated through factors such as metabolic syndrome, hepatic ischemia-reperfusion injury, or systemic inflammatory responses. Donors presenting with significantly elevated ALT and AST levels may therefore warrant more thorough assessment of kidney function prior to organ procurement. This observation needs further investigation.

Notably, after including recipient GFR measured three months post-transplant in the model, neither donor GFR nor donor ALT and AST levels remained significantly associated with the risk of graft loss. This finding suggests that recipient post-transplant GFR exerts a stronger influence on graft outcomes than donor-specific characteristics.

The associations observed between graft loss and recipient factors such as age, ischemic heart disease, atrial fibrillation, chronic heart failure, and end-stage renal disease appear to be mediated primarily through an increased risk of recipient mortality. This is supported by the observation that these factors were significantly associated only with all-cause graft loss, but not with death-censored graft loss. In this study, death-censored graft function was the most important factor as it provides an idea of the risk of losing kidney graft function at the individual. In contrast, overall graft survival, including all-cause loss due to any cause, provides information on graft outcomes at the population level but less directly captures the functional potential of the graft at the individual level.

The association between recipient diabetes and the risk of graft loss is well established [12]. Interestingly, nephropathy of unknown origin also demonstrated a statistically significant association with graft loss in multifactorial models (Models 6–8). This may be attributable to the higher incidence of recurrent graft pathology, as evidenced by the number of "on-demand" graft biopsies performed [13]. However, graft outcomes can vary widely depending on the underlying disease, such as recurrent IgA nephropathy [14] or focal segmental glomerulosclerosis [15], highlighting the critical need for accurate verification of CKD etiology in patients on the kidney transplant waiting list.

Based on these analyses, we developed an online application, accessible across platforms, designed to visualize the relationship between donor and recipient characteristics and the risk of graft loss [16].

STUDY LIMITATIONS

This study was retrospective in design. To enhance objectivity, no donors were excluded based on specific criteria; instead, all effective donors meeting the expanded criteria during the study period were included in the analysis.

The observation period in this study was limited to four years post-transplant, and therefore, the identified risk factors may primarily reflect medium-term outcomes.

When assessing graft function, we did not account for proteinuria, nor the potential overestimation of GFR due to hyperfiltration. Additionally, some potentially important factors, such as biopsy results, were not included because of limited observations, uncorrectable assumptions, or the inability to control for collider bias (Berkson's paradox).

CONCLUSION

The main risk factors for loss of kidney transplant function are recipient diabetes mellitus, nephropathy of unknown origin, and sensitization to HLA class II antigens. Donor age, although a key biological determinant, was not associated with the risk of graft loss. The effect of donor age on graft outcomes appears to be mediated through donor GFR. However, once recipient GFR measured three months post-transplant is included in the model, donor GFR no longer retains statistical significance.

The authors declare no conflict of interest.

REFERENCES

1. *Ferreira E, Costa J, Romãozinho C, Santos L, Macário F, Bastos C et al*. Long-Term Outcomes of Kidney Transplantation From Expanded-Criteria Deceased Donors: A Single-Center Experience. *Transplant Proc*. 2017 May; 49 (4): 770–776. doi: 10.1016/j.transproceed.2017.01.051.
2. *Maggiore U, Oberbauer R, Pascual J, Viklicky O, Dudley C, Budde K et al.* Strategies to increase the donor pool and access to kidney transplantation: an international perspective. *Nephrol Dial Transplant*. 2015 Feb; 30 (2): 217–222. doi: 10.1093/ndt/gfu212.
3. *Querard AH, Le Borgne F, Dion A, Giral M, Mourad G, Garrigue V et al.* Propensity score-based comparison of the graft failure risk between kidney transplant recipients of standard and expanded criteria donor grafts: Toward increasing the pool of marginal donors. *Am J Transplant*. 2018 May; 18 (5): 1151–1157. doi: 10.1111/ajt.14651.
4. *Metzger RA, Delmonico FL, Feng S, Port FK, Wynn JJ, Merion RM*. Expanded criteria donors for kidney transplantation. *Am J Transplant*. 2003; 3 Suppl 4: 114–125. doi: 10.1034/j.1600-6143.3.s4.11.x.
5. *Gautier SV, Khomyakov SM*. Organ donation and transplantation in the Russian Federation in 2022. 15th Report from the Registry of the Russian Transplant Society.

Russian Journal of Transplantology and Artificial Organs. 2023; 25 (3): 8–30. https://doi.org/10.15825/1995-1191-2023-3-8-30.

6. *Pascual J, Zamora J, Pirsch JD*. A systematic review of kidney transplantation from expanded criteria donors. *Am J Kidney Dis*. 2008 Sep; 52 (3): 553–586. doi: 10.1053/j.ajkd.2008.06.005.
7. *Cakmak U, Merhametsiz O, Ay N*. The Impact of Living Kidney Donor Glomerular Filtration Rate on Graft Survival. *Medicina (Kaunas)*. 2025 Mar 25; 61 (4): 580. doi: 10.3390/medicina61040580.
8. *Gaillard F, Courbebaisse M, Kamar N, Rostaing L, Del Bello A, Girerd S et al*. The age-calibrated measured glomerular filtration rate improves living kidney donation selection process. *Kidney Int*. 2018 Sep; 94 (3): 616–624. doi: 10.1016/j.kint.2018.05.016.
9. *Waas T, Schulz A, Lotz J, Rossmann H, Pfeiffer N, Beutel ME et al.* Distribution of estimated glomerular filtration rate and determinants of its age dependent loss in a German population-based study. *Sci Rep*. 2021 May 13; 11 (1): 10165. doi: 10.1038/s41598-021-89442-7.
10. *Irish GL, Coates PT, Clayton PA*. Association of Admission, Nadir, and Terminal Donor Creatinine With Kidney Transplantation Outcomes. *Kidney Int Rep*. 2021 May 15; 6 (8): 2075–2083. doi: 10.1016/j.ekir.2021.05.005.
11. *Bellini MI, Nozdrin M, Pengel L, Knight S, Papalois V*. How good is a living donor? Systematic review and meta-analysis of the effect of donor demographics on post kidney transplant outcomes. *J Nephrol*. 2022 Apr; 35 (3): 807–820. doi: 10.1007/s40620-021-01231-7.
12. *Liu C, Chen Q, Sun Z, Liang G, Yan F, Niu Y*. Pretransplant Diabetes Mellitus and Kidney Transplant Outcomes: A Systematic Review and Meta-Analysis. *Transplant Proc*. 2024 Dec; 56 (10): 2149–2157. doi: 10.1016/j.transproceed.2024.10.032.
13. *Stolyarevich ES, Zhilinskaya TR, Artyuhina (Rudakova) LYu, Kim IG, Tomilina NA*. Morphological structure of renal graft dysfunction depending on the time after transplantation. *Russian Journal of Transplantology and Artificial Organs*. 2018; 20 (S1): 102–103.
14. *Uffing A, Pérez-Saéz MJ, Jouve T, Bugnazet M, Malvezzi P, Muhsin SA et al.* Recurrence of IgA Nephropathy after Kidney Transplantation in Adults. *Clin J Am Soc Nephrol*. 2021 Aug; 16 (8): 1247–1255. doi: 10.2215/CJN.00910121.
15. *Uffing A, Pérez-Sáez MJ, Mazzali M, Manfro RC, Bauer AC, de Sottomaior Drumond F et al.* Recurrence of FSGS after Kidney Transplantation in Adults. *Clin J Am Soc Nephrol*. 2020 Feb 7; 15 (2): 247–256. doi: 10.2215/CJN.08970719.
16. Estimation of the probability of loss of renal graft function (web application). https://bankeevda.shinyapps.io/100725/.

The article was submitted to the journal on 23.06.2025

DOI: 10.15825/1995-1191-2025-4-57-66

IMPACT OF KIDNEY TRANSPLANTATION ON ERECTILE FUNCTION AND REPRODUCTIVE HEALTH IN MEN WITH CHRONIC KIDNEY DISEASE

S.S. Kariev[1], F.R. Nasyrov[1], Sh.Sh. Shavakhabov[1], S.Kh. Ibragimov[2], Z.T. Matkarimov[2], E.R. Ibadov[1]

[1] Republican Specialized Scientific and Practical Medical Center for Urology, Tashkent, Uzbekistan

[2] Republican Specialized Scientific and Practical Medical Center for Surgery, Tashkent, Uzbekistan

Objective: to evaluate the impact of kidney transplantation (KT) on erectile function and reproductive health in men with chronic kidney disease (CKD). **Materials and methods.** A prospective study was conducted involving 276 male patients (mean age 44.3 ± 5.8 years) with CKD who underwent KT from a living related donor. Erectile function was assessed using the International Index of Erectile Function (IIEF-5). Penile hemodynamics were evaluated by Doppler ultrasonography of the penile arteries, while hormonal status was determined by measuring serum testosterone, luteinizing hormone, and follicle-stimulating hormone (FSH) levels. Reproductive function was assessed by semen analysis and testicular volume measurements at five time points: baseline, at high azotemia, and at 3, 6, and 12 months post-transplantation. Management of post-transplant erectile dysfunction included phosphodiesterase type 5 inhibitors (IIEF-5, 5 mg daily for 3 months, followed by 20 mg on demand), pelvic floor muscle exercises, vacuum therapy, and physiotherapy. **Results.** After 12 months of follow-up, erectile function was fully restored in 65.6% of patients. The proportion of moderate-to-mild erectile dysfunction decreased to 9.4%, while mild dysfunction persisted in 25% of patients, primarily due to residual vascular, hormonal, and psychoemotional factors. The mean IIEF-5 score increased significantly from 13.2 ± 0.1 to 21.2 ± 0.2 ($p < 0.001$). The average peak systolic velocity in the right cavernous artery rose from 5.6 ± 0.1 cm/s to 7.2 ± 0.1 cm/s ($p < 0.001$). Serum testosterone levels increased from 4.6 ± 0.1 ng/ml to 5.6 ± 0.2 ng/ml ($p < 0.001$), and the proportion of patients with normospermia grew from 37.3% to 61.2% ($p < 0.001$). Erectile dysfunction persisted in 34.4% of patients despite therapy. **Conclusion.** The findings demonstrate a significant restoration of erectile function and fertility in most patients following KT and supported by comprehensive management of residual vascular, hormonal, and psychoemotional disorders.

Keywords: chronic kidney disease, erectile dysfunction, kidney transplantation, hormonal status, penile Doppler ultrasound, spermatogenesis.

INTRODUCTION

Erectile dysfunction (ED) is a significant complication of chronic kidney disease (CKD), affecting approximately 70–86% of patients, including those on hemodialysis (77–84%) and peritoneal dialysis (up to 84%) [1–3]. In recent decades, the mechanisms underlying ED and reproductive disorders in CKD have been actively investigated. These conditions are typically multifactorial, resulting from a combination of hormonal imbalances, uremic toxicity, vascular lesions, and metabolic problems. The importance of this issue extends beyond its physical consequences, as ED also profoundly affects patients' psycho-emotional state, often leading to social isolation and a reduced overall quality of life [4–6].

The effect of kidney transplantation (KT) on erectile function (EF) has drawn considerable attention, as KT not only prolongs survival but also enhances quality of life in patients with CKD. By normalizing hormonal function, KT can improve patients' sexual health (libido) [7–10]. However, the prevalence of ED after KT remains high at 46% [8, 11–13].

Data confirming the effect of KT on EF remain limited due to the small number of available studies, underscoring the need for further scientific research. The relevance of the present study lies in the comprehensive assessment of factors influencing EF recovery in patients after KT.

Unlike previous fundamental studies that focused on histological research, we presented clinically significant correlations between restoration of penile hemodynamics, hormonal balance, and spermatogenesis indicators. The novelty of this study lies in the integration of long-

Corresponding author: Sardor Ibragimov. Address: 10, Kichik Khalka Yuli str., Tashkent, 100115, Uzbekistan. Phone: 99 (890) 327-92-89. E-mail: dr.sardor.ibragimov@gmail.com

term prospective observation with a simultaneous evaluation of reproductive health and varicocele, an approach not previously implemented within a single research protocol. This methodology enabled us to identify key predictors of successful EF recovery that are relevant to clinical practice.

The aim of the study was to evaluate the effect of KT on EF and reproductive health in men with CKD.

MATERIALS AND METHODS

This study was based on a prospective analysis of treatment outcomes in 276 men with CKD who underwent KT from a living related donor at the Republican Specialized Scientific and Practical Medical Center for Surgery (Tashkent, Uzbekistan) and subsequently received treatment for ED at the Republican Specialized Scientific and Practical Medical Center for Urology (Tashkent, Uzbekistan).

Patient mean age was 34.9 ± 1.9 years. The majority (83.7%) were young adults (18–44 years), while 12.3% were middle-aged (45–59 years) and 4.0% were elderly (60–74 years).

The primary cause of stage 5 CKD was chronic glomerulonephritis (88.8%). Other causes included polycystic kidney disease (2.9%), CKD of unknown etiology (2.5%), urolithiasis (2.2%), chronic pyelonephritis (1.4%), type II diabetes mellitus, and congenital anomalies of the urinary tract (1.1% each).

The study complied with the Helsinki Declaration. All participants gave informed consent, and the study protocol was approved by the local ethics committee.

The inclusion criteria were as follows: men with preserved EF, a permanent sexual partner, stable graft function, and no concomitant diseases in the acute or decompensated stage (such as diabetes or stage II–III arterial hypertension).

The study design included the following stages of observation and EF assessment in patients with CKD:

– Baseline stage – assessment of EF status prior to development of severe renal failure.
– High azotemia stage – stage 5 CKD, characterized by accumulation of uremic toxins and systemic dysfunction, including impaired EF.
– Three months after KT – the first follow-up period, reflecting the early adaptation phase, initial stabilization of hormonal levels, and improvement in hemodynamic parameters.
– Six months after KT – mid-term assessment, during which further recovery of endothelial function and hormonal balance is expected.
– Twelve months after KT – long-term assessment to record the final therapeutic outcomes, including complete or partial restoration of EF.

To ensure data representativeness at the baseline stage (before the onset of severe chronic renal failure), the study included patients who had been registered at the transplant center as candidates for living-related KT and had undergone standard pre-transplant evaluation, including assessment of EF and reproductive health. This approach provided reliable baseline data before the onset of end-stage renal disease.

EF was evaluated using the International Index of Erectile Function (IIEF-5) questionnaire, with the following classification: severe ED (≤7), moderate (8–11), mild to moderate (12–16), mild (17–21), and no ED (22–25). Penile hemodynamics were assessed by ultrasound (US) with Doppler imaging of the penile arteries to determine the peak systolic velocity (PSV) in the cavernous and dorsal arteries. The hormonal profile – including serum testosterone, luteinizing hormone (LH), and follicle-stimulating hormone (FSH) – was analyzed using the enzyme-linked immunosorbent assay (ELISA) method. Testicular volume was measured using ultrasound and verified using an orchidometer. Reproductive function was evaluated by semen analysis, assessing the frequency of normospermia, asthenospermia, oligospermia, oligoasthenoteratozoospermia (OAT syndrome), and azoospermia among the study participants. Varicocele was diagnosed by scrotal ultrasound with Doppler imaging and classified according to severity (grades 1–3).

In the management of persistent ED after KT, patients received first-line therapy with phosphodiesterase type 5 (PDE-5) inhibitors – either sildenafil (5 mg daily) or tadalafil (2.5–5 mg daily) for an initial 3-month course. Thereafter, treatment was continued with standard therapeutic doses (sildenafil 20–50 mg or tadalafil 10–20 mg) administered on demand approximately 30 minutes before sexual intercourse. The pharmacological therapy was supplemented with a pelvic floor muscle exercise program to enhance penile blood flow, vacuum therapy (10 daily sessions followed by 12 sessions every other day), and physiotherapy sessions (15 minutes daily for 10 days).

Descriptive and comparative statistical methods were used to analyze the collected data. Data accumulation, correction, systematization, and visualization were performed using Microsoft Office Excel 2016. Statistical analysis was conducted with IBM SPSS Statistics v.26 (IBM Corporation, USA). Descriptive statistics were used to characterize the clinical and demographic parameters of patients, including the calculation of mean values (M), standard deviations (m), and percentage distributions. To evaluate statistically significant differences across the various stages of observation, a one-way analysis of variance (ANOVA) was applied. The chi-square test (χ^2) was used to analyze categorical variables.

RESULTS

In the initial period (before KT), according to the IIEF-5 scale, most patients (52.5%) had no signs of ED, while 47.5% had mild ED (Table 1).

However, at the high azotemia stage, all patients lost normal EF: 87.0% presented with mild to moderate ED, and 12.3% had moderate ED. Three months after KT, EF began to recover – the proportion of patients with mild to moderate ED decreased to 68.8%, while 21.7% showed mild ED.

After 6 months, 72.5% of recipients still had mild to moderate ED, 23.6% had moderate impairment, and 4.0% demonstrated mild ED. By 12 months post-transplant, 65.6% of patients had fully restored normal EF, while the proportion with moderate to mild ED declined to 9.4%, and mild ED persisted in 25.0% of cases.

An analysis of the mean IIEF-5 scores in the cohort of 276 KT recipients confirmed that patients with a transplanted kidney show EF recovery (Fig. 1).

The mean IIEF-5 score before KT was 21.6 ± 0.1, but it declined to 13.2 ± 0.1 at the high azotemia stage, indicating a marked deterioration in erection. In the first 3 months after KT, a partial improvement was observed (15.0 ± 0.1), followed by a further increase to 18.4 ± 0.2 after 6 months. By 12 months post-transplant, the index had almost returned to its preoperative level, reaching 21.2 ± 0.2. According to ANOVA, these changes were statistically significant ($F(4.1375) = 702.33$; $p < 0.001$), confirming a consistent trend of EF recovery (Fig. 1).

In parallel with EF improvement, penile blood flow also showed positive changes, as reflected by the increase in PSV in both the cavernous and dorsal arteries (Table 2).

The initial PSV values were 6.5 ± 0.1 cm/s in the right cavernous artery, 6.3 ± 0.1 cm/s in the left cavernous artery, and 12.4 ± 0.2 cm/s in the dorsal artery. At the high azotemia stage, these values decreased to 5.6 ± 0.1, 5.4 ± 0.1, and 10.7 ± 0.2 cm/s, respectively, indicating a deterioration in penile arterial blood flow.

During the first year after KT, gradual recovery of penile hemodynamics was observed. After 3 months, PSV increased to 5.8 ± 0.1, 5.7 ± 0.1, and 11.2 ± 0.2 cm/s; after 6 months, to 6.3 ± 0.1, 6.1 ± 0.1, and 12.1 ± 0.2 cm/s; and by 12 months, reached 7.2 ± 0.1, 7.1 ± 0.1, and 13.9 ± 0.2 cm/s, surpassing baseline levels. These differences were statistically significant according to ANOVA ($F(4.1375) = 194.69$; $p < 0.001$ for the right cavernous artery; $F(4.1375) = 68.40$; $p < 0.001$ for the left cavernous artery; $F(4.1375) = 43.09$; $p < 0.001$ for the dorsal artery).

Testicular volume showed no significant changes (Fig. 2).

Initially, the right testicular volume was 16.9 ± 0.2 cm^3, and the left was 12.8 ± 0.2 cm^3. At the high azotemia

Table 1

Erectile dysfunction (ED) severity according to the IIEF-5 scale at different stages of the study

ED severity (based on IIEF-5 score)		Baseline	High azotemia stage	3 months post-KT	6 months post-KT	12 months post-KT
Severe ED	n	0	0	0	0	0
	%	0.0%	0.0%	0.0%	0.0%	0.0%
Moderate ED	n	0	34	26	65	0
	%	0.0%	12.3%	9.4%	23.6%	0.0%
Moderate–mild ED	n	0	240	190	200	26
	%	0.0%	87.0%	68.8%	72.5%	9.4%
Mild ED	n	131	2	60	11	69
	%	47.5%	0.7%	21.7%	4.0%	25.0%
No ED	n	145	0	0	0	181
	%	52.5%	0.0%	0.0%	0.0%	65.6%
Total	n	276	276	276	276	276
	%	100.0%	100.0%	100.0%	100.0%	100.0%

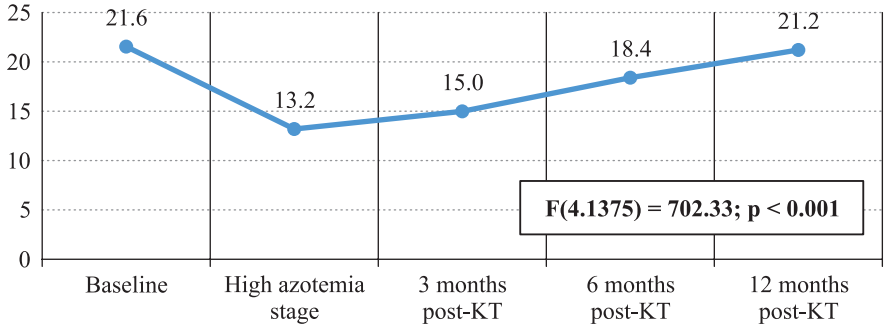

Fig. 1. Mean IIEF-5 scores in the kidney transplant group

stage, these values decreased slightly to 16.6 ± 0.2 cm^3 and 12.3 ± 0.2 cm^3, respectively. During the year following KT, only minor fluctuations were observed: after 3 months, the volumes remained nearly unchanged (16.5 ± 0.2 and 12.3 ± 0.2 cm^3); after 6 months, there was a modest increase to 16.8 ± 0.2 and 12.5 ± 0.2 cm^3; and by 12 months, the values slightly decreased again to 16.3 ± 0.2 and 12.1 ± 0.2 cm^3.

A statistically significant difference was noted only for the right testicle ($F(4.1375) = 3.66$; $p = 0.006$), whereas the left testicle showed no significant changes ($F(4.1375) = 2.09$; $p = 0.08$).

An analysis of hormonal status revealed a consistent trend in the dynamics of testosterone, LH, and FSH levels (Table 3). The testosterone level, initially 5.2 ± 0.2 ng/ml, decreased to 4.6 ± 0.1 ng/ml during high azotemia. Three months after KT, a slight increase was noted (4.7 ± 0.1 ng/ml), followed by further rises after 6 months (5.1 ± 0.1 ng/ml) and 12 months (5.6 ± 0.2 ng/ml) – ($F(4.1375) = 16.1$; $p < 0.001$).

LH level decreased from 8.9 ± 0.1 mIU/mL at baseline to 7.8 ± 0.1 mIU/mL with high azotemia, followed by a gradual increase to 8.0 ± 0.1 mIU/mL after 3 months, 8.6 ± 0.1 mIU/mL after 6 months, and 9.5 ± 0.1 mIU/mL after 1 year ($F(4.1375) = 81.2$; $p < 0.001$). A similar trend was observed for FSH, which decreased from 6.3 ± 0.1 to 5.5 ± 0.1 mIU/mL during high azotemia, followed by a recovery to 6.8 ± 0.1 mIU/mL after 12 months ($F(4.1375) = 22.5$; $p < 0.001$).

No cases of right-sided varicocele were identified at any stage of the study among all 276 patients. Analysis of left-sided varicocele (Fig. 3) showed that, initially, 22.1% of patients had grade 2 varicocele, with no cases of grade 3. However, at the stage of high azotemia,

Table 2

Mean peak systolic velocity (PSV) in the cavernous arteries during Doppler ultrasound examination

Study stage	Right cavernous artery (n = 276)	Left cavernous artery (n = 276)	Dorsal artery (n = 276)
	M ± m	M ± m	M ± m
Baseline	6.5 ± 0.1	6.3 ± 0.1	12.4 ± 0.2
High azotemia stage	5.6 ± 0.1	5.4 ± 0.1	10.7 ± 0.2
3 months post-KT	5.8 ± 0.1	5.7 ± 0.1	11.2 ± 0.2
6 months post-KT	6.3 ± 0.1	6.1 ± 0.1	12.1 ± 0.2
1 year post-KT	7.2 ± 0.1	7.1 ± 0.1	13.9 ± 0.2
ANOVA	$F(4.1375) = 194.7$; $p < 0.001$	$F(4.1375) = 68.4$; $p < 0.001$	$F(4.1375) = 43.1$; $p < 0.001$

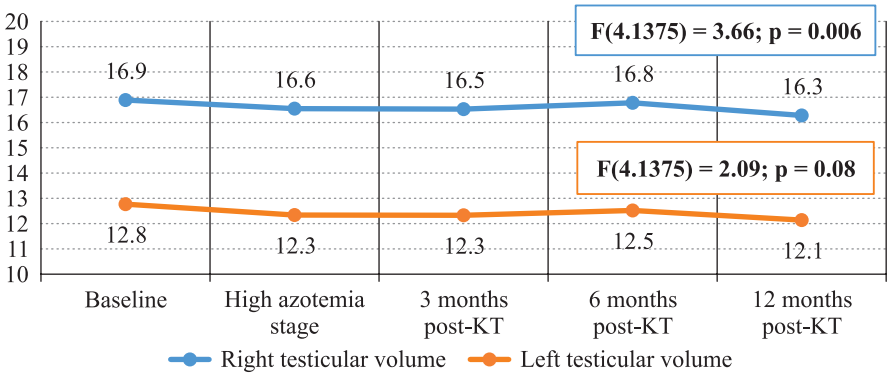

Fig. 2. Mean right and left testicular volumes in the kidney transplant group

Table 3

Mean serum levels of key hormones regulating reproductive function in the KT group

Stage	Testosterone (ng/mL, n = 276)	LH (mIU/mL, n = 276)	FSH (mIU/mL, n = 276)
	M ± m	M ± m	M ± m
Baseline	5.2 ± 0.2	8.9 ± 0.1	6.3 ± 0.1
High azotemia stage	4.6 ± 0.1	7.8 ± 0.1	5.5 ± 0.1
3 months post-KT	4.7 ± 0.1	8 ± 0.1	5.7 ± 0.1
6 months post-KT	5.1 ± 0.1	8.6 ± 0.1	6.1 ± 0.1
1 year post-KT	5.6 ± 0.2	9.5 ± 0.1	6.8 ± 0.1
ANOVA	$F(4.1375) = 16.1$; $p < 0.001$	$F(4.1375) = 81.2$; $p < 0.001$	$F(4.1375) = 22.5$; $p < 0.001$

22.1% of patients developed grade 3 varicocele, while grade 2 was not recorded.

After 3 months, the proportion of grade 3 left-sided varicocele decreased to 18.8%, and remained unchanged after 6 months ($\chi^2 = 76.5$; $p < 0.01$).

Significant changes were also observed in semen analysis (Fig. 4).

At the initial stage, normospermia was detected in 59.1% of patients, while asthenozoospermia – characterized by reduced sperm motility – was noted in 40.9%. Other spermatogenesis disorders (oligospermia, OAT syndrome, and azoospermia) were absent. At the high azotemia stage (stage 2), the proportion of normospermia decreased to 37.3%, while asthenozoospermia increased to 54.0%. Additionally, new cases of oligospermia (5.8%), OAT syndrome (1.8%), and azoospermia (1.1%) appeared, indicating suppression of spermatogenesis due to uremic intoxication and hormonal imbalance.

Three months after KT (stage 3), a slight improvement was noted: normospermia increased to 38.8%, asthenozoospermia decreased to 47.5%, though the incidence of OAT syndrome rose to 6.5%. After 6 months (stage 4), spermatogenesis showed marked recovery: normospermia increased to 52.9%, asthenozoospermia decreased to 35.1%, and the rates of oligozoospermia and OAT syndrome stabilized. By 12 months (stage 5), the recovery became most pronounced: normospermia reached 61.2%, exceeding baseline levels, while asthenozoospermia declined further to 27.5%. Although the proportion of oligospermia slightly increased to 7.2%, the rates of OAT syndrome (2.2%) and azoospermia (1.8%) continued to decline.

Thus, at the high azotemia stage (before KT), there was a marked deterioration in spermatogenesis, manifested by a decrease in normospermia and an increase in the frequency of pathological conditions, including asthenozoospermia, oligozoospermia, OAT syndrome, and azoospermia. Already 3 months post-transplant, improvement in the main indicators was evident, particularly an increase in the proportion of normospermia. After 6 and 12 months, there was a further restoration of fertility, with normospermia rising to 61.2% and asthenozoospermia decreasing to 27.5%.

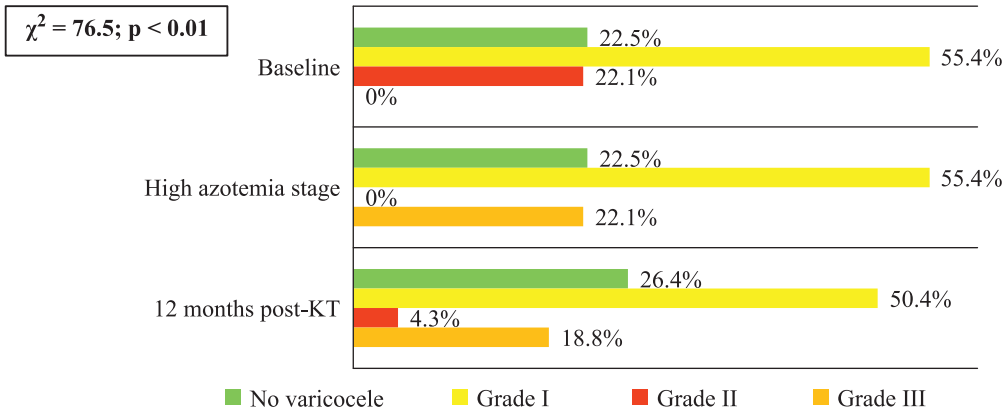

Fig. 3. Distribution of cases with or without left-sided varicocele in the kidney transplant group

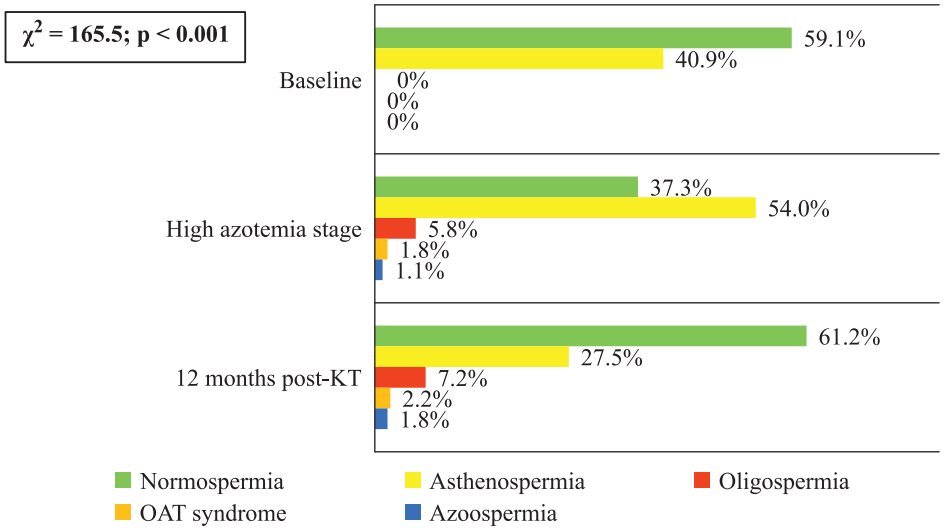

Fig. 4. Distribution of patients in the kidney transplant group according to changes in semen analysis parameters over time

The chi-square test for the distribution of spermogram types across KT stages yielded a value of $\chi^2 = 103.23$, with 16 degrees of freedom and $p < 0.001$, indicating statistically significant differences in the dynamics of spermogram parameters at various stages. These results confirm the positive effect of KT on the recovery of spermatogenesis and fertility potential in male patients.

Analysis of KT outcomes showed that 65.6% (181 of 276) of patients achieved complete restoration of EF within 1 year after KT, primarily due to normalization of vascular tone, improved cavernous arterial blood flow, and hormonal balance. However, 34.4% (95 of 276) of recipients continued to experience mild to moderate ED 1 year after KT, despite normalized renal function and improved systemic hemodynamics. These patients were categorized into five main groups according to factors that could explain why they still had ED (Table 4).

In the group of patients with vascular factors, the persistent ED was primarily attributed to long-term CKD, which led to irreversible vascular changes and progressive atherosclerosis. Clinically, these patients demonstrated a significant reduction in PSV in the cavernous arteries compared to those with restored EF. To correct ED, several therapeutic interventions were implemented. PDE-5 inhibitors (sildenafil, tadalafil) were prescribed, with a positive effect observed in 80% (24 of 30) of patients, while 20% showed no response due to severe vascular disorders. Additional management included statin and antiplatelet therapy to address systemic atherosclerosis, and the use of vasodilators (prostaglandin E1) in cases of severe arterial insufficiency, yielding a moderate effect in 36.7% (11 of 30) of patients. Physiotherapy programs, such as magnetotherapy and laser therapy, were also applied to improve regional blood flow, demonstrating 50% effectiveness (15 of 30). In two cases of advanced cavernous fibrosis, surgical treatment was performed in the form of penile implant surgery, while an additional 6 patients (20%) were indicated for this intervention.

In the group with persistent hormonal disorders, including hypogonadism and hyperprolactinemia (n = 25; 26.3%), several targeted therapeutic interventions were implemented. Testosterone replacement therapy was administered to patients with confirmed hypogonadism, resulting in clinical improvement in 72% (18 of 25) of cases. Dopamine agonists such as cabergoline and bromocriptine were prescribed for hyperprolactinemia, leading to positive dynamics in 80% (20 of 25) of patients. Additionally, metformin was used in individuals with insulin resistance, improving glucose and insulin sensitivity and indirectly enhancing EF in 40% (10 of 25) of cases.

Table 4

Summary of potential causes of persistent erectile dysfunction (ED) in kidney transplant recipients

Possible causes of persistent ED after KT	n	%
Vascular disorders (atherosclerosis, cavernous fibrosis, diabetic angiopathy)	30	31.6%
Hormonal and metabolic disorders (hypogonadism, hyperprolactinemia)	25	26.3%
Psychoemotional and neurological factors (depression, anxiety, polyneuropathy)	18	18.9%
Vascular anastomosis with the internal iliac artery leading to reduced penile blood flow	12	12.6%
Energy deficiency and sarcopenia (low body mass index, catabolic state)	10	10.5%

In the next group, comprising 18 of 95 patients (18.9%), the predominant factors were severe psychoemotional disturbances (depression, anxiety) and neurological disorders (polyneuropathy). Depression and anxiety contributed to psychogenic ED through reduced libido, whereas polyneuropathy disrupted nervous regulation of erections.

In this group, 61% of patients exhibited depressive disorders, 44% had sleep disorders, elevated cortisol levels, and chronic fatigue, while 28% reported reduced sensitivity in the penis and perineum. The therapeutic interventions included psychotherapeutic approaches such as cognitive-behavioral therapy and group therapy, which resulted in improvement in 50% of cases. The use of antidepressants (selective serotonin reuptake inhibitors in minimal doses) led to a positive effect in 65% of patients. Anxiolytics were administered when necessary to manage anxiety disorders, showing improvement in 45% of cases. Additionally, physiotherapy techniques aimed at stimulating peripheral nerve conduction (electrostimulation) improved nerve regulation in 35% of patients.

Patients with low BMI and sarcopenia (n = 10, 10.5%) had a general energy deficiency, which adversely affected endocrine function and erectile capacity. Mean BMI in this group was 18.9 kg/m^2, and serum albumin levels were below 3.5 g/dL, indicating a catabolic state. Testosterone level was approximately 25% lower than that of patients with restored EF. The therapeutic measures taken included: high-protein diet and nutritional support, resulting in a BMI increase of 1.5–2 kg/m^2 within 6 months; structured exercise programs (strength training), which produced an average muscle mass gain of 6% over 4 months; use of anabolic agents under endocrinological supervision, achieving improvement in 55% of cases; and correction of the catabolic state using amino acid complexes, leading to improvement in the general condition in 70% of patients.

Thus, 65.6% of patients recovered normal EF after KT, whereas 34.4% continued to experience moderate or mild ED associated with various etiological factors – vascular (31.6%), hormonal (26.3%), psychoemotional (18.9%), anatomical (12.6%), and energy deficiency (10.5%). Therapeutic correction included the use of PDE-5 inhibitors (80%), hormone therapy (72–80%),

psychotherapy (50–65%), physiotherapy (35–50%), nutritional support (70%), and surgical interventions (20%). Effective recovery required a comprehensive approach that addressed each patient's dominant risk factors.

It is also important to emphasize the influence of urological complications on EF recovery, observed in 8 recipients after KT. Among these, 4 patients (50%) had urinary tract obstruction, 2 (25%) were diagnosed with vesicoureteral reflux (VUR), and 2 (25%) had neurogenic urinary dysfunction. All patients in this subgroup presented with moderate to severe ED (IIEF-5: 12–18 points). Management of ureteral obstruction included endoscopic dilation (n = 3), neocystostomy (n = 1), PDE-5 inhibitor therapy (improvement in 3 out of 4 cases), physiotherapy (2 patients), and testosterone replacement therapy (1 patient).

Overall, for urological complications, a comprehensive treatment strategy, combining surgical correction, antibiotic therapy, physiotherapy, and vasoactive medications, proved effective in restoring EF. However, patients with severe vascular disorders may require penile implant surgery. These findings highlight that timely detection and correction of urological complications after KT increase the likelihood of EF recovery.

DISCUSSION

ED and reproductive disorders in patients with CKD and after KT remain pressing areas of clinical research due to their significant impact on patients' quality of life and overall health. In recent years, numerous studies have focused on developing diagnostic approaches to better identify and differentiate the underlying mechanisms of ED. Studies emphasize that hormonal and vascular abnormalities, including hypogonadism, hyperprolactinemia, and cavernous ischemia, play a leading role in the pathogenesis of persistent ED in this population [1, 3].

Despite the overall positive effect of KT, complete recovery of EF is not achieved in all recipients. According to Rahman et al., a systematic review demonstrated that KT leads to improved IIEF-5 scores, yet 20–50% of patients continue to experience varying degrees of ED post-transplant. The persistence of these disorders was primarily associated with long dialysis duration, advanced age, type of vascular anastomosis, and immunosuppressive therapy [7]. Similarly, Spirito et al. evaluated erectile and ejaculatory function at 6 and 12 months post-KT and observed a significant decline in sexual health quality at the 6-month follow-up, which remained stable throughout the year. In their cohort, the mean IIEF-5 score decreased significantly at 6 months ($p < 0.001$), remaining unchanged at 12 months ($p = 0.228$), correlating strongly with ejaculation disorders [14].

A study by El Hennawy et al. demonstrated that in patients with stage 5 CKD on dialysis, EF deteriorates; however, a positive trend is observed after KT. In their single-center crossover study, the authors assessed EF using the IIEF-5 one month before and one year after KT, revealing that KT recipients achieved significantly better results compared to dialysis patients [15].

In our study, the dynamics of IIEF-5 scores similarly showed a progressive recovery of EF after KT. Before transplantation, during the high azotemia stage, all patients exhibited varying degrees of ED. Twelve months post-KT, 65.6% of patients regained normal EF, confirmed by an increase in mean IIEF-5 scores from 13.2 ± 0.1 to 21.2 ± 0.2 ($p < 0.001$).

In addition to questionnaire-based assessments, laboratory parameters associated with the development of ED in CKD patients have been actively explored. Wang et al. reported that decreased testosterone levels and hyperprolactinemia are key risk factors for ED in this population [16], while Zhang et al. demonstrated that dyslipidemia and impaired glucose metabolism significantly contribute to vascular disorders underlying erectile impairment [17].

Miron et al. presented data showing that 70% of patients continued to experience ED 12 months after KT, despite normal laboratory values. In these cases, medication-related and vascular factors had a greater impact than testosterone or creatinine levels [12]. Antonucci et al. found that testosterone and prolactin levels were directly correlated with the severity of ED: 65% of patients with hypogonadism and hyperprolactinemia continued to experience moderate ED despite normal graft function [18].

A meta-analysis by Kang et al., which included 9 studies, showed that after KT, testosterone levels increased by an average of 1.1 ng/mL, prolactin levels decreased by 6.2 ng/mL, and the incidence of ED declined by 32% compared to patients on dialysis. These findings confirm the hormonal dependence of EF recovery following KT [19].

According to our data, patients after KT showed a consistent and statistically significant improvement in hormonal parameters: testosterone levels increased to 5.6 ± 0.2 ng/mL, exceeding baseline values; LH levels reached 9.5 ± 0.1 mIU/mL; and FSH levels reached 6.8 ± 0.1 mIU/mL.

Instrumental diagnostic methods, including pharmacodopplerography and shear wave elastography, are actively used to assess vascular alterations in patients with ED. Zhang et al. investigated the diagnostic potential of shear wave elastography in differentiating vasculogenic from non-vasculogenic ED. Their findings demonstrated that this method has high sensitivity and specificity for detecting fibrotic changes in the corpora cavernosa in patients with CKD and after KT [17].

Morphological studies of penile and testicular tissues also play an important role in understanding the pathogenesis of ED. Perri et al. analyzed cavernous body biopsies and identified pronounced fibrotic alterations that persisted even after successful KT, which may ex-

plain the persistence of ED in this patient group [20]. Similarly, Lundy et al. examined histological changes in the testes before and after KT and found that, despite the elimination of uremia, many patients continued to show signs of delayed spermatogenesis and morphological changes in Sertoli cells [21]. The same study confirmed that normalization of reproductive hormone levels after KT contributes to improvements in sperm parameters, including concentration, motility, and morphology of spermatozoa [21]. However, the use of immunosuppressive drugs – particularly calcineurin inhibitors and mTOR inhibitors – may adversely affect spermatogenesis and overall reproductive function.

In our study, we also examined vascular changes in ED by recording penile arterial blood flow dynamics using Doppler ultrasound. The results showed a gradual restoration of vascular perfusion following KT. By month 12, PSV exceeded baseline levels, reaching 7.2 ± 0.1 cm/s in the right cavernous artery, 7.1 ± 0.1 cm/s in the left cavernous artery, and 13.9 ± 0.2 cm/s in the dorsal artery, which correlated with an improvement in EF. All changes were statistically significant ($p < 0.001$).

Thus, both literature data and our findings confirm that KT promotes EF recovery in most patients with CKD, as evidenced by improvements in IIEF-5 scores, hormonal parameters, and penile arterial blood flow. After 12 months, normal EF was restored in 65.6% of patients, accompanied by increases in testosterone, LH, and FSH levels above baseline values. Enhanced vascular perfusion also correlated strongly with improved EF. However, a subset of patients continued to experience ED, primarily due to persistent vascular, hormonal, and medication-related factors. These results underscore the importance of a comprehensive diagnostic and therapeutic approach that includes hormonal and vascular monitoring, especially in the context of immunosuppressive therapy

However, our study has several limitations. The absence of a control group of dialysis patients limited the ability to perform a comparative analysis of the effects of different renal replacement therapies on erectile function. In addition, potential variations in the influence of specific immunosuppressive drugs on vascular and hormonal regulation were not considered.

CONCLUSION

The findings demonstrate that KT promotes effective restoration of EF and fertility in most patients, while targeted management of persistent vascular, hormonal, and psychoemotional disorders further enhances outcomes.

The authors declare no conflict of interest.

REFERENCES

1. *Efremov EA, Bekov RR, Dudareva AA, Krasnyak SS, Perlin DV.* Epidemiology and etiological factors of erectile dysfunction in patients on dialysis and after renal transplantation. *Russian Journal of Transplantology and Artificial Organs.* 2011; 13 (1): 50–55. (In Russ.). https://doi.org/10.15825/1995-1191-2011-1-50-55.
2. *Wang CJ, Cukor D, Johansen KL.* Sexual dysfunction among patients with chronic kidney disease. *Semin Nephrol.* 2021 Nov; 41 (6): 534–549. https://doi.org/10.1016/j.semnephrol.2021.10.006.
3. *Kadyrov ZA, Odilov AYu, Sadulloev FS.* Erectile dysfunction in kidney disease: a review of the literature. *Andrologiya i genital'naya khirurgiya = Andrology and Genital Surgery.* 2021; 22 (1): 13–20. (In Russ.). https://doi.org/10.17650/1726-9784-2021-22-1-13-20.
4. *Popov SV, Orlov IN, Grin' EA, Malevich SM, Gul'ko AM, Topuzov TM et al.* Erectile dysfunction: new technologies and approaches in diagnostics and treatment. *Urology Herald.* 2020; 8 (2): 78–92. (In Russ.). https://doi.org/10.21886/2308-6424-2020-8-2-78-92.
5. *Pizzol D, Xiao T, Yang L, Demurtas J, McDermott D, Garolla A et al.* Prevalence of erectile dysfunction in patients with chronic kidney disease: a systematic review and meta-analysis. *Int J Impot Res.* 2021 Jul; 33 (5): 508–515. https://doi.org/10.1038/s41443-020-0295-8.
6. *Kamalov AA, Matskeplishvili ST, Chaliy ME, Okhobotov DA, Sorokin NI, Strigunov AA et al.* Vascular erectile dysfunction: a comprehensive approach to diagnosis. *Experimental and Clinical Urology.* 2021; 14 (1): 68–76. https://doi.org/10.29188/2222-8543-2021-14-1-68-76.
7. *Rahman IA, Rasyid N, Birowo P, Atmoko W.* Effects of renal transplantation on erectile dysfunction: a systematic review and meta-analysis. *Int J Impot Res.* 2022 Aug; 34 (5): 456–466. https://doi.org/10.1038/s41443-021-00419-6.
8. *Pan J, Zheng Z, Wang W, Hu D, Yao R, Chen Y et al.* Time-dependent analysis of erectile dysfunction in kidney transplant recipients: insights from four distinct time periods. *BMC Infect Dis.* 2024 Jul 24; 24 (1): 728. https://doi.org/10.1186/s12879-024-09611-7.
9. *Schulz T, Niesing J, Homan van der Heide JJ, Westerhuis R, Ploeg RJ, Ranchor AV.* Great expectations? Pre-transplant quality of life expectations and distress after kidney transplantation: a prospective study. *Br J Health Psychol.* 2014 Nov; 19 (4): 823–838. https://doi.org/10.1111/bjhp.12081.
10. *Miron A, Stefan AE, Nistor I, Kanbay M, Covic A, Morosanu C, Covic A.* The impact of renal transplantation on sexual function in males with end-stage kidney disease: a systematic review and meta-analysis. *Int Urol Nephrol.* 2023 Mar; 55 (3): 563–577. https://doi.org/10.1007/s11255-022-03442-8.
11. *Muehrer RJ, Lanuza DM, Brown RL, Djamali A.* Sexual concerns among kidney transplant recipients. *Clin Transplant.* 2014 Nov; 28 (11): 1294–1302. doi: 10.1111/ctr.12454.
12. *Miron A, Nistor I, Moroșanu C, Siriţeanu L, Pricop C, Puia D, Covic A.* Prevalence, risk factors, and severity of erectile dysfunction following renal transplantation. *Int Urol Nephrol.* 2025 Apr; 57 (4): 1151–1173. https://doi.org/10.21203/rs.3.rs-5202315/v1.

13. *Miron A, Nistor I, Morosanu C, Siriteanu L, Covic A.* Clinical Implications and Risk Factors for Erectile Dysfunction in Kidney Transplant: A Single-Center Assessment. *Cureus.* 2023 Apr 24; 15 (4): e38088. https://doi.org/10.7759/cureus.38088.
14. *Spirito L, Manfredi C, Carrano R, Trinchieri A, Salemi F, Sciorio C et al.* Impact of Kidney Transplantation on Male Sexual Function: Results from a Ten-Year Retrospective Study. *J Sex Med.* 2020 Nov; 17 (11): 2191–2197. https://doi.org/10.1016/j.jsxm. 2020.07.014.
15. *El Hennawy HM, Safar O, Faifi ASA, Shalkamy O, Alqahtani Y, Nazer WE et al.* Does Kidney Transplantation Help Young Patients on Dialysis With Erectile Dysfunction? A Single-center Study. *Urology.* 2022 Nov; 169: 120–124. https://doi.org/10.1016/j.urology.2022.07.042.
16. *Wang Q, Guo Y, Zhang H, Qin X, Zhang C, Zhou W.* The value of shear wave elastography combined with red blood cell distribution width in evaluating arterial erectile dysfunction. *BMC Urol.* 2024 Sep 19; 24 (1): 205. https://doi.org/10.1186/s12894-024-01579-5.
17. *Zhang DK, Li YL, Guan JB, Li ZX, Sun M.* The feasibility study of shear wave elastography in the diagnosis of erectile dysfunction. *Sci Rep.* 2024 Nov 15; 14 (1): 28111. https://doi.org/10.1038/s41598-024-78849-7.
18. *Antonucci M, Palermo G, Recupero SM, Bientinesi R, Presicce F, Foschi N et al.* Male sexual dysfunction in patients with chronic end-stage renal insufficiency and in renal transplant recipients. *Arch Ital Urol Androl.* 2016 Jan 14; 87 (4): 299–305. https://doi.org/10.4081/aiua.2015.4.299.
19. *Kang J, Tian J, Lu Y, Song Y, Liu X.* Erectile function after kidney transplantation: A meta-analysis. *Transl Androl Urol*. 2020 Oct; 9 (5): 1967–1979. https://doi.org/10.21037/tau-20-604.
20. *Perri A, Izzo G, Lofaro D, La Vignera S, Brunetti A, Calogero AE, Aversa A.* Erectile Dysfunction after Kidney Transplantation. *J Clin Med.* 2020 Jun 25; 9 (6): 1991. https://doi.org/10.3390/jcm9061991.
21. *Lundy SD, Vij SC.* Male infertility in renal failure and transplantation. *Transl Androl Uro.* 2019 Apr; 8 (2): 173–181. https://doi.org/10.21037/tau.2018.07.16.

The article was submitted to the journal on 16.04.2025

DOI: 10.15825/1995-1191-2025-4-67-73

PEDIATRIC LIVER TRANSPLANTATION IN UZBEKISTAN: FIRST CLINICAL CASE AND OUTCOME ANALYSIS

K.O. Semash[1], T.A. Dzhanbekov[1], M.M. Nasyrov[1], A.R. Monakhov[2], P.M. Gadzhieva[2], S.A. Masyutin[2]

[1] National Children's Medical Center, Tashkent, Republic of Uzbekistan
[2] Shumakov National Medical Research Center of Transplantology and Artificial Organs, Moscow, Russian Federation

Background. Liver transplantation (LT) remains the only life-saving option for children with end-stage liver disease. In Uzbekistan, a national LT program was launched in 2018; however, pediatric LT had not been performed until recently. **Objective:** to report the first documented case of related pediatric LT in the Republic of Uzbekistan and to highlight key aspects of postoperative management, including rejection crises, recurrent autoimmune hepatitis (AIH), and the innovative use of bortezomib for treating steroid-resistant rejection. **Materials and methods.** A 15-year-old patient with liver cirrhosis secondary to AIH was selected for transplantation. The right hepatic lobe from a living donor was transplanted following comprehensive preoperative evaluation and preparation. The procedure involved surgical intervention followed by a multistage postoperative treatment protocol. **Results.** The transplant procedure was successful. However, in the early postoperative period, the patient developed a rejection crisis that proved resistant to standard therapy with glucocorticosteroids and antithymocyte globulin. Subsequent evaluation revealed a recurrent AIH. Bortezomib was administered as part of the therapeutic strategy, leading to normalization of laboratory parameters and restoration of graft function. **Conclusion.** This first case of pediatric LT in Uzbekistan demonstrates the feasibility of performing complex surgical interventions and managing challenging postoperative complications. The use of bortezomib for steroid-resistant rejection associated with AIH highlights a potentially promising therapeutic approach. These results mark an important step forward in the development of transplant care in the country.

Keywords: liver transplantation; pediatric liver transplantation; living-related liver transplantation; autoimmune hepatitis; acute transplant rejection; recurrent autoimmune hepatitis; bortezomib.

INTRODUCTION

Liver transplantation has proven to be a life-saving treatment for patients with end-stage liver disease, including pediatric patients [1, 2]. The first pediatric liver transplant (LT) was performed by Thomas Starzl in 1963 on a two-year-old child with biliary atresia [3]. Unfortunately, the patient died from uncontrolled intraoperative bleeding. Following this case, and until the early 1980s, the only technically feasible option for children was orthotopic transplantation of a whole liver from a deceased donor, whose organ size closely matched that of the recipient [4]. However, because of the limited availability of pediatric donors, up to 50% of children on waiting lists died before receiving a transplant [5].

The development of surgical techniques enabling the use of liver segments from adult donors revolutionized pediatric transplantation. A major milestone was the introduction of living donor liver transplantation (LDLT), with the first successful cases in children with biliary atresia reported in 1988 [6, 7]. Over time, related LDLT became a leading approach in many pediatric transplant programs worldwide [1]. In countries where organ donation from deceased donors was prohibited, LDLT remained the only available option [4]. Currently, the outcomes of pediatric LT have improved significantly due to advances in surgical techniques, perioperative management, and rehabilitation approaches [1, 8].

Uzbekistan, a developing country in Central Asia, initiated her LT program in 2018 with the support and direct involvement of Academician Sergey Gautier of the Russian Academy of Sciences. Despite this, notable progress was not achieved until 2021 [9]. By the end of 2023, only one medical center in the country regularly performed liver transplants [10]. Because of legislative restrictions prohibiting the use of organs from deceased donors, only LDLT is currently possible in Uzbekistan [11]. Furthermore, pediatric LT had not been performed in the country until very recently.

This paper presents a clinical observation of a related liver transplant in a child, performed at the National Children's Medical Center in Tashkent, Uzbekistan. To the best of our knowledge, this represents the first documented case of pediatric LT in the Republic of Uzbekistan.

Corresponding author: Konstantin Semash. Address: 294, Parkentskaya str., Yashnobod District, Tashkent, 100171, Uzbekistan. Phone: +998 (94) 090-89-05. E-mail: mail@doctorsemash.com

CLINICAL CASE

This clinical case was approved by the Ethics Committee of the National Children's Medical Center (protocol No. 55-56-24/29.12.2024). The patient's parents provided written informed consent for the use of medical data for scientific research, with full preservation of anonymity.

Examination and preparation for surgery

The 14-year-old boy was admitted to our center in October 2023 with complaints of progressive abdominal distension and blood in his stool. The patient had no history of liver disease or other significant comorbidities. Initial evaluation raised suspicion of chronic liver disease. The patient was referred for comprehensive diagnostic examination in accordance with our center's clinical protocol, including a complete blood count, biochemical profile, coagulation profile tests, and liver ultrasound.

Laboratory tests revealed cytolytic syndrome (ALT 115 U/L, AST 215 U/L), elevated bilirubin levels (63 μmol/L), hypoalbuminemia (28 g/L), and coagulopathy (INR 1.8, prothrombin index 44%, fibrinogen 1.65 g/L). Ultrasonography showed increased hepatic echogenicity, irregular liver contours, hepatosplenomegaly, and ascites.

Given the presence of gastrointestinal bleeding and evidence of portal hypertension, esophagogastroduodenoscopy (EGD) was performed, which revealed grade 3 esophageal varices according to the Paquet classification. Multislice contrast-enhanced computed tomography (MSCT) confirmed cirrhosis, hepatomegaly, splenomegaly, portal hypertension, and ascites.

Considering the endemic situation in Central Asia, viral hepatitis B and C were ruled out. Wilson's disease was also excluded. Autoimmune screening revealed high titers of antinuclear antibodies (ANAs), anti-smooth muscle antibodies (ASMAs), and anti-neutrophil cytoplasmic antibodies (ANCAs). Based on these findings, cirrhosis secondary to AIH (AIH) was diagnosed.

At the initial examination, the patient's MELD score was 20, which served as the basis for recommending LT. At that time, however, there were no pediatric LT programs in Uzbekistan, and the family had limited financial means to afford surgery abroad. Considering these circumstances, along with our team's prior experience in developing LT programs [9], we resolved to initiate a LT program at the National Children's Medical Center.

Preparation for the procedure – including acquisition of essential equipment, specialist training, and patient preparation – took one year. During this period, the patient remained under outpatient observation and received courses of conservative therapy in the hospital whenever his condition worsened. Given the patient's body weight (65 kg) and the presence of portal hypertension, potential donors for right-lobe liver transplantation were assessed, with a required graft-to-recipient weight ratio (GRWR) of at least 1%.

Following the established protocol [11], four potential donors were evaluated: the patient's father, mother, uncle, and aunt. The mother was excluded due to ABO incompatibility, while the uncle and aunt were deemed unsuitable because of hepatitis B infection. The father was identified as a suitable donor, with favorable vascular anatomy and a GRWR of 1.69%. However, his body mass index (BMI) was 34.6 kg/m^2 (106 kg at a height of 175 cm), and elastography revealed grade 2 steatosis. The father was recommended to adjust his diet and exercise. Over the course of a year, he successfully reduced his weight to 83 kg, lowering his BMI to 27.1 kg/m^2; repeat elastography revealed no steatosis.

Upon hospitalization for preoperative preparation in November 2024, the patient's MELD score had risen to 23. In view of coagulopathy, impaired hepatic synthetic function, and erosive changes in the gastric mucosa identified during control EGD, the patient received transfusions of fresh frozen plasma (FFP) and albumin, along with gastroprotective therapy. MSCT confirmed severe portal hypertension, portal vein dilation up to 2.8 cm, and splenomegaly.

Surgery

The surgical technique has been described in detail in our previous reports [9, 11]. The donor underwent right hemihepatectomy, with the surgery lasting for 435 minutes and intraoperative blood loss of 100 ml. The graft weighed 1006 g, corresponding to a GRWR of 1.65%. Primary warm ischemia time was 45 seconds. The graft was implanted into the recipient using the classic technique with complete clamping of the inferior vena cava. Cold ischemia time was 1 hour 35 minutes, and secondary warm ischemia time was 31 minutes. Arterial anastomosis was performed with a continuous twisted suture, and biliary reconstruction was carried out with a Roux-en-Y hepaticojejunostomy and biliary stent placement. The recipient's procedure lasted 665 minutes, with a total blood loss of 800 ml.

Postoperative rehabilitation

In the early postoperative period, the patient remained in the intensive care unit. Planned extubation was performed 8 hours after surgery, but 30 minutes later, the patient developed bronchospasm with oxygen desaturation to 56%, requiring reintubation. A second extubation attempt 3 hours later was successful.

By the end of the second postoperative day, the patient developed postoperative delirium, characterized by motor agitation, obsessive-compulsive behavior, limb tremors, and sleep disturbances. In view of thrombocytopenia and coagulopathy, MSCT and MRI of the brain were performed to rule out organic brain pathology, with

no abnormalities detected. Given the potential neurotoxic effects of tacrolimus, a neurologist recommended anticonvulsant therapy (valproic acid) and haloperidol to treat delirium. Electroencephalogram (EEG) monitoring excluded seizures or latent epileptic activity, leading to discontinuation of anticonvulsants. Delirium resolved only by postoperative day 6, and the patient was transferred to the ward on day 7.

Induction immunosuppressive therapy included basiliximab (days 0 and 4) and methylprednisolone (500 mg) after reperfusion. Tacrolimus was initiated at the end of postoperative day 3. Up to day 4, graft function steadily improved, with declining cytolysis markers and bilirubinemia. From postoperative day 4, however, bilirubin levels began to rise (predominantly direct fraction, Fig.), while cytolysis markers, alkaline phosphatase, and gamma-glutamyl transpeptidase continued to decrease. CMV hepatitis, hepatitis B and C, and biliary and vascular complications were ruled out. Due to thrombocytopenia and coagulopathy, a graft biopsy was not feasible. This increase in bilirubin was empirically attributed to acute rejection, and methylprednisolone pulse therapy (20 mg/kg/day for 3 days) was initiated on day 5, followed by tapering.

The lack of response suggested steroid-resistant rejection, prompting administration of equine antithymocyte globulin (ATG) at 1 mg/kg/day for 3 days. However, ATG was discontinued after the third dose due to severe side effects from ATG (polyneuropathy, headache, hypertension) and lack of therapeutic effect. Despite progressive hyperbilirubinemia, cytolysis and cholestasis markers remained stable.

Toxic liver injury, including tacrolimus-induced hepatotoxicity, was suspected. All potentially hepatotoxic drugs were discontinued, and tacrolimus was switched to azathioprine, but laboratory parameters did not improve.

Screening revealed recurrent AIH, with elevated antinuclear and antineutrophil cytoplasmic antibodies. During this period, the patient also developed progressive cytolytic syndrome (Fig.). A literature review identified several reports on the use of bortezomib for severe immune-mediated conditions [12–19].

The patient underwent plasmapheresis followed by subcutaneous bortezomib at a calculated dose of 1.31 mg/m^2. A sustained positive effect was observed by day 4 after the first dose: bilirubin levels decreased from 532 μmol/L to 276 μmol/L, and liver function normalized. The concomitant elevation of transaminases

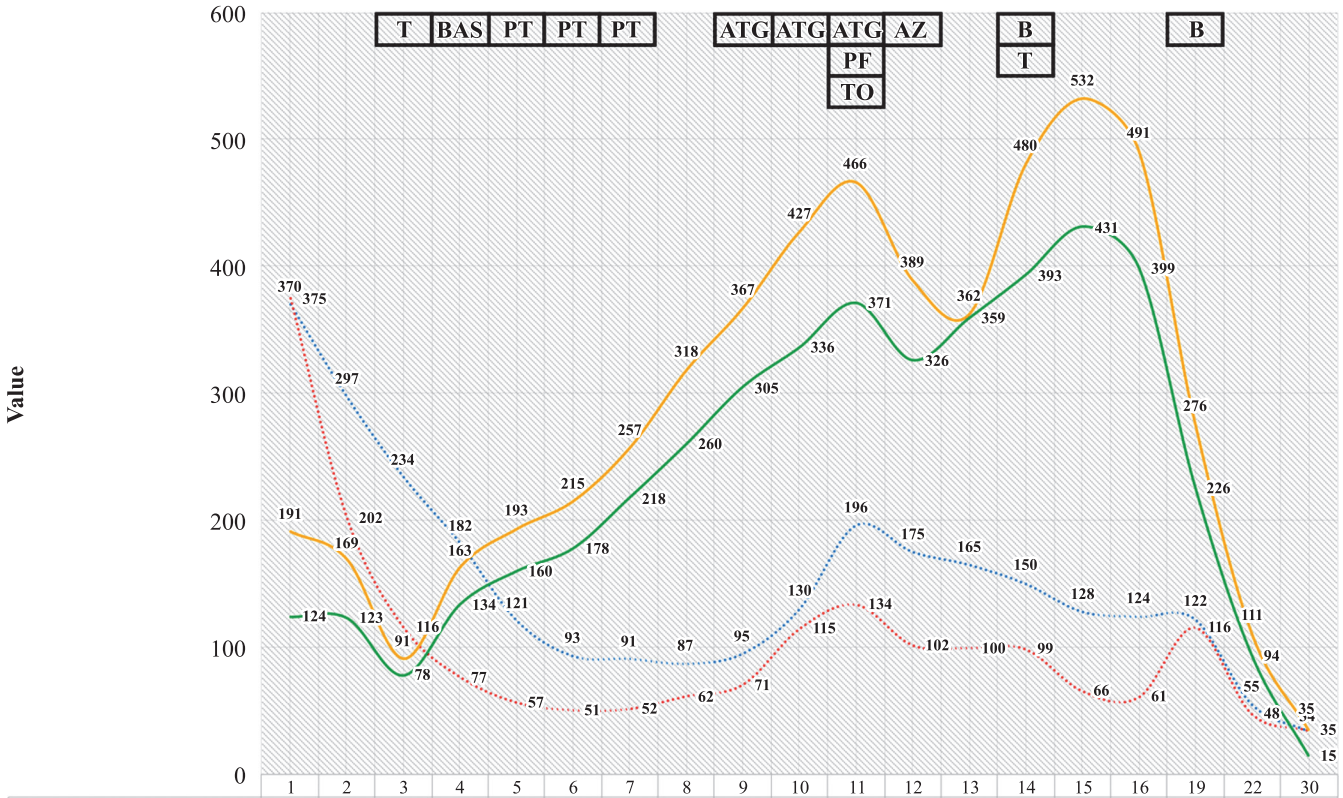

	1	2	3	4	5	6	7	8	9	10	11	12	13	14	15	16	19	22	30
ALT, U/L	370	297	234	182	121	93	91	87	95	130	196	175	165	150	128	124	122	55	34
AST, U/L	375	202	116	77	57	51	52	62	71	115	134	102	100	99	66	61	116	48	35
Total bilirubin, μmol/L	191	169	91	163	193	215	257	318	367	427	466	389	362	480	532	491	276	111	35
Direct bilirubin, μmol/L	124	123	78	134	160	178	218	260	305	336	371	326	359	393	431	399	226	94	15

Fig. Dynamics of laboratory parameters following living-related liver transplantation under different immunosuppressive regimens. Abbreviations: T, tacrolimus administration; BAS, basiliximab administration; PT, methylprednisolone pulse therapy; ATG, antithymocyte globulin administration; PF, plasmapheresis; TO, tacrolimus discontinuation; AZ, azathioprine administration; B, bortezomib administration

was attributed to tacrolimus toxicity, confirmed by a high plasma level (14.2 ng/dL). Immunosuppressive therapy was subsequently adjusted.

A second dose of bortezomib was administered seven days after the initial administration. By postoperative day 30, the patient's blood counts had fully normalized, and follow-up testing showed no detectable antinuclear or antineutrophil cytoplasmic antibodies.

The postoperative course was uneventful, with no surgical complications. He was discharged under outpatient follow-up. His current immunosuppressive regimen includes tacrolimus, methylprednisolone, and azathioprine.

DISCUSSION

This first successful pediatric LT in Uzbekistan marks a major milestone in the country's transplantation program. Until recently, pediatric LT had not been performed, and this achievement highlights the high level of training, coordination, and professionalism of the multidisciplinary team at the National Children's Medical Center.

What makes this case particularly noteworthy is not only the technical success of the transplantation itself but also the challenging postoperative course. The patient developed a rejection crisis that proved refractory to standard therapy with glucocorticosteroids and ATG, necessitating the use of innovative treatment approaches. The introduction of bortezomib was decisive in stabilizing the patient's condition and preventing graft loss.

Recurrent AIH following LT, although rare, represents a clinically significant complication requiring prompt detection and targeted intervention [12–14]. Literature reports indicate that the risk of post-transplant rejection in patients with AIH can reach up to 65%, while the risk of recurrent AIH is approximately 33% [11, 15, 16].

In this case, reactivation of the autoimmune process manifested as an isolated increase in bilirubin despite stable cytolysis and cholestatic enzyme levels, complicating the diagnostic process. We would like to emphasize that a definitive diagnosis could not be established due to the inability to perform a graft biopsy; however, international protocols support the possibility of diagnosis based on laboratory parameters alone [13], which was applied here.

Several risk factors for recurrent AIH were present in this patient, including young age, the presence of specific HLA alleles (notably HLA-DR3, associated with higher relapse risk), elevated autoantibody titers at the time of transplantation, and an HLA-DR3 mismatch between donor and recipient. Each of these factors is linked to recurrent AIH [12–16].

The use of bortezomib for steroid-resistant rejection and recurrent AIH appears promising, despite limited evidence in the literature [17–19]. Bortezomib, a proteasome inhibitor, induces apoptosis of plasma cells [17] and has been reported in some centers as effective for treating rejection unresponsive to conventional therapy after LT [18]. However, to our knowledge, no prior cases have described its use in pediatric LT. In this case, bortezomib administration resulted in normalization of bilirubin levels and full restoration of graft function.

Importantly, while a peak bilirubin level >461 μmol/L after transplantation is typically considered critical – with graft loss or patient death occurring in more than 95% of cases [20] – our patient, with a peak bilirubin of 532 μmol/L, achieved complete graft recovery. In our prior experience, we reported four cases of early acute rejection after LT [9], two of which were fatal, though none occurred in AIH patients. This case marks the first use of bortezomib in our practice.

The favorable outcome underscores the value of a multidisciplinary approach, involving surgeons, hepatologists, anesthesiologists, immunologists, neurologists, and intensive care specialists. The experience gained during this first pediatric LT in Uzbekistan will contribute to the development of a national transplant program and to improved treatment outcomes for children with end-stage liver disease.

This case highlights important directions for future research: optimizing immunosuppressive regimens, refining monitoring strategies for recurrent autoimmune disease, and defining the role of drugs such as bortezomib in managing post-transplant complications.

ACKNOWLEDGMENTS

The authors would like to express their deepest gratitude to:

– The Director of the National Children's Medical Center, **Bakhtiyar Umarov**, and the Deputy Director for Medical Care, **Shukhrat Salakhitdinov**, for their invaluable support in organizing and financing the transplant program.
– **Academician Sergey Gautier**, Director of the Shumakov National Medical Research Center of Transplantology and Artificial Organs, for his professional consultations and assistance in conducting the first pediatric liver transplant in Uzbekistan.
– **Davron Tulyaganov**, Director General of the Republican Scientific Center for Emergency Medical Care; **Umid Salimov**, Head of the Liver Transplant Program of the Republican Scientific Center for Emergency Medical Care; **Akrom Akhmedov**, transplant surgeon at the Vakhidov Republican Specialized Scientific and Practical Medical Center for Surgery; and **Abbos Adkhamov**, Director of the ShifoNur Clinic, for providing essential equipment required for the successful completion of the transplant.
– **Alla Syrkina**, neurologist at the Shumakov National Medical Research Center of Transplantology and Artificial Organs, for her expert neurological consultations during the postoperative period.

Your contributions were a vital link to the successful realization of the first pediatric liver transplantation in the Republic of Uzbekistan.

The authors declare no conflict of interest.

REFERENCES

1. *Gautier SV, Tsiroulnikova OM, Moysyuk YG, Akhaladze DG, Tsiroulnikova IE, Silina OV et al*. Liver transplantation in children: six-year experience analysis. *Russian Journal of Transplantology and Artificial Organs*. 2014; 16 (3): 54–62. (In Russ.). https://doi.org/10.15825/1995-1191-2014-3-54-62.
2. *Smith SK, Miloh T.* Pediatric Liver Transplantation. *Clin Liver Dis*. 2022; 26 (3): 521–535. https://doi.org/10.1016/j.cld.2022.03.010.
3. *Otte JB.* History of pediatric liver transplantation. Where are we coming from? Where do we stand? *Pediatr Transplant*. 2002; 6 (5): 378–387. https://doi.org/10.1034/j.1399-3046.2002.01082.x.
4. *Spada M, Riva S, Maggiore G, Cintorino D, Gridelli B*. Pediatric liver transplantation. *World J Gastroenterol*. 2009; 15 (6): 648–674. https://doi.org/10.3748/wjg.15.648.
5. *Martin BE, Ong EG*. Pediatric liver transplantation: an overview. *Pediatr Child Health*. 2017; 27 (12): 546–551. https://doi.org/10.1016/j.paed.2017.07.008.
6. *Strong RW, Lynch SV, Ong TH, Matsunami H, Koido Y, Balderson GA*. Successful liver transplantation from a living donor to her son. *N Engl J Med*. 1990 May 24; 322 (21): 1505–1507. https://doi.org/10.1056/NEJM199005243222106.
7. *Raia S, Nery JR, Mies S.* Liver transplantation from live donors. *Lancet*. 1989 Aug 26; 2 (8661): 497. https://doi.org/10.1016/s0140-6736(89)92101-6.
8. *Mogul DB, Luo X, Bowring MG, Chow EK, Massie AB, Schwarz KB et al*. Fifteen-Year Trends in Pediatric Liver Transplants: Split, Whole Deceased, and Living Donor Grafts. *J Pediatr*. 2018 May; 196: 148–153.e2. https://doi.org/10.1016/j.jpeds.2017.11.015.
9. *Semash K, Dzhanbekov T, Akbarov M, Mirolimov M, Usmonov A, Razzokov N et al.* Implementation of a living donor liver transplantation program in the Republic of Uzbekistan: a report of the first 40 cases. *Clin Transplant Res*. 2024; 38 (2): 116–127. https://doi.org/10.4285/ctr.24.0013.
10. *Porkhanov VA, Ismailov SI, Nazyrov FG, Popov AY, Babadzhanov AK, Lishchenko AN et al.* Rodstvennaya transplantatsiya pecheni v Respublike Uzbekistan: nyneshnee sostoyanie i perspektivy razvitiya [Living related liver transplantation in the Republic of Uzbekistan: current status and development prospects]. *Khirurgiia (Mosk)*. 2023; (11): 34–46. https://doi.org/10.17116/hirurgia202311134.
11. *Semash K.* Evaluation and Management of Living Donors in the Setting of Living Donor Liver Transplant Program in the Republic of Uzbekistan. *Exp Clin Transplant*. 2024; 22 (9): 664–674. https://doi.org/10.6002/ect.2024.0148.
12. *Montano-Loza AJ, Ronca V, Ebadi M, Hansen BE, Hirschfield G, Elwir S et al.* International Autoimmune Hepatitis Group (IAIHG). Risk factors and outcomes associated with recurrent autoimmune hepatitis following liver transplantation. *J Hepatol*. 2022 Jul; 77 (1): 84–97. https://doi.org/10.1016/j.jhep.2022.01.022.
13. *Patel YA, Henson JB, Wilder JM, Zheng J, Chow SC, Berg CL et al*. The impact of human leukocyte antigen donor and recipient serotyping and matching on liver transplant graft failure in primary sclerosing cholangitis, autoimmune hepatitis, and primary biliary cholangitis. *Clin Transplant*. 2018 Oct; 32 (10): e13388. https://doi.org/10.1111/ctr.13388.
14. *Harputluoglu M, Caliskan AR, Akbulut S*. Autoimmune hepatitis and liver transplantation: Indications, and recurrent and *de novo* autoimmune hepatitis. *World J Transplant*. 2022 Mar 18; 12 (3): 59–64. https://doi.org/10.5500/wjt.v12.i3.59.
15. *Montano-Loza AJ, Rodríguez-Perálvarez ML, Pageaux GP, Sanchez-Fueyo A, Feng S.* Liver transplantation immunology: Immunosuppression, rejection, and immunomodulation. *J Hepatol*. 2023 Jun; 78 (6): 1199–1215. https://doi.org/10.1016/j.jhep.2023.01.030.
16. *Mercado LA, Gil-Lopez F, Chirila RM, Harnois DM*. Autoimmune Hepatitis: A Diagnostic and Therapeutic Overview. *Diagnostics (Basel)*. 2024 Feb 9; 14 (4): 382. https://doi.org/10.3390/diagnostics14040382.
17. *Tajima T, Hata K, Okajima H, Nishikori M, Yasuchika K, Kusakabe J et al*. Bortezomib Against Refractory Antibody-Mediated Rejection After ABO-Incompatible Living-Donor Liver Transplantation: Dramatic Effect in Acute-Phase? *Transplant Direct*. 2019 Sep 19; 5 (10): e491. https://doi.org/10.1097/TXD.0000000000000932.
18. *Lee CF, Eldeen FZ, Chan KM, Wu TH, Soong RS, Wu TJ et al*. Bortezomib is effective to treat acute humoral rejection after liver transplantation. *Transplant Proc*. 2012 Mar; 44 (2): 529–531. https://doi.org/10.1016/j.transproceed.2012.01.051.
19. *Jiang H, Guo H, Yang B, Zhao Y, Wei L, Chen Z, Chen D.* Acute Antibody-Mediated Rejection in Liver Transplant Recipients with Autoimmune Liver Disease: A Clinical and Pathologic Study of 4 Cases. *J Pers Med*. 2023; 13 (1): 41. https://doi.org/10.3390/jpm13010041.
20. *Marubashi S, Dono K, Nagano H, Asaoka T, Hama N, Kobayashi S et al*. Postoperative hyperbilirubinemia and graft outcome in living donor liver transplantation. *Liver Transpl*. 2007 Nov; 13 (11): 1538–1544. https://doi.org/10.1002/lt.21345.

The article was submitted to the journal on 25.12.2024

DOI: 10.15825/1995-1191-2025-4-74-86

URGENT LVAD IMPLANTATION IN CHILDREN ON PERIPHERAL VA-ECMO SUPPORT

V.N. Poptsov, D.V. Ryabtsev, E.A. Spirina, A.A. Kuznetsova, V.V. Kolyadina, A.Ch. Chartaev, A.S. Epremian, A.K. Solodovnikova, A.S. Ignatkina, Ya.S. Karina

Shumakov National Medical Research Center of Transplantology and Artificial Organs, Moscow, Russian Federation

Background. Heart transplantation (HT) remains the primary surgical treatment for children with end-stage chronic heart failure (CHF). More than 30% of pediatric HT candidates require short- or long-term mechanical circulatory support (MCS) due to refractoriness to medical therapy. In recent years, the use of left ventricular assist device (LVAD) systems has expanded not only in teenagers and middle-aged children but also in younger and smaller patients. **Objective:** to investigate the perioperative course of emergency LVAD implantation in children with critical hemodynamic compromise (INTERMACS profile I) requiring short-term MCS via peripheral veno-arterial extracorporeal membrane oxygenation (VA-ECMO). **Materials and methods.** We studied 25 patients under 18 years of age (12 girls, 48.0%; 13 boys, 52.0%) who had a HeartMate III LVAD LVAD implanted between January 1, 2021, and June 30, 2024. The severity of pre-implantation CHF was classified according to INTERMACS profiles: I (n = 4, 16.0%), II (n = 9, 36.0%), and III (n = 12, 48.0%). Patients were divided into two groups based on the need for VA-ECMO prior to LVAD implantation: the VA-ECMO–LVAD group (n = 4, 16.0%) and the LVAD group (n = 21, 84.0%). **Results.** The VA-ECMO–LVAD group (n = 4) did not differ significantly from the LVAD group (n = 21) in age, sex, or underlying disease. Intraoperatively, there were no significant differences between groups in the duration of cardiopulmonary bypass, doses of sympathomimetic cardiotonics, or the use of inhaled nitric oxide. The VA-ECMO–LVAD group showed a trend toward greater intraoperative blood loss and transfusion requirements ($p > 0.05$). In the postoperative period, blood loss volumes were similar between groups. However, patients in the VA-ECMO–LVAD group more frequently required re-sternotomy (25% *vs* 9.5%, $p < 0.05$), had a longer duration of postoperative mechanical ventilation (1.79-fold, $p < 0.05$), more often required renal replacement therapy (2.5-fold, $p = 0.166$), and had significantly longer ICU stays (2.75-fold, $p = 0.041$). In the VA-ECMO–LVAD group, the incidence of severe acute right ventricular dysfunction was significantly higher (25.0% *vs* 9.5%, $p = 0.016$). No significant difference in postoperative hospital mortality was observed between the two groups. **Conclusion.** Emergency implantation of an LVAD system in children with critical hemodynamic instability requiring preoperative short-term MCS using peripheral VA-ECMO has demonstrated high effectiveness. However, careful consideration should be given to the presence and severity of multiple organ dysfunction before and after LVAD implantation, as well as perioperative blood loss. These factors largely determine the anesthetic and resuscitative management strategies, as well as the immediate outcomes of long-term MCS.

Keywords: pediatric heart failure, heart transplantation, mechanical circulatory support, VA-ECMO, left ventricular assist device, right ventricular dysfunction.

INTRODUCTION

Heart transplantation (HT) remains the primary surgical treatment for children of various age groups with end-stage chronic heart failure (CHF) [1]. More than 30% of children who are candidates for HT require some form of mechanical circulatory support (MCS), either short-term or long-term, due to refractoriness to drug therapy [2]. The choice of MCS method in children depends on multiple factors, including the urgency of intervention, the type and severity of intracardiac hemodynamic disorders, the degree of organ dysfunction, and the child's anthropometric parameters [3]. In recent years, there has been a marked increase in the implantation of left ventricular assist device (LVAD) systems not only in adolescents and middle-aged children but also in younger and smaller patients [4, 5].

In children with severe systemic hemodynamic disorders, veno-arterial extracorporeal membrane oxygenation (VA-ECMO) with central or peripheral cannulation remains the most commonly used method of short-term MCS. This technique enables rapid restoration of hemodynamics and stabilization of the patient's clinical condition [6]. In both adults and children presenting with critical hemodynamic instability corresponding to INTERMACS level I, VA-ECMO serves as an effective bridge to long-term MCS, including implantable left

Corresponding author: Vitaly Poptsov. Address: 1, Shchukinskaya str., Moscow, 123182, Russian Federation. Phone: (963) 644-96-39. E-mail: poptsov_vit@mail.ru

ventricular assist devices (iLVAD), or to heart transplantation [7, 8]. However, emergency LVAD implantation in pediatric patients at INTERMACS level I who require preoperative VA-ECMO is associated with an increased risk of postoperative complications and adverse outcomes [9].

The aim of this study was to investigate the perioperative course of emergency LVAD implantation in children with critical hemodynamic instability requiring pre-implantation peripheral VA-ECMO (pVA-ECMO) support (INTERMACS profile I).

MATERIALS AND METHODS

The study included 25 patients (<18 years of age), comprising 12 girls (48.0%) and 13 boys (52.0%), who had an LVAD implanted between 2021 and June 30, 2024. In all cases, the HeartMate III LVAD system was used. The age of the patients ranged from 5 to 17 years (mean 11.0 ± 3.5; median 11.5 [8.8; 14.0] years). Nine patients (36.0%) were between 5–10 years old, and sixteen (64.0%) were between 11–17 years old. Body weight ranged from 14.2 to 91 kg (mean 39.5 ± 20.2; median 34.5 [25.0; 54.0] kg), with 60% (n = 15) weighing less than 40 kg. Height ranged from 115 to 187 cm (mean 150.3 ± 23.2; median 154.0 [129.5; 163.5] cm), and 32% (n = 8) were shorter than 130 cm. Body surface area (BSA) ranged from 0.64 to 2.17 m^2 (mean 1.30 ± 0.47 m^2), with 56% (n = 14) having a BSA below 1.3 m^2. Body mass index (BMI) ranged from 10.4 to 26.2 kg/m^2 (mean 18.2 ± 5.1 kg/m^2).

The underlying cardiac pathologies leading to CHF were as follows: dilated cardiomyopathy in 22 patients (88.0%), hypertrophic cardiomyopathy in 2 (8.0%), and restrictive cardiomyopathy in 1 (4.0%).

The severity of pre-implantation CHF was classified according to the INTERMACS profiles: profile I in 4 patients (16.0%), profile II in 9 (36.0%), and profile III in 12 (48.0%).

In 4 patients (16.0%), 2 girls and 2 boys aged 12–14 years (mean 13.0 ± 0.8), pVA-ECMO was used prior to LVAD implantation due to critical systemic hemodynamic disorders (INTERMACS profile I).

All patients (n = 25) were divided into two study groups based on the need for pVA-ECMO before LVAD implantation: the VAECMO–LVAD group (n = 4, 16.0%) and the LVAD group (n = 21, 84.0%). A comparative analysis was conducted to evaluate differences in pre-implantation status, intraoperative parameters, and early postoperative outcomes between the two groups.

Data collection, statistical processing, and comparative analysis were performed using Microsoft Excel and IBM SPSS Statistics software. Quantitative variables were expressed as mean ± standard deviation (M ± SD) for normally distributed data or as median and interquartile range (Me [Q1; Q3]) for non-normally distributed data. The Student's t-test or Mann–Whitney U test was applied for comparison of continuous variables, depending on data distribution. Categorical variables were presented as numbers (n) and percentages (%) of the number of observations. For small sample sizes, quantitative observations were analyzed using Fisher's exact test.

STUDY RESULTS

The VA-ECMO–LVAD group (n = 4; 16.0%) did not differ significantly from the LVAD group (n = 21; 84.0%) in terms of age, sex, or underlying disease (Table 1). In both groups, the proportion of female patients was approximately 50%.

Patients in the VA-ECMO–LVAD group had significantly greater height, weight, BMI, and BSA compared with those in the LVAD group. Consistent with the critical nature of their pre-implantation condition, these patients also exhibited more severe manifestations of CHF, as reflected by a higher NYHA functional class: 4.0 ± 0.0 in the VA-ECMO–LVAD group versus 3.2 ± 0.7 in the LVAD group (p = 0.01).

In three of the four patients in the VA-ECMO–LVAD group, cannulation and connection to the pVA-ECMO circuit were performed in the operating room, while in one patient, these procedures were carried out in the intensive care unit during cardiopulmonary resuscitation (CPR). In this case, restoration of spontaneous cardiac activity and systemic hemodynamics was achieved only after initiation of extracorporeal support. The interval between the onset of conventional CPR and start of extracorporeal CPR was 24 minutes.

Prior to initiation of pVA-ECMO, systemic and central hemodynamic parameters in these patients (n = 4) were as follows: mean arterial pressure (mAP) – 49.2 ± 5.3 mmHg, central venous pressure (CVP) – 14.5 ± 4.9 mmHg, mean pulmonary artery pressure (mPAP) – 35.8 ± 12.7 mmHg, pulmonary artery wedge pressure (PAWP) – 27.8 ± 9.8 mmHg, and cardiac index (CI) – 1.46 ± 0.3 L/min/m^2. All patients required cardiotonic therapy, including dopamine (7.4 ± 2.1 μg/kg/min, n = 3), dobutamine (5.8 μg/kg/min, n = 1), and adrenaline (40.8 ± 11.8 ng/kg/min, n = 3).

Before initiation of short-term MCS, echocardiographic assessment showed a right ventricular size of 2.9 ± 0.5 cm, left ventricular end-diastolic volume (LVEDV) of 223.5 ± 38.3 mL, and left ventricular ejection fraction (LVEF) of 21.3 ± 7.2%. Laboratory parameters were as follows: pH – 7.301 ± 0.08, base excess (BEb) – –4.5 ± 0.7 mmol/L, blood lactate – 4.9 ± 1.4 mmol/L, urea – 9.9 ± 8.4 (7.4 [5.41; 11.9]) mmol/L, creatinine – 62.8 ± 40.2 (57.9 [33.9; 126.65]) μmol/L, total bilirubin – 84.8 ± 49.8 (84.6 [38.23; 100.5]) μmol/L, ALT – 502.6 ± 583.0 (300.5 [153.5; 649.0]) U/L, AST – 104.7 ± 47.6 (95.5 [80.75; 112.75]) U/L, and INR – 2.04 ± 0.22 (1.90 [1.93; 2.06]).

The duration of pVA-ECMO before LVAD implantation was 3.8 ± 0.9 days, with an extracorporeal blood

flow rate of 3.2 ± 0.9 L/min, or 1.8 ± 0.4 L/min/m^2. Before LVAD implantation, total bilirubin decreased to 69.6 ± 38.5 (69.15 [38.23; 100.5]) μmol/L (p = 0.648), ALT to 308.2 ± 370.0 (183.45 [89.18; 402.55]) U/L (p = 0.746), and AST to 68.8 ± 26.8 (62.10 [50.40; 80.44]) U/L (p = 0.241). A downward trend was also observed in international normalized ratio (INR) values to 1.71 ± 0.21 (1.65 [1.58; 1.78]) (p = 0.073), although these changes were not statistically significant.

In the LVAD-only group, 10 (47.6%) of 21 patients required intravenous cardiotonic therapy prior to implantation. Dopamine was administered in 6 patients (28.6%) at dosages of 2–12 μg/kg/min (mean 4.3 ± 3.9; median 3.0 [2.0; 4.0] μg/kg/min), and dobutamine in 4 patients (19.0%) at dosages of 1–5 μg/kg/min (mean 3.2 ± 1.8; median 3.0 [2.25; 4.0] μg/kg/min). The duration of preimplantation cardiotonic therapy ranged from 1–16 days, averaging 3.7 ± 1.9 days (median 2.75 [2.0; 5.0]).

Table 1

Demographic, anthropometric, and clinical characteristics of children before implantation of a left ventricular assist device (n = 25)

Indicator	Patient group		p-value
	VA-ECMO–LVAD	LVAD	
Count (n)	4	21	
Age, years M ± o Me [Q1; Q3]	 13.0 ± 0.8 13.0 [12.75; 13.25]	 10.6 ± 3.7 11.0 [7.0; 14.0]	0.253
Female n/%	 2/50.0	 10/47.6	1.0
Height, cm M ± o Me [Q1; Q3]	 171.3 ± 15.2 172.5 [162.0; 181.75]	 142.8 ± 20.5 144.0 [128.0; 158.0]	0.025
Weight, kg M ± o Me [Q1; Q3]	 68.3 ± 21.2 69.0 [54.5; 82.75]	 34.1 ± 15.1 32.0 [21.0; 38.0]	0.004
BMI, kg/m^2 M ± o Me [Q1; Q3]	 22.7 ± 3.3 23.0 [20.7; 25.0]	 15.5 ± 3.7 14.6 [12.9; 16.4]	0.006
Body surface area, m^2 M ± o Me [Q1; Q3]	 1.80 ± 0.36 1.80 [1.57; 2.04]	 1.17 ± 0.33 1.20 [0.89; 1.35]	0.008
Heart disease: DCM, n/% HCM, n/% RCM, n/% Other, n/%	 4/100 0/0.0 0/0.0 0/0.0	 17/80.9 1/4.8 1/4.8 2/9.5	1.00
Chronic HF severity (Strazhesko–Vasilenko classification) Stage IIa, n/% Stage IIb, n/% Stage 3, n/%	 0/0.0 1/25.0 3/75.0 0/	 6/2.8.6 11/52.4 4/19.0	
NYHA functional classification III IV M ± o Me [Q1; Q3]	 0/0.0 4/100 4.0 ± 0.0 0/0.0	 16/76.2 5/23.8 3.1 ± 0.7 0/0.0	0.010
INTERMACS, level I, n/% II, n/% III, n/% IV, n/% M ± o Me [Q1; Q3]	 4/100 0/0.0 0/0.0 0/0.0 4.0 ± 0.0 4.0 [4.0; 4.0]	 0/0.0 10/47.6 10/47.6 1/4.8 2.6 ± 0.6 3.0 [2.0; 3.0]	 <0.0001

Abbreviations: VA-ECMO, veno-arterial extracorporeal membrane oxygenation; LVAD, left ventricular assist device; BMI, body mass index; DCM, dilated cardiomyopathy; HCM, hypertrophic cardiomyopathy; RCM, restrictive cardiomyopathy; HF, heart failure; NYHA, New York Heart Association; INTERMACS, Interagency Registry for Mechanically Assisted Circulatory Support.

A comparative analysis of the pre-implantation status of patients in both groups revealed no statistically significant intergroup differences in central or systemic hemodynamic parameters (Table 2). However, patients in the VA-ECMO–LVAD group showed significantly lower levels of hemoglobin, erythrocytes, thrombocytes, and lactate in mixed venous blood, accompanied by significantly higher levels of leukocytes, total bilirubin, ALT, AST, and INR prior to LVAD implantation.

LVAD implantation was performed in all patients under cardiopulmonary bypass (CPB) conditions. The two groups did not differ significantly in CPB duration, doses of sympathomimetic cardiotonics, or the need for intraoperative inhaled nitric oxide therapy (Table 3). However, patients in the VA-ECMO–LVAD group exhibited a greater, though not statistically significant ($p > 0.05$), intraoperative blood loss and higher transfusion volumes.

Analysis of the postoperative period revealed that, despite the absence of differences in postoperative blood loss, patients in the VA-ECMO–LVAD group more often required re-sternotomy (25% vs. 9.5%, $p < 0.05$), had a 1.79-fold longer duration of postoperative mechanical ventilation ($p < 0.05$), a 2.5-fold higher need for renal replacement therapy ($p = 0.166$), and a 2.75-fold longer ICU stay ($p = 0.041$) compared with the LVAD group (Table 4).

In the VA-ECMO–LVAD group, the incidence of severe acute right ventricular failure (ARVF) was significantly higher compared with the LVAD group (25.0% vs. 9.5%, $p = 0.016$).

Table 2

Laboratory and biochemical parameters of children before implantation of a left ventricular bypass system (n = 25)

Indicator	Patient group		p-value
	VA-ECMO–LVAD	LVAD	
Count (n)	4	21	
mAP, mmHg M ± o Me [Q1; Q3]	 69.8.0 ± 5.3 69.5 [66.25; 73.0]	 66.0 ± 12.1 66.0 [62.0; 70.0]	0.548
HR, in min M ± o Me [Q1; Q3]	 127.0 ± 43.0 133.5 [106.25; 154.25]	 94.5 ± 21.5 95.0 [86.0; 106.0]	0.028
RAP, mmHg M ± o Me [Q1; Q3]	 7.3 ± 5.0 7.5 [4.50; 11.25]	 9.8 ± 4.7 9.0 [8.0; 11.0]	0.344
mPAP, mmHg M ± o Me [Q1; Q3]	 28.2 ± 19.0 25.0 [23.0; 34.75]	 30.4 ± 13.3 25.0 [20.0; 38.0]	0.853
PCWP, mmHg M ± o Me [Q1; Q3]	 19.5 ± 10.1 17.0 [15.5; 26.0]	 22.1 ± 9.3 20.0 [16.0; 27.0]	0.675
TPG, mmHg M ± o Me [Q1; Q3]	 8.7 ± 4.5 9.5 [6.5; 11.45]	 8.3 ± 5.8 6.0 [5.0; 11.0]	0.767
CI M ± o Me [Q1; Q3]	 1.86 ± 0.98 1.64 [1.16; 2.38]	 1.91 ± 0.55 1.9 [1.60; 2.60]	0.850
PVR, Wood's unit M ± o Me [Q1; Q3]	 2.61 ± 1.26 2.56 [1.50; 3.88]	 3.74 ± 2.38 2.71 [1.73; 6.23]	0.208
Hemoglobin, g/L M ± o Me [Q1; Q3]	 97.8 ± 9.4 96.0 [91.25; 102.5]	 122.1 ± 14.7 122.0 [111.0; 133.0]	0.004
RBC, $\times 10^{12}$/L M ± o Me [Q1; Q3]	 3.71 ± 0.93 3.52 [3.33; 3.91]	 4.47 ± 0.54 4.60 [4.13; 4.80]	0.030
WBC, $\times 10^{9}$/L M ± o Me [Q1; Q3]	 12.5 ± 4.3 12.0 [9.58; 14.88]	 7.94 ± 1.85 7.70 [6.40; 9.10]	0.019
Platelets, $\times 10^{9}$/L M ± o Me [Q1; Q3]	 94.0 ± 60.3 100.5 [59.0; 135.50]	 285.1 ± 89.1 284.0 [202.0; 344.0]	0.0002

End of Table 2

Indicator	Patient group		p-value
	VA-ECMO–LVAD	LVAD	
Urea, mmol/L M ± o Me [Q1; Q3]	 9.9 ± 8.4 7.40 [5.41; 11.88]	 7.8 ± 3.8 7.10 [4.99; 9.02]	0.344
Creatinine, μmol/L M ± o Me [Q1; Q3]	 62.8 ± 40.2 57.88 [83.99; 86.65]	 53.3 ± 10.7 52.00 [48.6; 60.7]	0.334
Total bilirubin, μmol/L M ± o Me [Q1; Q3]	 69.6 ± 38.5 69.15 [38.23; 100.5]	 18.7 ± 7.4 16.38 [13.20; 24.23]	0.002
ALT, U/L M ± o Me [Q1; Q3]	 308.2 ± 370 183.45 [89.18; 402.55]	 52.7 ± 100.0 22.3 [10.3; 31.6]	0.0044
AST, U/L M ± o Me [Q1; Q3]	 68.8 ± 26.8 62.10 [50.40; 80.44]	 58.8 ± 66.5 33.0 [25.19; 47.0]	0.081
Total protein, g/L M ± o Me [Q1; Q3]	 65.1 ± 4.3 66.25 [53.88; 67.45]	 69.0 ± 7.5 70.0 [63.40; 76.30]	0.236
INR M ± o Me [Q1; Q3]	 1.71 ± 0.21 1.65 [1.58; 1.78]	 1.41 ± 0.46 1.30 [1.10; 1.15]	0.029
pH (venous) M ± o Me [Q1; Q3]	 7.38 ± 0.08 7.40 [7.30; 7.40]	 7.37 ± 0.08 7.40 [7.30; 7.42]	0.821
Base excess (BE), mmol/L M ± o Me [Q1; Q3]	 –0.31 ± 2.66 –0.30 [–0.95; 1.15]	 0.65 ± 3.65 1.10 [–2.03; 3.73]	0.624
Sodium (Na), mmol/L M ± o Me [Q1; Q3]	 138.8 ± 8.4 136.0 [135.00; 139.75]	 135.9 ± 3.4 136.0 [134.00; 137.00]	0.85
Lactate, mmol/L M ± o Me [Q1; Q3]	 1.50 ± 0.57 1.30 [1.10; 1.70]	 1.05 ± 0.37 1.0 [0.80; 1.10]	0.041
PvO_2, mmHg M ± o Me [Q1; Q3]	 39.4 ± 6.4 39.00 [35.15; 43.25]	 36.7 ± 5.9 35.6 [36.50; 44.00]	0.543
SvO_2, % M ± o Me [Q1; Q3]	 70.05 ± 5.82 69.25 [65.35; 73.95]	 61.39 ± 9.61 59.40 [54.80; 64.90]	0.045

Abbreviations: VA-ECMO, veno-arterial extracorporeal membrane oxygenation; LVAD, left ventricular assist device; mAP, mean arterial pressure; HR, heart rate; RAP, right atrial pressure; mPAP, mean pulmonary artery pressure; PCWP, pulmonary capillary wedge pressure; TPG, transpulmonary gradient; CI, cardiac index; PVR, pulmonary vascular resistance; RBC, red blood cells; WBC, white blood cells; ALT, alanine aminotransferase; AST, aspartate aminotransferase; INR, international normalized ratio; PvO_2, mixed venous partial pressure of oxygen; SvO_2, mixed venous oxygen saturation.

Table 3

Intraoperative parameters in children undergoing LVAD implantation (n = 25)

Indicator	Patient group		p-value
	VA-ECMO–LVAD	LVAD	
Count (n)	4	21	
CPB duration M ± o Me [Q1; Q3]	 80.5 ± 18.0 75.0 [67.0; 88.50]	 87.9 ± 42.6 78.0 [69.00; 90.00]	0.739
Intraoperative blood loss, mL M ± o Me [Q1; Q3]	 1375.0 ± 914.2 1200.0 [800.0; 1775.0]	 605.3 ± 624.7 400.0 [300.0; 700.0]	0.046

End of Table 3

Indicator	Patient group		p-value
	VA-ECMO–LVAD	LVAD	
RBC transfusion n/% mL	4/100 692.5 ± 167.4 650.0 [607.50; 735.00]	13/61.9 422.4 ± 149.1 340.0 [310.0; 602.5]	0.001
FFP transfusion, n/% mL	4/100 1102.5 ± 347.6 1230.0 [1005.0; 1327.5]	21/100 767.7 ± 264.8 760.0 [570.0; 1000.0]	0.001
Platelet transfusion n/% mL	3/75.0 276.7 ± 40.4 300.0 [265.0; 300.0]	4/19.0 185.0 ± 69.5 185.0 [127.5; 242.5]	0.019
iNO therapy n/% ppm	4/100 17.5 ± 5.0 20.0 [17.5; 20.0]	12/57.1 20.3 ± 6.9 20.0 [19.28; 20.00]	0.260
Adrenaline (end of surgery) n/% mcg/kg/min	3/75.0 30.0 ± 10.0 30.0 [25.0; 35.0]	8/38.1 28.9 ± 23.7 20.0 [10.0; 40.0]	0.288 0.929
Dopamine (end of surgery) n/% mcg/kg/min	4/100 5.8 ± 0.5 6.0 [5.75; 6.00]	12/57.1 4.6 ± 2.4 4.0 [4.0; 4.0]	0.260 0.337
Dobutamine (end of surgery) n/% mcg/kg/min	1/25 2.0	7/33.1 4.1 ± 2.3 20.0 [10.0; 40.0]	0.267

Abbreviations: VA-ECMO, veno-arterial extracorporeal membrane oxygenation; LVAD, left ventricular assist device; CPB, cardiopulmonary bypass; RBC, red blood cell; FFP, fresh frozen plasma; iNO, inhaled nitric oxide.

Table 4

Postoperative parameters in children after LVAD implantation (n = 25)

Indicator	Patient group		p-value
	VA-ECMO–LVAD	LVAD	
Count (n)	4	21	
Resternotomy n/%	1/25	2/9.5	0.016
Blood loss, mL M ± o Me [Q1; Q3]	400.0 ± 173.2 300.00 [300.00; 375.00]	397.9 ± 164.9 320.00 [300.00; 500.00]	0.991
Mechanical ventilation, hours M ± o Me [Q1; Q3]	21.3 ± 13.1 17.50 [6.25; 27.0]	11.89 ± 7.2 7.0 [5.0; 19.0]	0.047
Adrenaline therapy, days M ± o Me [Q1; Q3]	5.0 ± 4.2 3.0 [2.50; 5.50]	4.2 ± 2.9 3.5 [2.0; 5.75]	0.641
Right ventricular bypass n/%	1/25	2/9.5	0.016
RRT (CVVHDF) n/%	2/50	3/14.3	0.166
WBC (max), $\times 10^9$/L M ± o Me [Q1; Q3]	18.9 ± 9.6 16.00 [14.55; 19.75]	16.1 ± 5.6 16.5 [13.05; 19.45]	0.421
Platelets (min), $\times 10^9$/L M ± o Me [Q1; Q3]	55.0 ± 52.4 77.0 [33.5; 115.25]	108.6 ± 43.1 40.0 [52.5; 133.50]	0.027

End of Table 4

Indicator	Patient group		p-value
	VA-ECMO–LVAD	LVAD	
Hemoglobin (Hb), g/dL M ± o Me [Q1; Q3]	 7.8 ± 0.8 8.30 [7.68; 8.70]	 8.1 ± 0.9 7.8 [7.4; 8.60]	0.542
Urea (max), mmol/L M ± o Me [Q1; Q3]	 19.4 ± 5.4 17.60 [11.53; 22.50]	 10.6 ± 6.9 9.40 [6.71; 15.85]	0.025
Creatinine (max), μmol/L M ± o Me [Q1; Q3]	 92.7 ± 24.8 78.5 [65.89; 91.75]	 68.9 ± 20.4 68.0 [49.15; 83.85]	0.049
Total bilirubin (max), μmol/L M ± o Me [Q1; Q3]	 108.0 ± 41.5 87.00 [59.60; 117.75]	 51.9 ± 41.0 46.10 [21.55; 71.50]	0.020
ALT (max), U/L M ± o Me [Q1; Q3]	 418.9 ± 380.2 180.2 [68.99; 446.2]	 128.6 ± 218.9 41.3 [27.15; 125.50]	0.041
AST (max), U/L M ± o Me [Q1; Q3]	 109.7 ± 62.6 109.9 [79.0; 147.09]	 127.6 ± 79.7 135.1 [79.40; 200.85]	0.677
Total protein (min), g/L M ± o Me [Q1; Q3]	 59.7 ± 3.2 59.00 [56.74; 61.25]	 62.6 ± 6.5 60.0 [55.93; 64.65]	0.398
INR (max) M ± o Me [Q1; Q3]	 2.17 ± 0.56 1.80 [1.48; 2.25]	 1.70 ± 0.35 1.60 [1.50; 2.00]	0.035
ICU stay, days M ± o Me [Q1; Q3]	 10.8 ± 4.4 11.00 [7.50; 14.25]	 5.3 ± 4.7 4.0 [2.00; 6.00]	0.041
In-hospital mortality n/%	0/0.0	3/14.3	1.000

Abbreviations: ALV, artificial ventilation of the lungs; RRT, renal replacement therapy; CVVHDF, continuous venovenous hemodiafiltration; WBC, white blood cells; ALT, alanine aminotransferase; AST, aspartate aminotransferase; INR, international normalized ratio; ICU, intensive care unit.

This hemodynamic complication developed in one patient in the VA-ECMO–LVAD group. To ensure adequate LVAD performance, the patient was transitioned from pVA-ECMO to a transcutaneous paracorporeal right ventricular assist circuit using the right femoral vein–right internal jugular vein configuration, with return cannulation into the pulmonary artery according to the previously described technique [10]. ARVD also occurred in two patients in the LVAD group. In the first case, transcutaneous paracorporeal right ventricular bypass was performed, while in the second case – due to the child's small anthropometric parameters – a paracorporeal right ventricular bypass with central cannulation was used, following the right atrium–pulmonary artery configuration. Patients in the VA-ECMO–LVAD group showed more pronounced clinical and laboratory signs of hepatorenal syndrome in the postoperative period. However, no significant differences in in-hospital postoperative mortality were observed between the groups.

DISCUSSION

Implantable LVADs have become an increasingly popular method of long-term MCS not only in adults but also in children. This trend is largely driven by continuous technological advancements, including device miniaturization, enhanced hemocompatibility, and improved thromboresistant properties, which collectively allow for a reduction in the intensity of anticoagulant and antiplatelet therapy. These improvements have contributed to a lower incidence of thrombotic and hemorrhagic complications, as well as a prolonged duration of assisted circulation [11].

According to the Pedimacs international registry (2024, 2025), implantable LVADs are now the leading modality of long-term MCS in pediatric patients, accounting for approximately 37–39% of all cases [12, 13]. The introduction of the HeartWare® Ventricular Assist Device (HVAD) into clinical practice has further expanded the feasibility of long-term MCS in children with smaller anthropometric parameters [14]. Notably, growing clinical experience has demonstrated the safety and efficacy

of LVAD implantation in children with a body surface area below 1.3 m^2 [15].

Many factors determine the immediate and long-term outcomes of LVAD implantation, including the severity of preimplantation CHF, degree of organ dysfunction, and urgency with which MCS is initiated [16]. The optimal timing for LVAD implantation in patients with CHF is before the onset of cardiogenic shock or acute decompensation of CHF [17]. Nevertheless, in about half of patients, the preimplantation hemodynamic status corresponds to INTERMACS profiles I–II [18]. The appropriateness of LVAD implantation in patients with critical hemodynamic disorders (cardiogenic shock, acute decompensation of CHF) remains a subject of debate, as these patients have increased risk of intraoperative and early postoperative complications [19], including right ventricular dysfunction, cerebrovascular and infectious events, pump thrombosis, and hemolysis [17]. Importantly, the clinical efficacy of LVAD support is significantly lower in patients presenting with preimplantation multiple dysfunction, primarily liver dysfunction/insufficiency arising from severe decompensated CHF [20].

Prior to LVAD implantation, 51–87% of patients with hemodynamic profiles corresponding to INTERMACS level I require pVA-ECMO. This intervention is indicated in cases of cardiogenic shock and/or life-threatening cardiac arrhythmias refractory to antiarrhythmic therapy [21, 22]. The principal causes of such severe preimplantation hemodynamic compromise in patients with an INTERMACS profile I classification are acute myocardial infarction, decompensated ischemic or dilated cardiomyopathy, and acute myocarditis [22].

According to H.-Y. Fu et al. (2023), emergency LVAD implantation in children (median age, 9.6 years) was required in 72.7% of cases, with 66.7% of all patients – and 91.7% of those with an INTERMACS I profile – receiving preimplantation VA-ECMO support [23]. LVAD implantation in patients presenting with cardiogenic shock but without prior short-term MCS is associated with high early postoperative mortality (23.8–28.6%) [24, 25]. Therefore, LVAD implantation should be performed before the onset of cardiogenic shock and severe impairment of organ perfusion, whereas patients with critical hemodynamic instability should undergo implantation following prior short-term MCS [26].

Short-term MCS prior to LVAD implantation enhances hemodynamic stability, restores organ perfusion, and mitigates multiple organ dysfunction, thereby improving the outcomes of subsequent long-term MCS [27, 28]. Several modalities of short-term MCS are used in pediatric patients, with the choice determined by the nature and severity of central hemodynamic impairment and the patient's anthropometric characteristics [29]. Among these, VA-ECMO with central or peripheral cannulation is the most widely employed, including in the pre-LVAD period [31, 32]. VA-ECMO provides both hemodynamic and respiratory support, particularly in the presence of pulmonary gas exchange disorders secondary to cardiogenic shock [27]. The use of VA-ECMO as the primary method of extracorporeal life support (ELS) in critical hemodynamic states has enabled the implementation of the concepts of MCS continuity ("bridge-to-bridge") and treatment optimization ("bridge-to-decision") [33]. For prolonged pre-implantation MCS, lasting up to a month or more, mono- or biventricular bypass with central cannulation using the CentriMag perfusion system based on magnetic levitation technology is employed [34].

Acute ischemic injury leading to renal ("shock kidney") and hepatic ("shock liver") dysfunction is a strong predictor of mortality following LVAD implantation [35]. LVAD implantation is contraindicated in patients with severe hyperbilirubinemia resulting from irreversible ischemic injury to the biliary epithelium and shock-induced secondary sclerosing cholangitis. Acute ischemic renal injury is associated with a high incidence (up to 45.5%) of renal replacement therapy (RRT) during the early postoperative period in patients who received pre-implantation short-term MCS. In our study, RRT was required 3.5 times more frequently after LVAD implantation in children who underwent pre-implantation VA-ECMO compared with those without prior MCS (50% vs. 14.3%). Nevertheless, pre-implantation VA-ECMO in patients with critical hemodynamic compromise is regarded as an important strategy to prevent the progression of renal failure in the post-implantation period [36].

Both in our study and in reports by other authors, the use of VA-ECMO prior to LVAD implantation contributed to improved systemic hemodynamics (increased mAP and decreased CVP) and enhanced organ function, as reflected by reductions in total bilirubin, serum creatinine, and hepatic transaminases (ALT, AST) by the time of LVAD implantation [21]. In our study, the duration of pre-implantation VA-ECMO support ranged from 1 to 16 days, with a mean of 3.7 ± 4.9 (1.00 [1.00; 5.00]) days. In other studies, the interval between initiation of short-term MCS and subsequent LVAD implantation averaged 4–7 days, which was attributed to the need for more sustained regression of multiple organ dysfunction [22].

D. Schibisky et al. (2017) reported that in 93.3% of patients receiving short-term MCS prior to LVAD implantation, the pre-implantation clinical status improved to INTERMACS level III TCS (temporary circulatory support) with VA-ECMO use [22]. Similarly, J.B. Durinka et al. (2014) recommended continuing short-term MCS until full normalization of organ function, with a median duration of 12.1 days [37]. However, other studies have highlighted the negative impact of prolonged pre-implantation VA-ECMO on LVAD outcomes. D. Tsyganenko et al. (2019) showed that VA-ECMO exceeding 7 days prior to LVAD implantation is an independent predictor of mortality in patients subsequently receiving long-term MCS [38]. Mortality among pati-

ents with LVADs was 9.4 times higher (75% vs. 8%) when VA-ECMO was used for more than 14 days before implantation, compared with shorter durations of pre-implantation support [37].

Volumetric overload of the left ventricle in the setting of progressive systolic dysfunction is one of the recognized complications of short-term MCS using the VA-ECMO method prior to LVAD implantation. This condition may necessitate surgical interventions aimed at unloading the left heart chambers. For this purpose, an additional drainage cannula can be inserted either through a minithoracotomy or by percutaneous transseptal puncture [39]. In the latter case, the resulting atrial septal defect is subsequently closed after LVAD implantation by percutaneous insertion of an intracardiac occluder.

The incidence of multiple organ failure (renal and/or hepatic dysfunction), as well as hemorrhagic and infectious complications (leukocytosis, pneumonia, bacteremia), following LVAD implantation is higher in patients who required pre-implantation VA-ECMO. This is attributed not only to the specific characteristics of this short-term MCS method but also to more severe preoperative disturbances in hemodynamics, hemostasis, and organ function [39]. Decreased hemoglobin and platelet levels during VA-ECMO increase the risk of hemorrhagic complications and contribute to greater intraoperative blood loss during subsequent LVAD implantation [39]. Consistent with previous studies [5], our findings demonstrated increased intraoperative blood loss, higher rates of re-sternotomy, and greater transfusion requirements in patients with pre-implantation VA-ECMO. These factors may explain the longer duration of postoperative mechanical ventilation and ICU stay observed in this subgroup of patients with implantable LVAD.

Acute right ventricular failure (ARVF) develops in 6–40% of patients after LVAD implantation. This complication occurs more frequently in patients presenting with pre-implantation cardiogenic shock and is associated with several factors, including hemodynamic instability, elevated CVP, dependence on cardiotonic and vasopressor support, and the need for mechanical ventilation. In cases of severe hemodynamic compromise due to ARVF developing against the background of left ventricular failure, temporary paracorporeal right ventricular bypass or continuation of pre-implantation VA-ECMO in the early post-implantation period is indicated [22, 36].

The use of VA-ECMO before LVAD implantation helps to prevent post-implantation ARVF by improving systemic hemodynamics, reducing elevated CVP, and facilitating weaning from mechanical ventilation to spontaneous breathing. Given the high risk of ARVF in patients with INTERMACS profile I, several studies recommend maintaining VA-ECMO support for the first four days after LVAD implantation [36]. In our study, severe ARVF developed significantly more often in the VA-ECMO–LVAD group, which may be related to the shorter duration of VA-ECMO use prior to LVAD implantation compared with other reports. We believe that paracorporeal right ventricular bypass represents a more effective MCS method for ARVF occurring after LVAD implantation, as it provides superior hemodynamic conditions for optimal LVAD performance.

In the absence of recovery of right ventricular function sufficient to ensure adequate LVAD performance, urgent heart transplantation is indicated [42]. Delayed initiation of right ventricular bypass adversely affects not only the outcomes of LVAD implantation but also those of subsequent urgent heart transplantation in cases of irreversible right ventricular dysfunction [43].

Our study did not reveal a negative impact of urgent LVAD implantation or pre-implantation VA-ECMO use on the immediate outcomes of long-term MCS in children.

CONCLUSION

Our experience confirms the high efficacy of urgent left ventricular assist device implantation in pediatric patients with critical hemodynamic instability requiring preoperative short-term mechanical circulatory support using peripheral veno-arterial extracorporeal membrane oxygenation. The presence and severity of multiple organ dysfunction, both before and after LVAD implantation, as well as the extent of perioperative blood loss, must be carefully considered, as these factors critically influence anesthetic management, postoperative intensive care strategies, and the immediate outcomes of long-term mechanical circulatory support.

The authors declare no conflict of interest.

REFERENCES

1. *Cleveland JD, Kumar SR*. Current opinion in pediatric heart transplantation. *Curr Opin Organ Transplant*. 2021 Jun 1; 26 (3): 290–295. doi: 10.1097/MOT.0000000000000870. PMID: 33938465.
2. *Hetzer R, Javier MFDM, Delmo Walter EM*. Role of paediatric assist device in bridge to transplant. *Ann Cardiothorac Surg*. 2018 Jan; 7 (1): 82–98. doi: 10.21037/acs.2018.01.03. PMID: 29492386; PMCID: PMC5827126.
3. *O'Connor MJ, Lorts A, Davies RR, Fynn-Thompson F, Joong A, Maeda K et al*. Early experience with the HeartMate 3 continuous-flow ventricular assist device in pediatric patients and patients with congenital heart disease: A multicenter registry analysis. *J Heart Lung Transplant*. 2020 Jun; 39 (6): 573–579. doi: 10.1016/j.healun.2020.02.007. Epub 2020 Feb 13. PMID: 32111350.
4. *Cabrera AG, Sundareswaran KS, Samayoa AX, Jeewa A, McKenzie ED, Rossano JW et al*. Outcomes of pediatric patients supported by the HeartMate II left ventricular assist device in the United States. *J Heart Lung Trans-*

plant. 2013 Nov; 32 (11): 1107–1113. doi: 10.1016/j.healun.2013.07.012. Epub 2013 Aug 31. PMID: 24002006.

5. *Cao I, Italiano EG, Bertelli F, Motta R, Castaldi B, Pergola V et al*. Intracorporeal LVAD implantation in pediatric patients: A single-center 10 years' experience. *Artif Organs*. 2024 Apr; 48 (4): 408–417. doi: 10.1111/aor.14716. Epub 2024 Feb 21. PMID: 38380771.
6. *Yang L, Ye L, Fan Y, He W, Zong Q, Zhao W, Lin R*. Outcomes following venoarterial extracorporeal membrane oxygenation in children with refractory cardiogenic disease. *Eur J Pediatr*. 2019 Jun; 178 (6): 783–793. doi: 10.1007/s00431-019-03352-5. Epub 2019 Mar 4. PMID: 30834480.
7. *Kurihara C, Kawabori M, Sugiura T, Critsinelis AC, Wang S, Cohn WE et al*. Bridging to a Long-Term Ventricular Assist Device With Short-Term Mechanical Circulatory Support. *Artif Organs*. 2018 Jun; 42 (6): 589–596. doi: 10.1111/aor.13112. Epub 2018 Feb 23. PMID: 29473181.
8. *Peer SM, Koehl DA, Cantor RS, Kirklin JK, Sinha P*. Effect of preoperative extracorporeal membrane oxygenation therapy on postventricular assist device outcomes: an analysis of the STS Pedimacs database. *Eur J Cardiothorac Surg*. 2022 Nov 3; 62 (6): ezac485. doi: 10.1093/ejcts/ezac485. PMID: 36227147.
9. *Lamba HK, Kim M, Santiago A, Hudson S, Civitello AB, Nair AP et al*. Extracorporeal membrane oxygenation as a bridge to durable left ventricular assist device implantation in INTERMACS-1 patients. *J Artif Organs*. 2022 Mar; 25 (1): 16–23. doi: 10.1007/s10047-021-01275-3. Epub 2021 May 13. PMID: 33982206.
10. *Poptsov VN, Spirina EA, Ryabtsev DV, Solodovnikova AK, Epremian AS*. Experience with percutaneous right ventricular support in the early post-left ventricular assist device implantation period (clinical case report and literature reviews). *Russian Journal of Transplantology and Artificial Organs*. 2023; 25 (1): 77–89. https://doi.org/10.15825/1995-1191-2023-1-77-89.
11. *Jefferson HL, Kent WDT, MacQueen KT, Miller RJH, Holloway DD, Fatehi Hassanabad A*. Left ventricular assist devices: A comprehensive review of major clinical trials, devices, and future directions. *J Card Surg*. 2021 Apr; 36 (4): 1480–1491. doi: 10.1111/jocs.15341. Epub 2021 Jan 21. PMID: 33476443.
12. *Griffiths ER, Profsky MP, Mokshagundam D, Boucek K, Amdani S, Davies RR et al*. Pedimacs Investigators. Eighth Annual Society of Thoracic Surgeons Pedimacs Report. *Ann Thorac Surg*. 2025 Mar; 119 (3): 513–522. doi: 10.1016/j.athoracsur.2024.12.020. Epub 2025 Jan 14. PMID: 39818264.
13. *Peng DM, Davies RR, Simpson KE, Shugh SB, Morales DLS, Jacobs JP et al*. Pedimacs Investigators. Seventh Annual Society of Thoracic Surgeons Pedimacs Report. *Ann Thorac Surg*. 2024 Apr; 117 (4): 690–703. doi: 10.1016/j.athoracsur.2023.11.035. Epub 2023 Dec 18. PMID: 38123046.
14. *Nassar MS, Hasan A, Chila T, Schueler S, Pergolizzi C, Reinhardt Z et al*. Comparison of paracorporeal and continuous flow ventricular assist devices in children: preliminary results. *Eur J Cardiothorac Surg*. 2017 Apr 1; 51 (4): 709–714. doi: 10.1093/ejcts/ezx006. PMID: 28329112.
15. *Schweiger M, Hussein H, de By TMMH, Zimpfer D, Sliwka J, Davies B et al*. Use of Intracorporeal Durable LVAD Support in Children Using HVAD or HeartMate 3-A EUROMACS Analysis. *J Cardiovasc Dev Dis*. 2023 Aug 17; 10 (8): 351. doi: 10.3390/jcdd10080351. PMID: 37623364; PMCID: PMC10455245.
16. *Frigerio M.* Left Ventricular Assist Device: Indication, Timing, and Management. *Heart Fail Clin*. 2021 Oct; 17 (4): 619–634. doi: 10.1016/j.hfc.2021.05.007. Epub 2021 Jul 22. PMID: 34511210.
17. *Zubarevich A, Zhigalov K, Szczechowicz M, Arjomandi Rad A, Vardanyan R, Torabi S et al*. Rescue extracorporeal life support as a bridge to durable left ventricular assist device. *Int J Artif Organs*. 2022 Apr; 45 (4): 371–378. doi: 10.1177/03913988211053874. Epub 2021 Oct 21. PMID: 34674570; PMCID: PMC8921882.
18. *Molina EJ, Shah P, Kiernan MS, Cornwell WK 3rd, Copeland H, Takeda K et al*. The Society of Thoracic Surgeons Intermacs 2020 Annual Report. *Ann Thorac Surg*. 2021 Mar; 111 (3): 778–792. doi: 10.1016/j.athoracsur.2020.12.038. Epub 2021 Jan 16. PMID: 33465365.
19. *Piffard M, Nubret-Le Coniat K, Simon O, Leuillet S, Rémy A, Barandon L, Ouattara A*. Independent risk factors for ICU mortality after left ventricular assist device implantation. *Artif Organs*. 2020 Feb; 44 (2): 153–161. doi: 10.1111/aor.13540. Epub 2019 Sep 2. PMID: 31318978.
20. *Demirozu ZT, Hernandez R, Mallidi HR, Singh SK, Radovancevic R, Segura AM et al*. HeartMate II left ventricular assist device implantation in patients with advanced hepatic dysfunction. *J Card Surg*. 2014 May; 29 (3): 419–423. doi: 10.1111/jocs.12318. Epub 2014 Mar 19. PMID: 24641429.
21. *Han JJ, Chung J, Chen CW, Gaffey AC, Sotolongo A, Justice C et al*. Different Clinical Course and Complications in Interagency Registry for Mechanically Assisted Circulatory Support 1 (INTERMACS) Patients Managed With or Without Extracorporeal Membrane Oxygenation. *ASAIO J*. 2018 May/Jun; 64 (3): 318–322. doi: 10.1097/MAT.0000000000000674. PMID: 28938306.
22. *Schibilsky D, Haller C, Lange B, Schibilsky B, Haeberle H, Seizer P et al.* Extracorporeal life support prior to left ventricular assist device implantation leads to improvement of the patients INTERMACS levels and outcome. *PLoS One*. 2017 Mar 30; 12 (3): e0174262. doi: 10.1371/journal.pone.0174262.
23. *Fu HY, Chou HW, Lai CH, Tsao CI, Lu CW, Lin MT et al*. Outcomes of pediatric patients supported with ventricular assist devices single center experience. *J Formos Med Assoc*. 2023 Feb; 122 (2): 172–181. doi: 10.1016/j.jfma.2022.09.008. Epub 2022 Oct 1. PMID: 36192294.
24. *Kirklin JK, Naftel DC, Kormos RL, Stevenson LW, Pagani FD, Miller MA et al*. Fifth INTERMACS annual report: risk factor analysis from more than 6,000 mechanical circulatory support patients. *J Heart Lung Transplant*. 2013 Feb; 32 (2): 141–156. doi: 10.1016/j.healun.2012.12.004. Erratum in: *J Heart Lung Transplant*. 2015 Oct; 34 (10): 1356. Timothy Baldwin, J [corrected to Baldwin, JT]. PMID: 23352390.

25. *Kirklin JK, Naftel DC, Pagani FD, Kormos RL, Stevenson L, Miller M, Young JB*. Long-term mechanical circulatory support (destination therapy): on track to compete with heart transplantation? *J Thorac Cardiovasc Surg*. 2012 Sep; 144 (3): 584–603; discussion 597–598. doi: 10.1016/j.jtcvs.2012.05.044. Epub 2012 Jul 15. PMID: 22795459; PMCID: PMC3443856.
26. *Boyle AJ, Ascheim DD, Russo MJ, Kormos RL, John R, Naka Y et al*. Clinical outcomes for continuous-flow left ventricular assist device patients stratified by pre-operative INTERMACS classification. *J Heart Lung Transplant*. 2011 Apr; 30 (4): 402–407. doi: 10.1016/j.healun.2010.10.016. Epub 2010 Dec 18. PMID: 21168346.
27. *Bermudez CA, Rocha RV, Toyoda Y, Zaldonis D, Sappington PL, Mulukutla S et al*. Extracorporeal membrane oxygenation for advanced refractory shock in acute and chronic cardiomyopathy. *Ann Thorac Surg*. 2011 Dec; 92 (6): 2125–2131. doi: 10.1016/j.athoracsur.2011.07.029. Epub 2011 Oct 7. PMID: 21982150.
28. *Shah P, Pagani FD, Desai SS, Rongione AJ, Maltais S, Haglund NA et al.* Mechanical Circulatory Support Research Network. Outcomes of Patients Receiving Temporary Circulatory Support Before Durable Ventricular Assist Device. *Ann Thorac Surg*. 2017 Jan; 103 (1): 106–112. doi: 10.1016/j.athoracsur.2016.06.002. Epub 2016 Aug 28. PMID: 27577033.
29. *Moisă ȘM, Burlacu A, Brinza C, Cinteză E, Butnariu LI, Țarcă E et al*. An Up-to-Date Literature Review on Ventricular Assist Devices Experience in Pediatric Hearts. *Life (Basel)*. 2022 Nov 30; 12 (12): 2001. doi: 10.3390/life12122001. PMID: 36556366; PMCID: PMC9788166.
30. *Shugh SB, Riggs KW, Morales DLS*. Mechanical circulatory support in children: past, present and future. *Transl Pediatr*. 2019 Oct; 8 (4): 269–277. doi: 10.21037/tp.2019.07.14. PMID: 31728319; PMCID: PMC6825962.
31. *Abreu S, Brandão C, Trigo C, Rodrigues R, Pinto F, Fragata J*. Mechanical circulatory support in children: Strategies, challenges and future directions. *Rev Port Cardiol*. 2022 May; 41 (5): 371–378. English, Portuguese. doi: 10.1016/j.repc.2021.03.011. Epub 2022 Mar 16. PMID: 36062636.
32. *Kozik D, Alsoufi B*. Pediatric mechanical circulatory support – a review. *Indian J Thorac Cardiovasc Surg*. 2023 Jul; 39 (Suppl 1): 80–90. doi: 10.1007/s12055-023-01499-3. Epub 2023 Mar 27. PMID: 37525715; PMCID: PMC10386992.
33. *Hoefer D, Ruttmann E, Poelzl G, Kilo J, Hoermann C, Margreiter R et al*. Outcome evaluation of the bridge-to-bridge concept in patients with cardiogenic shock. *Ann Thorac Surg*. 2006 Jul; 82 (1): 28–33. doi: 10.1016/j.athoracsur.2006.02.056. PMID: 16798182.
34. *Mohite PN, Zych B, Popov AF, Sabashnikov A, Sáez DG, Patil NP et al*. CentriMag short-term ventricular assist as a bridge to solution in patients with advanced heart failure: use beyond 30 days. *Eur J Cardiothorac Surg*. 2013 Nov; 44 (5): e310–e315. doi: 10.1093/ejcts/ezt415. Epub 2013 Aug 29. PMID: 23990618.
35. *Yang JA, Kato TS, Shulman BP, Takayama H, Farr M, Jorde UP et al*. Liver dysfunction as a predictor of outcomes in patients with advanced heart failure requiring ventricular assist device support: Use of the Model of End-stage Liver Disease (MELD) and MELD eXcluding INR (MELD-XI) scoring system. *J Heart Lung Transplant*. 2012 Jun; 31 (6): 601–610. doi: 10.1016/j.healun.2012.02.027. Epub 2012 Mar 28. PMID: 22458997; PMCID: PMC3358456.
36. *Riebandt J, Haberl T, Mahr S, Laufer G, Rajek A, Steinlechner B et al*. Preoperative patient optimization using extracorporeal life support improves outcomes of INTERMACS Level I patients receiving a permanent ventricular assist device. *Eur J Cardiothorac Surg*. 2014 Sep; 46 (3): 486–492; discussion 492. doi: 10.1093/ejcts/ezu093. Epub 2014 Mar 18. PMID: 24648428.
37. *Durinka JB, Bogar LJ, Hirose H, Brehm C, Koerner MM, Pae WE et al*. End-organ recovery is key to success for extracorporeal membrane oxygenation as a bridge to implantable left ventricular assist device. *ASAIO J*. 2014 Mar-Apr; 60 (2): 189–192. doi: 10.1097/MAT.0000000000000043. PMID: 24399062.
38. *Tsyganenko D, Gromann TW, Schoenrath F, Mueller M, Mulzer J, Starck C et al*. Predictors of mid-term outcomes in patients undergoing implantation of a ventricular assist device directly after extracorporeal life support. *Eur J Cardiothorac Surg*. 2019 Apr 1; 55 (4): 773–779. doi: 10.1093/ejcts/ezy351. PMID: 30445489.
39. *Sorensen EN, Griffith BP, Feller ED, Kaczorowski DJ*. Outcomes with temporary mechanical circulatory support before minimally invasive centrifugal left ventricular assist device. *J Card Surg*. 2020 Jul; 35 (7): 1539–1547. doi: 10.1111/jocs.14655. Epub 2020 Jun 24. PMID: 32579786.
40. *Das BB, Trivedi J, Deshpande SR, Alsoufi B, Slaughter MS*. Recent Era Outcomes of Mechanical Circulatory Support in Children With Congenital Heart Disease as a Bridge to Heart Transplantation. *ASAIO J*. 2022 Mar 1; 68 (3): 432–439. doi: 10.1097/MAT.0000000000001468. PMID: 35213887.
41. *Simpson KE, Kirklin JK, Cantor RS, Mehegan M, Lamour JM, Guleserian KJ et al*. Right heart failure with left ventricular assist device implantation in children: An analysis of the Pedimacs registry database. *J Heart Lung Transplant*. 2020 Mar; 39 (3): 231–240. doi: 10.1016/j.healun.2019.11.012. Epub 2019 Nov 28. PMID: 31926747.
42. *Bhama JK, Kormos RL, Toyoda Y, Teuteberg JJ, McCurry KR, Siegenthaler MP*. Clinical experience using the Levitronix CentriMag system for temporary right ventricular mechanical circulatory support. *J Heart Lung Transplant*. 2009 Sep; 28 (9): 971–976. doi: 10.1016/j.healun.2009.04.015. PMID: 19716053.
43. *Morgan JA, John R, Lee BJ, Oz MC, Naka Y*. Is severe right ventricular failure in left ventricular assist device recipients a risk factor for unsuccessful bridging to transplant and post-transplant mortality. *Ann Thorac Surg*. 2004 Mar; 77 (3): 859–863. doi: 10.1016/j.athoracsur.2003.09.048. PMID: 14992887.

The article was submitted to the journal on 30.07.2025

DOI: 10.15825/1995-1191-2025-4-87-94

EVALUATION OF THE EFFECTIVENESS OF NOVEL POLYPROPYLENE MEMBRANES FOR EXTRACORPOREAL MEMBRANE OXYGENATION

V.K. Bogdanov[1], Ts. Liang[2], Ch. Long[2], D.M. Bondarenko[1], V.A. Elenkin[1], A.P. Kuleshov[1], N.V. Vasiliev[3], N.V. Grudinin[1]

[1] Shumakov National Medical Research Center of Transplantology and Artificial Organs, Moscow, Russian Federation

[2] Hangzhou Cobetter Filtration Equipment Co., Ltd, Hangzhou, People's Republic of China

[3] Spetsmedtekhnika, St. Petersburg, Russian Federation

Objective: to assess the gas transport performance of new polypropylene (PP) membranes manufactured by Cobetter Filtration® (China) for use in extracorporeal circulation, and to compare their efficacy with the original 3M® PP membrane (USA) using both an extracorporeal hydrodynamic test bench and *in vivo* animal experiments. **Materials and methods.** Three experimental groups were established for bench and animal testing: a) Experimental – PP membrane 380/280 (n = 3); b) Experimental – PP membrane 300/200 (n = 3); c) Control – original 3M® PP membrane (n = 3). A total of 18 oxygenators were evaluated, including 12 experimental oxygenators with the Cobetter Filtration® membranes and 6 control oxygenators with 3M® membranes. The primary outcome was the oxygenation index (OI), reflecting the gas transport function of the membrane oxygenators. **Results.** During bench testing, the OI of the PP 300/200 membrane decreased from 509 ± 27 at baseline to 422 ± 31 after 240 minutes, showing no significant difference compared with the PP 380/280 membrane, which decreased from 487 ± 15 to 385 ± 20 ($p > 0.05$). In contrast, oxygenators with the original 3M® membrane exhibited significantly higher OI values, declining from 713 ± 46 to 612 ± 39 over the same period. In animal experiments, the initial OI in the 3M® control group exceeded the threshold of 300, measuring 439 ± 13, whereas the experimental groups recorded lower values: 392 ± 27 (PP 380/280) and 411 ± 8 (PP 300/200), with $p < 0.05$. By 60 minutes, OI values were similar across all groups ($p = 1$). At the end of the 5-hour acute observation, OI values were 325 ± 29 (PP 380/280) and 355 ± 33 (PP 300/200), with no statistically significant difference between the experimental groups ($p > 0.05$). **Conclusion.** The experimental PP membranes demonstrated comparable effectiveness to the original 3M® products, suggesting their potential for enhancing the safety and biocompatibility of extracorporeal circulation procedures.

Keywords: transplantology, perfusion physiology, artificial circulation, membrane oxygenation, polypropylene membrane.

INTRODUCTION

Today, membrane oxygenation is an essential technique for maintaining gas exchange during cardiac surgery. Despite the long evolution of this life-saving technology, polypropylene (PP) membranes have attracted intense research interest due to their unique properties, such as high chemical resistance, relatively low cost, and favorable mechanical strength [1].

Historically, research in the field of membrane oxygenation has been directed toward identifying the optimal material for gas exchange and achieving the ideal balance between biocompatibility and non-traumatic interaction with blood cells, which has been an enduring challenge. These efforts led to the development of disc, screen, bubble, and film oxygenators for extracorporeal gas exchange in cardiac surgery, paralleling the rapid rise of cardiac surgery as a distinct medical specialty [2–4].

In the early stages of development, various materials such as cellophane and polyethylene were used as gas exchange surfaces. However, the bubble direct-flow oxygenator, developed and commercialized by Richard DeWall and C. Walton Lillehei in 1955, became a life-saving device that dominated clinical practice for the next 25 years [5]. It was only natural that bubble oxygenators were eventually replaced by membrane oxygenators, a transition made possible by the introduction of microporous materials with unique properties [6].

The first commercially available microporous Teflon-based oxygenator, developed by Baxter-Travenol™ (USA), represented a major technological milestone. Distinguished by its pronounced hydrophobicity, it ensured complete separation between the gas phase and the

Corresponding author: Vladimir Bogdanov. Address: 1, Shchukinskaya str., Moscow, 123182, Russian Federation. Phone: (900) 110-42-41. E-mail: bogdanovv@bk.ru

patient's blood while also providing thermoregulatory functionality [7–9]. Shortly thereafter, Cobe Laboratories (USA) introduced the Variable Prime Cobe Membrane Lung™, based on a porous PP membrane, which closely resembles modern designs [10, 11]. From that point forward, within just 5–10 years, the global adoption of extracorporeal blood oxygenation technology based on PP membranes expanded rapidly – a dominance that continues to define clinical practice today.

The experience gained from commercially successful products and the findings of international research groups demonstrate that PP is a unique material with remarkable biocompatibility. It elicits no immune response upon contact with the body's internal environment and induces minimal production of pro-inflammatory cytokines. Furthermore, its pronounced hydrophobicity prevents the adhesion of blood cells, thrombus formation, and plasma proteins, thereby broadening the safe operational range of oxygenators utilizing PP membranes, even under challenging conditions such as high hematocrit or thrombocytosis. These properties are essential for ensuring the safety and efficacy of PP-based systems in extracorporeal circulatory support [12].

The chemical properties of PP play a crucial role in its suitability for medical applications:

1. Chemical inertness
   – PP has high chemical inertness, remaining resistant to a wide range of chemicals, including acids and alkalis. This stability prevents adverse reactions with blood components or other agents present within the oxygenation circuit.
2. Corrosion resistance
   – PP is not prone to corrosion, which makes it highly reliable for prolonged use. Since oxygenators operate in complex environments where various fluids may coexist with blood, corrosion resistance is a critical criterion.
3. Surface modifiability
   – The surface of PP membranes can be chemically modified to enhance their properties. For instance, increasing the hydrophilicity of the membrane surface improves its compatibility with blood and reduces the risk of thrombosis. Such modifications may involve the addition of specific functional groups or the use of polymeric or inorganic coatings.
4. Thermal stability
   – PP has a broad range of thermal stability, allowing its safe use under various temperature conditions. This is important because sterilization protocols typically involve exposure to high temperatures.
5. Porosity
   – PP membranes can be manufactured with controlled porosity, enabling optimization of their gas exchange capacity. The porous architecture enhances oxygen permeability, facilitating more efficient gas transfer between the blood and gaseous environments [13, 14].

At present, the leading global manufacturer of membranes and materials for extracorporeal blood circulation and oxygenation systems is 3M® (USA), which effectively maintains a dominant position in the production of polymer materials. However, interest in this field is expanding rapidly within the international medical device industry. Notably, Cobetter Filtration® (China) has achieved substantial progress through continuous refinement of the physical and chemical properties of PP membranes. The main directions of such improvements include optimization of structural porosity, as well as application of polymeric and inorganic surface coatings with tunable characteristics.

The objective of this international study is to investigate the performance of a modified PP membrane, assess its functional effectiveness, and conduct a comparative analysis of its gas exchange characteristics relative to the standard 3M® membrane.

RESEARCH DESIGN

Two types of PP membranes under investigation were supplied by Cobetter Filtration™, while the prototype oxygenators were assembled at a certified production facility with the technical support of Special and Medical Equipment™. The specifications of the test samples are presented in Table.

The tests were conducted at Shumakov National Medical Research Center of Transplantology and Artificial Organs in Moscow and included two sequential stages: bench tests and research on an experimental model of large animals. All membrane samples underwent molecular and microscopic diagnostics. The electron microscopy findings for PP membrane 300/200 are presented in Fig. 1.

In addition, infrared radiation analysis was performed during the membrane study (Fig. 2). The results confirmed that the quality parameters of all tested membranes were fully consistent with international reference data [15].

Table

Main characteristics of experimental polypropylene membranes

Specification	PP 380/280 membrane	PP 300/200 membrane
Wall thickness (μm)	50 ± 10	50 ± 10
Outer diameter (μm)	380 ± 20	300 ± 20
Inner diameter (μm)	280 ± 20	200 ± 20
Tensile strength (cN)	≥150	≥150
Elongation at break (%)	≥400	≥400
Nitrogen flow (ml/cm^2·min·bar)	50 ± 30	50 ± 30
Number of capillaries (cap/cm)	16.7 ± 1	20.5 ± 1
Angle ratio (°)	>12	>12

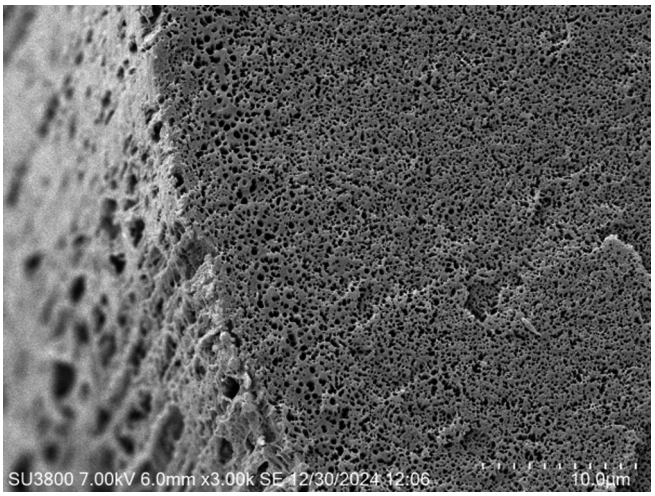

Fig. 1. Electron microscopy of PP 300/200 membrane

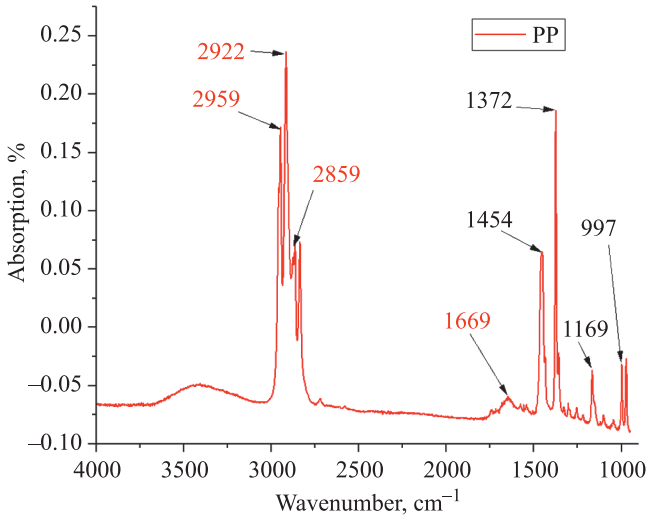

Fig. 2. Fourier transform infrared (FTIR) spectra of a PP fiber sample

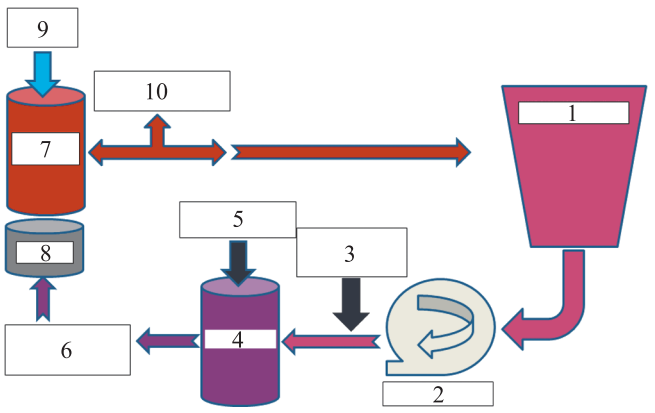

Fig. 3. Diagram of the low-volume hydrodynamic test bench. 1 – Reservoir with donor whole blood; 2 – Centrifugal pump of the ECMO device; 3 – Flow, temperature, and bubble sensor; 4 – Deoxygenator; 5 – Source of deoxygenated gas mixture; 6 – Pressure sensor #1 and sampling port #1; 7 – Tested oxygenator; 8 – Temperature control device; 9 – Oxygen mixture source; 10 – Pressure sensor #2 and sampling port #2

A sheep model was selected for the *in vivo* evaluation of the experimental membrane samples. A total of nine Romanov sheep (n = 9), each weighing 30–35 kg, were included in the study and divided into groups. All animal experiments were approved by the Committee on Biological Safety and Bioethics and conducted in accordance with the European Convention for the Protection of Vertebrate Animals Used for Experimental and Other Scientific Purposes and Directive 2010/63/EU. The animals were maintained under controlled laboratory conditions: temperature 22 ± 2 °C, humidity 65%, and a 12-hour light/dark cycle. Feeding and access to sterilized water were regulated according to physiological needs. A two-week quarantine period was observed prior to experimentation. Three groups were identified for the study: experimental (group 1, PP membrane 380/280, n = 3), experimental (group 2, PP membrane 300/200, n = 3), control (group 3, original PP membrane 3M®, n = 3). For bench testing, corresponding membrane groups with identical sample sizes and names were used for comparison.

MATERIALS AND METHODS

The first stage of experimental testing involved laboratory bench testing. A custom low-volume hydrodynamic bench was constructed, incorporating an original Nipro® oxygenator (Japan) that enriched the blood with carbon dioxide to simulate venous blood (exhalation phase). The test oxygenator, equipped with a Cobetter Filtration™ membrane (Groups 1 and 2), and the reference oxygenator with a 3M® membrane (Group 3) were supplied with pure oxygen. The perfusion circuit was filled with whole donor blood treated with a citrate anticoagulant. The configuration of the hydrodynamic setup is shown in Fig. 3.

As shown in the diagram above, a gas mixture of 5% CO_2 and 95% N_2 was delivered to the Nipro® oxygenator at a flow rate of 700 mL/min, while pure oxygen was supplied to the test or control oxygenators at 1 L/min. Blood circulated continuously at 37 °C and 1 L/min. To evaluate the gas transport efficiency of each membrane – quantified as the oxygenation index (OI) – blood flow was increased to 3 L/min for 15 minutes. Pressure sensors were positioned before and after the oxygenator to monitor the pressure differential, which remained constant at 80 mmHg throughout the tests. Blood samples were collected hourly from both the inlet (venous) and outlet (arterial) ports for analysis. The test lasted 240 minutes.

After bench testing, we studied oxygenators on sheep in three groups, fully replicating the extracorporeal circulation technique (infrared and cardiopulmonary bypass) used in cardiac surgery (Fig. 4).

The cardiopulmonary bypass (CPB) system was connected following standard clinical protocols. The test lasted for five hours (300 minutes), with the volumetric

perfusion rate adjusted according to each animal's weight and body surface area, ranging from 2.77 to 2.94 L/min. Gas flow rate was maintained at 1 L/min with an FiO_2 of 0.5. All blood parameters were kept within physiological limits. Pressure gradients were continuously recorded before and after the oxygenator. Heparin was administered as the anticoagulant, with activated clotting time (ACT) maintained below 400 seconds. Mechanical ventilation was discontinued during CPB.

Statistical analysis was conducted using StatTech v. 3.1.10 (StatTech LLC, Russia). The normality of quantitative variables was assessed with the Shapiro–Wilk test ($n < 50$). Normally distributed data were summarized as mean (M) ± standard deviation (SD) with 95% confidence intervals (CI). To compare three or more related groups, a one-way repeated-measures analysis of variance was used. Differences were considered statistically significant at $p < 0.05$.

RESULTS

As a result of bench testing, satisfactory blood oxygen saturation values were obtained for both types of new polypropylene membranes compared with the original 3M® membrane. Fig. 5 illustrates the dynamics of oxygen concentration changes, corresponding to the calculated OI, after blood passage through the oxygenators with the tested membranes relative to the 3M® reference membrane at a blood flow rate of 3 L/min.

No statistically significant difference in oxygenation performance was observed between the two experimental samples. The PP 300/200 membrane showed an OI of 509 ± 27 at baseline and 422 ± 31 after 240 minutes of testing, while the PP 380/280 membrane showed an OI of 487 ± 15 initially and 385 ± 20 at the final time point ($p > 0.05$).

In contrast, the oxygenators equipped with the original 3M® membrane exhibited significantly higher OI – 713 ± 46 at baseline and 612 ± 39 after 240 minutes ($p < 0.05$). Despite an average oxygen concentration difference of approximately 100 mmHg between the Cobetter Filtration® and 3M® membranes, all experimental membranes maintained oxygen levels exceeding normal physiological oxygen level.

Further *in vivo* testing on large animal models under infrared conditions with standardized perfusion and homeostatic parameters confirmed the high efficiency of Cobetter Filtration® membranes compared with the original 3M® oxygenators. Consistent with bench test results, arterial blood oxygenation index remained the principal comparative parameter, as shown in Fig. 6.

Although the initial OI values in the 3M® control group exceeded the threshold level (439 ± 13), the respiratory index values in groups 1 (PP 300/200) and 2 (PP 380/280) were slightly lower – 392 ± 27 and 411 ± 8, respectively ($p < 0.05$). However, by 60 minutes, the OI values across all groups had equalized, as indicated by $p = 1$, reflecting comparable oxygenation performance. At the end of five hours (300 minutes) of observation in the acute experiment, OI values in the PP 380/280 group were 325 ± 29, and in the PP 300/200 group 355 ± 33, with no statistically significant differences between these experimental groups ($p > 0.05$). In contrast, the control group with the 3M® membrane demonstrated a marked decline in oxygenation capacity by the end of the expe-

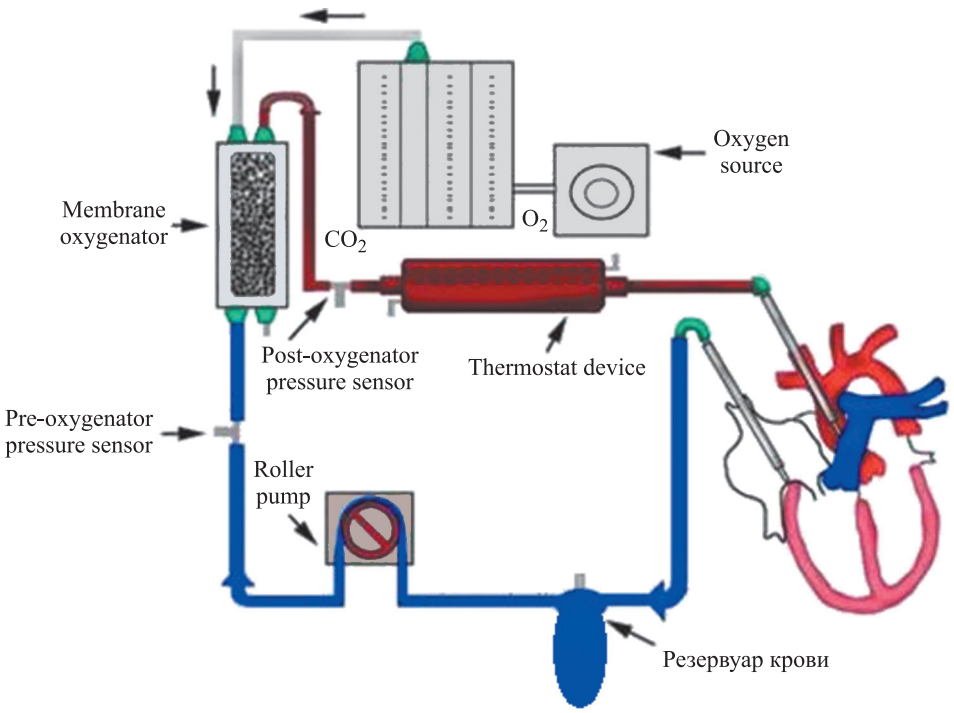

Fig. 4. Diagram of the extracorporeal circuit for artificial blood circulation

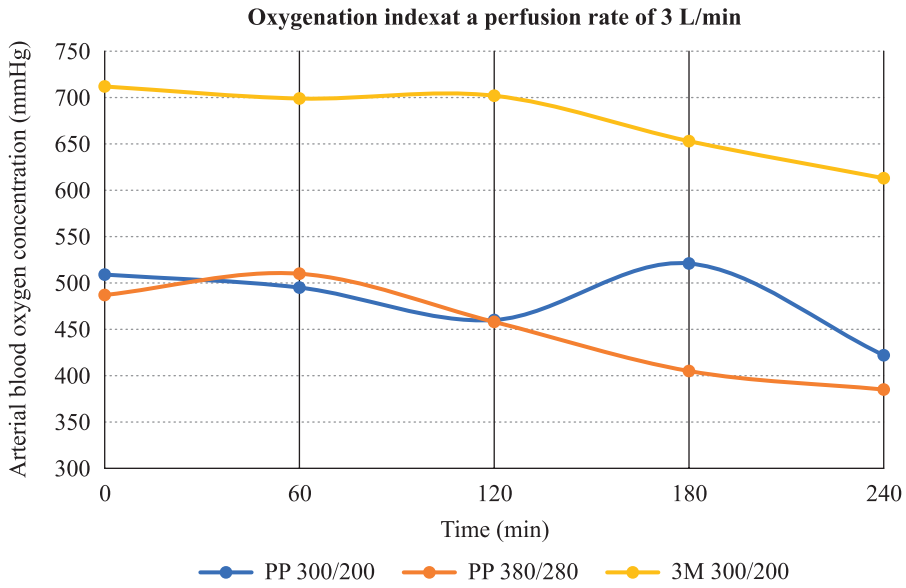

Fig. 5. Changes in oxygenation index in the tested membranes in bench tests

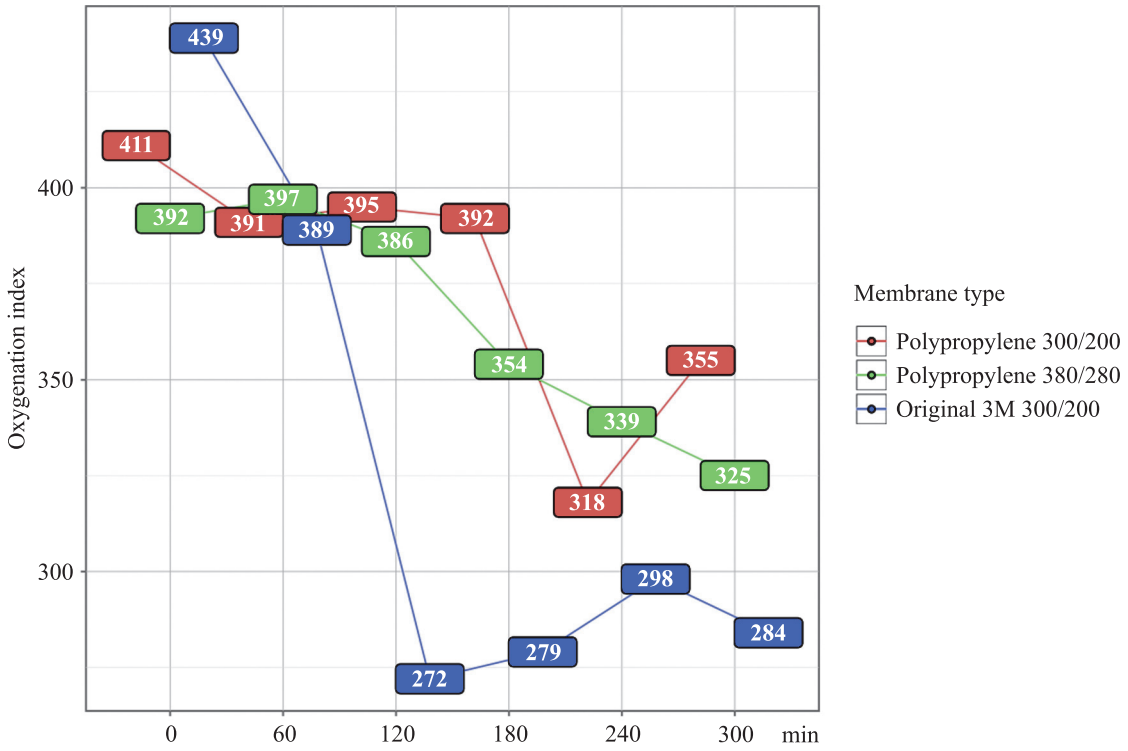

Fig. 6. Changes in oxygenation index in the tested membranes in the animal model

riment, with OI values dropping to 284 ± 18. The differences between the 3M® membrane and the Cobetter Filtration® membranes were statistically significant ($p = 0$), indicating a decrease in the oxygenating efficiency of the original 3M® oxygenator over time.

DISCUSSION

The results of this study demonstrate that Cobetter Filtration® polypropylene membranes are comparable in performance to the established 3M® polypropylene membranes, and under certain conditions, they even exhibit superior functional characteristics. In experimental settings that closely simulated clinical practice, oxygenators equipped with PP 300/200 and PP 380/280 membranes showed significantly higher OI values compared to those with the original 3M® membranes, maintaining consistently elevated OI levels throughout the 5-hour observation period.

This performance suggests that during prolonged cardiopulmonary bypass, Cobetter Filtration® membranes

possess advantages over the 3M® membranes, including more stable gas exchange, lower plasma leakage, and reduced thrombus formation within the interstitial spaces. The results were further supported by data on carbon dioxide elimination: while bench tests showed comparable CO_2 removal rates across all three groups (8.93 ± 1.25 mmHg, $p > 0.05$), experiments in large animal models revealed a progressive decline in CO_2 elimination with the 3M® membrane – from 6.74 ± 0.83 to 3.29 ± 0.17 mmHg over five hours. In contrast, the Cobetter Filtration® oxygenators maintained stable CO_2 elimination values (7.51 ± 1.77 mmHg) throughout the entire 300-minute test, with the difference reaching statistical significance ($p = 0.039$).

Along with blood gas composition indicators, blood pressure before and after the oxygenators was evaluated. In the control group, the transmembrane pressure gradient increased notably, from 19 ± 6 mmHg at baseline to over 30 mmHg after 300 minutes. Meanwhile, in both experimental groups, the gradient remained stable throughout the 5-hour perfusion period (22 ± 4.7 mmHg), indirectly indicating lower intermembrane thrombosis in the Cobetter Filtration® membranes.

CONCLUSION

The evolution of extracorporeal circulatory support has a long and dynamic history, and the devices themselves have undergone significant changes and modifications. Nevertheless, the core element of membrane oxygenation – the gas exchange membrane – has remained largely unchanged since its first clinical application. Today, intensive research is focused on enhancing the mechanical strength and biocompatibility of polypropylene.

The findings of this study possess both scientific significance and commercial potential, demonstrating that the newly developed Cobetter Filtration® polypropylene membranes exhibit comparable effectiveness to the established 3M® membranes. This opens new avenues for advancing membrane oxygenation technologies, ultimately improving procedural safety for patients.

The authors declare no conflict of interest.

REFERENCES

1. *Melchior RW, Sutton SW, Harris W, Dalton HJ*. Evolution of membrane oxygenator technology for utilization during pediatric cardiopulmonary bypass. *Pediatric Health Med Ther*. 2016 Jun 28; 7: 45–56. doi: 10.2147/PHMT.S35070. PMID: 29388637; PMCID: PMC5683297.
2. *Dennis C, Spreng DS Jr, Nelson GE, Karlson KE, Nelson RM, Thomas JV et al.* Development of a pump-oxygenator to replace the heart and lungs: an apparatus applicable to human patients, and application to one case. *Ann Surg*. 1951 Oct; 134 (4): 709–721. doi: 10.1097/00000658-195113440-00017.
3. *Mustard WT, Thomson JA*. Clinical experience with the artificial heart-lung preparation. *Can Med Assoc J*. 1957; 76: 265–269.
4. *Berne RM, Cross FS, Hirose Y, Jones RD, Kay EB*. Evaluation of a rotating disk-type reservoir oxygenator. *Proc Soc Exp Biol Med*. 1956; 93: 210–214. doi: 10.3181/00379727-93-22710.
5. *Lillehei CW, Cohen M, Warden HE, Read RC, Aust JB, Dewall RA, Varco RL.* Direct vision intracardiac surgical correction of the tetralogy of Fallot, pentalogy of Fallot, and pulmonary atresia defects; report of first ten cases. *Ann Surg*. 1955 Sep; 142 (3): 418–442. doi: 10.1097/00000658-195509000-00010. PMID: 13249340; PMCID: PMC1465089.
6. *Hossain MT, Shahid MA, Mahmud N, Habib A, Rana MM, Khan SA, Hossain MD*. Research and application of polypropylene: a review. *Discov Nano*. 2024 Jan 2; 19 (1): 2. doi: 10.1186/s11671-023-03952-z. PMID: 38168725; PMCID: PMC10761633.
7. *Gunaydin S*. Clinical significance of coated extracorporeal circuits: a review of novel technologies. *Perfusion*. 2004; 19 (Suppl 1): S33–S41. doi: 10.1191/0267659104pf718oa.
8. *Gunning AJ, Hodgson DC, Burrows P*. Travenol plastic-bag oxygenator in open-heart surgery. *Lancet*. 1965 Mar 13; 1 (7385): 584–585. doi: 10.1016/s0140-6736(65)91152-9. PMID: 14250087.
9. *Karlson KE, Massimino RM, Cooper GN Jr, Singh AK*. Initial clinical experience with a low pressure drop membrane oxygenator for cardiopulmonary bypass in adult patients. *Am J Surg*. 1984 Apr; 147 (4): 447–450. doi: 10.1016/0002-9610(84)90003-5. PMID: 6424487.
10. *Vyas A, Bishop MA*. Extracorporeal Membrane Oxygenation in Adults. 2023 Jun 21. In: StatPearls [Internet]. Treasure Island (FL): StatPearls Publishing; 2025 Jan. PMID: 35015451.
11. *Lim MW*. The history of extracorporeal oxygenators. *Anaesthesia*. 2006 Oct; 61 (10): 984–995. doi: 10.1111/j.1365-2044.2006.04781.x. PMID: 16978315.
12. *Syed A, Kerdi S, Qamar A*. Bioengineering Progress in Lung Assist Devices. *Bioengineering (Basel)*. 2021 Jun 28; 8 (7): 89. doi: 10.3390/bioengineering8070089. PMID: 34203316; PMCID: PMC8301204.
13. *Fang X, Sun C, Dai P, Xian Z, Su W, Zheng C et al*. Capillary Force-Driven Quantitative Plasma Separation Method for Application of Whole Blood Detection Microfluidic Chip. *Micromachines (Basel)*. 2024 May 1; 15 (5): 619. doi: 10.3390/mi15050619. PMID: 38793192; PMCID: PMC11122923.
14. *Xiao Z, Sun L, Yang Y, Feng Z, Dai S, Yang H et al*. High-Performance Passive Plasma Separation on OSTE Pillar Forest. *Biosensors (Basel)*. 2021 Sep 25; 11 (10): 355. doi: 10.3390/bios11100355. PMID: 34677311; PMCID: PMC8534190.
15. *Zięba-Palus J.* The usefulness of infrared spectroscopy in examinations of adhesive tapes for forensic purposes. *Forensic Sci Criminol*. 2017; 2 (2): 1–9. doi: 10.15761/FSC.1000112.

The article was submitted to the journal on 13.07.2025

DOI: 10.15825/1995-1191-2025-4-95-102

TOTAL HIP REPLACEMENT IN A HEART TRANSPLANT RECIPIENT WITH MULTIPLE COMORBIDITIES: A CASE REPORT

V.Yu. Murylev[1, 2], P.M. Elizarov[1, 2], P.A. Drozdov[2, 3], G.A. Kukovenko[1, 2], M.P. Elizarov[1, 2], A.V. Muzychenkov[1, 2], G.S. Michailyants[3], S.S. Alekseev[2], A.I. Rudnev[1, 2], K.G. Yakovlev[2], D.O. Golubkin[1]

[1] Sechenov University, Moscow, Russian Federation
[2] Botkin Hospital, Moscow, Russian Federation
[3] Russian Medical Academy of Continuous Professional Education, Moscow, Russian Federation

Background. According to available literature, recipients of solid organ transplants have a progressively increased risk of developing aseptic necrosis and osteoarthritis due to long-term corticosteroid and immunosuppressive therapy. Approximately 5% of transplant recipients develop femoral head avascular necrosis (FHAN). In such cases, the gold standard of treatment is total hip replacement (THR). However, this approach carries a high risk of postoperative infectious complications. **Clinical case.** A patient was admitted in Moscow at the City Center for Bone and Joint Endoprosthetics, Botkin Hospital for a planned THR. Six years earlier, she had undergone a heart transplant. Her clinical profile was further complicated by multiple comorbidities, placing her in a high-risk category for perioperative complications according to the ASA classification. **Conclusion.** Despite the high intraoperative and postoperative risks, THR was the only viable option to improve the patient's quality of life, given the progression of FHAN.

Keywords: femoral head avascular necrosis, endoprosthetics, hip joint, osteoarthritis, organ transplantation, immunosuppression.

INTRODUCTION

According to the 26th official report of the International Society for Heart and Lung Transplantation, more than 85,000 heart transplantations have been performed worldwide to date [1]. Lifelong immunosuppressive therapy in these patients may put them at increased risk of postoperative complications. Among these, orthopedic complications occur in approximately 20% of heart transplant (HT) recipients, with femoral head avascular necrosis (FHAN) being the most prevalent [2]. Reported incidence rates of FHAN in this population range from 3% to 9% [3–5]. According to Leonard et al. [6], the average time to joint replacement surgery after HT is seven years, with patients diagnosed with FHAN often requiring earlier endoprosthetic replacements. There are reports indicating that FHAN may be associated with long-term use of high doses of immunosuppressants [3, 5, 7–9]. In such cases, total hip replacement (THR) remains the gold standard of treatment. Prior investigations have shown that solid organ transplant recipients who have undergone hip replacement surgery achieve pain relief, improved joint function, and enhanced overall quality of life [8].

Our paper presents a clinical case of a patient who underwent successful total hip prosthetic replacement and was followed up dynamically for four years after a heart transplant performed in 2017. A distinctive feature of this case was the patient's unfavorable comorbid profile, which contributed to a high anesthetic risk according to the American Society of Anesthesiologists (ASA) classification.

CLINICAL CASE

Patient V., female, born in 1946, had a long-standing history of arterial hypertension with maximum recorded blood pressure values reaching 200/100 mmHg, although in recent years she had noted a tendency toward hypotension. At the time of admission, her weight was 95 kg, height 179 cm, and body mass index (BMI) 29.6 kg/m^2. She first considered herself ill in 1994, when she began experiencing dyspnea during physical exertion. An electrocardiogram (ECG) at that time revealed frequent ventricular extrasystoles. In 2008, she was diagnosed for the first time with dilated cardiomyopathy, paroxysmal atrial fibrillation, and frequent ventricular and supraventricular extrasystoles. By 2012, the patient exhibited signs of intraventricular and interventricular dyssynchrony, prompting the implantation of a biventricular cardioverter-defibrillator (CRT-D). In March 2013, a disturbance of atrial pacing was detected, necessitating atrial lead implantation. Over the subsequent years, the patient was repeatedly hospitalized for decompensated chronic heart failure (CHF). She was placed on the HT

Corresponding author: Pavel Drozdov. Address: 15, apt. 8, Brusilova str., Moscow, 117148, Russian Federation. Phone: (962) 985-04-41. E-mail: dc.drozdov@gmail.com

waiting list, and in 2017, underwent orthotopic HT at Shumakov National Medical Research Center of Transplantology and Artificial Organs. The postoperative course was uneventful.

A few months after the HT, the patient began experiencing progressively increasing pain in the right hip joint and her limp worsened. The pain gradually became constant and debilitating, necessitating the use of additional walking support. Over time, she developed pain in the lumbar spine, which was attributed to pelvic obliquity resulting from a developing flexion-adduction contracture of the right hip joint. Outpatient magnetic resonance imaging (MRI) of the pelvis was performed, revealing characteristic features of aseptic necrosis of the femoral head (ANFH) (Fig. 1). An incidental radiographic finding revealed FHAN.

On physical examination, the patient ambulated with a cane in her left hand, demonstrating pronounced limping of the right lower limb, persistent external rotation of the right hip by approximately 10 degrees, and a sharp decrease in weight-bearing capacity on the right leg. Movement within the right hip joint was restricted and elicited sharp pain.

Radiographic evaluation revealed asymmetry of the pelvic ring and uneven narrowing of the right hip joint space, with sclerosis of the subchondral bone. The right femoral head is mushroom-shaped with bone structure changes in the form of lucencies alternating with areas of thickening. In the lateral aspect, a cystic lucency with partial cortical destruction was identified. The femoral head was positioned in an anterolateral subluxation, and massive marginal osteophytes were present (Fig. 2).

At the time of referral to the endoprosthetics center, the patient was receiving maintenance immunosuppressive therapy consisting of tacrolimus 1.5 mg twice daily and mycophenolic acid 360 mg twice daily. In addition to her history of HT, she had experienced deep vein thrombosis of the lower extremities, which progressed to post-thrombophlebitic disease. Her comorbid conditions included polyosteoarthrosis (nodular, erosive variant), secondary gout, secondary hyperparathyroidism, and hypothyroidism – the latter being medically compensa-

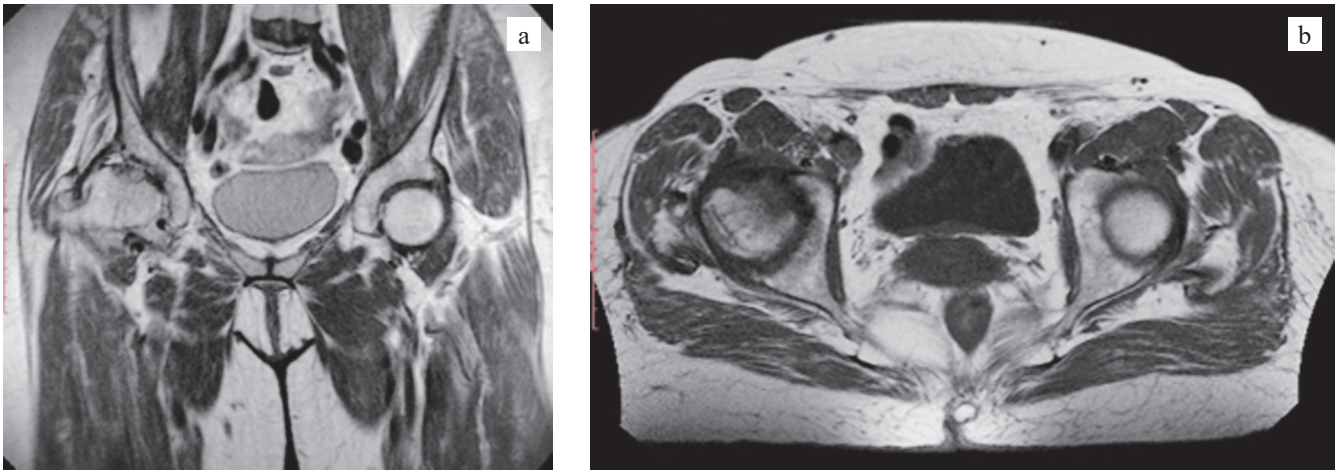

Fig. 1. MRI of the right hip joint showing the FHAN area: a, frontal projection; b, axial projection

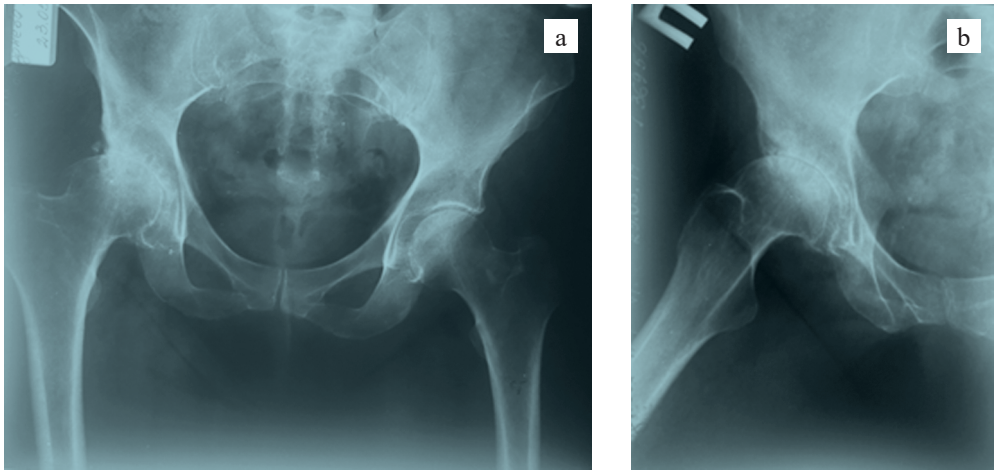

Fig. 2. Preoperative X-ray in anteroposterior projection demonstrating FHAN on the right and grade III coxarthrosis: a, general pelvic view; b, image of the right hip joint

ted. Cardiovascular assessment revealed ischemic heart disease (IHD) and transplant coronary artery disease, as well as chronic heart failure (CHF), stage IIA, functional class II (NYHA). Consequently, her anesthetic risk according to ASA classification was very high.

Despite these challenges, total hip arthroplasty represented the only viable option to relieve the severe pain syndrome that significantly impaired her quality of life, restore weight-bearing capacity of the right lower limb, and recover functional joint mobility.

Although the procedure carried substantial perioperative risks due to the patient's unfavorable comorbid background and ongoing immunosuppressive therapy, reports of successful surgical management of FHAN in solid-organ transplant recipients have been documented in international literature. Taking these precedents into account, a decision was made to proceed with THR surgery.

From a technical standpoint, the THR procedure in this patient did not differ significantly from that performed in the general population. A cementless endoprosthesis was implanted without technical difficulties (Fig. 3).

In the postoperative period, the patient received targeted antibiotic therapy with meropenem 1 g once daily and linezolid 300 mL (2 mg/mL). Anticoagulant therapy with enoxaparin sodium 4000 anti-Xa IU/0.4 mL subcutaneously once daily was initiated on postoperative day 1.

An important intraoperative objective was to minimize blood loss, as excessive hemorrhage could result in serious complications in a heart transplant recipient. Additionally, close monitoring for myocardial ischemia was essential, since denervation of the transplanted heart may mask typical anginal symptoms.

Preoperative hemoglobin levels were 121 g/L. Intraoperative blood loss was estimated at 350 mL, and within the first 24 hours postoperatively, an additional 480 mL of blood loss was recorded. As a result, hemoglobin levels decreased to 83 g/L. Despite comprehensive conservative therapy, including transfusion of 985 mL of red blood cells, 850 mL of fresh frozen plasma, and 300 mL of 10% albumin solution, hemoglobin levels only increased to 105 g/L.

On postoperative day 3, the patient's general condition deteriorated, and persistent edema was observed in the postoperative suture site. An ultrasound examination was performed to identify potential fluid collections. A hypoechoic interstitial lesion measuring up to 18 mL was detected at a depth of 7–8 cm, consistent with soft tissue hematoma. By evening, repeat ultrasound of the posterior surface of the right hip joint revealed a larger hematoma measuring approximately 350 mL.

A contrast-enhanced computed tomography (CT) scan of the right thigh confirmed the presence of a localized fluid collection (approximately 200 mL) along the posterior surface of the femur, with diffuse soft tissue edema. There were no clinical or laboratory signs of ongoing bleeding. A tendency toward hypocoagulation was noted; therefore, the anticoagulant therapy prescribed by protocol was discontinued.

A repeat contrast-enhanced CT scan of the right hip revealed persistent fluid accumulation within the muscle tissue of the operated limb, without evidence of extravasation. Two days later, an ultrasound-guided diagnostic puncture of the fluid collection was performed, yielding approximately 27 mL of hematoma consisting of dark coagulated blood. Laboratory tests revealed moderate hypocoagulation affecting the platelet component, with a hemoglobin level of 99 g/L. Based on these findings, a decision was made to withhold anticoagulant therapy. The postoperative wound healing process proceeded without complications.

A follow-up ultrasound conducted three days later showed two organized soft tissue hematomas measuring 152 mL and 38 mL. Five days later, the ultrasound

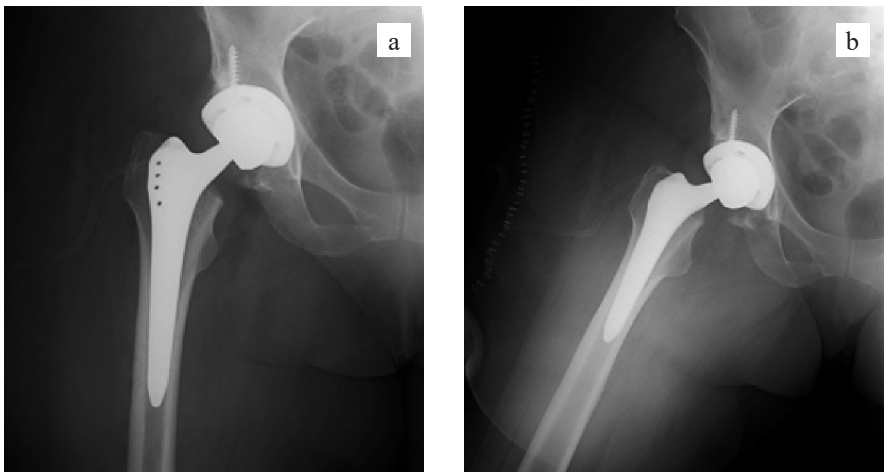

Fig. 3. X-ray on the first postoperative day following total hip arthroplasty of the right hip using a Zimmer–Biomet cementless endoprosthesis (IT cup, Alloclassic stem): a, hip joint in neutral position; b, hip joint in abduction position

showed positive dynamics, with a reduction in hematoma volume to 35 mL and 15 mL on the day before suture removal.

The patient's mobilization and rehabilitation followed the standard activation protocol used for individuals undergoing similar arthroplasty procedures. On postoperative day 1, the patient was able to sit up independently, and by day two, she stood and walked unassisted. Sutures were removed on postoperative day 14, with primary intention wound healing observed.

RESULTS

The Harris Hip Score (HHS) questionnaire was used to assess hip joint function before and after THR. According to standard interpretation, scores of 90–100 indicate excellent results, 80–89 good, 70–79 fair, and below 70 unsatisfactory outcomes [10]. In the preoperative questionnaire, the patient's HHS score was 43.8 points. Postoperatively, the patient was followed up for four years, with comprehensive evaluations conducted at 3, 6, 12, and 24 months, and subsequently annually after surgery.

Preoperative and postoperative examination of the range of motion (ROM) of the operated hip joint over time is presented in Table.

During the first two years following surgery, ROM in the operated hip joint showed a progressive increase. Over the subsequent two years of follow-up (total observation period: four years), ROM indicators remained within the previous estimated range.

Although the patient's HHS remained below 70 during the first 6 months postoperatively, she reported a high level of satisfaction with the surgery owing to marked pain relief and restoration of limb support. One year after THR, the HHS had improved to 82 points, and the ROM in the joint further increased. After two years, the score reached 84 points.

It is noteworthy that the patient's complete rehabilitation within four months was somewhat limited by pain in the contralateral hip joint, where coxarthrosis had developed secondary to FHAN. This was followed by unloading of this joint due to the operated leg, and the pain in it decreased.

Throughout the observation period, we followed a uniform postoperative protocol, the same as for non-transplant patients. X-rays were performed both pre- and postoperatively. Early postoperative imaging confirmed proper implantation, stable fixation and possible malposition of the endoprosthesis, while long-term follow-up radiographs demonstrated satisfactory osseointegration of the prosthetic components, possible osteolysis, polyethylene wear, and possible heterotopic ossification around it. At later stages, it was used to assess the position of the implant and its stability (Figs. 4, 5).

Table

Clinical assessment of the range of motion in the right hip joint

	Flexion	Extension	Abduction	Adduction	Rotation	
					Internal	External
Before surgery	120	175	20	5	0	5
3 months after surgery	100	180	30	5	5	15
6 months after surgery	90	180	40	10	10	15
1 year after surgery	70	180	40	15	15	15
2, 3, and 4 years after surgery	70	180	45	15	15	20

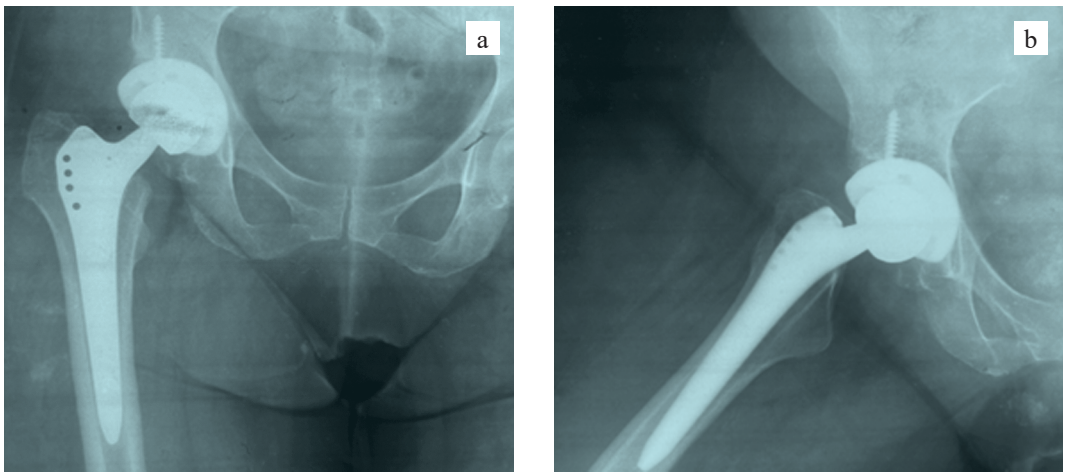

Fig. 4. X-ray six months after total hip arthroplasty of the right hip (Zimmer–Biomet cementless endoprosthesis, IT cup, Alloclassic stem): a, hip joint in neutral position; b, hip joint in abduction position

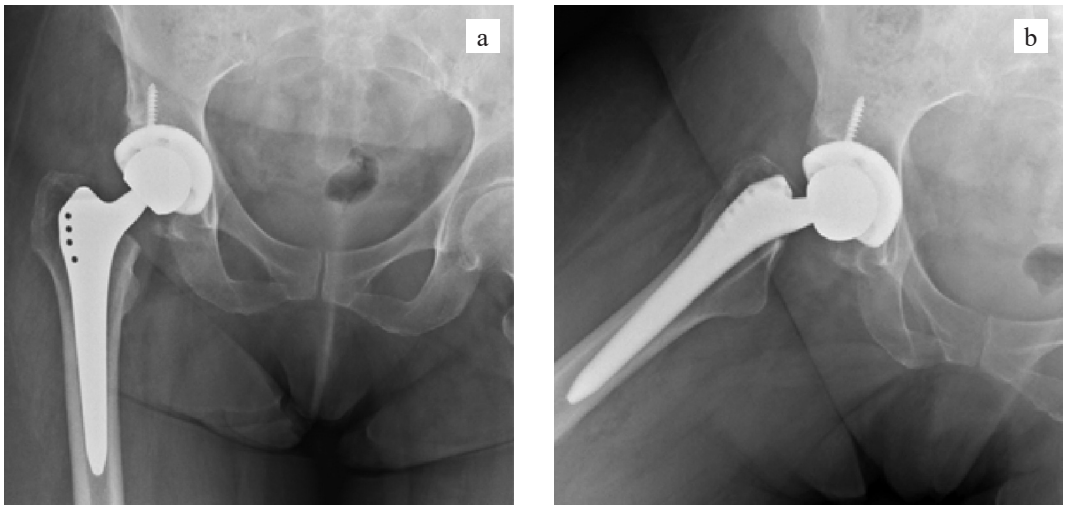

Fig. 5. X-ray four years after total hip arthroplasty of the right hip showing a correct and stable position of the endoprosthesis with evidence of osteointegration: a, hip joint in neutral position; b, hip joint in abduction position

DISCUSSION

The incidence of hip arthroplasty in patients with previous heart transplantation remains relatively rare, and there are limited reports in the international literature addressing this clinical situation. Nevertheless, available studies indicate that organ transplant recipients are at an increased risk of developing FHAN and osteoarthritis, primarily due to long-term corticosteroid and immunosuppressive therapy, with approximately 5% of patients developing FHAN after transplantation [5, 11–12].

In a study by Wu et al. in 2022 published data on 119 hip replacement surgeries performed over 20 years [13]. The leading indication for THR was FHAN (54.6%), followed by severe degenerative joint disease (39.4%), fractures (2.5%), arthritis (1.7%), Perthes disease (0.8%), and osteodysplasia (0.8%). The study further compared outcomes of arthroplasty among recipients of heart, kidney, liver, and lung transplants. Out of 182 hip and knee replacements performed, heart transplant recipients accounted for only 10% of cases.

Patients with transplanted hearts and kidneys tended to be younger compared to those who had undergone liver or lung transplantation, yet they presented with a higher anesthetic risk according to the ASA classification. Despite these risks, the overall outcomes of endoprosthetic replacement were encouraging: implant survival rates reached 95.6% at 1 year and 92.1% at 4 years. Revision surgery was necessary in only 8 cases, of which one patient was a heart transplant recipient.

In the study by Chalmers et al. [14], the 2-year implant survival rate was 95%, and the 5-year survival rate was 94%, with no significant differences depending on the type of implant. Importantly, the authors found no statistically significant association between implant survival and the type of transplanted organ.

A distinctive feature of THR in heart transplant recipients is the necessity for lifelong immunosuppressive therapy, which significantly increases the risk of postoperative infectious complications [9]. In managing such patients, a personalized approach is essential. Adjustment of immunosuppressive regimens and administration of any concomitant medications should be performed in coordination with the transplant center overseeing the patient's long-term care.

The highest incidence of postoperative infections among solid organ recipients is observed in kidney transplant patients [15–16]. This finding is supported by Cavanaugh et al. [17]. Klement et al. further corroborated these observations, demonstrating that patients with kidney transplants undergoing THR exhibit a significantly higher risk of infectious complications compared to non-transplant patients [18].

Comparative analyses between standard THR cohorts and patients with previous solid organ transplantation consistently indicate an elevated risk of infectious complications during the first 90 postoperative days. However, studies also show that by 2 years post-arthroplasty, there is no significant difference in the frequency of complications [19–20].

Given the increased risk of postoperative infectious complications in transplant recipients, perioperative antibiotic prophylaxis is indicated for this patient population. Leonard et al. analyzed 18 cases of total joint arthroplasty performed in HT recipients at Penn State Health Milton S. Hershey Medical Center, where antibiotic prophylaxis was administered intraoperatively and continued for 72 hours postoperatively. Cefazolin was the standard antibiotic of choice, while vancomycin or clindamycin was used in patients with penicillin hypersensitivity [6].

We concur with previous authors who argue that standard antibiotic regimens are generally sufficient for perioperative infection prevention in such cases [21].

However, our case presented unique clinical challenges due to the patient's extensive comorbidities. The development of a large postoperative soft tissue hematoma, despite adequate wound drainage, represented a significant risk factor for secondary infection, particularly in the context of ongoing immunosuppressive therapy and postoperative anemia. That is why we elected to extend the antibiotic course beyond standard practice, administering meropenem and linezolid for an additional 10 days.

N. Brown [22] reported a high postoperative mortality rate among transplant recipients undergoing arthroplasty. Conversely, Navalle et al. [23] found no significant increase in mortality compared to non-transplant patients undergoing similar orthopedic procedures. According to Wu [13], the mortality rate among solid organ recipients was 2.9% one year after arthroplasty and 23.7% four years postoperatively. Similarly, Chalmers et al. [14] reported mortality rates of 3.8% within the first two years and 13.3% within five years following arthroplasty in this patient population.

In our study, the heart transplant recipient underwent THR with favorable clinical and radiographic outcomes. Over a four-year follow-up period, the patient showed sustained implant stability and satisfactory joint function. She currently leads an active lifestyle, walks with a cane, and reports no discomfort in the operated hip joint.

Conclusion

From an orthopedic standpoint, hip replacement surgery in HT recipients does not present any specific technical deviations in terms of surgical access, implant selection, or procedural technique. In our observation, neither the duration of the operation, volume of intraoperative blood loss, nor postoperative recovery dynamics differed significantly from those seen in standard patients. Four years of follow-up demonstrated favorable functional outcomes, including complete resolution, and a marked improvement in the HHS score.

Successful orthopedic intervention in such high-risk patients is contingent upon a multidisciplinary approach within a specialized tertiary or transplant center, ensuring meticulous preoperative evaluation and preparation. This clinical case underscores that, despite the potentially high risk of possible complications in this patient cohort, THR in HT recipients can be considered a relatively safe and effective strategy to enhance overall quality of life and life expectancy.

The authors declare no conflict of interest.

REFERENCES

1. *Taylor DO, Stehlik J, Edwards LB, Aurora P, Christie JD, Dobbels F et al*. Registry of the International Society for Heart and Lung Transplantation: Twenty-sixth Official Adult Heart Transplant Report – 2009. *J Heart Lung Transplant.* 2009 Oct; 28 (10): 1007–1022. https://doi.org/10.1016/j.healun.2009.08.014.
2. *Egan B, O'Byrne JM, O'Farrell D, O'Donnell A, Wood AE, Neligan MC, O'Brien TM.* Orthopaedic complications following cardiac transplantation. *Ir Med J.* 1996 Jan-Feb; 89 (1): 26–27. PMID: 8984077.
3. *Bradbury G, Benjamin J, Thompson J, Klees E, Copeland J*. Avascular necrosis of bone after cardiac transplantation. Prevalence and relationship to administration and dosage of steroids. *J Bone Joint Surg Am.* 1994 Sep; 76 (9): 1385–1388. https://doi.org/10.2106/00004623-199409000-00014.
4. *León JL, Resines C, Zafra A*. Total hip arthroplasty in heart transplant patients. *Acta Orthop Belg.* 2007 Dec; 73 (6): 720–728. PMID: 18260484.
5. *Lieberman JR, Roth KM, Elsissy P, Dorey FJ, Kobashigawa JA*. Symptomatic osteonecrosis of the hip and knee after cardiac transplantation. *J Arthroplasty*. 2008 Jan; 23 (1): 90–96. https://doi.org/10.1016/j.arth.2007.01.006.
6. *Leonard GR, Davis CM 3rd*. Outcomes of total hip and knee arthroplasty after cardiac transplantation. *J Arthroplasty.* 2012 Jun; 27 (6): 889–894. https://doi.org/10.1016/j.arth.2011.12.030.
7. *Kulak CA, Borba VZ, Kulak Júnior J, Campos DJ, Shane E*. Post-transplantation osteoporosis. *Arq Bras Endocrinol Metabol.* 2010 Mar; 54 (2): 143–149. https://doi.org/10.1590/s0004-27302010000200009.
8. *Ledford CK, Watters TS, Wellman SS, Attarian DE, Bolognesi MP*. Risk versus reward: total joint arthroplasty outcomes after various solid organ transplantations. *J Arthroplasty.* 2014 Aug; 29 (8): 1548–1552. https://doi.org/10.1016/j.arth.2014.03.027.
9. *Khubutia MSh, Klyukvin IYu, Slastinin VV, Bogatsky GV, Bogolubsky YuA, Syutkin VE*. Hip replacement in female patient after liver transplantation (Case report). *Trudnyy patsiyent.* 2015; 13 (4): 21–23. (In Russ.).
10. *Harris WH*. Traumatic arthritis of the hip after dislocation and acetabular fractures: treatment by mold arthroplasty. An end-result study using a new method of result evaluation. *J Bone Joint Surg Am.* 1969 Jun; 51 (4): 737–755. PMID: 5783851.
11. *Lieberman JR, Scaduto AA, Wellmeyer E*. Symptomatic osteonecrosis of the hip after orthotopic liver transplantation. *J Arthroplasty.* 2000 Sep; 15 (6): 767–771. https://doi.org/10.1054/arth.2000.6635.
12. *Marston SB, Gillingham K, Bailey RF, Cheng EY*. Osteonecrosis of the femoral head after solid organ transplantation: a prospective study. *J Bone Joint Surg Am.* 2002 Dec; 84 (12): 2145–2151. https//doi.org/10.2106/00004623-200212000-00004.
13. *Wu CJ, Brekke AC, Hinton ZW, Kim BI, Ryan SP, Bolognesi MP, Seyler TM*. Total joint arthroplasty following solid organ transplants: complication and mid-term outcomes. *Int Orthop.* 2022 Dec; 46 (12): 2735–2745. https://doi.org/10.1007/s00264-022-05597-6.
14. *Chalmers BP, Ledford CK, Statz JM, Perry KI, Mabry TM, Hanssen AD, Abdel MP.* Survivorship after primary total hip arthroplasty in solid-organ transplant patients. *J Arthroplasty.* 2016 Nov; 31 (11): 2525–2529. https://doi.org/10.1016/j.arth.2016.04.012.

15. *Duplantier NL, Rivere AE, Cohen AJ, Chimento GF*. Hip and knee arthroplasty outcomes after abdominal organ transplantation. *J Surg Orthop Adv.* 2018 Summer; 27 (2): 119–124. PMID: 30084819.
16. *Klatt BA, Steele GD, Fedorka CJ, Sánchez AI, Chen AF, Crossett LS*. Solid organ transplant patients experience high rates of infection and other complications after total knee arthroplasty. *J Arthroplasty.* 2013 Jun; 28 (6): 960–963. https://doi.org/10.1016/j.arth.2013.02.005.
17. *Cavanaugh PK, Chen AF, Rasouli MR, Post ZD, Orozco FR, Ong AC*. Total joint arthroplasty in transplant recipients: in-hospital adverse outcomes. *J Arthroplasty.* 2015 May; 30 (5): 840–845. https://doi.org/10.1016/j.arth.2014.11.037.
18. *Klement MR, Penrose CT, Bala A, Green CL, Mather RC 3rd, Wellman SS et al.* Complications of total hip arthroplasty following solid organ transplantation. *J Orthop Sci.* 2017 Mar; 22 (2): 295–299. https://doi.org/10.1016/j.jos.2016.12.004.
19. *Upfill-Brown A, Hart CM, Hsiue PP, Burgess K, Chen CJ, Khoshbin A et al.* Revision total hip arthroplasty in solid organ transplant patients: a propensity score-matched cohort study for aseptic and infected revisions. *Arthroplast Today.* 2022 Jan 20; 14: 6–13. https://doi.org/10.1016/j.artd.2021.10.007.
20. *Upfill-Brown A, Wu SY, Hart C, Hsiue PP, Chen CJ, Ponzio D et al*. Revision total knee arthroplasty outcomes in solid organ transplant Patients, a matched cohort study of aseptic and infected revisions. *Knee.* 2022 Jan; 34: 231–237. https://doi.org/10.1016/j.knee.2021.12.007.
21. *Sperling JW, Cofield RH*. Case reports: shoulder arthroplasty in transplant recipients: a report of five cases. *Clin Orthop Relat Res.* 2006 Jan; 442: 273–275. https://doi.org/10.1097/01.blo.0000191271.57657.07.
22. *Brown N, Ralles S, Kroin E, Adams W, Wu K*. Complications of total joint arthroplasty in solid organ transplant patients versus a large control group. *J Clin Orthop Trauma.* 2020 Jan-Feb; 11 (1): 91–95. https://doi.org/10.1016/j.jcot.2019.07.018.
23. *Navale SM, Szubski CR, Klika AK, Schiltz NK, Desai PP, Barsoum WK*. The Impact of Solid Organ Transplant History on Inpatient Complications, Mortality, Length of Stay, and Cost for Primary Total Hip Arthroplasty Admissions in the United States. *J Arthroplasty.* 2017 Apr; 32 (4): 1107–1116.e1. doi: 10.1016/j.arth.2016.10.017.

The article was submitted to the journal on 4.04.2025

DOI: 10.15825/1995-1191-2025-4-103-109

HYBRID HEMODYNAMIC MODELING FOR OPTIMIZATION OF MECHANICAL CIRCULATORY SUPPORT SYSTEMS

A.I. Syrbu[1], A.O. Shevchenko[1, 2], N.V. Grudinin[1], A.S. Buchnev[1]

[1] Shumakov National Medical Research Center of Transplantology and Artificial Organs, Moscow, Russian Federation

[2] Sechenov University, Moscow, Russian Federation

Objective: to propose and justify approaches for improving the classical hemodynamic test bench, widely used to model the integration of mechanical circulatory support (MCS) systems. **Materials and methods.** The hemodynamic test bench consisted of multiple containers and resistors simulating systemic and pulmonary circulation, enabling the study of physiological conditions in heart failure (HF). The setup also included an auxiliary circulatory support pump and a pulsatile flow generator. **Results.** A mathematical model of the cardiovascular system was developed, capable of reproducing physiological states under conditions of pump-assisted circulation and pulsatile flow. Comparative evaluation of experimental and modeling results highlighted the advantages and limitations of different modeling methods. **Conclusion.** Based on these findings, strategies for further development of the hemodynamic test bench, aimed at enhancing its ability to simulate the impact of mechanical circulatory support on key hemodynamic parameters, were formulated and justified.

Keywords: mechanical circulatory support, hemodynamic test bench, mathematical modeling.

INTRODUCTION

Modern transplantology increasingly depends on engineering solutions designed to support the function of vital organs, including the heart [1, 2]. One of the most rapidly evolving fields involves the creation and optimization of mechanical circulatory support (MCS) systems, encompassing both extracorporeal and implantable pulsatile and continuous-flow pumps, as well as auxiliary devices for generating pulsatile blood flow [2–6].

Despite significant technological progress, one of the most critical stages in the development and clinical translation of MCS systems remains preclinical modeling and testing. Reproducing the physiological conditions under which these systems operate requires a high degree of precision, both in hydrodynamic performance and systemic physiological response [7, 8]. Consequently, continuous improvement of simulation platforms is essential, not only to accommodate the characteristics of novel devices, but also to integrate modern computational and mathematical modeling approaches.

The objective of this study is to substantiate proposals for the development of hemodynamic modeling complexes, using as an example the hemodynamic test bench designed and implemented at Shumakov National Medical Research Center of Transplantology and Artificial Organs [4, 5]. The work integrates the results of modeling, validation, and optimization of MCS parameters obtained by the authors, including a new technical device for generating pulsating flow [9–11].

MATERIALS AND METHODS

The hemodynamic test bench comprises an aortic (pulmonary artery) simulator, systemic and pulmonary hydraulic resistance, atrial reservoirs, an axial pump replicating the function of the left or right ventricles, an artificial ventricle simulator equipped with a pneumatic drive, and a sensor system for continuous monitoring of pressure and flow parameters. A schematic representation of the test bench configuration is presented in Fig. 1.

The physical component of the simulation complex – the hemodynamic test bench – enables the reproduction of key modes of cardiovascular system function through integration of mechanical and hydraulic elements. To enhance configurability, account for individual physiological variability, and model complex interaction scenarios with MCS devices, a mathematical model was developed. This model enables the prediction of hemodynamic responses to variations in device parameters, including those of the axial pump and pulsatile-flow generator (PFG) [9, 10].

The structure of the mathematical model (Fig. 2) consists of the following elements: left ventricle, left atrium, aortic, peripheral, and venous compartments, as well as coronary circulation, baroreceptor regulation, oxygen debt compensation, heart rate control circuits, and the aortic and mitral valves. In addition, the blocks describing the operation of the continuous flow pump and the pulsatile flow generator are highlighted with dotted lines [11].

Corresponding author: Arseniy Syrbu. Address: 1, Shchukinskaya str., Moscow, 123182, Russian Federation. Phone: (915) 453-98-55. E-mail: s_arseniy@outlook.com

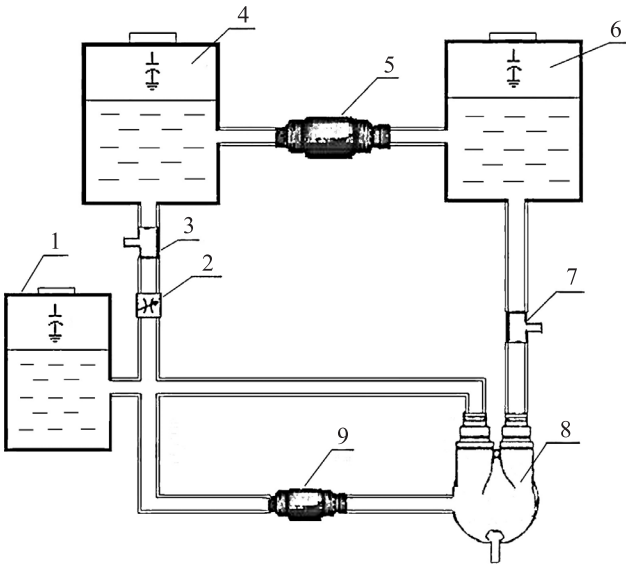

Fig. 1. Schematic diagram of the hemodynamic test bench: 1, arterial reservoir; 2, systemic hydraulic resistance; 3, arterial or pulmonary pressure sensor; 4, venous reservoir; 5, continuous-flow pump simulating systemic or pulmonary circulation; 6, reservoir simulating the pulmonary vein–left atrium system; 7, atrial pressure sensor; 8, artificial heart ventricle; 9, test VAD pump

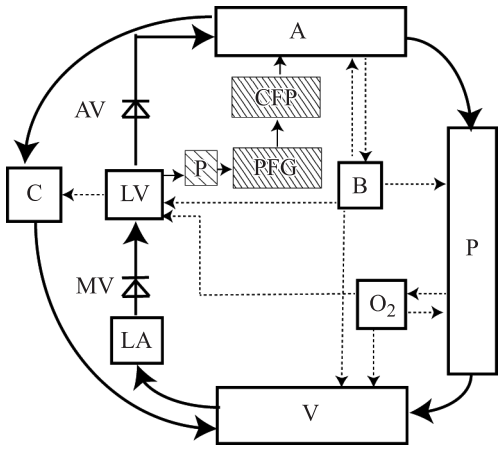

Fig. 2. Structural diagram of the mathematical model of the cardiovascular system with mechanical circulatory support. Abbreviations: LV, left ventricle; LA, left atrium; AO, aortic section; P, peripheral circulation; V, venous section; C, coronary vessels; B, baroreceptor regulation; O_2, oxygen debt regulation circuit; AV, aortic valve; MV, mitral valve; CFP, continuous-flow pump; PFG, pulsatile-flow generator

The diagram shows, with dotted lines, the added elements of the system: the continuous-flow pump, pulsatile flow generation devices, and a component simulating the occurrence of negative pressure in the left ventricle. Incorporating these modules – which represent the functional characteristics of MCS devices – into the previously developed mathematical model of the cardiovascular system makes it possible to account for their impact on key hemodynamic parameters.

RESULTS

The results of flow modeling through the MCS system obtained using the hemodynamic test bench are presented in Fig. 3.

For comparison, the results derived from the mathematical model under identical experimental conditions are shown in Fig. 4.

Analysis of the presented dependencies indicates that, although the obtained results are both qualitatively and quantitatively comparable, certain hydrodynamic phenomena are not fully captured by the model. Specifically, the lumped-parameter model fails to account for turbulent flow formation during the transition from systole to diastole and does not incorporate the non-Newtonian properties of blood.

On the other hand, the existing hemodynamic test bench cannot simulate specific physiological transitions, such as a shift from a state of rest to a state of physical exertion. Such constraints are typical of all bench-based hemodynamic systems.

In light of these limitations, recent years have seen increasing emphasis on the development of hybrid simulation platforms, integrating both physical test benches and computational mathematical models under a control system [12–18].

The results of this study make it possible to outline several proposals for optimizing the hemodynamic test bench developed at the Laboratory of Biotechnical Systems, Shumakov National Medical Research Center of Transplantology and Artificial Organs, with the overarching goal of enhancing the efficiency of MCS systems.

The goal of improving the test bench is to create a simulation test bench system that provides the ability to model the state of the cardiovascular system, taking into

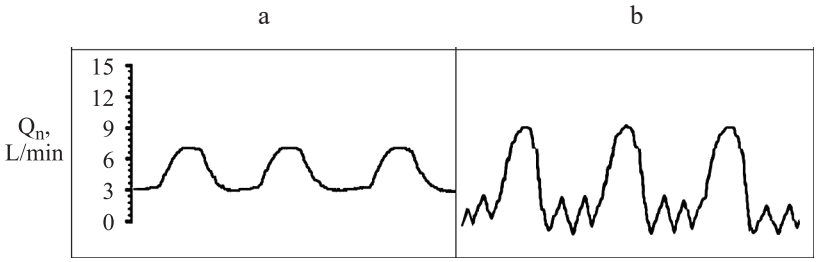

Fig. 3. Pump flow characteristics under continuous-flow conditions (a) and with connection to a pulsator (b), obtained on a hemodynamic stand. Interval = 1 s. Q_n – pump flow rate (L/min)

account heart failure, other pathologies, the level of physical activity, the presence of MCS systems, their characteristics, and modes of operation. At the same time, as shown by mathematical modeling results, it is essential to take into account the mechanisms of neurohumoral and baroreceptor regulation.

First of all, it is advisable to replace the existing analog controller of the heart simulator with a digital, reprogrammable real-time control module. At the same time, a set of algorithms for controlling the heart simulator can be pre-formed and tested on the mathematical model of the cardiovascular system developed in this work.

Additionally, the test bench should include controllable hydrodynamic resistances with high-precision pressure sensors. These components will enable closed-loop feedback control to account for the mechanisms of neurohumoral and baroreceptor regulation, similar to what was implemented in the mathematical model of the cardiovascular system developed in this work.

We recommend developing a pulsatile flow generator model with variable controlled pressure inside the chamber. Such a device would permit real-time tuning of generator parameters to reproduce blood flow that closely match the physiological characteristics of individual patients. Control signal parameters for the generator would be predefined in the mathematical model of the device.

The mathematical model described above can form the core of a hybrid (semi-natural) simulation platform. In this architecture the cardiovascular system's bulk hydraulics are realized on the hemodynamic test bench, while regulatory and adaptive mechanisms (baroreflex, neurohumoral feedback, exercise responses, etc.) are simulated in the computational module. Real-time measurements of pressure, flow and other state variables from the bench are streamed to the model, which computes corrective control signals and returns them to the bench to adjust resistances and chamber pressures.

A schematic overview of the proposed hybrid approach is shown in Fig. 5: solid lines denote fluid flows, and dotted lines indicate control signals from the computer part and back. A closely related concept has been previously discussed [19].

The following algorithm was developed to govern the operation of the proposed simulation test bench:

1) The model and test bench parameters are configured to simulate heart failure conditions;
2) The flow-pressure characteristics of the MCS device under investigation are entered into the model;
3) The test bench parameters are adjusted so that recorded pressures and flow rates correspond to clinical data;
4) It is then connected to a pulsatile flow generator (PFG);

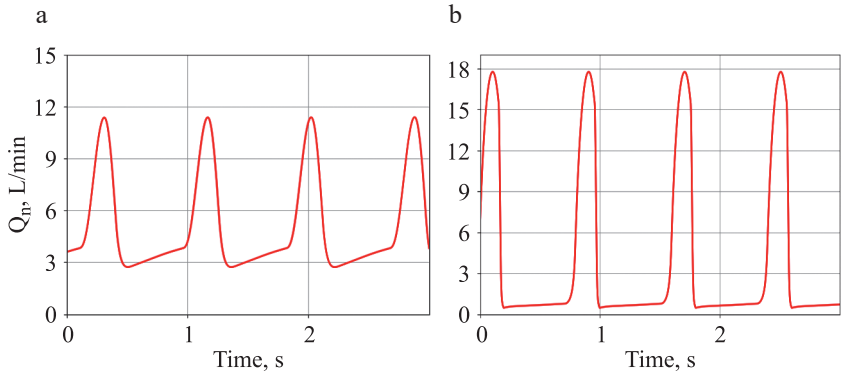

Fig. 4. Flow profiles through the pump under continuous-flow conditions (a) and with pulsator connection (b), obtained using a mathematical model. Interval = 1 s. Q_n – pump capacity (L/min)

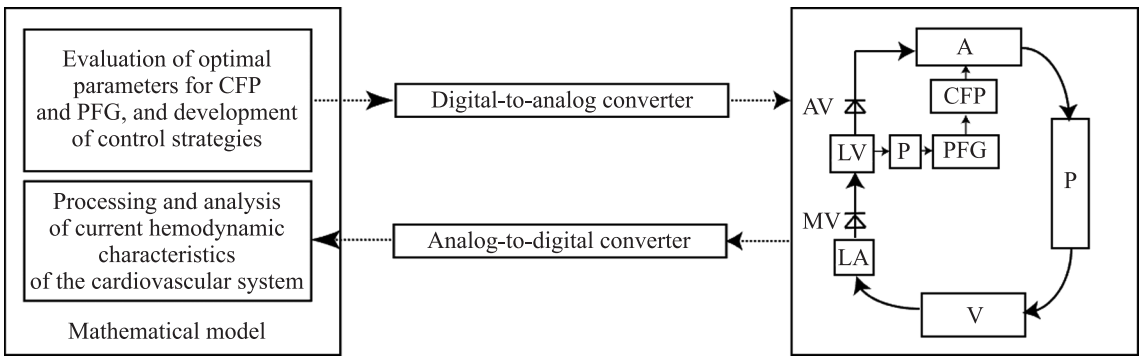

Fig. 5. Structural diagram of the proposed hybrid (semi-natural) simulation test bench

5) Experimental phase: A series of experiments is performed in which the parameters of the PFG, such as opening/closing pressures and hydraulic resistance, are systematically varied;
6) The resulting data are approximated and analyzed to determine the optimal pressure parameters within the PFG chamber and the maximum effective resistance of the generator and related elements;
7) The test bench settings are then adjusted in accordance with the identified optimal values;
8) A series of verification tests is conducted.

The core component of a next-generation computer model integrated into such a hybrid (semi-natural) simulation stand should be an intelligent analysis and control system capable of automatically analyzing hemodynamic data, recognizing the cardiovascular functional state of the system, and adaptively regulating the MCS parameters in real time. Such a computer model can be built on the basis of, for example, a multilayer neural networks and machine learning algorithms.

The following research directions should be identified as priority tasks for which the proposed hybrid modeling stand can be used:

1. Investigation of the rotor speed modulation algorithms aimed at increasing pulse pressure.
2. Investigation of the rotor speed modulation algorithms designed to ensure adaptive response to physical exertion and other conditions.
3. Study of the parameters of pulsatile-flow generation devices and their optimization.

Thus, the mathematical modeling of the cardiovascular system, incorporating the functional characteristics of MCS systems, enables the exploration of both existing and next-generation designs of continuous-flow pumps and pulsatile-flow generators. It also provides a framework for assessing the influence of various operational modes of these devices on the cardiovascular system under different conditions.

DISCUSSION

A comparison of results obtained from the hemodynamic test bench and from the mathematical model shows the need for a hybrid approach to more accurately characterize interactions between MCS devices and the cardiovascular system. Such an approach makes it possible to capture device-specific effects observed on the physical bench while simultaneously introducing physiologically meaningful feedback into the hydraulic system. Integrating physical and computational components within a single hybrid complex enables a closed-loop control architecture in which real-time data from the bench are streamed to the mathematical model, processed, and returned as control commands. This arrangement significantly broadens the functionality of the test bench and ensures a high level of physiological reliability of the experiments.

A review of the literature further corroborates the growing interest in the creation of hybrid simulation platforms among researchers in this field.

CONCLUSION

The development of hybrid simulation complexes marks a major advancement in the engineering support of extracorporeal circulation systems. The integration of a physical hemodynamic test bench with an adaptive mathematical model provides a new level of precision and flexibility in the testing, tuning, and validation of MCS systems.

Of particular relevance is the implementation of intelligent control algorithms enabling the personalization of MCS parameters. Furthermore, such systems can simplify and accelerate the preclinical evaluation of novel extracorporeal circulation systems.

Hybrid simulation complexes represent the foundation of a new generation of engineering medicine tools – systems that are intelligent, adaptive, and patient-centered.

The authors declare no conflict of interest.

REFERENCES

1. *Gautier SV.* Priority areas of scientific research in the field of transplantology and artificial organs. *Russian Journal of Transplantology and Artificial Organs*. (In Russ.). 2025; 27 (1): 6–7.
2. *Cameli M, Pastore MC, Campora A, Lisi M, Mandoli GE*. Donor shortage in heart transplantation: How can we overcome this challenge? *Front Cardiovasc Med*. 2022 Oct 17; 9: 1001002. doi: 10.3389/fcvm.2022.1001002.
3. *Kyriakopoulos CP, Kapelios CJ, Stauder EL, Taleb I, Hamouche R, Sideris K et al*. LVAD as a bridge to remission from advanced heart failure: current data and opportunities for improvement. *J Clin Med*. 2022 Jun 20; 11 (12): 3542. doi: 10.3390/jcm11123542.
4. *Itkin GP, Bychnev AS, Kuleshov AP, Drobyshev AA*. Haemodynamic evaluation of the new pulsatile-flow generation method *in vitro*. *Int J Artif Organs*. 2020 Mar; 43 (3): 157–164. doi: 10.1177/0391398819879939.
5. *Buchnev AS, Kuleshov AP, Esipova OYu, Drobyshev AA, Grudinin NV*. Hemodynamic evaluation of pulsatile-flow generating device in left ventricular assist devices. *Russian Journal of Transplantology and Artificial Organs*. 2023; 25 (1): 106–112. (In Russ.). https://doi.org/10.15825/1995-1191-2023-1-106-112.
6. *Itkin GP.* Ventricle assist device: past, present, and future nonpulsatile pumps. *Russian Journal of Transplantology and Artificial Organs*. 2009; 11 (3): 81–87. (In Russ.). https://doi.org/10.15825/1995-1191-2009-3-81-87.
7. *Fresiello L, Muthiah K, Goetschalckx K, Hayward C, Rocchi M, Bezy M et al*. Initial clinical validation of a hybrid in silico–*in vitro* cardiorespiratory simulator for comprehensive testing of mechanical circulatory support systems. *Front Physiol*. 2022 Oct 13; 13: 967449. doi: 10.3389/fphys.2022.967449.

8. *Pugovkin AA, Markov AG, Selishchev SV, Korn L, Walter M, Leonhardt S et al*. Advances in hemodynamic analysis in cardiovascular diseases investigation of energetic characteristics of adult and pediatric sputnik left ventricular assist devices during mock circulation support. *Cardiol Res Pract*. 2019 Nov 15; 2019: 4593174. doi: 10.1155/2019/4593174.
9. *Itkin GP, Nosov MS, Kuleshov AP, Drobyshev AA, Buchnev AS*. Blood flow control device in implantable extracorporeal circulation systems. Patent for a utility model. No. RU 201911 U1. Patent holder: Shumakov National Medical Research Center of Transplantology and Artificial Organs. 2020.
10. *Syrbu AI, Itkin GP, Kuleshov AP, Gaidai NA.* A mathematical model of neurohumoral regulation of the circulatory system. *Biomedical Engineering*. 2021; 55 (4): 41–44.
11. *Itkin GP, Syrbu AI, Kyleshov AP, Buchnev AS, Drobyshev AA*. Evaluation of the efficiency of a new pulsatile flow-generating circulatory-assist system in rotary blood pumps. Research on a mathematical model. *Russian Journal of Transplantology and Artificial Organs*. 2021; 23 (4): 73–78. (In Russ.). https://doi.org/10.15825/1995-1191-2021-4-73-78.
12. *Cappon F, Wu T, Papaioannou T, Du X, Hsu PL, Khir AW*. Mock circulatory loops used for testing cardiac assist devices: A review of computational and experimental models. *Int J Artif Organs*. 2021 Nov; 44 (11): 793–806. doi: 10.1177/03913988211045405.
13. *Gregory SD, Pauls JP, Wu EL, Stephens A, Steinseifer U, Tansley G, Fraser JF.* An advanced mock circulation loop for *in vitro* cardiovascular device evaluation. *Artif organs*. 2020 Jun; 44 (6): E238–E250. doi: 10.1111/aor.13636.
14. *Rapp ES, Pawar SR, Longoria RG*. Hybrid mock circulatory loop simulation of extreme cardiac events. *IEEE Trans Biomed Eng*. 2022 Sep; 69 (9): 2883–2892. doi: 10.1109/TBME.2022.3156963.
15. *Ochsner G, Amacher R, Amstutz A, Plass A, Daners MS, Tevaearai H et al*. A novel interface for hybrid mock circulations to evaluate ventricular assist devices. *IEEE Trans Biomed Eng*. 2013 Feb; 60 (2): 507–516. doi: 10.1109/TBME.2012.2230000. Epub 2012 Nov 27.
16. *Petrou A, Granegger M, Meboldt M, Daners MS*. A versatile hybrid mock circulation for hydraulic investigations of active and passive cardiovascular implants. *ASAIO J*. 2019 Jul; 65 (5): 495–502. doi: 10.1097/MAT.0000000000000851.
17. *Ślęzak M, Kopernik M, Szawiraacz K, Milewski G*. Assessment of blood flow parameters in a hybrid-digital model of the cardiovascular system applying recurrent neural networks. *Biomedical Signal Processing and Control*. 2024 Dec; 98: 106680. https://doi.org/10.1016/j.bspc.2024.106680.
18. *Syrbu AI, Itkin GP*. Optimization of the parameters of ventricular assist devices using computerized mathematical modeling of the cardiovascular system. *Biomedical Engineering*. 2022; 56 (2): 23–26.
19. *Jansen-Park SH, Mahmood MN, Müller I, Turnhoff LK, Schmitz-Rode T, Steinseifer U, Sonntag SJ*. Effects of interaction between ventricular assist device assistance and autoregulated mock circulation including Frank–Starling mechanism and baroreflex. *Artif Organs*. 2016 Oct; 40 (10): 981–991. doi: 10.1111/aor.12635.

The article was submitted to the journal on 25.07.2025

DOI: 10.15825/1995-1191-2025-4-110-124

PATHOGENIC AND THERAPEUTIC ROLES OF MESENCHYMAL STEM CELLS IN LIVER FIBROSIS

N.A. Onishchenko[1], M.Yu. Shagidulin[1, 2], A.A. Vaniukova[1], A.V. Kuzmina[2], A.O. Nikolskaya[1], E.A. Volkova[1], A.I. Kostysheva[2], I.A. Lychagin[2], K.A. Kazantseva[2], M.R. Ibragimova[2], A.M. Grigoriev[1], A.S. Ponomareva[1], Yu.B. Basok[1]

[1] Shumakov National Medical Research Center of Transplantology and Artificial Organs, Moscow, Russian Federation

[2] Sechenov University, Moscow, Russian Federation

The aim of this study was to conduct a comparative analysis of the bioregulatory role of mesenchymal stem cells (MSCs) in the liver under physiological conditions, in acute and chronic injury with fibrotic remodeling, and during therapeutic correction by implanting exogenous MSCs from healthy tissues into the body. The analysis showed that hepatic MSCs maintain structural homeostasis by interacting with tissue myofibroblasts and migrating immune cells. In acute liver injury that does not deplete adaptive reserves, hepatic (resident) MSCs regulate tissue homeostasis. Chronic injury that depletes adaptive reserves activates both immune cells and hepatic MSCs, leading to liver inflammation and the transdifferentiation of MSCs into myofibroblasts. These activated fibroblasts overproduce extracellular matrix components, thereby driving liver fibrosis progression. Exogenous apoptotic MSCs from healthy auto- or allogeneic tissues, when administered in cases of chronic liver injury, can compensate for deficient regulatory factors and restore metabolic regulation and structural homeostasis through their paracrine and trophic activity. Their therapeutic potential is maximized when their regulatory properties are enhanced prior to administration and when applied in recipients without irreversible liver injury.

Keywords: mesenchymal stem cells, chronic liver injury, liver fibrosis, regenerative medicine, cell therapy, cell-engineered constructs.

INTRODUCTION

The progression of chronic liver disease (CLD) and fibrosis or cirrhosis result from profound impairment of the liver's restorative regenerative capacity, creating conditions for persistent inflammation and ongoing tissue destruction. At present, liver transplantation remains the only effective treatment for irreversible liver damage in patients with CLD [1, 2]. However, the growing shortage of donor organs, coupled with the rising number of patients requiring transplantation, significantly limits access to this life-saving procedure.

Given these constraints, and in light of the limited efficacy of currently available antifibrotic therapies, there is a pressing need to explore alternative, more accessible and physiologically based treatment strategies that can enhance the liver's intrinsic regenerative potential. The use of mesenchymal stem cells (MSCs), derived from autologous or allogeneic human tissues, has emerged as a promising therapeutic approach.

By now, a considerable body of experimental and clinical evidence has demonstrated the beneficial effects of tissue-derived MSCs on liver structure and function in chronic fibrosing injury [3–5]. Several studies have even suggested the potential for regression of established fibrosis following MSC implantation. However, the fibrolytic properties of MSCs remain a subject of debate. Some researchers question these effects and, in contrast, report the possibility of enhanced fibrosis under certain conditions of MSC therapy [6, 7].

Such conflicting outcomes are likely related to insufficient consideration of several critical factors influencing therapeutic efficacy. These include the source of MSCs, the administered dose and frequency of administration, and the intrinsic bioregulatory potential of the cells – whether derived from healthy allogeneic donors or from patients with comorbidities such as chronic renal failure. Particularly important is the degree of reversibility of pre-existing structural (fibrotic) changes in the liver, which are thought to reflect the severity of the accompanying immune imbalance and the progression of immune deficiency, up to the stage of immune paralysis [8].

The inconsistency in outcomes reported for MSC-based therapy in fibrosing liver diseases, together with the need to enhance the therapeutic effectiveness of MSCs in the setting of progressive hepatic injury, prompted us to undertake a comparative assessment. Specifically, we aimed to evaluate the role of liver-resident MSCs in maintaining structural homeostasis during fibrosing in-

Corresponding author: Murat Shagidulin. Address: 1, Shchukinskaya str., Moscow, 123182, Russian Federation. Phone: (499) 196-87-90. E-mail: dr.shagidulin@mail.ru

jury and to investigate the therapeutic potential of MSCs derived from healthy tissues for correcting established structural disorders in the liver.

The objective of this study is to perform a comparative analysis of the bioregulatory role of resident liver MSCs in maintaining tissue homeostasis under damaging influences and during progression of destructive fibrotic processes. In addition, the study evaluates the corrective potential of exogenous MSCs derived from healthy tissues, with the aim of identifying factors that may enhance the efficacy of MSC-based antifibrotic therapy.

BIOLOGICAL PROPERTIES OF MSCS IN BODY TISSUES

MSCs are multipotent cells of mesodermal origin with properties characteristic of both stem and progenitor cells. They possess self-renewal capacity and can differentiate into mesodermal derivatives such as chondrocytes, osteoblasts, adipocytes, and skeletal muscle cells. Under specific culture conditions, MSCs may also differentiate into cells of ectodermal and endodermal lineages, including hepatocyte-like cells [5]. Currently, these cells have been described in detail, and the classical characteristic of MSCs is their phenotype [5]. Human MSCs express positive surface markers CD105, CD90, and CD73, while lacking hematopoietic and endothelial markers such as CD45, CD34, CD14, CD19, and HLA-DR. In mice, MSCs are characterized by positive expression of CD105, CD29, CD44, and stem cell antigen-1 (SCA-1), with negative expression of CD45, CD31, and lymphocyte antigen-76 (Ly76). Their multipotent (stem-like) properties are typically confirmed through differentiation into three main lineages: adipocytes, chondrocytes, and osteoblasts.

A unique feature of MSCs is their expression of MHC class I molecules and absence of MHC class II, B7-1, B7-2, CD40, and CD40L. This immunophenotype allows them to evade direct participation in immune responses and to exert immunosuppressive effects.

MSCs are present in virtually all body tissues, with particularly high abundance in mesoderm-derived tissues [9]. They can be efficiently harvested from bone marrow, adipose tissue, placenta, umbilical cord-derived Wharton's jelly, skeletal muscle, and skin, as well as from umbilical cord blood, amniotic fluid, and menstrual blood [5]. MSCs actively proliferate during cultivation, and their cell mass can be increased more than 100-fold without losing their multipotent differentiation potential [9].

The widespread presence of MSCs in various organs and tissues highlights their fundamental, non-specific role in maintaining structural and functional homeostasis, regulating adaptive and compensatory responses, and promoting both physiological and reparative regeneration [10]. These functions are mediated through direct interactions with neighboring cells in their microenvironment – primarily mesenchymal cells within the tissue and circulating immune cells [5].

In addition to direct cell-to-cell contact, MSCs exert regulatory effects via autocrine and paracrine signaling [11]. Through these mechanisms, they influence evolutionarily conserved pathways of programmed cell death and modulate the activity of key metabolic processes [4, 10–13]. Furthermore, MSCs demonstrate immune-evasive properties, including the ability to avoid innate immune recognition, counteract complement activation [14], and develop immunosuppressive activity in the presence of proinflammatory cytokines [15].

Importantly, MSC behavior is context-dependent. Their immunomodulatory effects vary according to the cytokine microenvironment and the residual adaptive and regulatory reserves of the tissue. Under these conditions, MSCs can exhibit both anti-inflammatory and proinflammatory effects, influencing the activity of innate and adaptive immune cells [9].

Thus, during tissue injury, the outcome of resident MSC activity depends on multiple factors, including the cytokine environment, the extent of tissue reserves, the diversity and coordination of surrounding cell types, and the severity and duration of inflammation. These variables may drive MSCs toward opposing outcomes in their interactions with mesenchymal cells – particularly fibroblasts and myofibroblasts (MFs). In their activated state, MFs are major producers of extracellular matrix (ECM) components.

The interaction between MSCs and MFs during acute exposure to a damaging factor supports tissue homeostasis and restorative regeneration – without fibrotic scarring – provided that the strength and duration of the effect of this factor on the tissue do not exceed the adaptive, compensatory, and regulatory reserves of the tissue. Under these conditions, MSCs contribute to maintaining balance by directly suppressing MF proliferation and the differentiation of other cells into MFs. They also induce expression of pro-apoptotic proteins in MFs [16] and attenuate their activation by inhibiting nuclear factor kappa B (NF-κB) signaling [17], thereby preventing initiation of a sustained inflammatory response.

In contrast, when stress-damaging effects are chronic, recurrent, or of high intensity, surpassing the tissue's evolutionary reserves of adaptation and regulation, the outcome shifts toward progressive fibrosis. In such settings, excessive and repeated tissue injury leads to necrosis and parenchymal dysfunction, often accompanied by apoptotic death of parenchymal cells due to prolonged functional overload. The release of intracellular products from necrotic and apoptotic cells – frequently carrying altered genetic and structural properties – triggers immune activation and recruits innate immune cells to the injury site, thereby sustaining chronic inflammation there.

At the same time, differentiation of resident MSCs (as stem/progenitor cells) into MFs is activated and the

activation of MFs (activated fibroblasts) increases uncontrollably, which is manifested by excessive production of extracellular matrix components and development of tissue fibrosis [9].

THE ROLE OF RESIDENT (LIVER) MSCS IN PREVENTING INFLAMMATION ESCALATION AND MAINTAINING LIVER TISSUE HOMEOSTASIS DURING ACUTE INJURY

In the acute phase of liver injury, when the adaptive and metabolic regulatory reserves of hepatocytes remain preserved, damage-associated molecules released from necrotic and apoptotic hepatocytes – including reactive oxygen species (ROS) and lipid peroxidation products – initiate an acute inflammatory response. These signals promote the recruitment of innate immune cells to the injury site through secretion of chemokines such as CCL-2, CCL-5, CXCL-1, and CXCL-15.

Initiation of the inflammatory cascade is not limited to hepatocytes alone. Other resident liver cell types also contribute significantly, most notably hepatic stellate cells (HSCs) and Kupffer cells (liver-resident macrophages), which enhance chemokine production [9].

It is believed that liver-resident MSCs also contribute to regulation of inflammatory responses. Bone marrow–derived MSCs, for example, have been shown to produce chemokines in response to danger signals such as circulating Toll-like receptor ligands. However, when proinflammatory signals arise at a stage when hepatic adaptive and metabolic reserves are not yet exhausted, MSCs exhibit strong immunosuppressive activity [15], thereby preventing escalation of acute inflammation.

Experimental data demonstrate that stimulation of MSCs with proinflammatory cytokines – including IFN-γ in combination with IL-1β or TNF-α – induces robust production of immunosuppressive molecules such as nitric oxide (NO), indoleamine 2,3-dioxygenase (IDO), prostaglandin E2 (PGE2), and transforming growth factor-β (TGF-β) [9]. These mediators suppress proinflammatory T-cell proliferation and promote the induction of regulatory, anti-inflammatory cell populations. Locally accumulated immunosuppressive factors around activated MSCs form specialized niches within the liver tissue, reshaping the immune microenvironment.

In particular, it has been shown that resident MSCs promote apoptosis of Th1 and Th2 cells, inhibit Th17 differentiation, and enhance regulatory T-cell (Treg) accumulation through high expression of iNOS, IDO, tumor necrosis factor–stimulated gene-6 (TSG-6), and matrix metalloproteinases (MMPs) [9]. These findings align with observations of increased Treg numbers and reduced Th17 infiltration in fibrotic liver tissue following transfusion of intact donor MSCs [18, 19].

Besides T cells, macrophages represent another key component of hepatic immune homeostasis. MSCs can reprogram macrophages toward an anti-inflammatory phenotype during monocyte-to-macrophage differentiation by secreting insulin-like growth factor-2 (IGF-2) [20]. Even under proinflammatory conditions, IGF-2–conditioned macrophages shift toward oxidative phosphorylation and upregulate programmed death ligand-1 (PD-1), acquiring immunosuppressive properties [20]. Interestingly, IGF-2 exerts a dose-dependent effect: at low concentrations, it binds the IGF-2 receptor on monocytes, driving anti-inflammatory macrophage differentiation; at high concentrations, it binds the insulin-like growth factor-1 (IGF-1) receptor, resulting in proinflammatory macrophages [21].

Taken together, recent evidence indicates that MSCs, when activated by acute inflammatory signals, play a pivotal role in restraining excessive immune responses and preserving liver homeostasis during injury. Proinflammatory macrophages, reprogrammed into anti-inflammatory phenotypes by MSC-derived IGF-2, act as additional regulators of tissue stability. By inhibiting early-stage inflammatory cascades, MSCs not only limit immune cell and cytokine-driven damage but also prevent activation of cells (PSCs, MSCs, and liver fibroblasts) capable of differentiating into macrophages, thereby mitigating fibrosis development.

THE ROLE OF RESIDENT (LIVER) MSCS IN MAINTAINING CHRONIC INFLAMMATION AND DEVELOPMENT OF LIVER FIBROSIS

The transition from acute to chronic inflammation reflects not only the depletion of energy reserves but also the exhaustion of adaptive and regulatory mechanisms in liver cells. Although chronic inflammation is characterized by lower levels of inflammatory mediators, these signals remain sufficient to stimulate MSCs to secrete chemokines and NO, thereby recruiting immune cells to damaged liver tissue [22]. However, the diminished expression of immunosuppressive molecules such as inducible NO synthase (iNOS) and indoleamine 2,3-dioxygenase (IDO) – which are crucial for directing MSC-dependent immunomodulation – limits the ability of MSCs to sustain their suppressive effect. Genetic studies have shown that deletion of iNOS in murine MSCs or IDO in human MSCs reduces the immunosuppressive potential of MSCs triggered by IFN-γ and TNF-α, leading to a more immunostimulatory effect [9]. Even under reduced cytokine levels, which are insufficient for optimal induction of iNOS or IDO, MSCs continue to be activated, secreting chemokines such as CXCL-9 and CCL-5. Under these conditions, MSCs acquire immunostimulatory properties, thereby perpetuating chronic inflammation [22]. Transforming growth factor-β (TGF-β) is recognized as a central cytokine driving liver fibrosis through activation of MFs. Notably, TGF-β sustains immune-mediated inflammation by suppressing iNOS expression induced by inflammatory cytokines in a SMAD3-dependent manner [23].

Chronic liver injury results in a critical reduction of functional hepatocyte mass. This creates conditions for hyperfunction of the remaining hepatocytes, their progressive apoptosis and death, and the persistence of chronic immune-inflammatory reactions coupled with oxidative stress. The latter, characterized by increased production of reactive oxygen species (ROS) and lipid peroxidation, further activates not only immune cells but also other mesenchymal populations in the liver, including hepatic stellate cells (HSCs), resident MSCs, and liver portal fibroblasts. Under conditions of cytokine imbalance, these cells – particularly HSCs and MSCs – upregulate TGF-β, proliferate, and differentiate into MFs. These MFs are the principal producers of ECM and key drivers of fibrogenesis, a pathological process of abnormal hyperplasia of connective tissue in the liver [24, 25].

Mechanisms of involvement of resident (hepatic) MSCs in the pathogenesis of liver fibrosis

In response to liver injury, liver MFs are activated and play a central role in regulating tissue repair and maladaptive remodeling. Multiple mesenchymal cell populations contribute to the pool of hepatic MFs, including HSCs, portal fibroblasts, circulating bone marrow–derived MSCs, and resident liver MSCs [5].

In vitro studies by Mishara et al. [9] showed that under cytokine imbalance, resident MSCs can serve as a source of MF accumulation, driving ECM production and promoting excessive fibrogenesis. Specifically, exposure of MSC cultures to TGF-β – one of the principal profibrotic cytokines – induced expression of α-smooth muscle actin (α-SMA), a hallmark marker of myofibroblastic differentiation. The observed increase in α-SMA–positive MFs, together with enhanced ECM production, provides direct evidence for the transition of MSCs into MFs. These findings suggest that the ability of MSCs to undergo phenotypic transformation and adopt MF functions *in vitro* reflects similar processes occurring *in vivo* under pathological conditions.

Kramann et al. [9] identified Gli-1 as a marker of resident (tissue) MSCs in the liver. In healthy mouse livers, Gli-1^+ MSCs accounted for only 0.02% of resident cells. However, in a carbon tetrachloride–induced model of liver fibrosis, the proportion of Gli-1^+ MSCs increased sharply to 39%. Importantly, their data demonstrated that resident, rather than circulating, Gli-1^+ cells differentiate into MFs during liver injury.

Although resident MSCs contribute significantly to the MF population, the predominant source of MFs (up to 80%) and excessive ECM during fibrosis is attributed to HSCs. In their quiescent state, HSCs exhibit pericyte-like properties and store vitamin A and lipids. Upon chronic liver injury, inflammatory cytokines secreted by hepatocytes and immune cells activate HSCs, leading to upregulation of α-SMA and transition into MFs, which then drive fibrotic ECM deposition [5].

Activation of HSCs and subsequent fibrogenesis are further amplified by proinflammatory cytokines and profibrotic growth factors – including IL-6, IL-1β, TNF-α, TGF-β, and platelet-derived growth factor (PDGF) – secreted by neighboring epithelial and endothelial cells, infiltrating immune cells, and resident fibroblasts [24, 25].

The proposed mechanisms of resident (liver) MSC involvement in the pathogenesis of fibrosis are illustrated schematically in Fig. 1.

Molecular and genetic mechanisms of fibrogenesis

Multiple key molecules are involved in the process of tissue fibrosis [5]. Among these, the most critical are TGF-β, proinflammatory cytokines, integrins, transmembrane receptors, and other signaling factors.

TGF-β is considered the central driver of fibrosis. Following tissue injury, fibroblasts secrete TGF-β, which signals through two types of receptors – TβRI and TβRII – to orchestrate local inflammation, macrophage activation, and immune responses during fibrogenesis. It has also been shown that TGF-β, secreted by macrophages during liver fibrosis, synergizes with other profibrotic mediators, including PDGF and MMPs, to amplify inflammatory signaling and promote progression toward cirrhosis. These effects are mediated primarily via the canonical TGF-β1/Smad pathway as well as the non-canonical PI3K–AKT signaling cascade [5].

TGF-β signaling pathways are in turn coordinated by transcription factors such as PU.1, which activates a broad set of profibrotic genes in fibroblasts and the production of excess ECM [26–28].

Cytokines, particularly the proinflammatory interleukins IL-1 to IL-17, are recognized as important inducers of fibrogenesis, acting synergistically with TGF-β signaling pathways. Among them, IL-17, secreted primarily by $CD4^+$ T lymphocytes, has been shown to play a key role in the development of fibrosis in many tissues, including the liver [29].

In contrast, IL-13, produced by Th2 lymphocytes, promotes fibrosis independently of TGF-β, most likely through its direct stimulatory effect on collagen-producing fibroblasts. The pivotal role of these cytokines in fibrosis development is further supported by experimental findings demonstrating that mice deficient in IL-13, IL-4R, or IL-13Rβ1 show reduced tissue fibrosis following various forms of injury [5].

Integrins, being transmembrane cell receptors, mediate interactions between the ECM and the intracellular cytoskeleton and play a critical role in fibrosis by regulating cellular adhesion, migration, and signaling. Several synergistic mechanisms linking integrin-mediated signaling with TGF-β activation and ECM remodeling, leading to fibrosis activation, have been studied. TGF-β, in its in-

active state, exists as a complex with latency-associated peptide (LAP) and latent TGF-β-binding protein [30]. Certain integrins bind to this latent complex and trigger TGF-β activation. Specifically, integrin αvβ6 has been shown to activate TGF-β through binding to LAP, thereby contributing to fibrotic processes in several organs, including the liver. Furthermore, integrins α8β1 and α11β1 are markedly upregulated in HSCs, where they promote liver fibrosis through TGF-β activation [31].

Disruptions in the gut microbiome have also been shown to influence the progression of liver fibrosis [32]. In patients with CLD, bacterial translocation and the entry of microbial metabolites into the liver occur due to increased intestinal permeability. As a result of intestinal dysbiosis, the liver's innate immune system becomes activated, leading to the production of proinflammatory cytokines that stimulate HSCs and enhance ECM deposition, thereby promoting fibrogenesis [33]. Experimental studies further support this mechanism: blockade of Toll-like receptor 4 (TLR-4) in mice or suppression of intestinal microbial influence using antibiotics slows the development of liver fibrosis.

The progression of liver fibrosis is also associated with alterations in various genetic and molecular regulatory pathways. Previous studies [5] have demonstrated that hepatocyte apoptosis, an initiating event in fibrosis, is mediated by genes involved in programmed cell death, including death receptors (e.g., TRAIL, Bcl-xL, Fas), proapoptotic pathway components (such as caspase-3), and natural killer T (NKT) cells. Furthermore, it has been shown [34] that the transition from fibrosis to cirrhosis is accompanied by significant changes in the mRNA expression of several key genes (tweak, fn14, ang, vegfa, cxcl12, and mmp-9), as well as by altered interactions among them. During the late stage of fibrosis, at the point of transition to cirrhosis, the highest number of correlations between the expression levels of these target genes is still observed. However, as cirrhosis develops, these intergene connections weaken or disappear almost completely, reflecting profound molecular reorganization, metabolic dysregulation in cirrhotic tissue, and the decompensation of the regulatory functions of MSCs.

MECHANISMS OF THE THERAPEUTIC EFFECT OF EXOGENOUS MSCS ON A DAMAGED LIVER

Unlike endogenous (resident) liver MSCs, exogenous MSCs, whether autologous (derived from adipose tissue) or allogeneic/xenogeneic (isolated from healthy donor tissues) [4, 35], retain their full regulatory potential and capacity to maintain tissue homeostasis. Numerous preclinical and clinical studies have shown that the therapeutic effects of healthy exogenous MSCs in fibrosing liver diseases are mediated through activation of evolutionarily conserved mechanisms of stress adaptation and cellular survival. Following transplantation, exogenous MSCs often undergo a spontaneous transition into states of apoptosis or necrosis in response to the new microenvironment [10–13].

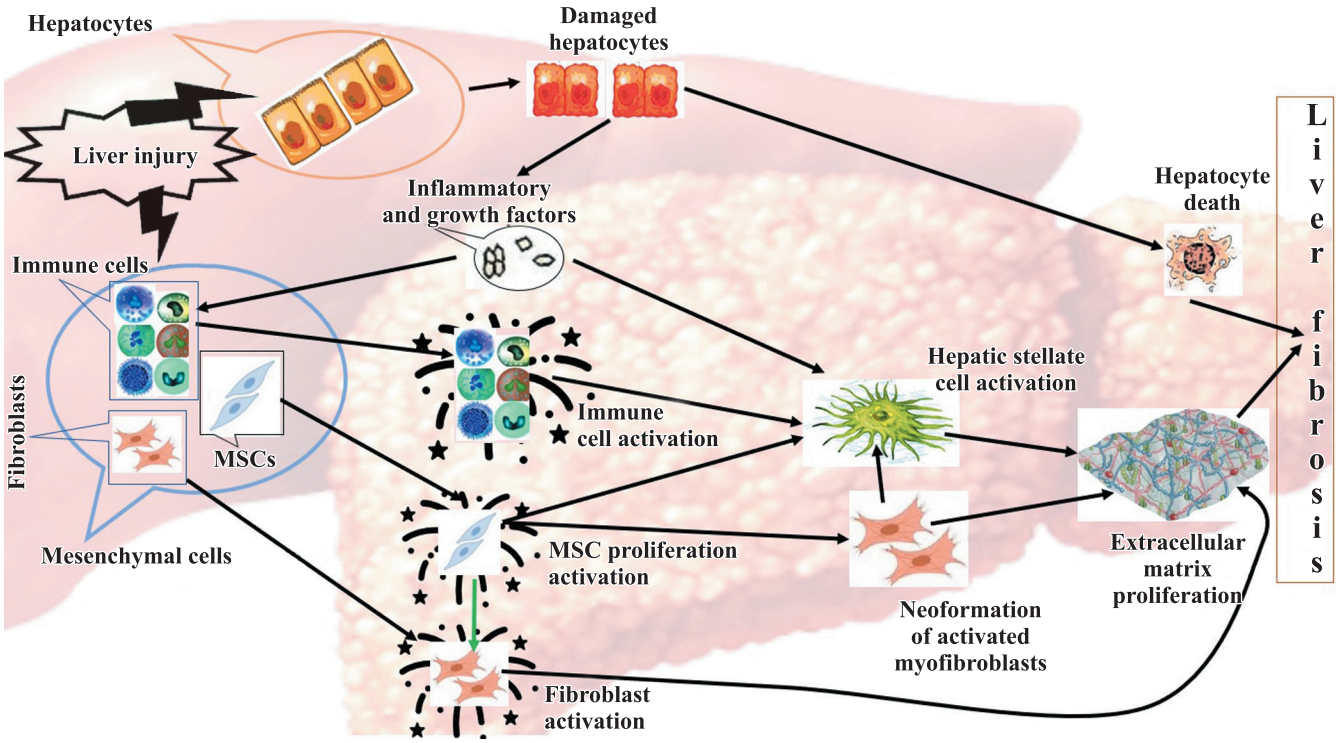

Fig. 1. Schematic representation of the role of resident (hepatic) MSCs in the pathogenesis of liver fibrosis. Arrows indicate the interactions developing between liver cells under chronic damaging effects

During apoptosis, MSCs release a broad spectrum of paracrine and trophic factors, including extracellular vesicles (exosomes, microvesicles, and apoptotic bodies), growth factors, proteases, hormones, diverse RNA species, cytokines, and chemokines [10, 36]. These secreted components exert potent regulatory effects: they protect damaged hepatocytes, suppress the activation of HSCs and MFs, promote the degradation of ECM components, and modulate immune responses, thereby attenuating inflammatory activity within the liver.

A recent meta-analysis evaluating the mechanisms and efficacy of MSC-based therapy in preclinical models of liver fibrosis confirmed that MSCs derived from various tissue sources significantly improve hepatic function, reduce HSC activation through inhibition of the profibrogenic factor TGF-β, and significantly reduce the extent of fibrotic tissue [37]. Notably, the antifibrotic effects were most pronounced when MSCs derived from bone marrow-derived MSCs were used, compared with those obtained from other sources.

Protection of damaged hepatocytes

The pathway by which exogenous MSCs participate in liver regeneration is directly linked to their production of paracrine factors during apoptosis and necrobiosis [38]. Both conditioned medium derived from MSC cultures and MSCs themselves, used alone or in combination with growth factors such as VEGF, have been shown to effectively suppress hepatocyte death and stimulate hepatic regeneration [39, 40].

Exosomes isolated from MSCs can inhibit ferroptosis, a specific form of programmed cell death, by stabilizing SLC7A11 protein levels in hepatocytes during CCl_4-induced liver injury [41]. In addition, MSCs exert hepatoprotective effects via paracrine signaling that activates autophagy, an essential cellular mechanism initiating tissue regeneration [42]. The microRNA Let-7a-5p, delivered through MSC-derived exosomes, has been shown to enhance hepatocyte autophagy and promote regenerative processes in the liver by modulating the mitogen-activated protein kinase-3 (MAP4K3) pathway [43]. Through these tightly regulated molecular pathways, MSCs limit hepatocyte injury, promote survival signaling, and attenuate the progression of liver fibrosis.

Inhibition of HSC and MF activity

To control the progression of fibrosis, one of the principal therapeutic strategies involves suppressing HSCs activation. Consequently, the inhibitory influence of MSCs on HSCs is of particular interest when evaluating the antifibrotic efficacy of MSC-based therapies. Experimental models of liver fibrosis have shown that MSC transplantation can attenuate fibrosis by inhibiting HSC proliferation and inducing their apoptosis [44]. Several other studies have confirmed the suppressive effect of MSCs on HSCs [45, 46]. Umbilical cord–derived MSCs have been shown to downregulate TGF-β1 expression through paracrine signaling [47]. Similarly, adipose tissue–derived MSCs induce cell-cycle arrest of HSCs in the G0/G1 phase of the mitotic cycle , leading to diminished synthesis of profibrogenic proteins and attenuation of fibrotic progression [44, 48]. The antifibrotic effects of MSCs are also mediated through modulation of several signaling pathways, including Notch, Hippo/YAP/Id1 [45, 46], PI3K/AKT/mTOR [44], and p38 MAPK/NF-κB, via regulation of the miR-20a-5p/TGF-βR2 axis [48]. In addition, MSCs inhibit fibrosis by interfering with the Hedgehog/SMO pathway, a central regulator of fibrogenesis [49]. It is believed that human umbilical cord MSCs also suppress HSC proliferation by inhibiting Smad3 protein expression while upregulating Smad7 expression [47].

There is evidence that MSCs play a key role in the process of ECM degradation [40, 48]. MFs can internalize extracellular vesicles derived from MSCs, resulting in decreased type I collagen mRNA expression, and thus reduced ECM production by MFs [50]. These effects are likely mediated by microRNAs – particularly miR-21 and miR-29c – which interact with key signaling molecules involved in ECM synthesis. MSCs also produce enzymes that promote ECM remodeling, including matrix metalloproteinases (MMP-2 and MMP-9) and their tissue inhibitors (TIMP-1 and TIMP-2), which collectively reduce ECM accumulation in fibrotic areas [9].

Immunomodulation of the inflammatory microenvironment by MSCs

The immunomodulatory properties of MSCs play a crucial role in mitigating liver fibrosis [51]. It was found that through both direct interactions with microenvironmental cells and the secretion of paracrine immunoregulatory factors, such as heme oxygenase-1 (HO-1), nitric oxide (NO), prostaglandin E2 (PGE-2), indoleamine 2,3-dioxygenase (IDO), interleukin-6 (IL-6), and human leukocyte antigen-G5 (HLA-G5), MSCs exert potent immunosuppressive effects. These mechanisms enable MSCs to modulate both innate and adaptive immune responses by influencing the activity of natural killer (NK) cells, regulatory T cells (Tregs), myeloid-derived suppressor cells (MDSCs), neutrophils, macrophages, and T and B lymphocytes [22, 35, 52, 53].

Through these immunoregulatory actions, MSCs attenuate inflammation-induced liver injury [40] and reciprocally regulate immune responses to foster a microenvironment conducive to hepatic regeneration [54]. MSCs have been shown to alter T-lymphocyte phenotypes by increasing the population of $CD4^+CD25\text{^}high\text{^}CD45RA^+$ Tregs and modulating the secretion of cytokines associated with immune tolerance [22, 55]. Activation of autophagy in MSCs enhances their immunosuppressive effects on $CD4^+$ T cells, while in fibrotic liver tissue,

MSCs promote the differentiation of circulating monocytes into macrophages and induce the polarization of proinflammatory M1 macrophages toward the anti-inflammatory M2 phenotype, primarily through PGE-2–dependent mechanisms [9].

Circulating monocytes can mediate the systemic immunomodulatory effects of MSCs by engulfing apoptotic MSCs and transporting their regulatory molecules to sites of inflammation, thereby reinforcing systemic immunosuppression [56]. With the help of immunomodulatory factors, MSCs reduce inflammation-induced liver damage and create conditions for restorative regeneration [40].

Recent evidence also highlights that MSC-derived exosomes replicate the potent immunomodulatory and anti-inflammatory properties of MSCs [51, 57]. The regulatory role of exogenous apoptotic MSCs derived from healthy tissues in liver defibrotic processes is shown in Fig. 2.

WAYS TO ENHANCE THE REGULATORY AND ANTIFIBROTIC ACTIVITY OF EXOGENOUS MSCS

It is well established that the therapeutic efficacy of isolated apoptotic MSCs is not always pronounced, particularly in chronic fibrosing liver diseases. This limitation is primarily attributed to their isolation, poor survival rate, and gradual degradation within the recipient's body. Consequently, MSCs rapidly lose their ability to home to the liver, undergo hepatogenic differentiation, and secrete paracrine and trophic modulatory factors. These shortcomings significantly constrain their broad clinical application.

Preliminary adaptive preparation of MSCs

Numerous attempts have been made to enhance the regulatory potential of MSCs by altering their culture conditions and incorporating various factors into the culture medium that train (adapt) them to the effects of unconventional, deficient, or even unfavorable factors, including fibrogenic ones [58]. Factors used for pre-treatment of MSCs include growth factors, lipids, vitamins, hormones, inflammatory factors, and hypoxic conditions [9, 59].

Pre-co-cultivation of umbilical cord MSCs with Schisandrin B (one of the main components of Schisandra chinensis, which prevents the progression of fibrosis) [60], as well as treatment of MSCs with hepatocyte growth factor (HGF) or fibroblast growth factor 4 (FGF-4) before transplantation [61] contributed to the transdifferentiation of MSCs into hepatocyte-like cells, improved their engraftment, and enhanced the therapeutic effect in mice with CCL4-induced fibrosis. MSCs pre-treated with the hormone melatonin [58, 62] exhibited a high ability to homing to damaged hepatic tissue, preserved hepatocellular glycogen stores, and reduced the accumulation of collagen and lipids in fibrous liver tissue. Similar results were obtained using benzimidazole [63], eugenol [64], vitamin E [65], and L-theanine [66].

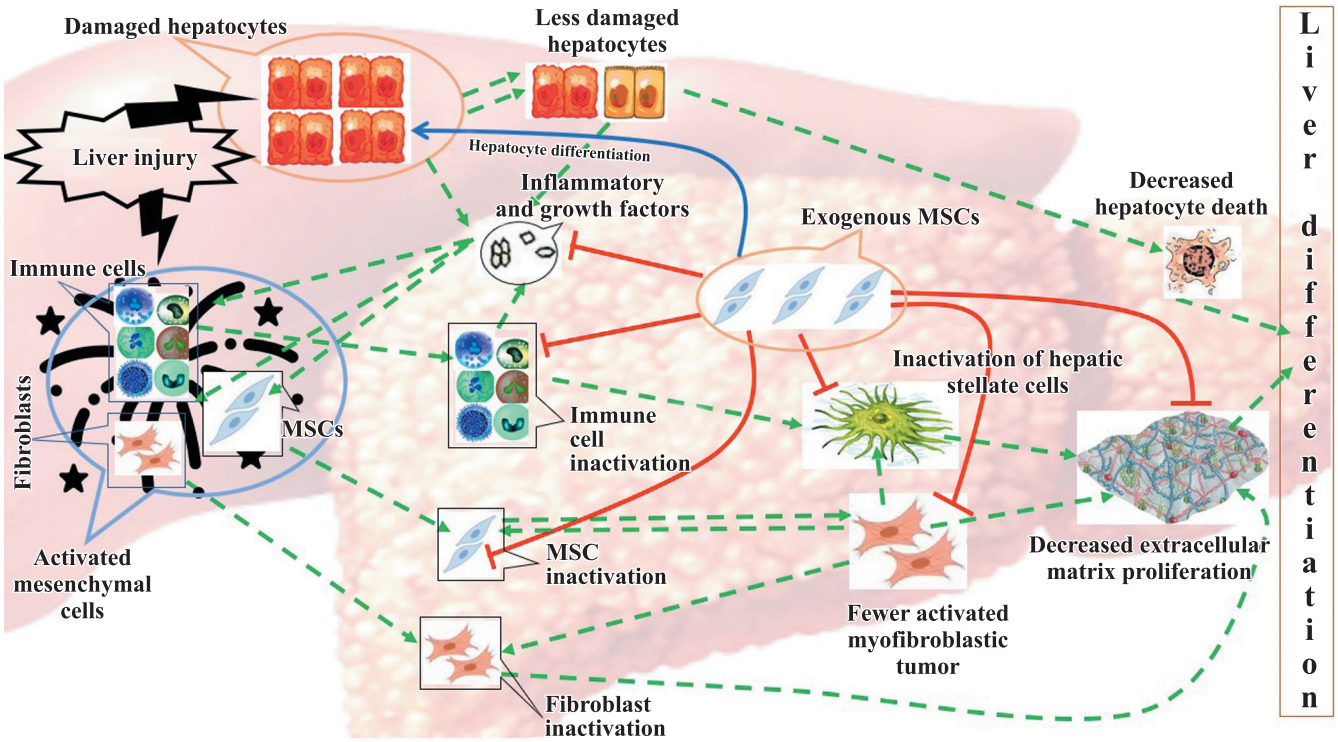

Fig. 2. Diagram showing the involvement of exogenous apoptotic MSCs isolated from healthy tissues in the processes of liver antifibrosis. Details in the text

Combined preparation of MSCs with platelet-rich plasma and HGF [67] significantly enhanced its antifibrotic effect, inhibited HSCs proliferation, inhibiting glycogen synthesis, prolongeing apoptosis, and promoting immunomodulation, transdifferentiation of MSCs into hepatocyte-like cells, secretion of trophic factors, cytokines, chemokines, and more effective regeneration of the damaged liver.

Among the factors that have a pronounced antifibrotic and regenerative effect, it is also worth highlighting preconditioning of MSCs with hypoxia [68], and pretreatment with proinflammatory factors – IFN-α2 [69], TLR4, and IFN-γ [70]. It turned out that pre-treatment of MSCs with pro-inflammatory factors induced higher levels of secretion of CSF-3, IL-8, and the chemokine CCL20 compared to untreated MSCs. In addition, treated MSCs exhibited higher therapeutic activity, and immunohistochemical analysis revealed the accumulation of neutrophils and an increase in MMP-8 activity in the liver [69]. Activation of MSCs via TLR4 and IFN-γ pathways led to downregulation of fibrosis-associated actin-SMA, TGF-β, and TNF-α in the liver.

Hypoxic preconditioning of MSCs also reduced collagen deposition and the number of cells expressing actin-SMA and TGF-β in the liver [68]. Recent studies have further emphasized the synergistic benefits of combining MSCs or their exosomes with chemical agents [67, 68, 71] in experimental models of liver fibrosis.

Genetic modification of MSCs

Genetic modification of MSCs using viral and non-viral vectors has been shown to enhance their capacity for homing, differentiation, and regeneration of fibrotic liver tissue. Modified MSCs overexpress genes that play key roles in liver repair and regeneration, including HGF [72], IGF-1, hepatocyte nuclear factor-4α (HNF-4α), FGF-4 and FGF-21, interleukin-10 (IL-10), and extracellular matrix protein-1 (ECM-1), each of which contributes to improved therapeutic outcomes in liver fibrosis [9].

Expression of the FOXA2 gene in MSCs has been found to promote liver antifibrosis, enhance hepatogenic differentiation, and upregulate several liver-specific genes such as α-fetoprotein, cytokeratin-18 (CK-18), HNF-1, and HGF. In addition to gene overexpression, miRNA modification has also been explored. For instance, upregulation of miR-122 in adipose-derived MSCs enhances their therapeutic efficacy in liver fibrosis by suppressing HSC activation and reducing collagen deposition [73]. IL-10 gene modification in MSCs has been shown to inhibit HSC activity and downregulate TNF-α expression in T lymphocytes and macrophages isolated from fibrotic liver tissue [74].

These findings suggest that modification of specific MSC genes may be a potential new strategy for enhancing the efficacy of liver fibrosis treatment.

Use of cell culture constructs from MSCs (spheroids and cell-engineered constructs)

It is known that three-dimensional (3D) cell cultures exhibit superior phenotypic stability and biological activity compared to traditional two-dimensional (2D) cultures. Studies evaluating the therapeutic potential of MSC spheroids [75] have shown that 3D-cultured MSCs possess enhanced multipotent differentiation capacity, stronger anti-inflammatory and regenerative properties, and secrete higher levels of cytokines. In a mouse model of liver cirrhosis, transplantation of MSC spheroids promoted hepatogenic differentiation, improved liver function, and produced an antifibrotic effect [76].

The higher functionality of 3D-cultured MSCs appears to be related to their increased stemness, as well as their anti-inflammatory and immunomodulatory functions, as indicated by the upregulation of stem cell markers (OCT-4, SOX2, NANOG), anti-inflammatory factors (IL-10, TSG-6, IDO), immunomodulatory molecules (HGF, VEGF, and CXCR4) [77], and activation of the TGF-β1/Smad signaling pathway [78]. In rhesus monkeys with experimental liver fibrosis, portal vein infusion of 3D MSC cultures resulted in the preservation of the spheroidal configuration within the liver for up to one hour post-injection. Even after 16 days, although the spheroids had dissociated into individual cells, viable MSCs remained present in the liver in significant quantities, indicating sustained homing ability [78].

To further prolong and enhance MSC functionality in chronic liver failure, researchers have developed and tested cell-engineered constructs (CECs) implanted directly into the liver. These constructs are based on biomimetic ECMs such as collagen-containing hydrogels (spherogels) [79], recombinant spidroin (rS1/9) – an analogue of spider silk proteins [80] – or decellularized liver matrices [81]. The constructs are typically seeded with bone marrow-derived MSCs in combination with hepatocytes at a 1:5 ratio. Multiple implantation of such CECs over a 90-day period resulted in accelerated and robust liver regeneration: by day 30, biochemical liver function parameters normalized, while structural regeneration and antifibrosis (reduction of ECM area) continued throughout the follow-up period.

Recently, a novel cell-engineering technology has been introduced for generating cell sheets–matrices using temperature-responsive culture dishes coated with poly(N-isopropylacrylamide) to promote MSC adhesion. Combining this technique with pre-treatment of MSCs using IC-2 – a derivative of ICG-001, an inhibitor of the Wnt/β-catenin signaling pathway that induces hepatic differentiation – has yielded a new strategy for treating chronic liver diseases [82–84]. Orthotopic implantation of MSCs in the form of engineered MSC–IC-2 sheets into the livers of CCl_4-induced fibrotic mice resulted in elevated expression of MMP-1 and MMP-14, inhibition

of HSC activation, and significant reduction of fibrosis severity.

It should be noted that most scientific studies devoted to developing ECM biopolymer mimetics for CECs generally follow two main approaches. The first focuses on using individual biopolymer components of ECM, such as collagen, hyaluronic acid, and gelatin (a collagen denaturation product), to regulate the morphological characteristics of the cell carrier and enable the incorporation of additional bioactive molecules. The second approach involves obtaining cell carriers from tissues through decellularization, which allows for maximal preservation of the native ECM composition but limits the ability to modify its structure, mechanical properties, and biodegradation rate.

A promising direction lies in combining both strategies to create next-generation carriers that closely replicate the natural ECM composition while possessing tailored physicochemical properties and the capacity for bioactive molecule incorporation. A macroporous morphology throughout the material is particularly favorable for effective cell colonization and vascularization. In this regard, using enzymatic hydrolysates of decellularized liver tissue as the basis for new materials appears especially promising, as cryostructuring can impart the desired structural and mechanical characteristics.

Previous studies have shown that cryostructurates derived from gelatin and hydrolysates can sustain long-term adhesion and proliferation of human adipose tissue-derived MSCs, as well as support albumin and urea synthesis by tissue-specific HepG2 hepatocellular carcinoma cells [85, 86]. This approach may help maintain the viability of MSCs and hepatocytes within CECs after implantation, thereby extending their functional lifespan *in vivo*.

However, it should be emphasized that enhancement of the therapeutic and antifibrotic effects of exogenous MSCs through these methods is feasible only when the recipient's liver has not undergone irreversible damage.

CONCLUSION

A comparative analysis of the regulatory properties of MSCs in healthy tissues, as well as in acute and chronic (fibrosing) liver injury, was conducted. In a healthy body, MSCs are present in virtually all tissues, where they maintain structural homeostasis and physiological tissue regeneration. They interact primarily with tissue myofibroblasts (MFs) and migrating immune cells, which, like MSCs, originate from the mesoderm.

During acute liver injury, when the extent and duration of the damaging factor do not exceed the adaptive capacity of tissue and cellular defense mechanisms, resident liver MSCs continue to regulate and preserve tissue homeostasis. In contrast, chronic (fibrosing) liver injury leads to progressive depletion of these adaptive and regulatory reserves, resulting in the activation of immune inflammatory cells and resident MSCs. Under such conditions, resident MSCs may transdifferentiate into MFs. These activated fibroblasts produce excessive amounts of extracellular matrix, driving hepatic fibrogenesis.

Exogenous MSCs derived from healthy autologous or allogeneic sources, after isolation, typically undergo reversible apoptosis but retain a high capacity to secrete regulatory and adaptive factors. When administered, apoptotic MSCs exert their effects mainly through paracrine and trophic signaling, compensating for deficits in the chronically injured liver and contributing to the restoration of tissue homeostasis.

Reliable restoration of metabolic regulation and structural integrity in the damaged liver using exogenous MSCs is achievable only when their regulatory activity is enhanced – through preconditioning with adaptive agents, genetic modification, or incorporation into bioengineered cell-matrix constructs – and when the residual regulatory capacity of the recipient's liver has not reached the threshold of irreversible damage.

To optimize clinical outcomes, it is essential to develop reliable and convenient criteria for predicting the individual therapeutic efficacy of exogenous MSCs in patients with chronic fibrosing liver diseases.

This study was supported by the Russian Science Foundation (grant No. 25-25-00425, https://rscf.ru/project/25-25-00425/).

The authors declare no conflict of interest.

REFERENCES

1. *Halliday N, Westbrook RH.* Liver transplantation: need, indications, patient selection and pre-transplant care. *Br J Hosp Med (Lond).* 2017; 78 (5): 252–259. doi: 10.12968/hmed.2017.78.5.252.
2. *Olivo R, Guarrera JV, Pyrsopoulos NT.* Liver Transplantation for Acute Liver Failure. *Clin Liver Dis.* 2018; 22 (2): 409–417. doi: 10.1016/j.cld.2018.01.014.
3. *Basok YuB, Ponomareva AS, Grudinin NV, Kruglov DN, Bogdanov VK, Belova AD, Sevastyanov VI.* Application of mesenchymal stromal cells in solid organ transplantation: challenges and prospects (systematic review). *Russian Journal of Transplantology and Artificial Organs.* 2025; 27 (1): 114–134. https://doi.org/10.15825/1995-1191-2025-1-114-134.
4. *Eom YW, Kang SH, Kim MY, Lee JI, Baik SK.* Mesenchymal stem cells to treat liver diseases. *Ann Transl Med*. 2020; 8: 563. doi: 10.21037/atm.2020.02.163.
5. *Qin L, Liu N, Bao CL, Yang DZ, Ma GX, Yi WH et al.* Mesenchymal stem cells in fibrotic diseases – the two sides of the same coin. *Acta Pharmacol Sin*. 2023; 44 (2): 268–287. doi: 10.1038/s41401-022-00952-0.
6. *Carvalho AB, Quintanilha LF, Dias JV, Paredes BD, Mannheimer EG, Carvalho FG et al.* Bone marrow multipotent mesenchymal stromal cells do not reduce fibrosis or improve function in a rat model of severe chronic

liver injury. *Stem Cells*. 2008; 26 (5): 1307–1314. doi: 10.1634/stemcells.2007-0941.

7. *Quante M, Tu SP, Tomita H, Gonda T, Wang SS, Takashi S et al.* Bone marrowderived myofibroblasts contribute to the mesenchymal stem cell niche and promote tumor growth. *Cancer Cell.* 2011; 19: 257–272. https://doi.org/10.1016/j.ccr.2011.01.020.
8. *Onishchenko NA, Nikolskaya AO, Shagidulin MYu.* Progressive dysfunction of the immune system as a factor preventing recoverable regeneration of the liver in chronic fibrosing diseases. *Pathological Physiology and Experimental Therapy, Russian journal*. 2023; 67 (3): 109–123. doi: 10.25557/0031-2991.2023.03.109-123.
9. *Yang X, Li Q, Liu W, Zong C, Wei L, Shi Y, Han Z.* Mesenchymal stromal cells in hepatic fibrosis/cirrhosis: from pathogenesis to treatment. *Cell Mol Immunol*. 2023; 20 (6): 583–599. doi: 10.1038/s41423-023-00983-5. Epub 2023 Feb 24. Erratum in: *Cell Mol Immunol*. 2023; 20 (6): 687–688. doi: 10.1038/s41423-023-01010-3.
10. *Kholodenko IV, Kholodenko RV, Majouga AG, Yarygin KN.* Apoptotic MSCs and MSC-Derived Apoptotic Bodies as New Therapeutic Tools. *Curr Issues Mol Biol*. 2022; 44 (11): 5153–5172. doi: 10.3390/cimb44110351.
11. *Gnecchi M, Danieli P, Malpasso G, Ciuffreda MC.* Paracrine mechanisms of mesenchymal stem cells in tissue repair. *Methods Mol Biol*. 2016; 1416: 123–146. https://doi.org/10.1007/978-1-4939-3584-0_7.
12. *Naji A, Favier B, Deschaseaux F, Rouas-Freiss N, Eitoku M, Suganuma N.* Mesenchymal stem/stromal cell function in modulating cell death. *Stem Cell Res Ther*. 2019; 10: 56. https://doi.org/10.1186/s13287-019-1158-4.
13. *Weiss DJ, English K, Krasnodembskaya A, Isaza-Correa JM, Hawthorne IJ, Mahon BP.* The necrobiology of mesenchymal stromal cells affects therapeutic efficacy. *Front Immunol*. 2019; 10: 1228. https://doi.org/10.3389/fimmu.2019.01228.
14. *Mishra VK, Shih HH, Parveen F, Lenzen D, Ito E, Chan TF, Ke LY.* Identifying the therapeutic significance of mesenchymal stem cells. *Cells*. 2020; 9: 1145. https://doi.org/10.3390/cells9051145.
15. *Wang Y, Fang J, Liu B, Shao C, Shi Y.* Reciprocal regulation of mesenchymal stem cells and immune responses. *Cell Stem Cell*. 2022; 29 (11): 1515–1530. https://doi.org/10.1016/j.stem.2022.10.001.
16. *Qiao H, Zhou Y, Qin X, Cheng J, He Y, Jiang Y.* NADPH oxidase signaling pathway mediates mesenchymal stem cell-induced inhibition of hepatic stellate cell activation. *Stem Cells Int*. 2018; 10: 1239143. https://doi.org/10.1155/2018/1239143.
17. *Lee C, Kim M, Han J, Yoon M, Jung Y.* Mesenchymal stem cells influence activation of hepatic stellate cells, and constitute a promising therapy for liver fibrosis. *Biomedicines*. 2021; 9: 1598. https://doi.org/10.3390/biomedicines9111598.
18. *Milosavljevic N, Gazdic M, Simovic Markovic B, Arsenijevic A, Nurkovic J, Dolicanin Z et al.* Mesenchymal stem cells attenuate liver fibrosis by suppressing Th17 cells – an experimental study. *Transpl Int*. 2018; 31: 102–115. https://doi.org/10.1111/tri.13023.
19. *Chen QH, Wu F, Liu L, Chen HB, Zheng RQ, Wang HL, Yu LN.* Mesenchymal stem cells regulate the Th17/Treg cell balance partly through hepatocyte growth factor *in vitro*. *Stem Cell Res Ther*. 2020; 11: 91. https://doi.org/10.1186/s13287-020-01612-y.
20. *Du L, Lin L, Li Q, Liu K, Huang Y, Wang X et al.* IGF-2 preprograms maturing macrophages to acquire oxidative phosphorylation-dependent anti-inflammatory properties. *Cell Metab*. 2019; 29: 1363–1375.e8. https://doi.org/10.1016/j.cmet.2019.01.006.
21. *Wang X, Lin L, Lan B, Wang Y, Du L, Chen X et al.* IGF2R-initiated proton rechanneling dictates an anti-inflammatory property in macrophages. *Sci Adv*. 2020; 6: eabb7389. https://doi.org/10.1126/sciadv.abb7389.
22. *Hu C, Wu Z, Li L.* Mesenchymal stromal cells promote liver regeneration through regulation of immune cells. *Int J Biol Sci*. 2020; 16: 893–903. https://doi.org/10.7150/ijbs.39725.
23. *Xu C, Yu P, Han X, Du L, Gan J, Wang Y et al.* TGF-beta promotes immune responses in the presence of mesenchymal stem cells. *J Immunol*. 2014; 192: 103–109. https://doi.org/10.4049/jimmunol.1302164.
24. *De Araújo Farias V, Carrillo-Gálvez AB, Martín F, Anderson P.* TGF-beta and mesenchymal stromal cells in regenerative medicine, autoimmunity and cancer. *Cytokine Growth Factor Rev*. 2018; 43: 25–37. https://doi.org/10.1016/j.cytogfr.2018.06.002.
25. *Kisseleva T.* The origin of fibrogenic myofibroblasts in fibrotic liver. *Hepatology*. 2017; 65: 1039–1043. https://doi.org/10.1002/hep.28948.
26. *Bernard NJ.* PU.1 pulls the strings in fibrotic disease. *Nat Rev Rheumatol*. 2019; 15: 187. https://doi.org/10.1038/s41584-019-0193-y.
27. *Wohlfahrt T, Rauber S, Uebe S, Luber M, Soare A, Ekici A et al.* PU.1 controls fibroblast polarization and tissue fibrosis. *Nature*. 2019; 566: 344–349. https://doi.org/10.1038/s41586-019-0896-x.
28. *Liu Q, Yu J, Wang L, Tang Y, Zhou Q, Ji S et al.* Inhibition of PU.1 ameliorates metabolic dysfunction and non-alcoholic steatohepatitis. *J Hepatol*. 2020; 73: 361–370. https://doi.org/10.1016/j.jhep.2020.02.025.
29. *Gu L, Xu Q, Cao H*. $1,25(OH)_2D_3$ protects liver fibrosis through decreasing the generation of TH17 cells. Med Sci Monit: *Int Med J Exp Clin Res*. 2017; 23: 2049–2058. https://doi.org/10.12659/msm.904271.
30. *Yokota T, McCourt J, Ma F, Ren S, Li S, Kim TH et al.* Type V collagen in scar tissue regulates the size of scar after heart injury. *Cell*. 2020; 182: 545–562.e523. https://doi.org/10.1016/j.cell.2020.06.030.
31. *Nishimichi N, Tsujino K, Kanno K, Sentani K, Kobayashi T, Chayama K et al.* Induced hepatic stellate cell integrin, α8β1, enhances cellular contractility and TGFβ activity in liver fibrosis. *J Pathol*. 2021; 253: 366–373. https://doi.org/10.1002/path.5618.
32. *Lee G, You HJ, Bajaj JS, Joo SK, Yu J, Park S et al.* Distinct signatures of gut microbiome and metabolites associated with significant fibrosis in nonobese NAFLD. *Nat Commun*. 2020; 11: 4982. https://doi.org/10.1038/s41467-020-18754-5.

33. *Koyama Y, Brenner DA*. Liver inflammation and fibrosis. *J Clin Invest*. 2017; 127: 55–64. https://doi.org/10.1172/jci88881.
34. *Lebedeva EI, Shastny AT, Babenko AS*. Model of toxic fibrosis in Wistar rats: morphologic and molecular genetic parameters of the transition point into cirrhosis. *Genes and Cells*. 2023; 18 (3): 219–234. https://doi.org/10.23868/gc546031.
35. *Alfaifi M, Eom YW, Newsome PN, Baik SK*. Mesenchymal stromal cell therapy for liver diseases. *J Hepatol*. 2018; 68: 1272–1285. https://doi.org/10.1016/j.jhep.2018.01.030.
36. *Cai H, Guo H*. Mesenchymal stem cells and their exocytotic vesicles. *Int J Mol Sci.* 2023; 24 (3): 2085. doi: 10.3390/ijms24032085.
37. *Wang X, Wang Y, Lu W, Qu J, Zhang Y, Ye J. Wang X et al.* Effectiveness and mechanisms of mesenchymal stem cell therapy in preclinical animal models of hepatic fibrosis: a systematic review and meta-analysis. *Front Bioeng Biotechnol*. 2024; 12: 1424253. doi: 10.3389/fbioe.2024.1424253.
38. *Driscoll J, Patel T*. The mesenchymal stem cell secretome as an acellular regenerative therapy for liver disease. *J Gastroenterol*. 2019; 54: 763–773. https://doi.org/10.1007/s00535-019-01599-1.
39. *Adas G, Koc B, Adas M, Duruksu G, Subasi C, Kemik O et al.* Effects of mesenchymal stem cells and VEGF on liver regeneration following major resection. *Langenbecks Arch Surg*. 2016; 401: 725–740. https://doi.org/10.1007/s00423-016-1380-9.
40. *Liu H, Wang X, Deng H, Huang H, Liu Y, Zhong Z et al.* Integrated Transcriptome and Metabolomics to Reveal the Mechanism of Adipose Mesenchymal Stem Cells in Treating Liver Fibrosis. *Int J Mol Sci*. 2023; 24 (22): 16086. doi: 10.3390/ijms242216086.
41. *Lin F, Chen W, Zhou J, Zhu J, Yao Q, Feng B et al.* Mesenchymal stem cells protect against ferroptosis via exosome-mediated stabilization of SLC7A11 in acute liver injury. *Cell Death Dis*. 2022; 13: 271. https://doi.org/10.1038/s41419-022-04708-w.
42. *Cheng Y, Wang B, Zhou H, Dang S, Jin M, Shi Y et al.* Autophagy is required for maintenance of liver progenitor cell functionality. *Cell Physiol Biochem*. 2015; 36 (3): 1163–1174. https://doi.org/10.1159/000430287.
43. *Lin D, Chen H, Xiong J, Zhang J, Hu Z, Gao J et al.* Mesenchymal stem cells exosomal let-7a-5p improve autophagic flux and alleviate liver injury in acuteon-chronic liver failure by promoting nuclear expression of TFEB. *Cell Death Dis*. 2022; 13: 865. https://doi.org/10.1038/s41419-022-05303-9.
44. *Zhang Z, Shang J, Yang Q, Dai Z, Liang Y, Lai C et al.* Exosomes derived from human adipose mesenchymal stem cells ameliorate hepatic fibrosis by inhibiting PI3K/Akt/mTOR pathway and remodeling choline metabolism. *J Nanobiotechnology*. 2023; 21 (1): 29. doi: 10.1186/s12951-023-01788-4.
45. *Yao L, Hu X, Yuan M, Liu P, Zhang Q, Wang Z et al.* Human umbilical cord-derived mesenchymal stromal cells alleviate liver cirrhosis through the Hippo/YAP/Id1 pathway and macrophage-dependent mechanism. *Int Immunopharmacol*. 2023; 123: 110456. doi: 10.1016/j.intimp.2023.110456.
46. *Liu H, Huang H, Liu Y, Yang Y, Deng H, Wang X et al.* Adipose-derived mesenchymal stem cells inhibit hepatic stellate cells activation to alleviate liver fibrosis via Hippo pathway. *Stem Cell Res Ther*. 2024; 15 (1): 378. doi: 10.1186/s13287-024-03988-7.
47. *Zhang LT, Peng XB, Fang XQ, Li JF, Chen H, Mao XR*. Human umbilical cord mesenchymal stem cells inhibit proliferation of hepatic stellate cells *in vitro*. *Int J Mol Med*. 2018; 41: 2545–52. https://doi.org/10.3892/ijmm.2018.3500.
48. *Gan L, Zheng L, Yao L, Lei L, Huang Y, Zeng Z, Fang N.* Exosomes from adipose-derived mesenchymal stem cells improve liver fibrosis by regulating the miR-20a-5p/TGFBR2 axis to affect the p38 MAPK/NF-κB pathway. *Cytokine*. 2023; 172: 156386. doi: 10.1016/j.cyto.2023.156386.
49. *Zong R, Zheng Y, Yan Y, Sun W, Kong L, Huang Y et al.* Mesenchymal stem cells-derived exosomes alleviate liver fibrosis by targeting Hedgehog/SMO signaling. *Hepatol Int*. 2024; 18 (6): 1781–1791. doi: 10.1007/s12072-024-10717-y.
50. *Basalova N, Sagaradze G, Arbatskiy M, Evtushenko E, Kulebyakin K, Grigorieva O et al.* Secretome of mesenchymal stromal cells prevents myofibroblasts differentiation by transferring fibrosis-associated microRNAs within extracellular vesicles. *Cells*. 2020; 9: 1272. https://doi.org/10.3390/cells9051272.
51. *Liu P, Yao L, Hu X, Wang Z, Xiong Z, Jiang Y*. Recent advances in the immunomodulation mechanism of mesenchymal stem cell therapy in liver diseases. *J Gastroenterol Hepatol*. 2023; 38 (7): 1099–1106. doi: 10.1111/jgh.16247.
52. *Feng X, Feng B, Zhou J, Yang J, Pan Q, Yu J et al.* Mesenchymal stem cells alleviate mouse liver fibrosis by inhibiting pathogenic function of intrahepatic B cells. *Hepatology*. 2024; 10.1097. doi: 10.1097/HEP.0000000000000831.
53. *Liu K, Wang FS, Xu R*. Neutrophils in liver diseases: pathogenesis and therapeutic targets. *Cell Mol Immunol*. 2021; 18: 38–44. doi: 10.1038/s41423-020-00560-0.
54. *Shi Y, Wang Y, Li Q, Liu K, Hou J, Shao C, Wang Y*. Immunoregulatory mechanisms of mesenchymal stem and stromal cells in inflammatory diseases. *Nat Rev Nephrol*. 2018; 14 (8): 493–507. doi: 10.1038/s41581-018-0023-5.
55. *Yang H, Sun J, Li Y, Duan WM, Bi J, Qu T*. Human umbilical cord-derived mesenchymal stem cells suppress proliferation of PHA-activated lymphocytes *in vitro* by inducing CD4(+)CD25(high)CD45RA(+) regulatory T cell production and modulating cytokine secretion. *Cell Immunol*. 2016; 302: 26–31. https://doi.org/10.1016/j.cellimm.2016.01.002.
56. *Wu HW, Chen HD, Chen YH, Mao XL, Feng YY, Li SW, Zhou XB*. The effects of programmed cell death of mesenchymal stem cells on the development of liver fibrosis. *Stem Cells Int*. 2023; 11: 4586398. doi: 10.1155/2023/4586398.

57. *Zheng Q, Zhang S, Guo WZ, Li XK*. The unique immunomodulatory properties of MSC-derived exosomes in organ transplantation. *Front Immunol*. 2021; 12: 659621. https://doi.org/10.3389/fimmu.2021.659621.
58. *Elzainy A, El Sadik A, Altowayan WM*. Comparison between the Regenerative and Therapeutic Impacts of Bone Marrow Mesenchymal Stem Cells and Adipose Mesenchymal Stem Cells Pre-Treated with Melatonin on Liver Fibrosis. *Biomolecules*. 2024; 14 (3): 297. doi: 10.3390/biom14030297.
59. *Ding F, Liu Y, Li J, Wei X, Zhao J, Liu X, Zhang L*. TC14012 enhances the anti-fibrosis effects of UC-MSCs on the liver by reducing collagen accumulation and ameliorating inflammation. *Stem Cell Res Ther*. 2024; 15 (1): 44. doi: 10.1186/s13287-024-03648-w.
60. *Jin M, Yi X, Zhu X, Hu W, Wang S, Chen Q et al.* Schisandrin B promotes hepatic differentiation from human umbilical cord mesenchymal stem cells. *iScience*. 2024; 27 (2): 108912. doi: 10.1016/j.isci.2024.108912.
61. *Shams S, Mohsin S, Nasir GA, Khan M, Khan SN*. Mesenchymal stem cells pretreated with HGF and FGF4 can reduce liver fibrosis in mice. *Stem Cells Int*. 2015; 2015: 747245. https://doi.org/10.1155/2015/747245.
62. *Mortezaee K, Khanlarkhani N, Sabbaghziarani F, Nekoonam S, Majidpoor J, Hosseini A et al.* Preconditioning with melatonin improves therapeutic outcomes of bone marrow-derived mesenchymal stem cells in targeting liver fibrosis induced by CCl_4. *Cell Tissue Res*. 2017; 369: 303–312. https://doi.org/10.1007/s00441-017-2604-1. (Retraction published *Cell Tissue Res*. 2025 Feb 17. doi: 10.1007/s00441-025-03959-1).
63. *Iqbal M, Shams S, Rafiq H, Khan M, Khan S, Sadique Khattak U et al.* Combinatorial therapeutic potential of stem cells and benzimidazol derivatives for the reduction of liver fibrosis. *Pharmaceuticals (Basel)*. 2023; 16 (2): 306. doi: 10.3390/ph16020306.
64. *Fathy M, Okabe M, M Othman E, Saad Eldien HM, Yoshida T*. Preconditioning of adipose-derived mesenchymal stem-like cells with eugenol potentiates their migration and proliferation *in vitro* and therapeutic abilities in rat hepatic fibrosis. *Molecules*. 2020; 25 (9): 2020. https://doi.org/10.3390/molecules25092020.
65. *Baig MT, Ghufran H, Mehmood A, Azam M, Humayun S, Riazuddin S*. Vitamin E pretreated Wharton's jelly-derived mesenchymal stem cells attenuate CCl4-induced hepatocyte injury *in vitro* and liver fibrosis *in vivo*. *Biochem Pharm*. 2021; 186: 114480. https://doi.org/10.1016/j.bcp.2021.114480.
66. *Lai YJ, Sung YT, Lai YA, Chen LN, Chen TS, Chien CT*. L-Theanine-treated adiposederived mesenchymal stem cells alleviate the cytotoxicity induced by N-nitrosodiethylamine in liver. *Tissue Eng Regen Med*. 2022; 19: 1207–1221. https://doi.org/10.1007/s13770-022-00472-2.
67. *Shivaramu S, Maiti SK, Banu SA, Kalaiselvan E, Sharun K, Mishra M et al.* Synergistic hepatoprotective effects of mesenchymal stem cells and platelet-rich plasma in a rat model of bile duct ligation-induced liver cirrhosis. *Cells*. 2024; 13 (5): 404. doi: 10.3390/cells13050404.
68. *Amansyah F, Budu B, Achmad MH, Daud NMAS, Putra A, Massi MN et al.* Secretome of Hypoxia-Preconditioned Mesenchymal Stem Cells Promotes Liver Regeneration and Anti-Fibrotic Effect in Liver Fibrosis Animal Model. *Pak J Biol Sci*: *PJBS*. 2024; 27 (1): 18–26. doi: 10.3923/pjbs.2024.18.26.
69. *Xie Y, Yao J, Yan M, Lin Y, Wei J, Wang H et al.* Pretreatment of UC-MSCs with IFN-α2 improves treatment of liver fibrosis by recruiting neutrophils. *J Transl Med*. 2023; 21 (1): 832. doi: 10.1186/s12967-023-04732-0.
70. *Liu C, Zhang YS, Chen F, Wu XY, Zhang BB, Wu ZD, Lei JX.* Immunopathology in schistosomiasis is regulated by TLR2,4- and IFN-gamma-activated MSC through modulating Th1/Th2 responses. *Stem Cell Res Ther*. 2020; 11: 217. https://doi.org/10.1186/s13287-020-01735-2.
71. *Xu Y, Wang XS, Zhou XL, Lu WM, Tang XK, Jin Y, Ye JS*. Mesenchymal stem cell therapy for liver fibrosis need "partner": Results based on a meta-analysis of preclinical studies. *World J Gastroenterol*. 2024; 30 (32): 3766–3782. doi: 10.3748/wjg.v30.i32.3766.
72. *Moon SH, Lee CM, Park SH, Jin Nam M*. Effects of hepatocyte growth factor gene-transfected mesenchymal stem cells on dimethylnitrosamine-induced liver fibrosis in rats. *Growth Factors*. 2019; 37: 105–119. https://doi.org/10.1080/08977194.2019.1652399.
73. *Lou G, Yang Y, Liu F, Ye B, Chen Z, Zheng M, Liu Y.* MiR-122 modification enhances the therapeutic efficacy of adipose tissue-derived mesenchymal stem cells against liver fibrosis. *J Cell Mol Med*. 2017; 21: 2963–2973. https://doi.org/10.1111/jcmm.13208.
74. *Choi JS, Jeong IS, Han JH, Cheon SH, Kim SW*. IL-10-secreting human MSCs generated by TALEN gene editing ameliorate liver fibrosis through enhanced antifibrotic activity. *Biomater Sci*. 2019; 7: 1078–1087. https://doi.org/10.1039/c8bm01347k.
75. *Zhang X, Hu MG, Pan K, Li CH, Liu R*. 3D spheroid culture enhances the expression of antifibrotic factors in human adipose-derived MSCs and improves their therapeutic effects on hepatic fibrosis. *Stem Cells Int*. 2016; 2016: 4626073. https://doi.org/10.1155/2016/4626073.
76. *Takahashi Y, Yuniartha R, Yamaza T, Sonoda S, Yamaza H, Kirino K et al.* Therapeutic potential of spheroids of stem cells from human exfoliated deciduous teeth for chronic liver fibrosis and hemophilia A. *Pediatr Surg Int*. 2019; 35: 1379–1388. https://doi.org/10.1007/s00383-019-04564-4.
77. *Lee S, Kim HS, Min BH, Kim BG, Kim SA, Nam H et al.* Enhancement of antiinflammatory and immunomodulatory effects of adipose-derived human mesenchymal stem cells by making uniform spheroid on the new nanopatterned plates. *Biochem Biophys Res Commun*. 2021; 552: 164–169. https://doi.org/10.1016/j.bbrc.2021.03.026.
78. *Li S, Fu X, Wang J, Yang H, Wang D, Dong X et al.* Therapeutic efficacy and *in vivo* distribution of human umbilical cord-derived mesenchymal stem cell spheroids transplanted via B-Ultrasound-guided percutaneous portal vein puncture in rhesus monkey models of liver fibrosis. *Stem Cell Res Ther*. 2024; 15 (1): 315. doi: 10.1186/s13287-024-03934-7.

79. *Shagidulin M, Onishchenko N, Sevastianov V, Krasheninnikov M, Lyundup A, Nikolskaya A et al.* Experimental Correction and Treatment of Chronic Liver Failure Using Implantable Cell-Engineering Constructs of the Auxiliary Liver Based on a Bioactive Heterogeneous Biopolymer Hydrogel. *Gels.* 2023; 9 (6): 456. https://doi.org/10.3390/gels9060456.
80. *Shagidulin M, Onishchenko N, Grechina A, Nikolskaya A, Krasheninnikov M, Lyundup A et al.* Recombinant spidroin microgel as the base of cell-engineered constructs mediates liver regeneration in rat. *Polymers (Basel).* 2022; 14 (15): 3179. https://doi.org/10.3390/polym14153179.
81. *Shagidulin MYu, Onishchenko NA, Basok YuB, Grigoriev AM, Kirillova AD, Nemets EA et al.* Functional efficiency of cell-engineered liver constructs based on tissue-specific matrix (experimental model of chronic liver failure). *Russian Journal of Transplantology and Artificial Organs*. 2020; 22 (4): 89–97. https://doi.org/10.15825/1995-1191-2020-4-89-97.
82. *Itaba N, Noda I, Oka H, Kono Y, Okinaka K, Yokobata T et al.* Hepatic cell sheets engineered from human mesenchymal stem cells with a single small molecule compound IC-2 ameliorate acute liver injury in mice. *Regen Ther*. 2018; 9: 45–57. https://doi.org/10.1016/j.reth.2018.07.001.
83. *Fukushima K, Itaba N, Kono Y, Okazaki S, Enokida S, Kuranobu N et al.* Secreted matrix metalloproteinase-14 is a predictor for antifibrotic effect of IC-2-engineered mesenchymal stem cell sheets on liver fibrosis in mice. *Regen Ther*. 2021; 18: 292–301. https://doi.org/10.1016/j.reth.2021.08.004.
84. *Itaba N, Kono Y, Watanabe K, Yokobata T, Oka H, Osaki M et al.* Reversal of established liver fibrosis by IC-2-engineered mesenchymal stem cell sheets. *Sci Rep*. 2019; 9: 6841. https://doi.org/10.1038/s41598-019-43298-0.
85. *Lozinsky VI, Kulakova VK, Grigoriev AM, Podorozhko EA, Kirsanova LA, Kirillova AD et al.* Cryostructuring of Polymeric Systems: 63. Synthesis of Two Chemically Tanned Gelatin-Based Cryostructurates and Evaluation of Their Potential as Scaffolds for Culturing of Mammalian Cells. *Gels*. 2022; 8 (11): 695. doi: 10.3390/gels8110695.
86. *Basok YuB, Grigoriev AM, Lozinsky VI, Kirsanova LA, Kulakova VK, Podorozhko EA et al.* Cryogenically Structured Extracellular Matrix Mimetic Based on a Concentrated Collagen-Containing Solution. *Inorg Mater Appl Res.* 2024; 15: 358–366. https://doi.org/10.1134/S2075113324020096.

The article was submitted to the journal on 11.04.2025

DOI: 10.15825/1995-1191-2025-4-125-132

SILK-BASED SCAFFOLDS FOR TISSUE ENGINEERING AND RECONSTRUCTIVE SURGERY: MECHANICAL AND STRUCTURAL PROPERTIES

E.I. Podbolotova[1, 2], A.R. Pashutin[1, 2], N.V. Grudinin[1], E.A. Volkova[1], O.I. Agapova[1], A.E. Efimov[1], I.I. Agapov[1]

[1] Shumakov National Medical Research Center of Transplantology and Artificial Organs, Moscow, Russian Federation

[2] Moscow Institute of Physics and Technology, Dolgoprudny, Russian Federation

Silk is a promising natural biomaterial that combines mechanical strength, biocompatibility, and controlled biodegradation, making it highly suitable for scaffold creation for clinical practice. This study investigates how different processing methods influence the morphological and mechanical characteristics of silk-based scaffolds. The findings showed that varying the processing conditions facilitates the production of materials with tailored properties, ranging from dense, mechanically robust structures to porous, rapidly degradable scaffolds. High-density samples (Fibroplen-Atlas) exhibited substantial mechanical stability, making them promising candidates for surgical applications in mechanically demanding areas such as ligaments, fascia, and tendons. In contrast, more porous scaffolds (Fibroplen-Gas) demonstrated accelerated biodegradation, which is advantageous for soft tissue regeneration. These results highlight the potential of silk scaffolds for personalized applications, where the balance between mechanical stability and biodegradation rate can be adjusted according to specific clinical needs.

Keywords: silk fibroin, mechanical properties, tissue engineering, biomaterials.

INTRODUCTION

In recent decades, biomedical technologies aimed at restoring and replacing damaged tissues and organs have developed rapidly. A key component of these technologies is biomaterials, which form the foundation for creating implants, scaffolds, and various medical devices. The performance of these materials is determined by their biocompatibility, biodegradability, and, critically, their mechanical properties, such as strength, elasticity, and resistance to physiological stresses, which must be optimized for specific clinical applications [1, 2]. These properties directly influence the integration of the implant within the tissue environment, its functional durability, and the overall effectiveness of regeneration [3, 4].

In regenerative medicine and tissue engineering, for instance, scaffolds must possess sufficient mechanical stability to preserve the architecture of the defect and provide structural support for cell attachment and proliferation until regeneration is complete. However, the required level of mechanical strength varies considerably with the anatomical site: dense, durable materials with prolonged resorption times are necessary for the replacement of tendons, ligaments, and fascial structures, whereas more elastic, rapidly degradable matrices are preferred for soft tissue engineering applications [5, 6].

Silk fibroin, derived from the cocoons of the silkworm *Bombyx mori*, is a promising natural polymer that has been extensively studied in recent years as a foundation for developing biocompatible and biodegradable matrices in regenerative medicine and tissue engineering [7–10]. Its high mechanical strength, chemical modifiability, and low immunogenicity make silk a versatile material suitable for a broad range of medical applications – from permanent tissue replacements to temporary scaffolds that promote the restoration of native biological structures [11].

Silk fibroin is a macromolecule with an ordered architecture in which highly crystalline regions (predominantly β-sheet structures) alternate with amorphous domains. The crystalline regions form a rigid framework that imparts high mechanical strength and resistance to enzymatic degradation, whereas the amorphous regions provide flexibility and elasticity [12]. The balance between these two domains determines the overall physical and mechanical properties of fibroin, which can be precisely tuned by modifying processing conditions.

Fibroin elicits minimal inflammatory response *in vivo* and supports cell adhesion, proliferation, and differentiation, especially with additional surface modification or when supplemented with bioactive molecules [13–17].

One of the key advantages of silk fibroin lies in its versatility and technological flexibility. By varying pro-

Corresponding author: Igor Agapov. Address: 1, Shchukinskaya str., Moscow, 123182, Russian Federation. Phone: (495) 231-60-42. E-mail: igor_agapov@mail.ru

cessing conditions, such as solvent composition, extraction time, and thermal or mechanical treatment, it is possible to deliberately tailor the morphology, degree of crystallinity, porosity, biodegradation rate, and mechanical performance of the material [18, 19]. This tunability enables the adaptation of silk-based scaffolds to a wide range of clinical applications.

The present study aims to elucidate the relationship between the extent of silk processing and the resulting changes in the mechanical and morphological characteristics of fibroin-based scaffolds. The primary objective is to determine how different fabrication approaches influence scaffold properties, thereby providing a rationale for selecting optimal processing parameters to create biomaterials that meet specific clinical requirements. This will allow for targeted design of scaffold types – ranging from dense, slowly resorbable structures to porous, rapidly degradable matrices – depending on the intended surgical application.

MATERIALS AND METHODS

Obtaining samples

Natural silk fabrics (EAC Declaration of Conformity, N RU D-CN.PA09.B.91575/23, Tianjin Textile Industrial Supply and Sale Co., Ltd., China) were used for the preparation of biodegradable scaffolds. Two types of silk fabrics differing in surface density – 15 g/m^2 and 155 g/m^2 – were employed in this study. Sample preparation was carried out according to previously described protocols [20–22].

The processing procedure included several sequential stages. Initially, the silk fabric was boiled in a 0.25% aqueous sodium bicarbonate ($NaHCO_3$) solution for 40 minutes in a water bath to remove sericin, followed by thorough rinsing in distilled water. The fabric was then reboiled in a fresh $NaHCO_3$ solution for 30 minutes, and this process was repeated three times to ensure complete sericin removal. After treatment, the samples were air-dried at room temperature until a constant weight was achieved.

The resulting materials were designated as “Fibroplen-Gas” (15 g/m^2) and “Fibroplen-Atlas” (155 g/m^2). These samples were used as model scaffolds for subsequent analyses.

Obtaining the solution

The purified silk fabrics were dissolved in a mixture of distilled water, 95% ethanol, and calcium chloride (Sharlab S.L., Spain) in a molar ratio of 8 : 2 : 1, respectively. The volume of the mixture was calculated at 1 mL of solution per 200 mg of fibroin. Dissolution was carried out in sealed test tubes at 90 °C for 40 minutes with constant stirring until a homogeneous solution was obtained.

The resulting solution was purified from calcium chloride and ethanol by dialysis against distilled water at 20 °C, with ten water changes performed at 30-minute intervals. Upon completion of dialysis, the solution was further purified by centrifugation at 3000 rpm for 15 minutes using a SIGMA 6K10 2000 W centrifuge (Sigma, Germany) to remove insoluble particles. The resulting solution was subsequently subjected to mass spectrometric analysis to verify its protein composition, assess its purity, and confirm its suitability for further use.

Mass spectrometry

An aliquot of the solution containing 20 μg of total protein was dried in a SpeedVac centrifugal vacuum concentrator (Savant, France) and resuspended in 20 μL of buffer containing 100 mM Tris-HCl (pH 8.5), 1% sodium deoxycholate, 10 mM TCEP, and 20 mM 2-chloroacetamide. The mixture was incubated at 85 °C for 10 minutes and subsequently cooled to room temperature. 0.4 μg of trypsin in 10 μl of 100 mM Tris-HCl (pH 8.5) was added to the solution, and the reaction mixture was incubated at 37 °C overnight. The reaction was terminated by adding an equal volume of 2% trifluoroacetic acid (TFA), after which the peptides were purified by solid-phase extraction on an SDB-RPS StageTip microcolumn made from an automatic pipette tip packed with SDB-RPS membrane (3M, USA). The column was sequentially washed with 1% TFA in ethyl acetate and 0.2% TFA in water, and peptides were eluted using 5% ammonium hydroxide in 60% acetonitrile. The eluate was dried completely and stored at –80 °C. Prior to analysis, peptides were reconstituted in 0.1% TFA and 2% acetonitrile in water.

Chromatographic–mass spectrometric analysis was performed on an Ultimate 3000 Nano LC system (Thermo Fisher Scientific) coupled to an Orbitrap Lumos Tribrid mass spectrometer (Thermo Fisher Scientific) via a nanoelectrospray ionization source. Peptides were first loaded onto a precolumn packed with Reprosil-Pur C18-AQ 5 μm sorbent and subsequently separated on a fused silica analytical column packed with Reprosil-Pur C18-AQ 1.9 μm sorbent. Chromatographic separation was carried out at room temperature using a binary solvent system: eluent A – 0.1% formic acid in water, and eluent B – 80% acetonitrile with 0.1% formic acid. Peptides were eluted with a linear gradient from 3% to 99% eluent B over 37 minutes at a flow rate of 500 nL/min.

The mass spectrometer operated in data-dependent acquisition (DDA) mode with the following parameters: MS1 resolution 60,000, mass range 350–1600 m/z, HCD fragmentation energy 30%, and MS2 resolution 15,000.

Data processing was performed using MaxQuant (v.2.4.2.0) and Perseus (v.2.0.10.0) software packages. Database searching was carried out against the *Bombyx mori* protein sequence database (UniProt, version 04.2025) using standard MaxQuant settings: trypsin

specificity, up to two missed cleavages, variable modifications (methionine oxidation, N-terminal acetylation), fixed modification (cysteine carbamidomethylation), and a false discovery rate (FDR) threshold of 1% at both peptide and protein levels.

Subsequent data analysis in Perseus included the exclusion of contaminants, reverse sequences, and proteins identified only by site. Relative protein quantification was performed using the relative intensity-based absolute quantification (iBAQ) algorithm.

Obtaining modified samples

Fibroplen-Gas and Fibroplen-Atlas samples were incubated in an aqueous–alcoholic solution of calcium chloride ($CaCl_2$) with a molar ratio of $CaCl_2$: ethanol : water = 1 : 2 : 8 at 46 °C. The treatment was continued until the complete loss of fabric integrity. The time required for full structural disintegration was 7 hours for Fibroplen-Gas and 4.5 hours for Fibroplen-Atlas samples; these durations were defined as representing 100% destruction.

Based on these reference points, incubation times corresponding to 20%, 40%, 60%, and 80% degrees of destruction were calculated proportionally. Upon completion of each treatment, the samples were thoroughly rinsed with distilled water to remove residual reagents and subsequently air-dried at room temperature until a constant weight was achieved.

The resulting scaffolds were sterilized in a Sanyo MLS-3020U autoclave (Sanyo, Japan) at 126 °C for 30 minutes. The modified scaffolds were designated with numerical indices reflecting the percentage of structural destruction.

Scanning electron microscopy

To compare the structural features of samples with different degrees of processing and to identify changes in surface morphology and microstructure resulting from tissue modification, the samples were examined using scanning electron microscopy (SEM). The samples were dehydrated by sequential immersion in ethanol solutions of increasing concentration (10%, 20%, 50%, 70%, and 95%), with each step lasting 30 minutes. After dehydration, the samples were mounted on glass slides and vacuum-dried for 1 hour using a Q150R ES rotary pump sputtering system (Quorum Technologies, UK). The dried samples were then coated with a 5 nm layer of gold under an argon atmosphere at an ion current of 20 mA and a pressure of 1 mbar, using the same Q150R ES system (Quorum Technologies, UK). Microscopic examination was carried out with a Tescan Vega3 SBU scanning electron microscope (Tescan, Czech Republic) operated at a voltage of 30 kV. The images were captured using VegaTC software (Tescan, Czech Republic).

Mechanical properties of samples

To assess the strength characteristics of the silk scaffolds, tensile tests were conducted using a universal tensile testing machine I1158M-2 (Tochpribor, Russia). Five rectangular specimens, each measuring 8 cm × 2.5 cm, were prepared from each type of fabric. The samples were fixed in the machine's clamps and subjected to uniaxial tensile loading at a crosshead speed of 50 mm/min until they broke. During the test, the relationship between the applied load and elongation was continuously measured. The tensile strength of each sample was calculated based on the maximum load at break and the corresponding strain.

Data processing

All quantitative data are presented as mean ± standard deviation (M ± SD). The Mann–Whitney U test was applied to evaluate statistical differences between groups. Differences were considered statistically significant at $p < 0.05$. Data analysis and graphical visualization were performed using OriginPro software (OriginLab Corporation, USA).

RESULTS AND DISCUSSION

Mass spectrometry analysis

Mass spectrometric analysis of the fibroin solution obtained from sericin-free satin silk tissue identified 50 protein sequence groups corresponding to *Bombyx mori* silk proteins (according to the UniProt database, version 04.2025). Protein identification and quantification performed using MaxQuant revealed that more than 97% of the total molar protein content was represented by fibroin light chains (42.3%), fibroin heavy chains (48.8%), and fibrohexamerin (P25) (6.1%). This composition corresponds closely to the native protein profile of fibroin extracted from *Bombyx mori* cocoons, confirming the high preservation of the native structure of silk after processing and confirms that the solution contains predominantly pure fibroin. Thus, it can be concluded that the pretreated silk tissue matrices retain the native biochemical composition characteristic of natural fibroin and can be used as a basis for creating biocompatible scaffolds.

Tissue morphology

SEM analysis of the samples revealed a clear relationship between the microstructural characteristics of the samples and the degree of modification. In the untreated samples, the fibers exhibited a dense and orderly arrangement with a smooth surface, retaining both their structural integrity and spatial organization. This was particularly evident in the samples with a denser weave (Fibroplen-Atlas). As the degree of processing increased (from 20% to 80%), progressive structural alterations were observed. The fiber surfaces became roughened,

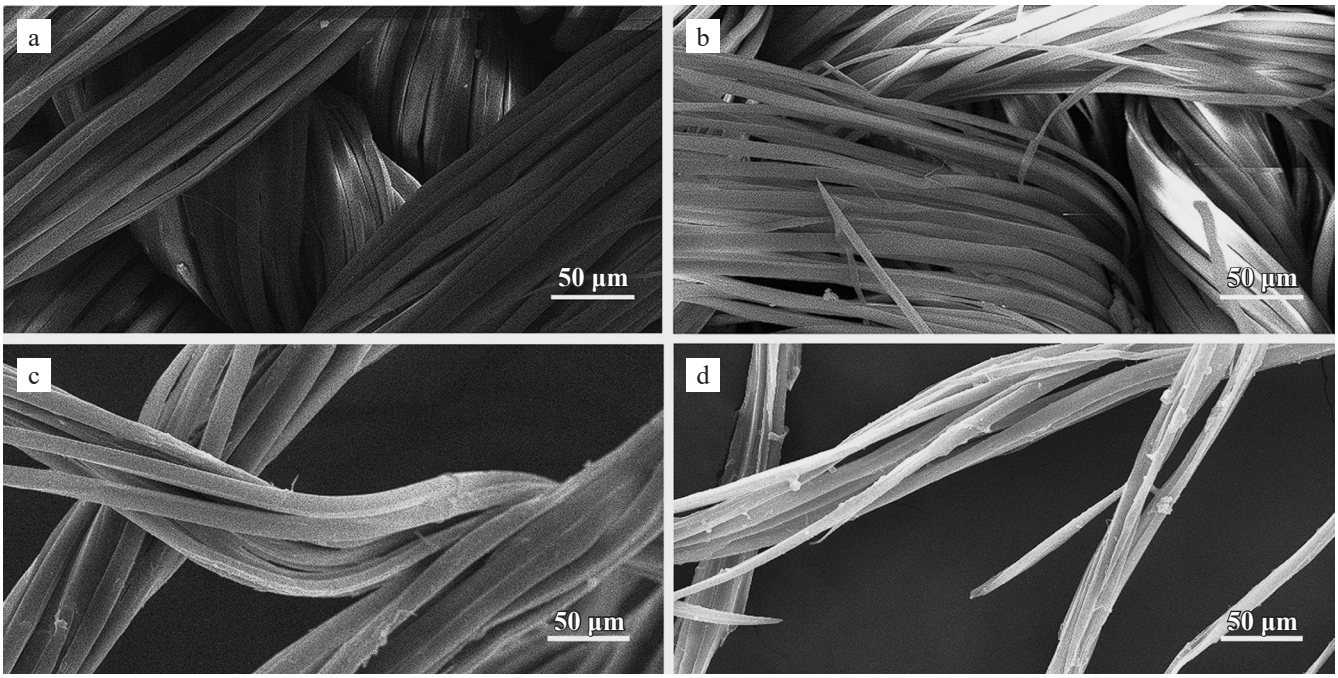

Fig. 1. Surface morphology of silk fabrics at different processing levels, according to scanning electron microscopy (SEM). a, Fibroplen-Atlas; b, Fibroplen-Atlas 80; c, Fibroplen-Gas; d, Fibroplen-Gas 80

Table

Tensile strength of silk scaffolds at different degrees of modification

Sample	Tensile strength (MPa)
A0	34.67 ± 2.80
A20	28.11 ± 2.30
A40	21.30 ± 1.90
A60	17.68 ± 1.50
A80	15.04 ± 1.30

Sample	Tensile strength (MPa)
G0	9.01 ± 0.80
G20	8.97 ± 0.80
G40	8.12 ± 0.70
G60	7.32 ± 0.65
G80	7.86 ± 0.70

with evident localized degradation, loosening of the network, and regions of thinning. Breaks formed in the fibrous network. At higher modification levels, the structure became less ordered, and the fabric became more porous and fragile (Fig. 1).

Mechanical properties

Mechanical testing of the silk scaffolds revealed pronounced differences in tensile strength, reflecting the influence of fabric density and structural organization on the mechanical behavior of the materials. The untreated Fibroplen-Atlas (A0) samples showed a maximum tensile strength of 34.67 ± 2.80 MPa (Fig. 2), which was significantly higher than that of the modified samples (A20–A80), where tensile strength varied from 28.11 ± 2.30 MPa to 15.04 ± 1.30 MPa. The Fibroplen-Gas samples, with lower fabric density, showed considerably reduced strength. The untreated G0 samples had a maximum tensile strength of 9.01 ± 0.80 MPa, which decreased to 7.86 ± 0.70 MPa following maximal modification (G80) (Table).

For Fibroplen-Atlas samples, a clear and statistically significant ($p < 0.05$) inverse relationship was observed between tensile strength and degree of processing. Increasing the incubation time in the calcium chloride–ethanol solution led to a gradual decline in mechanical strength, indicating progressive structural degradation of the fibroin matrix. A similar trend was noted for the Fibroplen-Gas samples, although with greater data variability.

DISCUSSION

The observed decrease in tensile strength with increasing degrees of modification is attributed to the partial disruption of the fibroin protein matrix, resulting in reduced structural integrity and mechanical stability of the scaffolds. This finding is consistent with previous studies [20, 22], which have shown that chemical processing of silk fibroin leads to a loss of crystallinity and partial unfolding of β-structures, thereby diminishing the strength of the material while accelerating its biodegradation.

The high-density Fibroplen-Atlas samples demonstrated superior mechanical performance, making them suitable for use in surgical applications that require long-

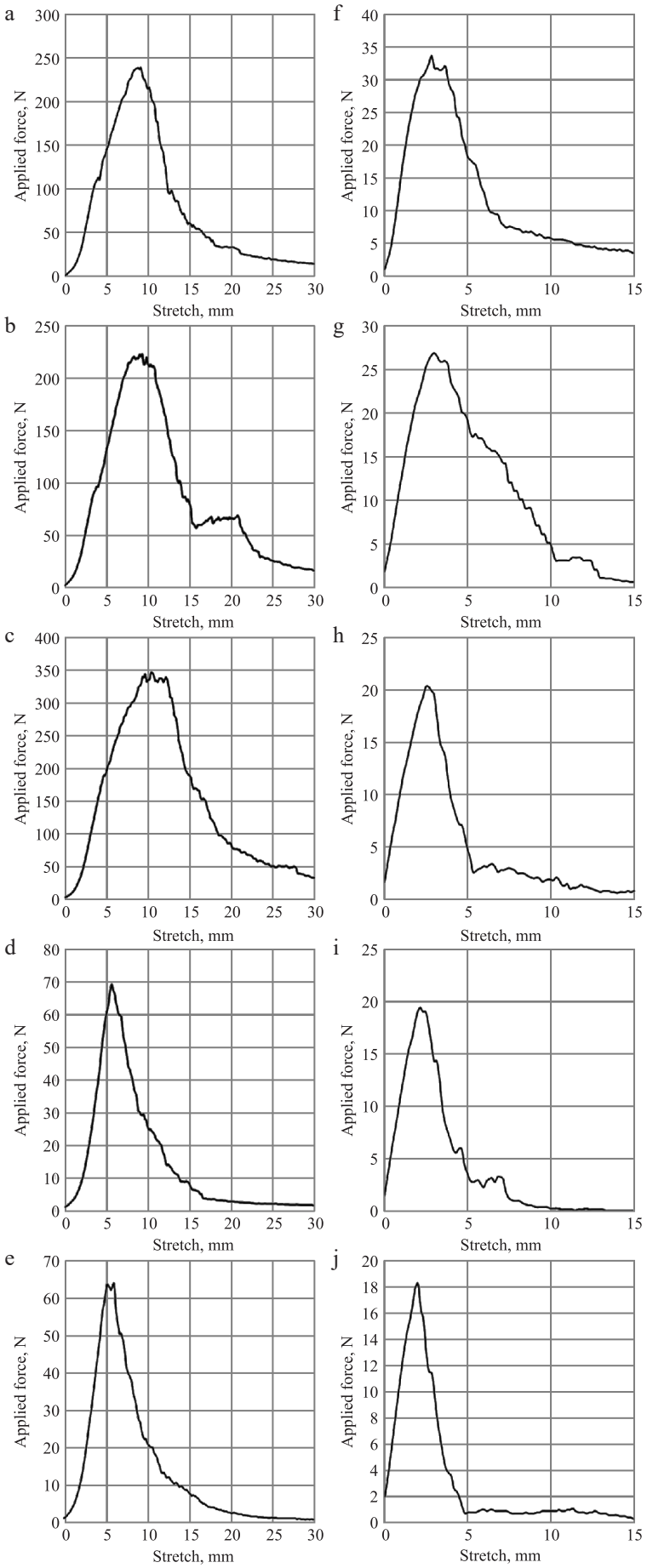

Fig. 2. Dependence of breaking force on time from the start of testing for silk scaffold samples A0–A80 (a–e) and G0–G80 (f–j). The maximum recorded value is taken as the breaking force of the scaffold

term mechanical reinforcement, such as tendon, fascia, and other structures subjected to significant stress, where it is necessary to maintain the stability of the framework for a long time after surgery, for example, in orthopedics and reconstructive surgery.

Indeed, high-strength silk matrices are already employed clinically in procedures such as rotator cuff reconstruction and knee ligament repair, where prolonged stability and resistance to stress are critical to successful postoperative outcomes [23–26].

At the same time, Fibroplen-Gas samples, characterized by a looser and more porous architecture, exhibited lower mechanical strength but a faster biodegradation rate, making them ideal for soft tissue surgery. Such materials hold promise for use in regenerative medicine, particularly for wound coverage, burn treatment, and plastic surgery, where temporary biodegradable matrices are required for accelerated epithelial and vascular growth.

CONCLUSION

This study demonstrated that physicochemical treatment of silk tissues exerts a pronounced influence on their morphological and mechanical properties, enabling the formation of scaffolds with distinct architectural characteristics. By varying treatment parameters, it was possible to obtain biomaterials with a controlled degree of protein matrix degradation, which in turn determined their mechanical strength and expected biodegradation kinetics.

High-density scaffolds fabricated from materials such as Fibroplen-Atlas exhibit pronounced mechanical strength and structural stability, making them highly promising for clinical applications that require long-term tissue support. In contrast, scaffolds with a less dense architecture (such as Fibroplen-Gas) display lower tensile strength but increased biodegradation rates, rendering them more suitable for use in tissue engineering and regenerative surgery, including the treatment of chronic wounds, burns, and creation of matrices.

Thus, the developed silk-based scaffolds demonstrate significant potential for adaptive use in clinical practice, where selection of material can be guided by the biomechanical demands of the target tissue and the desired rate of regeneration. The results confirm the feasibility of targeted modulation of the properties of silk biomaterials to meet specific therapeutic objectives.

ACKNOWLEDGEMENTS

The authors would like to thank Rustam H. Ziganshin for his assistance in performing the mass spectrometry analyses.

The authors declare no conflict of interest.

REFERENCES

1. *Wang L, Wang C, Wu S, Fan Y, Li X*. Influence of mechanical properties of biomaterials on degradability, cell behaviors and signaling pathways: current progress and challenges. *Biomater Sci*. 2020 May 21; 8 (10): 2714–2733. doi: 10.1039/d0bm00269k.
2. *Binyamin G, Shafi BM, Mery CM*. Biomaterials: A primer for surgeons. *Semin Pediatr Surg*. 2006 Nov; 15 (4): 276–283. doi: 10.1053/j.sempedsurg.2006.07.007.
3. O'Brien FJ. Biomaterials & scaffolds for tissue engineering. Materials Today. 2011; 14 (3): 88–95. doi: 10.1016/S1369-7021(11)70058-X.
4. *Efimov AE, Agapova OI, Safonova LA, Bobrova MM, Parfenov VA, Koudan EV et al.* 3D scanning probe nanotomography of tissue spheroid fibroblasts interacting with electrospun polyurethane scaffold. *Express Polymer Letters*. 2019; 13 (7): 632–641. doi: 10.3144/expresspolymlett.2019.53.
5. *Chan BP, Leong KW*. Scaffolding in tissue engineering: general approaches and tissue-specific considerations. *Eur Spine J*. 2008 Dec; 17 (Suppl 4): 467–479. doi: 10.1007/s00586-008-0745-3.
6. *Suamte L, Tirkey A, Barman J, Jayasekhar Babu P.* Various manufacturing methods and ideal properties of scaffolds for tissue engineering applications. *Smart Materials in Manufacturing*. 2023; 1: 100011. doi: 10.1016/j.smmf.2022.100011.
7. *Podbolotova EI, Agapova OI*. Biodegradable silk-based products for regenerative medicine. *Russian Journal of Transplantology and Artificial Organs*. 2024; 26 (4): 157–165. [In Russ, English abstract]. doi: 10.15825/1995-1191-2024-4-157-165.
8. *Prokudina ES, Senokosova EA, Antonova LV, Krivkina EO, Velikanova EA, Akentieva TN et al.* New Tissue-Engineered Vascular Matrix Based on Regenerated Silk Fibroin: *in vitro* Study. *Sovrem Tekhnologii Med*. 2023; 15 (4): 41–48. doi: 10.17691/stm2023.15.4.04. PMID: 38434192.
9. *Mantry S, Silakabattini K, Das PK, Sankaraiah J, Barik CS, Panda S et al*. Silk fibroin: An innovative protein macromolecule-based hydrogel/ scaffold revolutionizing breast cancer treatment and diagnosis – Mechanisms, advancements, and targeting capabilities. *Int J Biol Macromol*. 2025 Apr 5; 309 (Pt 2): 142870. doi: 10.1016/j.ijbiomac.2025.142870. PMID: 40194579.
10. *Sun W, Gregory DA, Tomeh MA, Zhao X*. Silk Fibroin as a Functional Biomaterial for Tissue Engineering. *Int J Mol Sci*. 2021 Feb 2; 22 (3): 1499. doi: 10.3390/ijms22031499. PMID: 33540895.
11. *De Giorgio G, Matera B, Vurro D, Manfredi E, Galstyan V, Tarabella G et al.* Silk Fibroin Materials: Biomedical Applications and Perspectives. *Bioengineering (Basel)*. 2024 Feb 9; 11 (2): 167. doi: 10.3390/bioengineering11020167. PMID: 38391652.
12. *Qi Y, Wang H, Wei K, Yang Y, Zheng RY, Kim IS, Zhang KQ*. A Review of Structure Construction of Silk Fibroin Biomaterials from Single Structures to Multi-Level Structures. *Int J Mol Sci*. 2017 Mar 3; 18 (3): 237. doi: 10.3390/ijms18030237. PMID: 28273799.

13. *Tian Z, Chen H, Zhao P*. Compliant immune response of silk-based biomaterials broadens application in wound treatment. *Front Pharmacol*. 2025 Feb 12; 16: 1548837. doi: 10.3389/fphar.2025.1548837.
14. *Jacobsen MM, Li D, Rim NG, Backman D, Smith ML, Wong JY*. Silk-fibronectin protein alloy fibres support cell adhesion and viability as a high strength, matrix fibre analogue. *Sci Rep*. 2017 Apr 5; 7: 45653. doi: 10.1038/srep45653.
15. *Safonova L, Bobrova M, Efimov A, Lyundup A, Agapova O, Agapov I.* A Comparative Analysis of the Structure and Biological Properties of Films and Microfibrous Scaffolds Based on Silk Fibroin. *Pharmaceutics*. 2021 Sep 26; 13 (10): 1561. https://doi.org/10.3390/pharmaceutics13101561.
16. *Safonova L, Bobrova M, Efimov A, Davydova L, Tenchurin T, Bogush V et al.* Silk Fibroin/Spidroin Electrospun Scaffolds for Full-Thickness Skin Wound Healing in Rats. *Pharmaceutics*. 2021 Oct 15; 13 (10): 1704. doi: 10.3390/pharmaceutics13101704.
17. *Gavrilova NA, Borzenok SA, Revishchin AV, Tishchenko OE, Ostrovkiy DS, Bobrova MM et al.* The effect of biodegradable silk fibroin-based scaffolds containing glial cell line-derived neurotrophic factor (GDNF) on the corneal regeneration process. *Int J Biol Macromol*. 2021 Aug 31; 185: 264–276. doi: 10.1016/j.ijbiomac.2021.06.040.
18. *Cao Y, Wang B*. Biodegradation of Silk Biomaterials. *Int J Mol Sci*. 2009 Mar 31; 10 (4): 1514–1524. doi: 10.3390/ijms10041514.
19. *Koh LD, Cheng Y, Teng CP, Khin YW, Loh XJ, Tee SY et al.* Structures, mechanical properties and applications of silk fibroin materials. *Progress in Polymer Science*. 2015 Jul; 46: 86–110. doi: 10.1016/j.progpolymsci.2015.02.001.
20. *Podbolotova EI, Pashutin AR, Efimov AE, Agapova OI, Agapov II*. *In vitro* Degradation Study of Tissue-Based Materials from Natural Silk for Regenerative Medicine. *Biomaterials*. 2024; 40 (3): 95–99. [In Russ, English abstract]. doi: 10.56304/S0234275824030104.
21. *Agapov II, Agapova OI, Efimov AE, Sokolov DYu, Bobrova MM, Safonova LA.* Sposob polucheniya biodegradiruemykh skaffoldov na osnove tkaney iz natural'nogo shelka. Patent na izobretenie RU2653428 S1, 08.05.2018.
22. *Agapov II, Podbolotova EI, Kirsanova LA, Grudinin NV, Pashutin AR, Agapova OI et al*. *In vitro* and *in vivo* Biodegradation of Silk Fabric Scaffolds. *Dokl Biol Sci*. 2025 Feb; 520 (1): 34–37. doi: 10.1134/S0012496624600519.
23. *Zheng Z, Ran J, Chen W, Hu Y, Zhu T, Chen X et al.* Alignment of collagen fiber in knitted silk scaffold for functional massive rotator cuff repair. *Acta Biomater*. 2017 Mar 15; 51: 317–329. doi: 10.1016/j.actbio.2017.01.041. PMID: 28093363.
24. *Chen X, Qi YY, Wang LL, Yin Z, Yin GL, Zou XH, Ouyang HW.* Ligament regeneration using a knitted silk scaffold combined with collagen matrix. *Biomaterials*. 2008 Sep; 29 (27): 3683–3692. doi: 10.1016/j.biomaterials.2008.05.017.
25. *Shang P, Xiang Y, Xing C, Chen S, Yuan F*. Procyanidin-crosslinked gradient silk fibroin composite nanofiber scaffold with sandwich structure for rotator cuff repair. *Biomater Adv*. 2025 Apr; 169: 214183. doi: 10.1016/j.bioadv.2025.214183.
26. *Fan H, Liu H, Wang Y, Toh SL, Goh JC*. Development of a silk cable-reinforced gelatin/silk fibroin hybrid scaffold for ligament tissue engineering. *Cell Transplant*. 2008; 17 (12): 1389–1401. doi: 10.3727/096368908787648047.

The article was submitted to the journal on 10.06.2025

DOI: 10.15825/1995-1191-2025-4-133-137

ADVANCES IN OVERCOMING IMMUNOLOGICAL AND PHYSIOLOGICAL BARRIERS IN XENOTRANSPLANTATION

D.A. Velikiy[1], Yu.B. Basok[1], N.V. Grudinin[1], O.E. Gichkun[1, 2], A.P. Trashkov[3], A.V. Varlachev[3], O.P. Shevchenko[1, 2]

[1] Shumakov National Medical Research Center of Transplantology and Artificial Organs, Moscow, Russian Federation
[2] Sechenov University, Moscow, Russian Federation
[3] Kurchatov Institute, Moscow, Russian Federation

The growing number of patients with severe organ diseases, along with the increasing demand for retransplantations, has intensified the global shortage of donor organs – the primary limitation to expanding transplant programs. Advances in genetic engineering and cell therapy technologies are opening new opportunities for the use of animal organs in human transplantation. Enhancing the efficacy and safety of this approach requires overcoming significant immunological and physiological barriers inherent in xenotransplantation. This review summarizes recent progress in genetic modification of donor animals, use of cell-based therapy in xenotransplantation, and prospects for clinical application.

Keywords: xenotransplantation, hyperacute rejection, genetic modification, cell therapy.

INTRODUCTION

Organ transplantation remains the only definitive treatment for many patients with end-stage organ failure. Advances in surgical techniques, postoperative care, and immunosuppressive therapy have significantly improved transplant outcomes. However, the primary factor limiting the expansion of transplant programs is the persistent shortage of donor organs. In 2023, a total of 1,817 kidney transplants were performed in the Russian Federation [1], while 53,874 patients were on hemodialysis [2].

One possible solution to this problem is the use of animal organs. In the mid-20th century, the first attempts at transplanting primate organs into humans were conducted in the United States. However, these early experiments yielded poor outcomes, with most recipients dying within weeks due to graft rejection. The subsequent decline in interest in xenotransplantation was driven not only by immunological incompatibility but also by concerns regarding the transmission of zoonotic infections. The discovery of retroviruses and the potential emergence of recombinant strains pathogenic to humans led to an almost complete halt in animal organ transplantation research [3].

However, recent advances in genetic engineering and cell therapy have revived interest in xenotransplantation. Although apes share a closer anatomical, physiological, and immunological resemblance to humans, they are not considered an optimal source of donor organs. Compared to primates, pigs present several key advantages: rapid growth to adult size, early reproductive maturity, large litter sizes, and relatively low maintenance costs. It is also important to note that there is a certain amount of accumulated experience in the field of genetic engineering in cloning pigs [4].

The purpose of this review is to analyze the latest data on methods of genetic modification of animals and the use of cell therapy in xenotransplantation, as well as to assess the prospects for its clinical application.

RISKS OF XENOTRANSPLANTATION

Genetic disparities between species create immunological barriers to successful xenotransplantation. Early attempts to transplant pig organs into primates were largely unsuccessful: within hours of reperfusion, recipients developed hyperacute rejection [5, 6]. This reaction is driven by the recognition of xenoantigens expressed on the vascular endothelial cells of the pig graft by preexisting “anti-pig” antibodies in the recipient’s circulation. The ensuing cascade involved antibody-mediated activation of the complement system, leading to endothelial inflammation, formation of the membrane attack complex, and subsequent vascular injury. This triggered coagulation pathway activation, resulting in interstitial hemorrhage, thrombosis, and ischemia, ultimately destroying the transplant [7].

Membrane-associated regulatory complement proteins play a crucial role in the development of rejection during xenotransplantation. These molecules, expressed on the surface of most cell types, suppress excessive complement activation and thereby protect healthy cells.

Corresponding author: Dmitriy Velikiy. Address: 1, Shchukinskaya str., Moscow, 123182, Russian Federation. Phone: (499) 193-87-62. E-mail: dim_vel@mail.ru

Similarly, coagulation regulatory factors present in the vascular endothelium maintain an anticoagulant state under normal conditions.

However, in xenotransplantation, porcine complement and coagulation regulatory proteins fail to interact efficiently with their primate counterparts. As a result, the xenograft becomes susceptible to uncontrolled complement activation and coagulation cascade dysregulation [8].

Another major obstacle to successful xenotransplantation is the risk of transmission of zoonotic infections. Therefore, animals – particularly pigs – used as organ donors must be bred under sterile, pathogen-free conditions and rigorously screened for infectious agents hazardous to humans, such as gamma (γ) herpesvirus, swine influenza virus, porcine cytomegalovirus, hepatitis E virus, and porcine endogenous retrovirus (PERV) [9].

Unlike other pathogens, PERV is integrated into the pig genome and cannot be eliminated through pharmacological or vaccination measures [9]. Although no cases of PERV transmission to humans or nonhuman primates have been documented during experimental xenotransplantations, genetic inactivation of PERV loci is considered a promising strategy to mitigate the potential risk of zoonotic transmission [10].

GENETIC MODIFICATION OF DONOR ANIMALS

A significant body of research in genetic engineering and animal cloning is currently focused on enhancing the compatibility of pig organs for xenotransplantation into humans. The creation of genetically modified pigs with multiple gene deletions and human transgene insertions should be aimed at overcoming key immunological and physiological barriers to successful pig-to-human organ transplantation [11].

The advancement of these methods has been largely driven by the development of the CRISPR/Cas9 genome editing system, which is derived from a natural bacterial antiviral defense mechanism. This technology enables the induction of site-specific double-stranded DNA breaks within the genome, facilitating targeted insertion or deletion of genes followed by cellular DNA repair [12].

Another necessary condition for genetic modification is the ability to obtain a line of animals with a modified genome. This is achieved by transferring the nuclei of genetically modified somatic cells into an enucleated animal oocyte (cloning). The combination of gene targeting via homologous recombination in cultured somatic cells followed by nuclear transfer allows for the production of multiple heritable genetic modifications for xenotransplantation purposes [13].

In recent years, a series of experimental studies have been conducted to identify optimal strategies for genetic modification of the pig genome aimed at minimizing the risk of xenograft rejection [10, 14, 15]. One of the most effective approaches reported involves the modification of ten key genes – specifically, the deletion of four porcine antigens combined with the insertion of six human transgenes.

The inactivated porcine genes include the major carbohydrate antigen αGal (Galactose-α-1,3-galactose) and two additional carbohydrate antigens, CMAH and β4GalNT2, which participate in the synthesis of N-glycolylneuraminic acid and the sialyl dimeric antigen, respectively. The growth hormone receptor gene (GHr) is also deleted to limit donor pig growth, maintaining body weight below 150 kg.

At the same time, six human genes were introduced: CD46 (membrane cofactor protein) and CD55 (decay-accelerating factor) as complement inhibitors; THBD (thrombomodulin) and EPCR (endothelial protein C receptor) as coagulation inhibitors; CD47 (integrin-associated protein), which inhibits T-cell and macrophage activation; and HO1 (heme oxygenase-1), an anti-inflammatory enzyme [16].

Prior to organ harvesting for xenotransplantation, it is necessary to study the genotype and phenotype of donor animals for the presence of all intended modifications and to rule out any unplanned changes, such as unintended CRISPR/Cas9-induced breaks or the random insertion of extra copies of human transgenes [17].

CELL THERAPY

One of the major challenges in xenotransplantation is the lack of an effective immunosuppressive regimen. A promising direction for improving xenograft outcomes lies in the application of cell-based therapies designed to enhance the effectiveness of organ transplantation by mitigating the adverse consequences of prolonged immunosuppression [18].

Mesenchymal stromal stem (MSCs) are known to possess a set of unique properties, including immunosuppressive effects. The therapeutic potential of MSCs is mediated by the secretion of numerous regulatory and trophic factors, exosomes, microvesicles, lipoproteins, microRNAs, as well as apoptotic bodies, which significantly enhance regenerative processes in damaged organs, stimulate angiogenesis, and prevent cell apoptosis, inflammation, and fibrosis [19].

Further optimization of MSC-based therapy in transplantation may involve their pre-activation. One of the most promising strategies is MSC activation through autophagy induction [20]. The combined use of methods of genetic modification of animals and cell therapy can increase the effectiveness of xenogeneic transplantation and achieve long-term survival of the xenograft.

CLINICAL OBSERVATIONS

In recent years, an increasing number of studies have reported on the outcomes of xenotransplantation of genetically modified pig organs in both brain-dead human

models and living recipients [21]. The use of brain-dead patients as recipients in such experiments is scientifically justified, as it allows for minimizing the risks associated with early clinical trials [22].

Nevertheless, this model has several important limitations, including short observation periods and unstable hemodynamics in brain-dead recipients, which may lead to hypoperfusion, ischemic injury, and inflammatory responses within the xenograft [23].

A notable clinical case was described by Kawai et al., who reported the transplantation of a genetically modified pig kidney into a 62-year-old patient with end-stage chronic kidney disease. In the early postoperative period, the recipient developed an episode of T-cell–mediated rejection, which was successfully treated with antithymocyte globulin. No subsequent rejection episodes were observed. The xenograft remained functionally active for two months until the patient died of acute coronary pathology unrelated to the transplant [24].

In another notable report, a research group described the xenotransplantation of a genetically engineered pig heart – modified with ten specific gene edits – into a living human recipient. On the first postoperative day, the xenograft demonstrated satisfactory cardiac function. However, by day 13, endomyocardial biopsy revealed signs of acute antibody-mediated rejection. Despite intensive immunosuppressive therapy, hemodynamic decompensation occurred on day 30, necessitating extracorporeal membrane oxygenation (ECMO). The patient was declared dead 10 days later. The authors attributed the graft failure primarily to the recipient's critical preoperative condition and the extensive transfusion of blood components, both of which likely contributed to the rejection [25].

In a study conducted by Tao et al., heterotopic xenotransplantation of a genetically modified pig liver was performed in a brain-dead human recipient. The xenograft maintained stable hepatic perfusion and functioned effectively for 10 days, producing both bile and porcine albumin. Histological analysis of biopsy specimens revealed C3d and C4d complement deposition, along with IgM and IgG staining, consistent with early humoral immune activation. Despite the short observation period, the non-physiological nature of the transplant and the use of a brain-dead recipient, the authors suggested that such xenotransplants may provide temporary metabolic and synthetic support through xenotransplantation, serving as a bridge to to possible allotransplantation [26].

CONCLUSION

Advances in genetic engineering have made it possible to create genetically modified lines of animals (primarily pigs) whose organs do not trigger hyperacute rejection during xenotransplantation to primates in experimental settings or to humans in clinical practice. However, species incompatibility remains a major challenge, as long-term xenograft survival still requires recipients to take high doses of immunosuppressive drugs, which significantly increases the risk of malignant tumors and infectious complications. To mitigate the adverse effects of prolonged immunosuppression, several immune tolerance–induction strategies have been proposed, including hematopoietic stem cell transplantation to achieve mixed chimerism, combined transplantation of a solid organ and thymus, and infusion of regulatory T cells. Clinical studies have demonstrated that formation of mixed chimerism in kidney recipients following allotransplantation from HLA-incompatible related donors may allow for reduction or complete discontinuation of immunosuppressive therapy [27].

At present, a synergistic approach combining genetic modification of donor animals to reduce the immunogenicity of their organs with cell-based therapies aimed at inducing immune tolerance to the xenograft appears to be the most promising direction. This approach may not only enhance the efficacy and safety of xenogeneic transplantation and ensure long-term survival of both the xenograft and recipient, but also provide new insights into the fundamental regulatory mechanisms underlying the immune response in interspecies transplantation.

The authors declare no conflict of interest.

REFERENCES

1. Transplantology: results and prospects. Vol. XV. 2023 / Ed. by S.V. Gautier. M.–Tver: Triada, 2024; 320.
2. *Shilov EM, Shilova MM, Rumyantseva EI, Batyushin MM, Bevzenko AYu, Belskikh AN et al*. Nephrological service of the Russian Federation 2023: Part I. Renal replacement therapy. *Clinical Nephrology*. 2024; 16 (1): 5–14. https://dx.doi.org/10.18565/nephrology.2024.1.5-14.
3. *Orlova OV*. Xenotransplantation of organs and tissues (the First Global consultation on regulatory requirements for xenotransplantation clinical trials). *Russian Journal of Transplantology and Artificial Organs*. 2008; 6: 6–11.
4. *Damas J, Corbo M, Kim J, Turner-Maier J, Farré M, Larkin DM et al.* Evolution of the ancestral mammalian karyotype and syntenic regions. *Proc Natl Acad Sci USA*. 2022 Oct 4; 119 (40): e2209139119. doi: 10.1073/pnas.2209139119.
5. *Cooper DK*. Xenotransplantation – state of the art. *Front Biosci (Landmark Ed).* 1996 Sep 1; 1 (4): 248–265. doi: 10.2741/a130.
6. *Mudur G*. Indian surgeon challenges ban on xenotransplantation. *BMJ*. 1999 Jan 9; 318 (7176): 79. doi: 10.1136/bmj.318.7176.79a.
7. *Hisadome Y, Eisenson DL, Santillan MR, Iwase H, Yamada K*. Pretransplant Screening for Prevention of Hyperacute Graft Loss in Pig-to-primate Kidney Xenotransplantation. *Transplantation*. 2024 Aug 1; 108 (8): 1749–1759. doi: 10.1097/TP.0000000000004958.
8. *Goerlich CE, Singh AK, Griffith BP, Mohiuddin MM*. The immunobiology and clinical use of genetically engineered porcine hearts for cardiac xenotransplantation.

Nat Cardiovasc Res. 2022 Aug; 1 (8): 715–726. doi: 10.1038/s44161-022-00112-x.
9. *Denner J*. Porcine endogenous retroviruses in xenotransplantation. *Nephrol Dial Transplant*. 2024 Jul 31; 39 (8): 1221–1227. doi: 10.1093/ndt/gfae023.
10. *Anand RP, Layer JV, Heja D, Hirose T, Lassiter G, Firl DJ et al*. Design and testing of a humanized porcine donor for xenotransplantation. *Nature*. 2023 Oct; 622 (7982): 393–401. doi: 10.1038/s41586-023-06594-4.
11. *Peterson L, Yacoub MH, Ayares D, Yamada K, Eisenson D, Griffith BP et al*. Physiological basis for xenotransplantation from genetically modified pigs to humans. *Physiol Rev*. 2024 Jul 1; 104 (3): 1409–1459. doi: 10.1152/physrev.00041.2023.
12. *Gostimskaya I*. CRISPR-Cas9: A History of Its Discovery and Ethical Considerations of Its Use in Genome Editing. *Biochemistry (Mosc)*. 2022 Aug; 87 (8): 777–788. doi: 10.1134/S0006297922080090.
13. *Wang X, Qu J, Li J, He H, Liu Z, Huan Y*. Epigenetic Reprogramming During Somatic Cell Nuclear Transfer: Recent Progress and Future Directions. *Front Genet*. 2020 Mar 18; 11: 205. doi: 10.3389/fgene.2020.00205.
14. *Yamamoto T, Iwase H, Patel D, Jagdale A, Ayares D, Anderson D et al*. Old World Monkeys are less than ideal transplantation models for testing pig organs lacking three carbohydrate antigens (Triple-Knockout). *Sci Rep*. 2020 Jun 17; 10 (1): 9771. doi: 10.1038/s41598-020-66311-3.
15. *Ariyoshi Y, Takeuchi K, Pomposelli T, Ekanayake-Alper DK, Shimizu A, Boyd L et al*. Antibody reactivity with new antigens revealed in multi-transgenic triple knockout pigs may cause early loss of pig kidneys in baboons. *Xenotransplantation*. 2021 Jan; 28 (1): e12642. doi: 10.1111/xen.12642.
16. *Eisenson D, Hisadome Y, Santillan M, Iwase H, Chen W, Shimizu A et al*. Consistent survival in consecutive cases of life-supporting porcine kidney xenotransplantation using 10GE source pigs. *Nat Commun*. 2024 Apr 18; 15 (1): 3361. doi: 10.1038/s41467-024-47679-6.
17. *Mohiuddin MM, Goerlich CE, Singh AK, Zhang T, Tatarov I, Lewis B et al*. Progressive genetic modifications of porcine cardiac xenografts extend survival to 9 months. *Xenotransplantation*. 2022 May; 29 (3): e12744. doi: 10.1111/xen.12744.
18. *Deo D, Marchioni M, Rao P*. Mesenchymal stem/stromal cells in organ transplantation. *Pharmaceutics*. 2022 Apr 4; 14 (4): 791. doi: 10.3390/pharmaceutics14040791.
19. *Han Y, Yang J, Fang J, Zhou Y, Candi E, Wang J et al*. The secretion profile of mesenchymal stem cells and potential applications in treating human diseases. *Signal Transduct Target Ther*. 2022 Mar 21; 7 (1): 92. doi: 10.1038/s41392-022-00932-0.
20. *Shravage BV, Turksen K*. Autophagy in stem cell maintenance and differentiation. 1st ed. Cham, Switzerland: Springer; 2022.
21. *Shirini K, Ladowski JM, Meier RPH*. Xenotransplantation Literature Update: January-June 2025. *Xenotransplantation*. 2025 Jul-Aug; 32 (4): e70072. doi: 10.1111/xen.70072.
22. *Montgomery RA, Griesemer AD, Segev DL, Sommer P*. The decedent model: A new paradigm for de-risking high stakes clinical trials like xenotransplantation. *Am J Transplant*. 2024 Apr; 24 (4): 526–532. doi: 10.1016/j.ajt.2024.01.035.
23. *Cooper DKC, Kobayashi T*. Xenotransplantation experiments in brain-dead human subjects – A critical appraisal. *Am J Transplant*. 2024 Apr; 24 (4): 520–525. doi: 10.1016/j.ajt.2023.12.020.
24. *Kawai T, Williams WW, Elias N, Fishman JA, Crisalli K, Longchamp A et al*. Xenotransplantation of a Porcine Kidney for End-Stage Kidney Disease. *N Engl J Med*. 2025 May 15; 392 (19): 1933–1940. doi: 10.1056/NEJMoa2412747.
25. *Griffith BP, Grazioli A, Singh AK, Tully A, Galindo J, Saharia KK et al*. Transplantation of a genetically modified porcine heart into a live human. *Nat Med*. 2025 Feb; 31 (2): 589–598. doi: 10.1038/s41591-024-03429-1.
26. *Tao KS, Yang ZX, Zhang X, Zhang HT, Yue SQ, Yang YL et al*. Gene-modified pig-to-human liver xenotransplantation. *Nature*. 2025 May; 641 (8064): 1029–1036. doi: 10.1038/s41586-025-08799-1.
27. *Podestà MA, Sykes M*. Chimerism-Based Tolerance to Kidney Allografts in Humans: Novel Insights and Future Perspectives. *Front Immunol*. 2022 Jan 5; 12: 791725. doi: 10.3389/fimmu.2021.791725.

The article was submitted to the journal on 2.07.2025

DOI: 10.15825/1995-1191-2025-4-138-145

ASSOCIATION BETWEEN *TGFB1* RS1800469 POLYMORPHISM AND POST-TRANSPLANT COMPLICATIONS IN PEDIATRIC LIVER RECIPIENTS

R.M. Kourabekova[1], O.E. Gichkun[1, 2], O.M. Tsirulnikova[1, 2], I.E. Pashkova[1], M.S. Vlasov[1], S.V. Meshcheryakov[1], O.P. Shevchenko[1, 2], S.V. Gautier[1, 2]

[1] Shumakov National Medical Research Center of Transplantology and Artificial Organs, Moscow, Russian Federation

[2] Sechenov University, Moscow, Russian Federation

Objective: to evaluate the association between carriage of the rs1800469 polymorphism of the *TGFB1* gene and the risk of post-transplant complications, rejection episodes, and infectious diseases in pediatric liver recipients. **Materials and methods.** The study included 219 pediatric liver recipients (92 boys, 127 girls), aged 2.4 to 204 months (median 8 months). Indications for liver transplantation (LT) were end-stage liver failure resulting from congenital or acquired liver diseases. Genotyping of the *TGFB1* rs1800469 polymorphism was performed using real-time polymerase chain reaction (PCR) with TaqMan probes. **Results.** A comparative analysis of the allele frequency of rs1800469 of the *TGFB1* gene was performed in three groups of pediatric liver recipients: (1) with versus without post-transplant complications, (2) with versus without rejection episodes, and (3) with versus without infectious complications. In all groups, allele frequencies conformed to Hardy–Weinberg equilibrium ($p > 0.05$). No significant differences in rs1800469 variant distribution were observed between recipients with and without overall complications or between those with and without rejection episodes. However, marked differences emerged between recipients with and without infectious complications: the C/C genotype was 1.9 times less frequent ($p = 0.0102$), the C allele was 1.3 times less frequent ($p = 0.0175$), and the T allele was 1.4 times more frequent ($p = 0.0175$) in the infection group. Under a dominant inheritance model, carriers of the T allele (C/T + T/T) had 2.53-fold higher odds of infection compared with those with the homozygous C/C genotype in the group of recipients with infections than in those without ($p = 0.0077$). **Conclusion.** In pediatric liver transplant recipients, the *TGFB1* polymorphic variant rs1800469 is not associated with either a complicated post-transplant course or the occurrence of graft rejection episodes. However, carriers of the T allele appear to have an increased risk of infectious complications compared with those with the homozygous C/C genotype. These findings suggest that the rs1800469 T allele may serve as a genetic marker for increased susceptibility to infections and could be considered in strategies for prevention of complications and individualized adjustment of immunosuppressive therapy.

Keywords: congenital liver diseases, liver transplantation, TGFB1 rs1800469, infectious complications.

INTRODUCTION

Liver transplantation remains the only definitive treatment for young children with end-stage liver failure resulting from congenital or acquired liver disease. However, post-transplantation, a range of complications may occur, arising either from immunosuppressive therapy or the underlying disease. The occurrence and severity of these complications may, in many cases, depend on the recipient's genetic profile. Thus, identification of genetic markers that reflect individual patient characteristics could facilitate the prediction, prevention, and management of post-transplant complications.

Several studies, including our own, have demonstrated that in pediatric liver transplant (LT) recipients, blood levels of transforming growth factor-β1 (TGF-β1), a pleiotropic cytokine with profibrogenic and immunosuppressive properties, may be associated with graft status, particularly with the development of rejection or transplant dysfunction [1–3]. These observations suggest that TGF-β1 may serve as a potential prognostic biomarker for post-transplant complications. Nevertheless, the causal relationship between protein levels and complications remains unclear: high levels of the cytokine may represent both a cause and a consequence of fibrotic processes [4, 5]. Given the multifactorial regulation of TGF-β1 expression, it is plausible that individual genetic determinants influencing cytokine production contribute to the pathogenesis of post-transplant complications [6, 7].

In patients with various pathological conditions, including liver diseases, an association has been established between circulating levels of TGF-β1 and carriage of the polymorphic variant rs1800469 in the *TGFB1* gene

Corresponding author: Rivada Kourabekova. Address: 1, Shchukinskaya str., Moscow, 123182, Russian Federation. Phone: (499) 190-53-41. E-mail: kourabr@yandex.ru

[8, 9]. This single-nucleotide polymorphism (SNP), also known as C(–509)T, represents a cytosine-to-thymine substitution in the gene's promoter region and is thought to influence transcription factor binding affinity [10]. Reporter gene assays have demonstrated that promoter constructs containing cytosine at position –509 exhibit significantly higher transcriptional activity than those carrying thymine [8].

Several studies have suggested that the carriage of specific *TGFB1* polymorphic alleles may contribute to the development of post-transplant complications, including acute rejection, graft fibrosis, and renal dysfunction [11–13]. Furthermore, the role of TGFB1 gene polymorphisms has been investigated in the pathogenesis of infectious diseases such as hepatitis B and C, human papillomavirus (HPV), and COVID-19 [14–16].

In adult patients with liver cirrhosis secondary to hepatitis B or C infection, significant differences have been observed in the frequencies of rs1800469 and rs1800470 variants compared to healthy controls, suggesting that these polymorphisms may influence both susceptibility to viral infection and predisposition to cirrhosis [17–19]. However, the direction of association varies across studies: while the T allele at position –509 (rs1800469) is most frequently linked to increased risk [18–20], other reports have implicated the C allele [8, 17] or found no significant associations at all [21].

No studies investigating the role of *TGFB1* gene polymorphisms in the development of post-LT complications among pediatric liver recipients were found in the available literature. Our previous research demonstrated that in children who underwent liver transplantation for various congenital and acquired liver diseases, the frequencies of individual variants rs1800469, rs1800470, and rs1800471 did not differ significantly from those in healthy controls. However, rare haplotypes of these polymorphic loci were significantly more common in recipients [22]. Analysis of *TGFB1* polymorphic loci and their haplotypes in specific subgroups, such as patients with biliary atresia or histologically confirmed fibrosis of the explanted liver, revealed significant differences compared to healthy individuals [23, 24]. The high prevalence of rare allelic variants and haplotypes of the *TGFB1* gene in children with liver disease suggests their potential association not only with progression to liver failure but also with development of post-transplant complications.

The present study aims to evaluate the risk of post-transplant complications, including rejection episodes and infectious diseases, in pediatric LT recipients carrying the rs1800469 polymorphic variant of the TGFB1 gene.

MATERIALS AND METHODS

The study included 219 pediatric LT recipients aged 2.4 to 204 months (median age, 8 months), comprising 92 boys and 127 girls. The investigation was conducted in accordance with a protocol approved by the Local Ethics Committee, Shumakov National Medical Research Center of Transplantology and Artificial Organs (Moscow, Russia).

Indications for liver transplantation were end-stage liver failure resulting from liver diseases, such as biliary atresia (BA), biliary hypoplasia (BH), Alagille syndrome, Caroli syndrome, and Byler disease, as well as rarer disorders such as Crigler–Najjar syndrome, Gierke disease, alpha-1 antitrypsin deficiency, tyrosinemia, fulminant and autoimmune hepatitis, cryptogenic cirrhosis, and others.

After transplantation, patients received double- or triple-drug immunosuppressive therapy, which included tacrolimus, corticosteroids, and mycophenolate mofetil. Routine follow-up and management of recipients were performed in accordance with the clinical guidelines of the Russian Transplant Society and the institutional protocols at Shumakov National Medical Research Center of Transplantology and Artificial Organs.

During the first year following transplantation, recipients developed various complications, including immune, infectious, vascular, biliary, surgical, and other postoperative disorders. Immune complications comprised episodes of acute cellular and antibody-mediated rejection, diagnosed based on a combination of laboratory parameters (elevated serum transaminases and/or bilirubin levels) and clinical manifestations such as jaundice, acholic or hypocholic stools, and occasionally skin itching.

Infectious complications included bacterial intestinal infections leading to cholangitis, bacterial pneumonia, generalized sepsis with systemic inflammatory response syndrome (SIRS), peritonitis secondary to intestinal perforation or obstruction, and cytomegalovirus (CMV) infection.

Genomic DNA was extracted from peripheral blood leukocytes using the QIAamp DNA Blood Mini Kit on an automated QIAcube™ platform (Qiagen, Germany), following the manufacturer's instructions.

Genotyping of the TGFB1 rs1800469 polymorphism was performed by real-time polymerase chain reaction (PCR) using TaqMan® probes (Applied Biosystems, USA) on a CFX96™ real-time PCR detection system (Bio-Rad, USA), according to the manufacturer's instructions.

The TaqMan assay (Assay ID: C_8708473_10) identifies allelic variants at the G/A locus of rs1800469, which are complementary to the C/T nucleotides on the other DNA strand.

Data collection and statistical evaluation were performed using Microsoft Excel. Analysis of genotype and allele frequencies for the studied SNP, as well as assessment of the potential influence of genotype on clinical traits, were carried out using the SNPstats software [22].

The odds ratio (OR) and its 95% confidence interval (CI) were calculated to estimate the strength of associations.

Genotype frequencies were expressed as a percentage of individuals in the cohort, while allele frequencies were expressed as a percentage of chromosomes, according to the formula:

$$\text{Allele frequency} = \frac{(2 \times \text{number of homozygotes}) + \text{number of heterozygotes}}{2 \times \text{total number of individuals}}$$

A p-value < 0.05 was considered statistically significant.

RESULTS

Table 1 presents the demographic and clinical characteristics of the pediatric LT recipients included in the study.

The majority of patients in the study cohort were children with congenital cholestatic liver diseases, the most common diagnosis being BA, which accounted for 48% of all cases. Three groups of LT recipients were analyzed: (1) with versus without post-transplant complications, (2) with versus without rejection episodes, and (3) with versus without infectious complications. In all examined groups, the distribution of rs1800469 alleles of the *TGFB1* gene was consistent with the Hardy–Weinberg equilibrium (p > 0.05).

To evaluate the potential association between post-transplant complications and the rs1800469 polymorphism of the *TGFB1* gene, a comparative analysis of genotype and allele frequencies was performed in pediatric LT recipients with complicated and uncomplicated postoperative courses (Fig. 1).

Table 1

Clinical and demographic characteristics of pediatric liver recipients

Characteristic	Value
Number of recipients, n	219
Age, median (range), months	8.4 (2.4–204)
Sex, number (%)	Male: 92 (42) Female: 127 (58)
Underlying disease, n (%)	219 (100)
BA	105 (48)
BH	24 (11)
Caroli syndrome	11 (5)
Alagille syndrome	10 (4.5)
Byler's disease	10 (4.5)
Others	59 (27)
Post-LT complications, n (%)	
Complication / No complication	131 (60) / 88 (40)
Rejection / No rejection	28 (13) / 191 (87)
Infections / No infections	52 (24) / 167 (76)

Abbreviations: BA, biliary atresia; BH, biliary hypoplasia; LT, liver transplant.

The analysis presented in Fig. 1 did not reveal any statistically significant differences in the frequencies of genotypes or alleles of the rs1800469 locus between pediatric LT recipients who developed complications and those who had an uneventful postoperative course during the first year after transplantation.

Fig. 2 shows the results of a comparative analysis of genotype and allele frequencies of the same locus in groups of recipients with and without graft rejections (labeled as "Rejection" and "No rejection" in the figure) during the first year following liver transplantation.

The results presented in Fig. 2 also showed no statistically significant differences in the frequencies of genotypes or alleles at the rs1800469 locus between recipients who experienced rejection episodes and those who did not.

A comparative analysis of genotype and allele frequencies at the rs1800469 polymorphic locus was further performed between groups of recipients with and without infectious complications that developed during the first year ppost-transplant (Fig. 3).

As shown in Fig. 3, statistically significant differences were observed in the distribution of genotypes and alleles of the rs1800469 locus between these two groups.

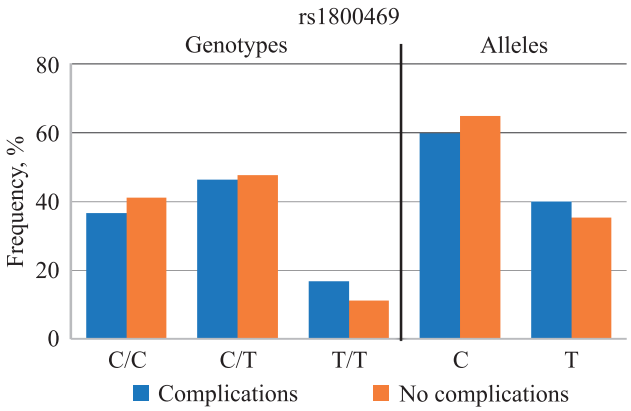

Fig. 1. Frequency of rs1800469 genotypes and alleles among recipients with and without complications

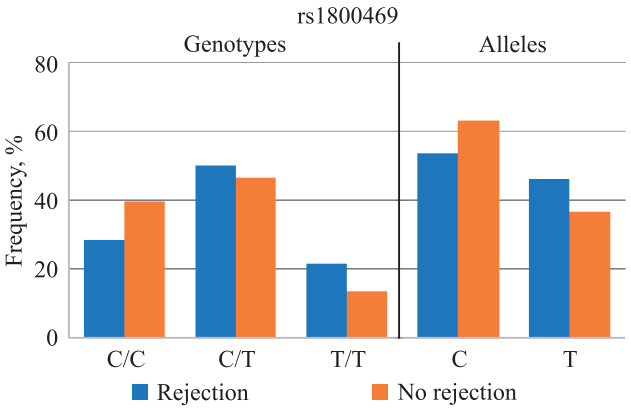

Fig. 2. Frequency of TGFB1 rs1800469 genotypes and alleles among recipients with and without graft rejection

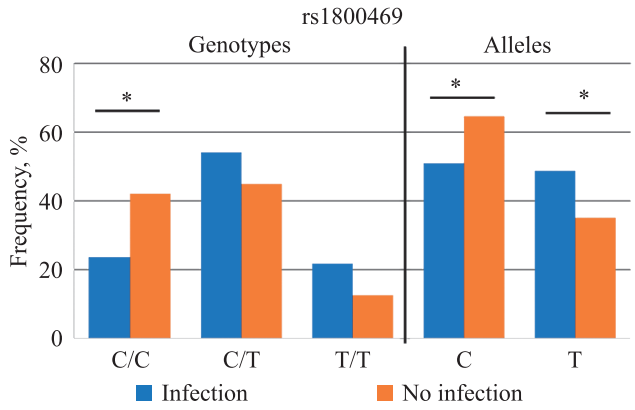

Fig. 3. Frequency of rs1800469 genotypes and alleles among recipients with and without infectious complications. * – $p < 0.05$

Table 2

Distribution of TGFB1 rs1800469 genotypes in gene–gene interaction models among liver recipients with infectious complications

Model	Genotype	Frequency, %		OR (95% CI)	p-value
		With infections	Without infections		
Codominant	C/C	23	43	Comparison group	0.028*
	C/T	58	44	**2.47 (1.17–5.19)**	
	T/T	19	13	**2.73 (1.04–7.16)**	
Dominant	C/C	23	43	Comparison group	0.0077*
	C/T + T/T	77	57	**2.53 (1.24–5.16)**	
Recessive	C/C + C/T	81	87	Comparison group	0.29
	T/T	19	13	1.57 (0.69–3.57)	
Overdominant	C/C + T/T	42	56	Comparison group	0.078
	C/T	58	44	1.76 (0.94–3.29)	

* – $p < 0.05$.

Among recipients with infectious complications, carriers of the homozygous C/C genotype were 1.9 times less frequent ($p = 0.0102$), the C allele was 1.3 times less frequent ($p = 0.0175$), and the T allele was 1.4 times more frequent ($p = 0.0175$) compared to recipients without infectious complications.

For a more detailed statistical assessment, the distribution of rs1800469 genotypes in recipients with and without infectious complications was analyzed under various models of allelic interaction (codominant, dominant, recessive, and overdominant). The corresponding genotype frequencies, odds ratios (ORs), and 95% confidence intervals (CIs) are summarized in Table 2.

As shown in Table 2, statistically significant differences were observed between groups with and without infectious complications under two genetic models. In the codominant model, the carrier frequency of the heterozygous C/T genotype was 2.47 times higher, and that of the homozygous T/T genotype was 2.73 times higher compared to the homozygous C/C variant. In the dominant model, carriers of the T allele (C/T + T/T) were 2.53 times more frequent than those with the C/C genotype in the compared recipient groups.

DISCUSSION

The development of post-transplant complications depends to a certain extent on the individual characteristics of the recipient's immune system. It is possible that the rs1800469 polymorphic locus of the *TGFB1* gene may serve as a potential genetic marker of predisposition to such complications.

In this study, we analyzed the distribution of genotypes at SNP rs1800469 among pediatric liver recipients with various types of post-transplant complications, identified a statistically significant association with infectious complications, and calculated the relative chance of their development in carriers of different variants of the *TGFB1* gene.

In the group of pediatric LT recipients who developed serious complications within the first year after transplantation, the frequencies of genotypes and alleles of the rs1800469 polymorphism of the *TGFB1* gene did not differ significantly from those observed in recipients with a favorable postoperative course. Some of the complications recorded – such as surgical, biliary, or vascular – are unlikely to be associated with immune mechanisms or with the activity of the cytokine TGF-β1. Therefore, the absence of a general association between the carriage of *TGFB1* polymorphic variants and the overall incidence of complications appears reasonable. Nonetheless, several studies have reported associations between *TGFB1* polymorphisms and broader clinical outcomes, including post-transplant survival after heart transplantation [25] and overall survival in hematopoietic stem cell recipients [26]. It is possible that in these cases, the observed relationships reflect, at least in part, the influence of cytokine TGF-β1 levels on the studied outcomes.

In the subgroup of pediatric liver recipients who developed acute rejection episodes, no statistically significant differences were found in the distribution of *TGFB1* polymorphic alleles compared with recipients without rejection. As noted in the introduction, there are currently no published data on the role of *TGFB1* polymorphism in the development of rejection following liver transplantation in children. However, in adult solid-organ recipients, several studies have demonstrated an association

between polymorphic variants of this cytokine gene and the incidence of rejection [11, 25]. Our previous study similarly found no significant association between circulating TGF-β1 levels and rejection episodes in pediatric liver recipients [3]. It is known that rejection occurs less frequently in pediatric liver recipients than in adults; therefore, the relatively small number of recipients with rejection episodes in this study (n = 28) may have limited the statistical power to detect genetic differences. It is also possible that the role of *TGFB1* polymorphic loci in the development of rejection may depend on factors such as the type of transplanted organ, recipient age, and ethnic background.

This study revealed a link between *TGFB1* polymorphism and the risk of developing post-LT infectious complications in children. Specifically, carriers of the T allele (C/T + T/T) of rs1800469 were found to develop infectious complications 2.5 times more frequently than recipients with the C/C genotype. Notably, in our previous study, no significant association was observed between circulating TGF-β1 levels measured before transplantation, and at one month and one year post-transplant, and the frequency of post-transplant infectious complications [3]. This finding may suggest that the genetic marker provides a more stable and sensitive indicator of susceptibility than the protein marker, whose concentration can be influenced by numerous environmental factors.

To our knowledge, no previous studies have investigated the role of TGFB1 genetic polymorphism in the development of infectious complications after liver transplantation in either pediatric or adult recipients. However, studies in adult patients with liver cirrhosis resulting from hepatitis B or C virus infection have shown that the presence of the T allele of rs1800469 is associated with an increased risk of infection in several populations [8, 18, 19]. In addition, these studies show that infected patients had higher levels of cytokine in their blood. Thus, our data, showing a higher incidence of infectious complications in carriers of the T allele, are broadly consistent with previous findings. Nevertheless, some reports have failed to identify significant differences in TGFB1 rs1800469 distribution between patients with infectious hepatitis and healthy controls [21, 27], which may be due to differences in study design and ethnic origin of the cohorts.

The findings of this study indicate that the rs1800469 polymorphism in the *TGFB1* gene in pediatric LT recipients is not associated with an unfavorable post-transplant course or an increased risk of graft rejection. However, carriage of this variant may be linked to the risk of developing infectious complications after liver transplantation. These results suggest that the rs1800469 locus could serve as a potential genetic marker for predicting post-transplant infectious complications in children and for optimizing immunosuppressive therapy to prevent infectious diseases. Further research is warranted to assess the prognostic value of the *TGFB1* rs1800469 polymorphism as a marker of infection risk and its possible relationship with individualized immunosuppressant requirements.

CONCLUSION

The risk of post-transplant complications may be influenced by both the expression level of the cytokine TGF-β1 and its genetic polymorphism. Analysis of the rs1800469 locus in the TGFB1 gene in pediatric liver recipients revealed no association between this variant and an overall complicated postoperative course or episodes of graft rejection. However, the odds ratio for carriers of the T allele (C/T + T/T genotypes) was 2.5 times higher than for carriers of the homozygous C/C genotype among recipients who developed infectious complications compared to those without infections. These findings suggest that carriage of the T allele of rs1800469 may increase susceptibility to post-transplant infections. This locus may therefore serve as a potential genetic marker for identifying patients at increased risk of infectious complications and for guiding individualized immunosuppressive therapy.

The authors declare no conflict of interest.

REFERENCES

1. *Briem-Richter A, Leuschner A, Krieger T, Grabhorn E, Fischer L, Nashan B et al*. Peripheral blood biomarkers for the characterization of alloimmune reactivity after pediatric liver transplantation. *Pediatr Transplant.* 2013 Dec; 17 (8): 757–764. doi: 10.1111/petr.12161.
2. *Hussein MH, Hashimoto T, AbdEl-Hamid Daoud G, Kato T, Hibi M, Tomishige H et al*. Pediatric patients receiving ABO-incompatible living related liver transplantation exhibit higher serum transforming growth factor-beta1, interferon-gamma and interleukin-2 levels. *Pediatr Surg Int.* 2011 Mar; 27 (3): 263–268. doi: 10.1007/s00383-010-2784-1.
3. *Kurabekova R, Tsirulnikova O, Pashkova I, Gichkun O, Mozheyko N, Gautier S, Shevchenko O*. Transforming growth factor beta 1 levels in the blood of pediatric liver recipients: Clinical and biochemical correlations. *Pediatr Transplant.* 2020 May; 24 (3): e13693. doi: 10.1111/petr.13693.
4. *Li MO, Wan YY, Sanjabi S, Robertson AK, Flavell RA*. Transforming growth factor-beta regulation of immune responses. *Annu Rev Immunol.* 2006; 24: 99–146. doi: 10.1146/annurev.immunol.24.021605.090737.
5. *Valva P, Casciato P, Diaz Carrasco JM, Gadano A, Galdame O, Galoppo MC et al*. The role of serum biomarkers in predicting fibrosis progression in pediatric and adult hepatitis C virus chronic infection. *PloS One.* 2011; 6 (8): e23218. doi: 10.1371/journal.pone.0023218.
6. *Grainger DJ, Heathcote K, Chiano M, Snieder H, Kemp PR, Metcalfe JC et al*. Genetic control of the circulating concentration of transforming growth factor type beta1. *Hum Mol Genet.* 1999 Jan; 8 (1): 93–97. doi: 10.1093/hmg/8.1.93.

7. *Awad MR, El-Gamel A, Hasleton P, Turner DM, Sinnott PJ, Hutchinson IV*. Genotypic variation in the transforming growth factor-beta1 gene: association with transforming growth factor-beta1 production, fibrotic lung disease, and graft fibrosis after lung transplantation. *Transplantation.* 1998 Oct 27; 66 (8): 1014–1020. doi: 10.1097/00007890-199810270-00009.
8. *Wang H, Zhao Y-P, Gao C-F, Ji Q, Gressner AM, Yang Z-X, Weiskirchen R*. Transforming growth factor β1 gene variants increase transcription and are associated with liver cirrhosis in Chinese. *Cytokine.* 2008 Jul; 43 (1): 20–25. doi: 10.1016/j.cyto.2008.04.013.
9. *Punia V, Agrawal N, Bharti A, Mittal S, Chaudhary D, Mathur A et al*. Association of TGF-β1 Polymorphism and TGF-β1 Levels With Chronic Hepatitis C and Cirrhosis: A Systematic Review and Meta-Analysis. *Cureus.* 2023 Jun 29; 15 (6): e41157. doi: 10.7759/cureus.41157. eCollection 2023 Jun.
10. *Shah R, Rahaman B, Hurley CK, Posch PE*. Allelic diversity in the *TGFB1* regulatory region: characterization of novel functional single nucleotide polymorphisms. *Hum Genet.* 2006 Mar; 119 (1–2): 61–74. doi: 10.1007/s00439-005-0112-y.
11. *Zhang XX, Bian RJ, Wang J, Zhang QY*. Relationship between cytokine gene polymorphisms and acute rejection following liver transplantation. *Genet Mol Res.* 2016 Apr 26; 15 (2): gmr.15027599. doi: 10.4238/gmr.15027599.
12. *Gichkun OE, Shevchenko OP, Kurabekova RM, Mozheiko NP, Shevchenko AO*. The rs1800470 Polymorphism of the *TGFB1* Gene Is Associated with Myocardial Fibrosis in Heart Transplant Recipients. *Acta Naturae.* 2021 Oct-Dec; 13 (4): 42–46. doi: 10.32607/actanaturae.11469.
13. *López-Ibor JV, Citores MJ, Portoles J, Gómez-Bueno M, Sánchez-Sobrino B, Muñoz A et al*. Role of TGF-β1 +869T>C polymorphism in renal dysfunction one year after heart transplantation. *J Heart Lung Transplant.* 2022 Dec; 41 (12): 1672–1678. doi: 10.1016/j.healun.2022.09.004.
14. *Guo P, Sun X, Feng X, Zhang C*. Transforming growth factor-β1 gene polymorphisms with liver cirrhosis risk: A meta-analysis. *Infect Genet Evol.* 2018 Mar; 58: 164–170. doi: 10.1016/j.meegid.2017.12.019.
15. *Trugilo KP, Cebinelli GCM, Pereira É R, Okuyama NCM, Cezar-Dos-Santos F, Castilha EP et al*. Haplotype Structures and Protein Levels of *TGFB1* in HPV Infection and Cervical Lesion: A Case-Control Study. *Cells.* 2022 Dec 25; 12 (1): 84. doi: 10.3390/cells12010084.
16. *Jahromi M, Al Otaibi T, Othman N, Mahmoud T, Nair P, Halim MA, Gheith O*. Transforming Growth Factor-β1 C (+869) T Codon 10 Gene Polymorphism Significantly Associated with Rates of SARS-CoV-2 in Kidney Transplant Recipients in Kuwait. *Exp Clin Transplant.* 2024 Jan; 22 (Suppl 1): 299–309. doi: 10.6002/ect.MESOT2023.P100.
17. *Wang H, Mengsteab S, Tag CG, Gao CF, Hellerbrand C, Lammert F et al*. Transforming growth factor-beta1 gene polymorphisms are associated with progression of liver fibrosis in Caucasians with chronic hepatitis C infection. *World J Gastroenterol.* 2005 Apr 7; 11 (13): 1929–1936. doi: 10.3748/wjg.v11.i13.1929.
18. *Mohy A, Fouad A*. Role of transforming growth factor-β1 in serum and –509C>T promoter gene polymorphism in development of liver cirrhosis in Egyptian patients. *Meta Gene.* 2014 Sep 9; 2: 631–637. doi: 10.1016/j.mgene.2014.08.002.
19. *De Brito WB, Queiroz MAF, da Silva Graça Amoras E, Lima SS, da Silva Conde SRS, Dos Santos EJM et al*. The *TGFB1* –509C/T polymorphism and elevated TGF-β1 levels are associated with chronic hepatitis C and cirrhosis. *Immunobiology.* 2020 Sep; 225 (5): 152002. doi: 10.1016/j.imbio.2020.152002.
20. *Falleti E, Fabris C, Toniutto P, Fontanini E, Cussigh A, Bitetto D et al*. TGF-beta1 genotypes in cirrhosis: relationship with the occurrence of liver cancer. *Cytokine.* 2008 Nov; 44 (2): 256–261. doi: 10.1016/j.cyto.2008.08.008.
21. *Wu XD, Zeng K, Gong CS, Chen J, Chen YQ*. Transforming growth factor-β genetic polymorphisms on development of liver cirrhosis in a meta-analysis. *Mol Biol Rep.* 2013 Jan; 40 (1): 535–543. doi: 10.1007/s11033-012-2090-1.
22. *Kurabekova RM, Gichkun OE, Tsirulnikova OM, Pashkova IE, Fomina VA, Shevchenko OP, Gautier SV*. Analysis of the Association between the Tgfb1 Gene Haplotype and Liver Diseases in Children. *Acta Naturae.* 2023 Jul-Sep; 15 (3): 75–81. doi: 10.32607/actanaturae.19425.
23. *Kurabekova RM, Gichkun OE, Tsirulnikova OM, Pashkova IE, Vakurova EA, Shevchenko OP, Gautier SV*. High incidence of rare *TGFB1* haplotypes in children with biliary atresia. *Russian Journal of Transplantology and Artificial Organs*. 2024; 26 (3): 168–175. doi: 10.15825/1995-1191-2024-3-168-175.
24. *Tsirulnikova OM, Gichkun OE, Kurabekova RM, Stakhanova EA, Pashkova IE, Vakurova EA, Shevchenko OP*. Native liver fibrosis in pediatric liver recipients: association with genetic polymorphism in the *TGFB1* gene. *Russian Journal of Transplantology and Artificial Organs*. 2024; 26 (4): 166–170. doi: 10.15825/1995-1191-2024-4-166-170.
25. *Van Setten J, Warmerdam EG, Groot OQ, de Jonge N, Keating B, Asselbergs FW*. Non-HLA Genetic Factors and Their Influence on Heart Transplant Outcomes: A Systematic Review. *Transplant Direct.* 2019 Jan 21; 5 (2): e422. doi: 10.1097/TXD.0000000000000859.
26. *Arrieta-Bolanos E, Mayor NP, Marsh SG, Madrigal JA, Apperley JF, Kirkland K et al*. Polymorphism in *TGFB1* is associated with worse non-relapse mortality and overall survival after stem cell transplantation with unrelated donors. *Haematologica.* 2016 Mar; 101 (3): 382–390. doi: 10.3324/haematol.2015.134999.
27. *Larijani MS, Rad LN, Nikbin M, Bahiraei N, Javadi F, Daneshvar M et al*. Impact of TGF-β1 Gene Polymorphism (rs1800469) on Treatment Response to Pegylated Interferon/Ribavirin in Iranian Patients with Hepatitis C. *Clin Lab.* 2016; 62 (4): 609–614. doi: 10.7754/clin.lab.2015.150807.

The article was submitted to the journal on 29.07.2025

DOI: 10.15825/1995-1191-2025-4-146-157

KIDNEY TRANSPLANTATION FROM EXPANDED CRITERIA DONORS. THE FIRST MULTICENTER COHORT STUDY IN THE RUSSIAN FEDERATION

D.A. Bankeev[1], A.B. Zulkarnaev[1], M.G. Minina[1, 2], V.S. Bogdanov[1], E.A. Tenchurina[1], V.M. Sevostyanov[1]

[1] Botkin Hospital, Moscow, Russian Federation

[2] Shumakov National Medical Research Center of Transplantology and Artificial Organs, Moscow, Russian Federation

The use of expanded criteria donors (ECDs) is an effective strategy to increase the availability of organs for transplantation. However, in Russia, there have been no large-scale studies evaluating the outcomes of kidney transplantation (KT) from ECDs. In Moscow, through successful implementation of an original organ donation model, considerable experience has been accumulated in managing donors who meet the UNOS expanded criteria for kidney donation. This paper presents the epidemiological characteristics of donors and recipients, as well as the medium-term outcomes of KT from ECDs. The study represents the first multicenter cohort study in the Russian Federation dedicated to kidney transplants from ECDs. The database was developed using systematized donor information from the Moscow Coordination Center for Organ Donation at Botkin Hospital for the period 2021–2022. During this time, 254 donors meeting UNOS expanded criteria underwent organ explantation at 21 hospitals in Moscow. The follow-up period for KT recipients was limited to four years. Recipient survival at 4 years after transplantation was 0.882 [95% CI 0.839–0.927], while overall graft survival (loss from any cause) was 0.806 [95% CI 0.739–0.880] and death-censored graft survival was 0.887 [95% CI 0.825–0.952]. Primary graft function was observed in 61.4% of recipients who received kidneys from ECDs. The medium-term survival rates of both recipients and grafts are acceptable and comparable to those reported in international studies, confirming the safety and effectiveness of expanding donor criteria to increase the number of kidney transplants.

Keywords: kidney transplantation, extended criteria donors, brain death, graft survival.

INTRODUCTION

According to data from the Russian Transplant Society registry [1] between January 1, 2021, and December 31, 2022, a total of 630 organ transplants from deceased donors were performed in Moscow. In 2021, among 298 effective donors (23.7 per million population), 290 (97.3%) were diagnosed with brain death. In 2022, 332 organ procurements were carried out (26.3 per million population), with 313 donors (94.3%) diagnosed with brain death. Overall, 254 donors (40.3%) met the UNOS criteria for expanded criteria donors (ECDs) [2].

According to UNOS [2], ECDs are defined as individuals aged 60 years and older, or aged 50–59 years with at least two of the following risk factors: a history of hypertension, death from acute cerebrovascular accident, or a serum creatinine level exceeding 1.5 mg/dL (132.6 μmol/L).

Although numerous studies have shown that kidney transplant (KT) outcomes from ECDs are somewhat inferior to those from standard criteria donors (SCDs) [2–5], their use remains an effective and necessary strategy to increase the availability of donor organs [5–9].

There are currently no large-scale studies in Russia evaluating the outcomes of KT from ECDs. However, according to data from the Russian Transplant Society, the proportion of donors aged over 60 years has increased significantly, from 10.7% in 2018 to 22.3% in 2023 [10]. It should also be noted that the donor and recipient pools, donor conditioning protocols, organ preservation times, and other procedural factors in Russia may differ considerably from those in other countries.

The objective of this study is to provide a comprehensive characterization of kidney donors meeting the expanded UNOS criteria, as well as to evaluate the medium-term outcomes of KT using such organs.

MATERIALS AND METHODS

This was a retrospective multicenter cohort study based on data systematically collected by the Moscow Coordination Center for Organ Donation at Botkin Hospital for the years 2021–2022. During this period, organs were procured across 21 hospitals from 254 donors who met the expanded UNOS criteria.

Corresponding author: Dmitry Bankeev. Address: 5/17, Vtoroy Botkinsky Proezd, Moscow, 125284, Russian Federation. Phone: (912) 743-09-97. E-mail: 79127430997@ya.ru

Descriptive statistics for quality indicators are presented as absolute frequencies and percentages. In some instances, the total number of observations may differ from n = 444 due to missing data for certain patients.

Quantitative variables were described as mean ± standard deviation for distributions close to normal, and as median (first and third quartiles) for non-normally distributed data. The normality of distribution was assessed through visual analysis of frequency histograms and quantile–quantile (Q–Q) plots.

Survival analysis was performed using the Kaplan–Meier method, with point estimates and 95% confidence intervals (95% CI) calculated. In the analysis of kidney graft survival, three types of estimates were considered: overall graft loss – defined as transplant loss due to any cause (events included recipient death with a functioning graft, surgical removal of a functioning graft for discontinuation of immunosuppressive therapy, or graft failure); death-censored graft loss – defined as graft removal or graft failure, with death of a recipient with a functioning graft treated as a censored event; graft loss only – defined as graft failure, while deaths with functioning grafts and elective removals for discontinuation of immunosuppression were treated as censored events.

RESULTS

General characteristics of donors and recipients

The general characteristics of kidney donors and recipients are presented in Table 1. Donors were slightly older than recipients, with a minimum donor age of 50 years (in accordance with the expanded donor criteria) and a minimum recipient age of 19 years. The mean body mass index (BMI) of donors exceeded 30 kg/m^2, indicating a predominance of overweight and obese individuals in this group.

The median length of hospital stay for donors was 51.5 hours [31.3; 85.8], ranging from 13.2 to 446.3 hours. In one case, organ procurement was performed on day 18 after admission; in all other cases, hospitalization did not exceed 10 days.

Most effective donors (248; 97.6%) were diagnosed with brain death due to acute cerebrovascular accident, while traumatic brain injury was identified as the cause of death in only 6 cases (2.4%).

Most donors had type O (I) or type A (II) blood – 94 (37.0%) and 95 (37.4%), respectively – whereas types B (III) and AB (IV) were less common, occurring in 42 (16.5%) and 23 (9.1%) donors, respectively.

Comorbid background of donors, conditioning and retrieval characteristics

Eighteen donors (7.1%) underwent successful cardiopulmonary resuscitation lasting from 5 to 40 minutes (median 15 [10; 20] minutes). More than half of the donors (146; 57.5%) exhibited glucose metabolism disorders, defined as either confirmed diabetes mellitus or the need for insulin administration during conditioning. In 37 cases (14.6%), diabetes mellitus had been previously diagnosed, while in 60 cases (23.6%), repeated insulin administration was required due to persistent hyperglycemia. It should be noted that glucose-containing solutions were not used during donor conditioning. The condition listed in Table 2 as systemic atherosclerosis refers to a

Table 1

General characteristics of effective organ donors diagnosed with brain death

Characteristics	Donors, n = 254	Recipients, n = 444
Age, years	58.3 (4.8), 50.0 to 74.0	51.6 (9.6), 19.0 to 72.0
Male / Female	155 (61.0%) / 99 (39.0%)	271 (60.2%) / 179 (39.8%)
Weight, kg	90.9 (18.2), 50.0 to 150.0	76.2 (16.1), 40.0 to 125.0
Body mass index, kg/m^2	30.8 (5.9), 18.4 to 54.7	25.8 (4.5), 13.6 to 38.4
Body surface area (BSA), m^2	2.1 (0.2), 1.5 to 2.7	1.9 (0.2), 1.3 to 2.6

Descriptive statistics: n (%); mean (SD), minimum and maximum; median [Q1; Q3], minimum and maximum.

Table 2

Comorbid background of organ donors

Donor characteristics	n = 254
Insulin administration during conditioning of potential donors	146 (57.5%)
Persistent hyperglycemia during donor conditioning	60 (23.6%)
Confirmed diabetes mellitus	37 (14.6%)
Signs of impaired glucose metabolism	146 (57.5%)
Confirmed arterial hypertension	251 (98.8%)
Systemic atherosclerosis	171 (67.3%)
Ischemic heart disease	242 (95.3%)
Chronic heart failure	135 (53.1%)
Administration of norepinephrine prior to organ retrieval	252 (99.2%)
Maximum norepinephrine dose, ng/kg/min	525 [330; 800], 60 to 3700
Administration of norepinephrine at the time of organ retrieval	212 (83.5%)
Norepinephrine dose at retrieval, ng/kg/min	150 [75.5; 340], 10 to 1200
Adrenaline, ng/kg/min	
0	247 (97.2%)
50	3 (1.2%)
100	2 (0.8%)
200	2 (0.8%)

Descriptive statistics: n (%); mean (SD), minimum and maximum; median [Q1–Q3], minimum and maximum.

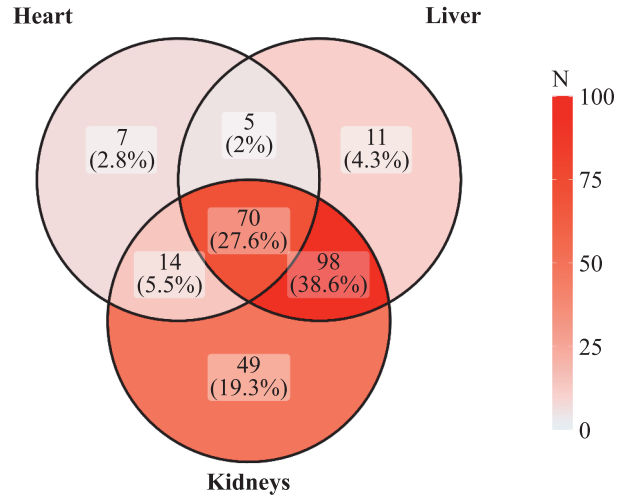

Fig. 1. Organ retrieval structure in donors

generalized form of vascular pathology characterized by multiple arterial lesions identified via instrumental diagnostic methods and visual inspection of accessible arteries during organ retrieval.

Almost all donors required vasopressor therapy (noradrenaline administration) before or during the conditioning phase. However, by the time of organ retrieval, the proportion of donors requiring noradrenaline had decreased significantly. Adrenaline was used in only 7 donors (2.8%), and none of these required its administration at the time of retrieval.

Most donors (182, 71.7%) underwent multi-organ procurement (Fig. 1). The liver was retrieved from 183 donors (71.7%), while the heart was procured from 96 donors (37.8%).

In 23 cases (9.1%), no kidneys were retrieved, and in 18 cases (7.1%), only one kidney was removed. In total, 444 kidneys were obtained from 254 donors, including 218 left and 226 right kidneys. The reasons for non-retrieval or refusal of transplantation are summarized in Table 3.

Laboratory data from 231 effective kidney donors, from whom at least one kidney was procured for transplantation, are presented in Table 4.

Recipients: causes of chronic kidney disease (CKD) and comorbidities

Predialysis transplantation was performed in 36 patients (8.4%). Before KT, 337 patients (78.4%) were on scheduled hemodialysis, 34 (7.9%) received peritoneal dialysis, and 23 (5.3%) underwent conversion of renal replacement therapy from peritoneal dialysis to hemodialysis. The duration of dialysis therapy among these patients ranged from 1 to 240 months (median 12 [12; 48] months). The causes of chronic renal failure (CRF) and the comorbidity profile of recipients are detailed in Tables 5 and 6, respectively.

Table 3

Reasons for refusal to harvest or transplant kidneys

Reason	Both kidneys (n = 23)	One kidney (n = 18)
Renal hypoplasia (shrunken kidneys)	7	4
Presence of hypoperfusion areas	4	–
Renal replacement therapy due to CKD stage 5D	3	–
Infected abdominal cavity	2	–
Presence of hypoperfusion and renal cyst areas	2	–
Shrunken kidneys and renal cysts	1	2
Renal cysts	1	5
Atherosclerotic renal artery atherosclerosis	1	3
Atherosclerotic renal artery and cyst atherosclerosis	1	–
Histologically confirmed renal formations	1	–
Hydronephrosis	–	1
Renal formation of unclear etiology	–	1
Absence of a kidney (anomaly or prior removal)	–	1
Parenchymal damage	–	1

Table 4

Laboratory parameters in effective kidney donors diagnosed with brain death

Donor characteristics	n = 231
Hemoglobin, g/L	141.2 (20.0), 75.0 to 199.0
Creatinine, μmol/L	
on admission	82.0 [67.0; 99.5], 33.0 to 262.0
maximum	92.0 [74.0; 118.5], 33.0 to 507.0
before retrieval	88.0 [70.0; 109.5], 33.0 to 507.0
Urea, mmol/L	
on admission	5.0 [4.0; 7.0], 2.0 to 15.0
maximum	7.0 [5.0; 8.0], 2.0 to 27.0
before retrieval	6.0 [5.0; 8.0], 2.0 to 27.0
Glomerular filtration rate (CKD-EPI), mL/min/1.73 m^2	
on admission	79.5 (21.0), 22.7 to 134.7
minimum	70.2 (24.4), 10.1 to 134.7
before retrieval	73.8 (23.8), 10.1 to 134.7
Alanine aminotransferase (ALT), U/L	
on admission	28.0 [23.0; 43.0], 7.0 to 406.0
maximum	31.0 [23.0; 54.0], 7.0 to 866.0
before retrieval	28.0 [21.0; 46.0], 7.0 to 866.0
Aspartate aminotransferase (AST), U/L	
on admission	25.0 [18.0; 36.0], 5.0 to 413.0
maximum	26.0 [19.0; 41.0], 5.0 to 1.090.0
before retrieval	24.5 [17.0; 36.0], 5.0 to 1.090.0

Descriptive statistics: mean (SD), minimum and maximum; median [Q1–Q3], minimum and maximum.

Recipients: immunological background

A large proportion of recipients had 3–5 HLA mismatches with their respective donors across the A, B, and DR loci. In 36 cases (8.2%), transplantation was performed despite mismatches in all three loci, whereas in 2 cases (0.5%), full HLA compatibility (no mismatches at all three loci) was observed. In 6 cases, the donor had blood group AB, a group with a notoriously limited recipient pool (Fig. 2).

More than half of the recipients (54.1%) had one mismatch at the DRB1 locus, while 19.9% had no mismatch at this locus. This distribution illustrates the positive impact of the regional regulatory framework, specifically, Order of the Moscow City Health Department No. 737 of October 19, 2017, titled "On the organization of medical

Table 5

Causes of chronic kidney disease in kidney transplant recipients

Cause of CKD	n = 444
Chronic glomerulonephritis	179 (41.6%)
Diabetic nephropathy	49 (11.4%)
Autosomal dominant polycystic kidney disease	61 (14.2%)
Hypertensive nephropathy (nephroangiosclerosis)	44 (10.2%)
Tubulointerstitial nephritis	25 (5.6%)
– Urolithiasis	14 (3.3%)
– Gout	9 (2.1%)
Secondary glomerulopathies	22 (5%)
– Anti-neutrophil cytoplasmic antibody (ANCA)-associated vasculitis	8 (1.9%)
– Antiphospholipid syndrome	3 (0.7%)
– Atypical hemolytic uremic syndrome	2 (0.5%)
– Thrombotic microangiopathy	2 (0.5%)
– Systemic lupus erythematosus	7 (1.6%)
Unknown cause	55 (12.2%)
Other	15 (3.3%)
– Nephrectomy (trauma or malignant tumor)	2 (0.4%)
– Developmental anomaly	13 (2.9%)

Table 6

Comorbid background of kidney transplant recipients

Recipient characteristics	n = 444
Arterial hypertension	428 (99.5%)
Ischemic heart disease	73 (17.0%)
Ischemic heart disease + history of coronary artery stenting	47 (10.9%)
Chronic heart failure	63 (14.7%)
Atrial fibrillation	26 (6.0%)
Diabetes mellitus	62 (14.4%)
With complications	44 (10.2%)
Without complications	18 (4.2%)
Peptic ulcer disease of the stomach and duodenum	21 (4.9%)
Chronic pyelonephritis	59 (13.7%)
Renoprivative state	30 (7.0%)
Chronic obstructive pulmonary disease	3 (0.7%)
History of acute cerebrovascular accident	15 (3.5%)
Malignant tumor	13 (3.0%)
Viral hepatitis C	35 (8.1%)
Viral hepatitis B	8 (1.9%)
HIV infection	2 (0.5%)
History of liver transplantation	1 (0.2%)
History of heart transplantation	1 (0.2%)
Hyperparathyroidism	235 (54.7%)
Multinodular goiter	7 (1.6%)
Autoimmune thyroiditis	9 (2.1%)
Thyrotoxicosis	4 (0.9%)
Gout	27 (6.3%)
Systemic lupus erythematosus	7 (1.6%)
Rheumatoid arthritis	1 (0.2%)
Thrombophilia	9 (2.1%)
Obliterating atherosclerosis of the lower extremities	5 (1.2%)

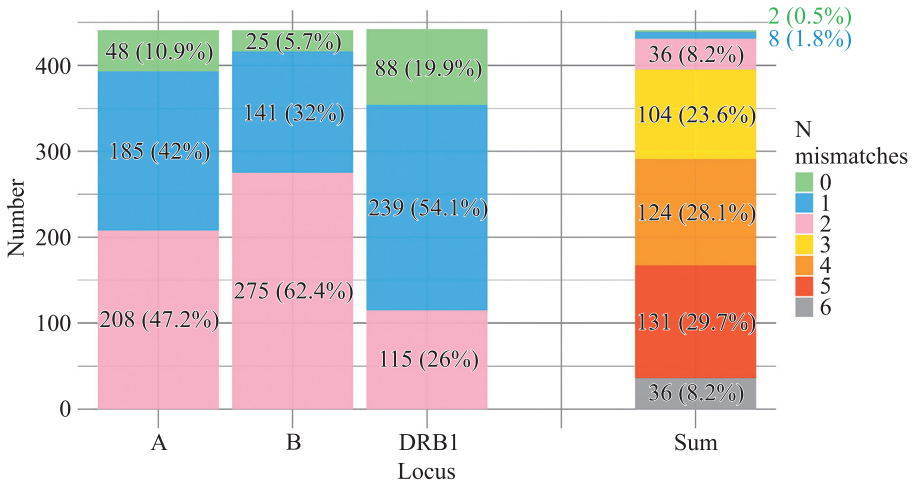

Fig. 2. Number of HLA mismatches. The number of donor antigens absent in each recipient was calculated

activities related to human organ donation and provision of surgical medical care (human organ and tissue transplantation) in the city of Moscow", which was implemented to improve the efficiency of donor-recipient matching within the transplant system of Moscow.

Pre-existing anti-HLA antibodies (mean fluorescence intensity, MFI >500 units) were identified in 73 recipients (16.4%). Class I antibodies (MFI >500) were detected in 40 recipients (9.2%), with median MFI of 2071.5 [1111.0; 3799] (range: 725–19,477). Class II antibodies (MFI >500) were found in 56 recipients (12.8%), with median MFI of 2618 [1305.5; 7269] (range: 526–20,772). For sensitization patterns, 17 recipients (3.8%) were sensitized to class I alone, 33 (7.4%) to class II alone, and 23 (5.2%) to both classes.

Recipients: characteristics of transplantation and the postoperative period

A total of 366 recipients (85.1%) underwent their first KT, 59 (13.7%) underwent their second, and 5 (1.2%) underwent their third. Median cold ischemia time was 14.4 hours [12.3; 17] (range: 6.9–26 hours). Median duration of hospitalization for recipients was 18 days [13; 26], varying between 5 and 106 days.

Induction therapy most frequently included a combination of basiliximab and methylprednisolone (362 patients, 84.2%). Antithymocyte globulin (ATG) combined with methylprednisolone was administered to 61 recipients (14.2%), while 4 (0.9%) received triple induction (basiliximab + ATG + methylprednisolone). Three patients (0.7%) received methylprednisolone alone.

Standard triple therapy – a calcineurin inhibitor (CNI), mycophenolate, and methylprednisolone – was administered to 403 recipients (93.9%). An everolimus-based regimen (everolimus + calcineurin inhibitor + methylprednisolone) was used in 24 patients (5.6%), while one recipient (0.2%) received everolimus + mycophenolate + methylprednisolone. Among those receiving CNIs, 390 (90.7%) were treated with tacrolimus, and 38 (8.8%) with cyclosporine A.

Delayed graft function (DGF), defined as the need for dialysis within the first postoperative week (regardless of the number of sessions), was observed in about one-third of recipients (147, 34.3%). The median number of hemodialysis sessions in this group was 3 [2; 6] (range: 1–26 sessions). Primary graft function was observed in 263 recipients (61.4%), while primary non-function occurred in 18 cases (4.2%).

Surgical or urological complications during hospitalization were recorded in about one-quarter of patients (109, 25.3%), while a combination of both types of complications occurred in 12 cases (2.8%). Among surgical complications, the most frequent was lymphocele of the transplant bed, diagnosed in 26 patients (5.9%). Other notable complications included retroperitoneal hematoma in 17 cases (3.8%) and postoperative wound infection in 11 cases (2.5%), of which 6 required vacuum-assisted closure (VAC). Reconstruction of transplant vessels was necessary in 9 cases (2.0%). Intraoperative bleeding and renal artery aneurysm of the transplant were each observed in one case (0.2%), and multiple surgical complications occurred in 8 recipients (1.8%).

Among urological complications, transplant pyelonephritis was the most common, developing in 40 recipients (9.0%). Ureteral necrosis occurred in 16 cases (3.6%), transplant hydronephrosis in 13 cases (3.0%), retroperitoneal urinary leakage in 12 cases (2.7%), and vesicoureteral reflux in 3 cases (0.7%). Combined urological complications were observed in 20 recipients (4.5%).

During the 4-year follow-up period, 272 recipients (61.2%) required rehospitalization between 1 and 8 times. A total of 567 rehospitalization episodes were recorded, corresponding to a frequency of 3.95 [95% CI 3.63–4.29] per 100 patient-months of follow-up. The most common reason for rehospitalization was the need for therapeutic intervention, including management of graft dysfunction or adjustment of immunosuppressive therapy, observed in 214 patients (48.2%). Combined causes included therapeutic intervention with distant surgical complications/diseases – 18 patients (4.1%); therapeutic intervention with distant urological complications/diseases – 17 patients (3.8%); urological complications/diseases alone – 14 patients (3.2%); surgical complications/diseases alone – 9 patients (2.0%).

Recipients: puncture biopsy results

During hospitalization for kidney transplantation, puncture biopsies were performed in 75 recipients (16.9%). No "zero" or routine control biopsies were performed in the early postoperative period. The indication for biopsy was graft dysfunction characterized by delayed recovery or absence of renal function.

After discharge, renal transplant biopsies were performed in 81 recipients (18.2%), as summarized in Table 7. The median time from transplantation to biopsy was 13.8 [6.1; 23.5] months, with a range of 2.9 to 44.7 months.

Recipients: recipient survival, graft survival, and graft function

Recipient survival is presented in Fig. 3. The estimated survival rates at 3 months, 1 year, 2 years, 3 years, and 4 years were 0.981 [95% CI 0.968–0.994], 0.950 [95% CI 0.929–0.971], 0.940 [95% CI 0.917–0.963], 0.910 [95% CI 0.881–0.939], and 0.882 [95% CI 0.839–0.927], respectively. During the follow-up period, 37 deaths were recorded. The leading causes of death included

acute myocardial infarction (n = 9), COVID-19 infection (n = 8), non-COVID-19-associated pneumonia (n = 8), sepsis (n = 5), and acute cerebrovascular accident (n = 3). Less common causes were peritonitis (n = 1), malignant neoplasm (n = 1), cardiac arrhythmia (n = 1), and acute hepatic failure with portal vein thrombosis (n = 1).

Kidney graft survival rates at 3 months, 1 year, 2 years, 3 years, and 4 years were as follows:

– For graft loss from any cause: 0.967 [95% CI 0.950–0.985], 0.926 [95% CI 0.900–0.952], 0.910 [95% CI 0.882–0.939], 0.876 [95% CI 0.843–0.911], and 0.806 [95% CI 0.739–0.880], respectively.
– For death-censored graft loss: 0.975 [95% CI 0.959–0.990], 0.956 [95% CI 0.936–0.977], 0.945 [95% CI 0.922–0.968], 0.936 [95% CI 0.911–0.961], and 0.887 [95% CI 0.825–0.952], respectively.
– For loss of graft function: 0.977 [95% CI 0.963–0.992], 0.958 [95% CI 0.939–0.979], 0.950 [95% CI 0.929–0.972], 0.941 [95% CI 0.917–0.965], and 0.896 [95% CI 0.835–0.961], respectively (Fig. 4).

The intensity (frequency) of events was highest during the first post-transplant year (Fig. 5).

The function of the transplanted kidney, assessed by the dynamics of estimated glomerular filtration rate (eGFR) and serum creatinine levels, is presented in Figs. 6 and 7, respectively.

Table 7

Puncture biopsy results

Biopsy result	Early period*, n = 75	Late period, n = 81
Donor pathology	30 (40.5%)	15 (18.5%)
Acute tubular necrosis	60 (81.1%)	25 (30.9%)
Focal segmental glomerulosclerosis	7 (9.5%)	20 (24.7%)
Interstitial fibrosis**	8 (10.8%)	39 (48.1%)
Percentage of interstitial fibrosis, %	22.5 [15; 35], 5 to 50	20 [15; 35], 5 to 70
Tubular atrophy	11 (14.9%)	39 (48.1%)
Calcineurin inhibitor toxicity	7 (9.5%)	8 (9.9%)
IgA nephropathy	0	3 (3.7%)
Thrombotic microangiopathy	2 (2.7%)	1 (1.2%)
Oxalosis	1 (1.4%)	0
Rejection	27 (36.0%)	41 (50.6%)
Acute cellular	11 (14.7%)	11 (13.8%)
Antibody-mediated	11 (14.7%)	15 (18.8%)
Acute mixed	5 (6.7%)	5 (6.3%)
Chronic active rejection	0	10 (12.3%)

Descriptive statistics: n (%); median [Q1–Q3], minimum and maximum. * Hospitalization for kidney transplantation. ** Among patients with interstitial fibrosis.

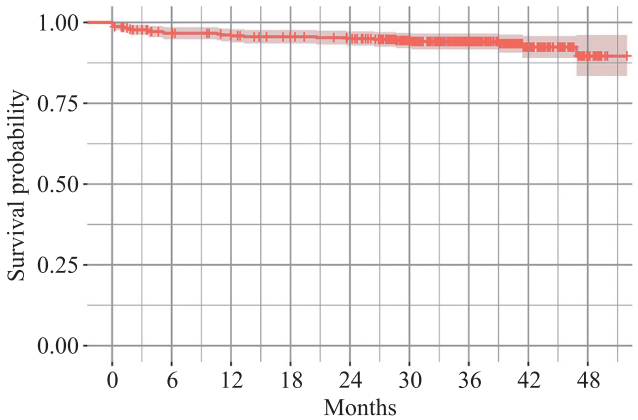

Fig. 3. Recipient survival. Survival function values are shown with 95% confidence intervals (CI)

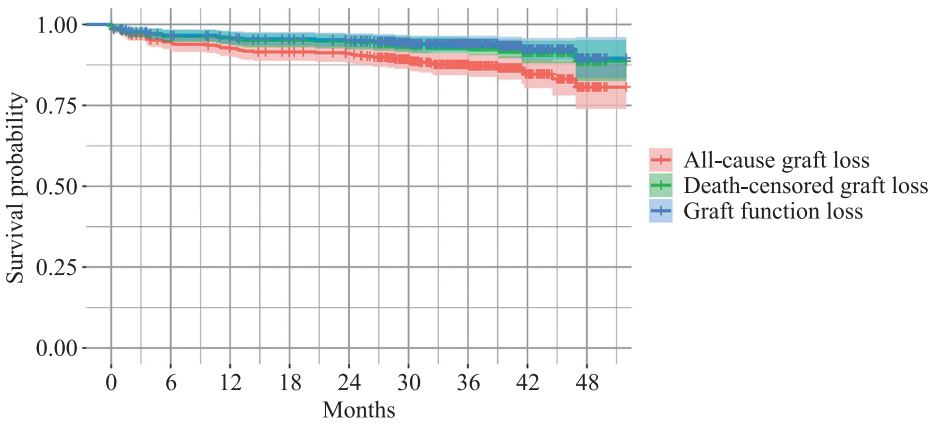

Fig. 4. Renal transplant survival. Survival rates and 95% confidence intervals (CI) are presented. Transplant loss for any reason: events included death of the recipient with a functioning transplant, retrieval of a functioning transplant for the purpose of discontinuing immunosuppressive therapy, or loss of transplant function. Death-censored graft loss: events included retrieval of a functioning graft for the purpose of discontinuing immunosuppressive therapy or loss of graft function; death of the recipient with a functioning graft was considered a censoring event. Transplant loss of function: events included graft loss; death of the recipient with a functioning graft and retrieval of a functioning graft for the purpose of discontinuing immunosuppressive therapy were considered censoring events

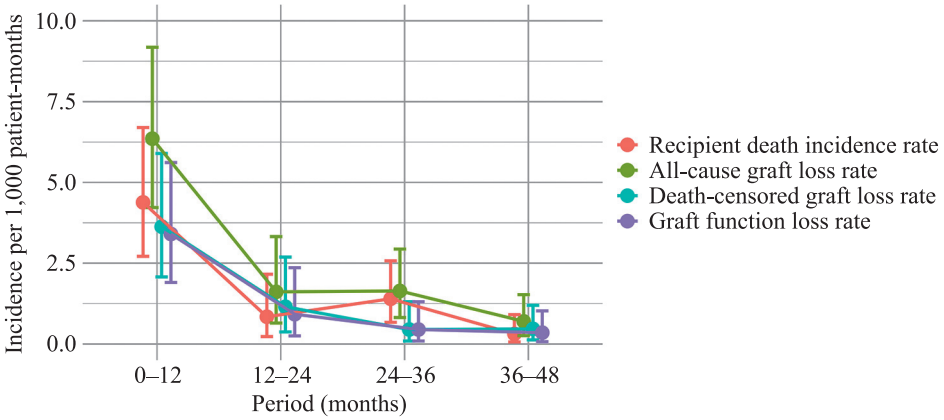

Fig. 5. Event intensity by follow-up period: recipient deaths, graft losses for any reason, death-censored graft losses, and graft function loss. Point estimates are shown with 95% confidence intervals (CI)

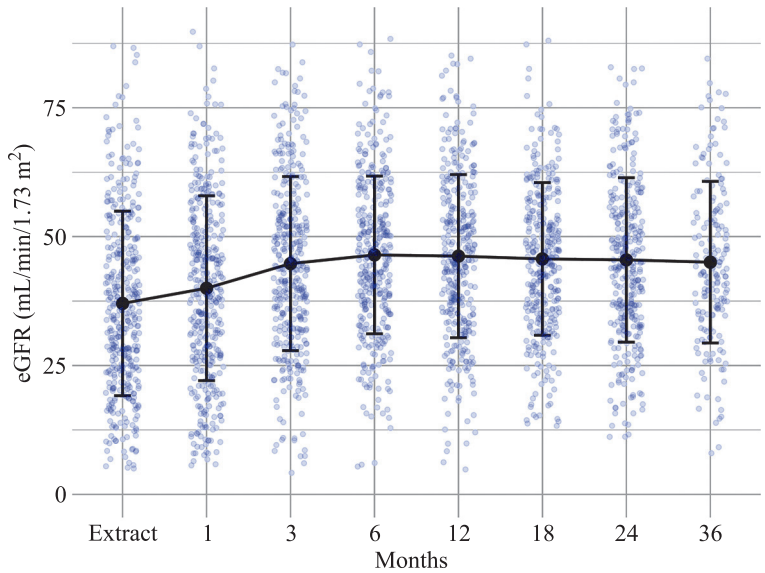

Fig. 6. Dynamics of estimated glomerular filtration rate (eGFR, CKD-EPI). Mean values with standard deviations and individual data points are presented

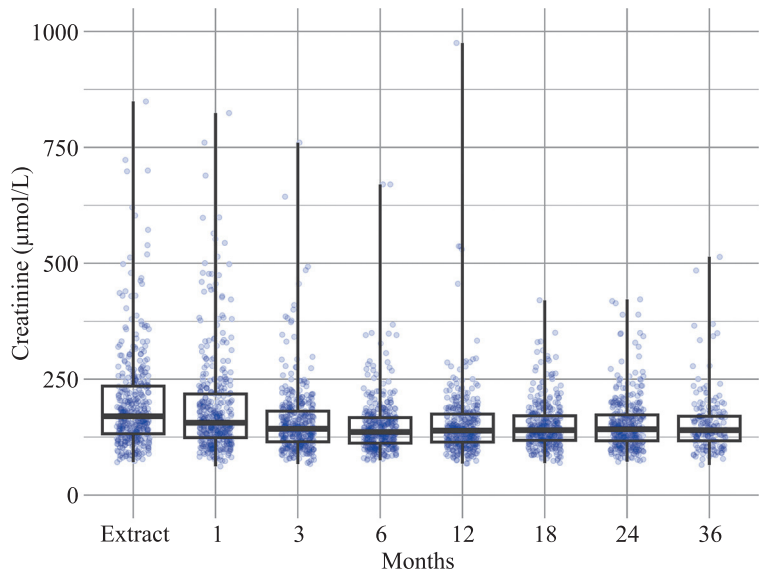

Fig. 7. Serum creatinine dynamics. Medians, first and third quartile limits, and individual values are presented

DISCUSSION

At present, there is a clear and steady trend toward an aging donor pool. According to Eurotransplant, between 2015 and 2024, the proportion of deceased donors aged ≥65 years increased from 22.4% to 26.4% [11]. In Spain, between 2014 and 2023, the proportion of donors aged 45–59 years remained nearly unchanged (28.7–29.2%), while the proportion aged 60–69 years rose from 23.8% to 27.2%, and those aged 70–79 years from 21.2% to 25.1% [12]. Querard et al. conducted a systematic review and meta-analysis of 32 studies comparing survival outcomes of kidney recipients from standard-criteria donors (SCDs) and expanded-criteria donors (ECDs). The pooled 5-year patient survival rates were 86.4% for SCDs and 78.4% for ECDs recipients [4]. A significant difference was also noted between European and North American data: in Europe, the 5-year survival rates for SCD and ECD recipients were 90.3% and 85.3%, respectively, whereas in North America they were considerably lower – 83.6% and 73.4% [13].

In a French prospective study published in the British Medical Journal in 2015, the 7-year graft survival rate was 80% for kidneys from ECDs and 88% for those from SCDs, demonstrating a moderately reduced graft viability but underscoring the continued clinical value of expanding donor criteria in the context of organ shortages [14].

The data presented support the necessity and feasibility of broadening kidney donation criteria, provided that donor–recipient pairing is carefully selected, risk is appropriately stratified, and perioperative management is optimized. Such an approach helps reduce patient mortality by reducing dialysis time, even while acknowledging potential limitations in long-term graft survival.

In the present study, anthropometric and gender-age characteristics of donors and recipients were generally comparable. The slight difference in mean age is down to the fact that the minimum age of a donor meeting the expanded criteria is 50 years.

A high incidence of diabetes mellitus and systemic atherosclerosis was observed among donors in this category. It is well established that donor diabetes is associated with poorer transplant outcomes [15, 16]. Moreover, kidneys obtained from ECDs may be more vulnerable to ischemic injury during preservation [17, 18]. These factors emphasize the need for further research aimed at identifying optimal allocation strategies for such organs and enhancing preservation technologies, particularly considering recent advances in machine perfusion systems.

In our study, the proportion of donors requiring inotropic support therapy to maintain hemodynamic stability at the time of organ retrieval decreased, indirectly reflecting the efficacy of donor optimization protocols. Nevertheless, increased azotemia and reduced GFR were noted in some donors, likely attributable to hemodynamic instability, high-dose inotropic therapy (including adrenaline administration), and the use of radiopaque contrast agents during brain death diagnosis. Despite these factors, current evidence indicates that acute kidney injury in donors prior to organ procurement is not associated with impaired medium-term graft outcomes [19–21].

An alarming yet common finding among KT recipients – including the general recipient population – is the increased incidence of recurrent renal pathology within 3–4 years after transplantation, particularly focal segmental glomerulosclerosis [22, 23]. This trend, also observed in Russia, is likely attributable to the lack of etiological verification of CKD prior to transplantation, as indirectly suggested by the high proportion (41.6%) of cases diagnosed as “chronic glomerulonephritis”.

The highest incidence of both recipient mortality and graft loss occurs during the first postoperative year. Nevertheless, long-term kidney graft survival in this cohort can be considered satisfactory, remaining comparable to that observed among recipients in the general population [24], and those receiving kidneys from SCDs [25]. Renal function improved significantly within six months after transplantation and remained relatively stable thereafter.

Comparable outcomes were reported in another study [26], which noted a high prevalence of hypertension and diabetes and elevated pre-donation creatinine levels, yet long-term recipient survival remained on par with that of transplants from SCDs. However, several other studies [27, 28], have demonstrated poorer graft outcomes in transplants from ECDs compared to standard donors. However, recipient survival remains higher than in patients maintained on dialysis while awaiting transplantation [29].

This publication presents descriptive statistics as well as recipient and graft survival rates. A detailed analysis of factors influencing recipient and transplant survival will be provided in a subsequent publication.

STUDY LIMITATIONS

The main limitation of this study is its retrospective design. However, inclusion of all transplants performed from donors meeting the inclusion criteria enhances the objectivity and representativeness of the findings. In several instances, particularly when characterizing comorbid conditions, it was not possible to retrospectively verify specific diagnoses, and the analysis therefore relied on data extracted from medical records. The assessment of the recipients’ comorbid background remains the most debatable aspect of the study. Nevertheless, the criteria for inclusion on the waiting list and for kidney transplantation in the analyzed cohort are largely standardized, suggesting that patients with decompensated extrarenal diseases were not included.

When describing biopsy results, the study did not apply the Banff classification, but rather focused on the rejection profile (cellular, antibody-mediated, or mixed) in order to obtain a larger number of patients in each category.

CONCLUSION

Approximately one-third of recipients who received kidneys from ECDs and from brain-dead donors developed delayed graft function. With increasing time after transplantation, the incidence of recurrent renal pathology also tended to rise. Nevertheless, the favorable 3- and 4-year graft survival rates observed in this study support the clinical effectiveness and feasibility of using ECDs as a viable strategy to increase the number of kidney transplants.

The authors declare no conflict of interest.

REFERENCES

1. *Gautier SV, Khomyakov SM*. Organ donation and transplantation in the Russian Federation in 2021. 14th Report from the Registry of the Russian Transplant Society. *Russian Journal of Transplantology and Artificial Organs*. 2022; 24 (3): 8–31. doi: 10.15825/1995-1191-2022-3-8-31.
2. *Metzger RA, Delmonico FL, Feng S, Port FK, Wynn JJ, Merion RM*. Expanded criteria donors for kidney transplantation. *Am J Transplant*. 2003; 3 Suppl 4: 114–125. doi: 10.1034/j.1600-6143.3.s4.11.x.
3. *Querard AH, Foucher Y, Combescure C, Dantan E, Larmet D, Lorent M et al.* Comparison of survival outcomes between Expanded Criteria Donor and Standard Criteria Donor kidney transplant recipients: a systematic review and meta-analysis. *Transpl Int*. 2016 Apr; 29 (4): 403–415. doi: 10.1111/tri.12736.
4. *Barreda Monteoliva P, Redondo-Pachón D, Miñambres García E, Rodrigo Calabia E*. Kidney transplant outcome of expanded criteria donors after circulatory death. *Nefrologia (Engl Ed)*. 2022 Mar-Apr; 42 (2): 135–144. doi: 10.1016/j.nefroe.2021.01.005.
5. *Sandes-Freitas TV de*. Expanded donor criteria in kidney transplantation: a suitable option to increase the donor pool in Brazil? *J Bras Nefrol*. 2016 Jul-Sep; 38 (3): 273–274. doi: 10.5935/0101-2800.20160040.
6. *Maggiore U, Oberbauer R, Pascual J, Viklicky O, Dudley C, Budde K et al.* Strategies to increase the donor pool and access to kidney transplantation: an international perspective. *Nephrol Dial Transplant*. 2015 Feb; 30 (2): 217–222. doi: 10.1093/ndt/gfu212.
7. *Schold JD, Hall YN*. Enhancing the expanded criteria donor policy as an intervention to improve kidney allocation: is it actually a “net-zero” model? *Am J Transplant*. 2010 Dec; 10 (12): 2582–2585. doi: 10.1111/j.1600-6143.2010.03320.x.
8. *Hwang JK, Park SC, Kwon KH, Choi BS, Kim JI, Yang CW et al.* Long-term outcomes of kidney transplantation from expanded criteria deceased donors at a single center: comparison with standard criteria deceased donors. *Transplant Proc*. 2014; 46 (2): 431–436. doi: 10.1016/j.transproceed.2013.11.061.
9. *Rouhi AD, Choudhury RA, Hoeltzel GD, Prins K, Yoeli D, Moore HB et al.* Uncontrolled donation after cardiac death kidney transplantation: Opportunity to expand the donor pool? *Am J Surg*. 2023 Jun; 225 (6): 1102–1107. doi: 10.1016/j.amjsurg.2022.12.014.
10. *Gautier SV, Khomyakov SM*. Organ donation and transplantation in the Russian Federation in 2023. 16th Report from the Registry of the Russian Transplant Society. *Russian Journal of Transplantology and Artificial Organs*. 2024; 26 (3): 8–31. doi: 10.15825/1995-1191-2024-3-8-31.
11. Eurotransplant International Foundation [Internet]. URL: https://statistics.eurotransplant.org/ (date of access: 13.06.2025).
12. www.ont.es/Actividad de donación y trasplante España 2023.pdf.
13. *Patel K, Brotherton A, Chaudhry D, Evison F, Nieto T, Dabare D, Sharif A.* All Expanded Criteria Donor Kidneys are Equal But are Some More Equal Than Others? A Population-Cohort Analysis of UK Transplant Registry Data. *Transpl Int*. 2023 Sep 4; 36: 11421. doi: 10.3389/ti.2023.11421.
14. *Aubert O, Kamar N, Vernerey D, Viglietti D, Martinez F, Duong-Van-Huyen JP et al*. Long term outcomes of transplantation using kidneys from expanded criteria donors: prospective, population based cohort study. *BMJ*. 2015 Jul 31; 351: h3557.
15. *Gilbert A, Scott D, Stack M, de Mattos A, Norman D, Rehman S et al.* Long-standing donor diabetes and pathologic findings are associated with shorter allograft survival in recipients of kidney transplants from diabetic donors. *Mod Pathol*. 2022 Jan; 35 (1): 128–134. doi: 10.1038/s41379-021-00927-2.
16. *Ahmad M, Cole EH, Cardella CJ, Cattran DC, Schiff J, Tinckam KJ, Kim SJ.* Impact of deceased donor diabetes mellitus on kidney transplant outcomes: a propensity score-matched study. *Transplantation*. 2009 Jul 27; 88 (2): 251–260. doi: 10.1097/TP.0b013e3181ac68a9.
17. *Kim SM, Ahn S, Min SI, Park D, Park T, Min SK et al.* Cold ischemic time is critical in outcomes of expanded criteria donor renal transplantation. *Clin Transplant*. 2013 Jan-Feb; 27 (1): 132–139. doi: 10.1111/ctr.12034.
18. *Johnston TD, Thacker LR, Jeon H, Lucas BA, Ranjan D*. Sensitivity of expanded-criteria donor kidneys to cold ischaemia time. *Clin Transplant*. 2004; 18 Suppl 12: 28–32. doi: 10.1111/j.1399-0012.2004.00214.x.
19. *Hall IE, Akalin E, Bromberg JS, Doshi MD, Greene T, Harhay MN et al.* Deceased-donor acute kidney injury is not associated with kidney allograft failure. *Kidney Int*. 2019 Jan; 95 (1): 199–209. doi: 10.1016/j.kint.2018.08.047.
20. *Van der Windt DJ, Mehta R, Jorgensen DR, Bou-Samra P, Hariharan S, Randhawa PS et al.* Donor acute kidney injury and its effect on 1-year post-transplant kidney allograft fibrosis. *Clin Transplant*. 2020 Feb; 34 (2): e13770. doi: 10.1111/ctr.13770.

21. *Pei J, Cho Y, See YP, Pascoe EM, Viecelli AK, Francis RS et al.* Impact of deceased donor with acute kidney injury on subsequent kidney transplant outcomes – an ANZDATA registry analysis. *PloS One*. 2021 Mar 25; 16 (3): e0249000. doi: 10.1371/journal.pone.0249000.
22. *Allen PJ, Chadban SJ, Craig JC, Lim WH, Allen RDM, Clayton PA et al.* Recurrent glomerulonephritis after kidney transplantation: risk factors and allograft outcomes. *Kidney Int*. 2017 Aug; 92 (2): 461–469. doi: 10.1016/j.kint.2017.03.015.
23. *Stolyarevich ES, Zhilinskaya TR, Artyukhina LYu, Kim IG, Zaydenov VA, Tomilina NA*. Morphological structure of late renal graft dysfunction and its effect for long-term results. *Russian Journal of Transplantology and Artificial Organs*. 2018; 20 (1): 45–54. [In Russ, English abstract]. doi: 10.15825/1995-1191-2018-1-45-54.
24. USRDS [Internet]. Annual Data Report. Available at: https://usrds-adr.niddk.nih.gov/. Accessed June 23, 2025.
25. *Ko KJ, Kim YH, Kwon KH, Kim MH, Jun KW, Hwang JK et al.* Kidney Transplantation Using Expanded-Criteria Deceased Donors: A Comparison With Ideal Deceased Donors and Non-Expanded-Criteria Deceased Donors. *Transplant Proc*. 2018 Dec; 50 (10): 3222–3227. doi: 10.1016/j.transproceed.2018.05.028.
26. *Fang X, Wang Y, Liu R, Zhu C, Wu C, He F et al.* Long-term outcomes of kidney transplantation from expanded criteria donors with Chinese novel donation policy: donation after citizens' death. *BMC Nephrol*. 2022 Oct 3; 23 (1): 325. doi: 10.1186/s12882-022-02944-y.
27. *Foroutan F, Friesen EL, Clark KE, Motaghi S, Zyla R, Lee Y et al.* Risk Factors for 1-Year Graft Loss After Kidney Transplantation. *Clin J Am Soc Nephrol*. 2019 Nov 7; 14 (11): 1642–1650. doi: 10.2215/CJN.05560519.
28. *Salguero J, Chamorro L, Gomez-Gomez E, Robles JE, Campos JP*. Midterm Outcomes of Kidney Transplantation from Expanded Criteria Donors After Circulatory Death: A Single-Center Retrospective Cohort Study. *Exp Clin Transplant*. 2023 Jun; 21 (6): 481–486. doi: 10.6002/ect.2023.0076.
29. *Hellemans R, Kramer A, De Meester J, Collart F, Kuypers D, Jadoul M et al*. Does kidney transplantation with a standard or expanded criteria donor improve patient survival? Results from a Belgian cohort. *Nephrol Dial Transplant.* 2021 Apr 26; 36 (5): 918–926. doi: 10.1093/ndt/gfab024.

The article was submitted to the journal on 22.08.2025

DOI: 10.15825/1995-1191-2025-4-158-172

DYSLIPIDEMIA AND LIPID-LOWERING THERAPY IN PATIENTS ON RENAL REPLACEMENT THERAPY: A LITERATURE REVIEW

A.V. Samburov, N.A. Khaibulina, T.L. Kulik, Sh.R. Galeev

Volzhsky Branch of Shumakov National Medical Research Center of Transplantology and Artificial Organs, Volzhsky, Russian Federation

Dyslipidemia in patients with chronic kidney disease (CKD), particularly those on renal replacement therapy (RRT), is a major risk factor for cardiovascular complications. The pathogenesis of lipid metabolism disorders in this population is multifactorial and influenced by the underlying kidney disease, the specific characteristics of RRT, and, in transplant recipients, the effects of immunosuppressive therapy. Despite the high prevalence and clinical significance of dyslipidemia in CKD, therapeutic strategies for its correction remain insufficiently studied. This review analyzes current pharmacologic approaches to the management of dyslipidemia and evaluates the potential for their application in patients receiving RRT. Literature search was conducted using electronic databases Medline/PubMed (https://pubmed.ncbi.nlm.nih.gov) and eLIBRARY/Russian Science Citation Index (https://www.elibrary.ru).

Keywords: dyslipidemia, chronic kidney disease, renal replacement therapy, hemodialysis, peritoneal dialysis, kidney transplantation.

INTRODUCTION

Patients with chronic kidney disease (CKD) are at a significantly increased risk of developing cardiovascular complications. The onset and progression of cardiovascular disease in this population are driven by A variety of factors, including dyslipidemia, hyperhomocysteinemia, chronic inflammation, oxidative stress, disturbances in calcium–phosphate metabolism, and endothelial dysfunction [1]. Evidence indicates that CKD progression is accompanied by a progressive deterioration of the lipid profile. The pathogenesis of dyslipidemia in CKD is complex and multifactorial, involving alterations in lipoprotein metabolism, oxidative stress, inflammatory processes, and declining renal function [2].

Among patients with CKD, those receiving renal replacement therapy (RRT) represent a subgroup at particularly high cardiovascular risk – the incidence of myocardial infarction in this cohort is approximately 20 times higher than in the general population. Data from routine coronary angiography in Japan revealed that 60% of patients on maintenance hemodialysis (HD) had asymptomatic stenosis of at least one coronary artery [3]. Thus, patients receiving RRT are more likely to have pronounced atherosclerotic changes. Importantly, dyslipidemia is not the sole mechanism underlying the progression of atherosclerosis in individuals with end-stage renal disease. These patients also possess unique metabolic and physiological characteristics that complicate the management and correction of dyslipidemia [4].

Numerous studies have demonstrated a clear association between serum cholesterol (SC) levels and the risk of cardiovascular events. In particular, a multifactorial risk study showed a progressive increase in mortality from coronary heart disease (CHD) with rising SC levels, beginning at 5.2 mmol/L; at 7.8 mmol/L, the risk of CHD-related mortality increased fourfold [5]. Data from the Framingham Heart Study further confirmed a direct correlation between total SC levels and CHD risk. Specifically, individuals with total SC levels of 7.8 mmol/L had approximately twice the risk of developing CHD compared with those with levels around 5.2 mmol/L [6].

Subsequent meta-analyses of the Framingham data reinforced the direct relationship between low-density lipoprotein (LDL) cholesterol levels and the incidence of CHD [7]. According to current clinical guidelines for the management of lipid disorders in very high-risk patients, the target LDL cholesterol level should be below 1.4 mmol/L, with at least a 50% reduction from baseline values. These guidelines also emphasize the pathogenic role of elevated lipoprotein(a) [Lp(a)] levels in increasing the risk of cardiovascular events [8].

Current approaches to lipid-lowering therapy (LLT) in patients undergoing RRT include the use of statins, ezetimibe, and proprotein convertase subtilisin/kexin type 9 (PCSK9) inhibitors, as well as other methods aimed at reducing serum cholesterol and lipoprotein(a) [Lp(a)] levels to lower the risk of cardiovascular complications.

Corresponding author: Andrey Samburov. Address: 86/1, Karbysheva str., Volgograd, 404133, Russian Federation. Phone: (8443) 21-25-15. E-mail: andru.samburov@gmail.com

Statins remain the cornerstone of LLT and can be prescribed to patients in the early stages of CKD. However, their use in individuals on RRT, particularly those on HD, requires caution and individualized risk assessment, since high-dose statin therapy in this group is often associated with an increased incidence of adverse effects. Ezetimibe may be used in combination with statins in patients on RRT, particularly when statin monotherapy fails to achieve target lipid levels.

PCSK9 inhibitors are considered an appropriate therapeutic option for RRT patients with persistently elevated LDL cholesterol levels despite maximally tolerated statin and ezetimibe therapy. These drugs may also be considered in patients with markedly elevated LDL levels, particularly when other interventions prove ineffective [1].

FEATURES OF LIPID METABOLISM IN PATIENTS WITH CKD RECEIVING RRT

The metabolism of endogenous and exogenous lipoproteins in healthy individuals (Fig. 1, Fig. 2) differs significantly from that in patients with CKD. These differences are primarily associated with a range of pathological factors caused by CKD.

IMPAIRED CLEARANCE OF TRIGLYCERIDE-RICH LIPOPROTEINS

Patients with CKD exhibit a reduced fractional catabolic rate of triglyceride (TG)-rich lipoproteins, including very low-density lipoproteins (VLDL), their subfractions VLDL1 and VLDL2, as well as intermediate-density lipoproteins (IDL) and apolipoprotein B-100 (apoB-100). This indicates impaired clearance mechanisms, resulting in the accumulation of these particles in plasma. In contrast, the synthetic rate of VLDL, IDL, and apoB-100 in CKD patients is comparable to that of healthy individuals, indicating that the primary disturbance lies in delayed degradation rather than excessive production of lipoproteins.

Apolipoprotein C-III (apoC-III) plays a key role in lipid metabolism disorders in patients with CKD. Normally, the kidneys filter and excrete apoC-III; however,

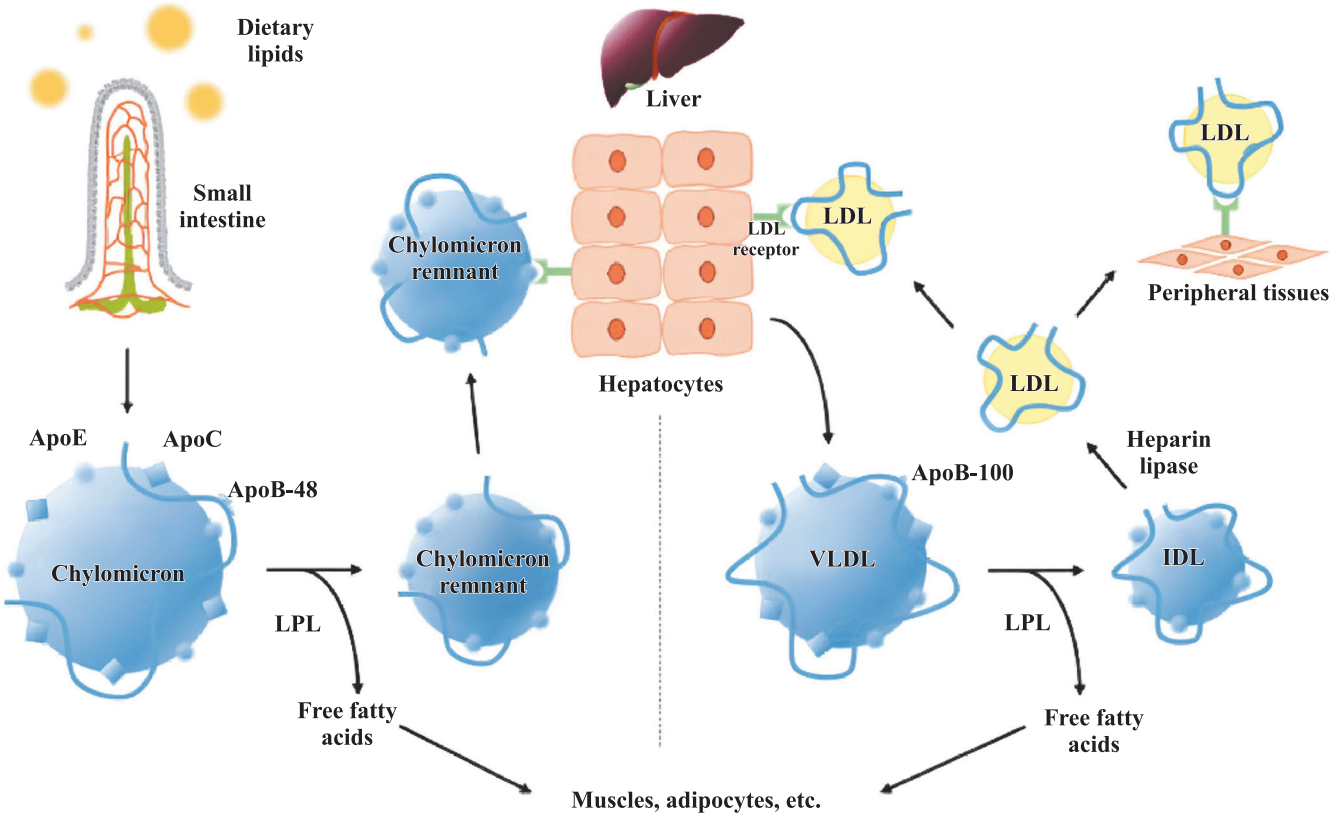

Fig. 1. Metabolic pathway of exogenous and endogenous lipoproteins. Dietary lipids are absorbed in the small intestine, where they are assembled into chylomicrons containing apolipoproteins C (apoC), E (apoE), and B-48 (apoB-48). These chylomicrons enter the bloodstream and are hydrolyzed by lipoprotein lipase (LPL) to release free fatty acids (FFAs), and shrink to chylomicron remnants. FFAs are taken up by peripheral tissues – such as skeletal muscle and adipose tissue – for energy or stored as fat. Chylomicron remnants are subsequently absorbed by the liver via low-density lipoprotein (LDL) receptors. Within hepatocytes, very low-density lipoproteins (VLDL), which also contain apolipoprotein B-100. VLDL is broken down by LPL in the blood into FFAs and intermediate-density lipoproteins (IDL). IDL is then converted by hepatic lipase into LDL, which transports cholesterol to peripheral tissues. Adapted from: Suh SH, Kim SW. Dyslipidemia in Patients with Chronic Kidney Disease: An Updated Overview

renal impairment leads to its systemic accumulation. In addition, uremic inflammation enhances hepatic synthesis of apoC-III through cytokine-mediated pathways, particularly via interleukin-6 (IL-6) and tumor necrosis factor-α (TNF-α). Elevated plasma apoC-III levels are strongly correlated with slowed catabolism of VLDL and its subfractions, as apoC-III inhibits the activity of lipoprotein lipase (LPL) and hepatic lipase.

LPL is a key enzyme responsible for hydrolyzing triglycerides (TG) contained in chylomicrons and VLDL into free fatty acids and glycerol, which are subsequently utilized for energy production or stored in adipose tissue (Fig. 3). ApoC-III not only suppresses LPL activity but also interferes with apoE-mediated receptor binding, thereby reducing hepatic clearance of remnant particles. CKD patients also have elevated plasma levels of apolipoprotein B-48, a marker of chylomicrons and their remnants, reflecting impaired intestinal lipoprotein metabolism [9].

Changes in LDL receptor function play a major role in impaired catabolism of LDL particles in patients with CKD. Expression of LDL receptors is significantly reduced in CKD, a phenomenon largely associated with the chronic inflammatory state characteristic of this

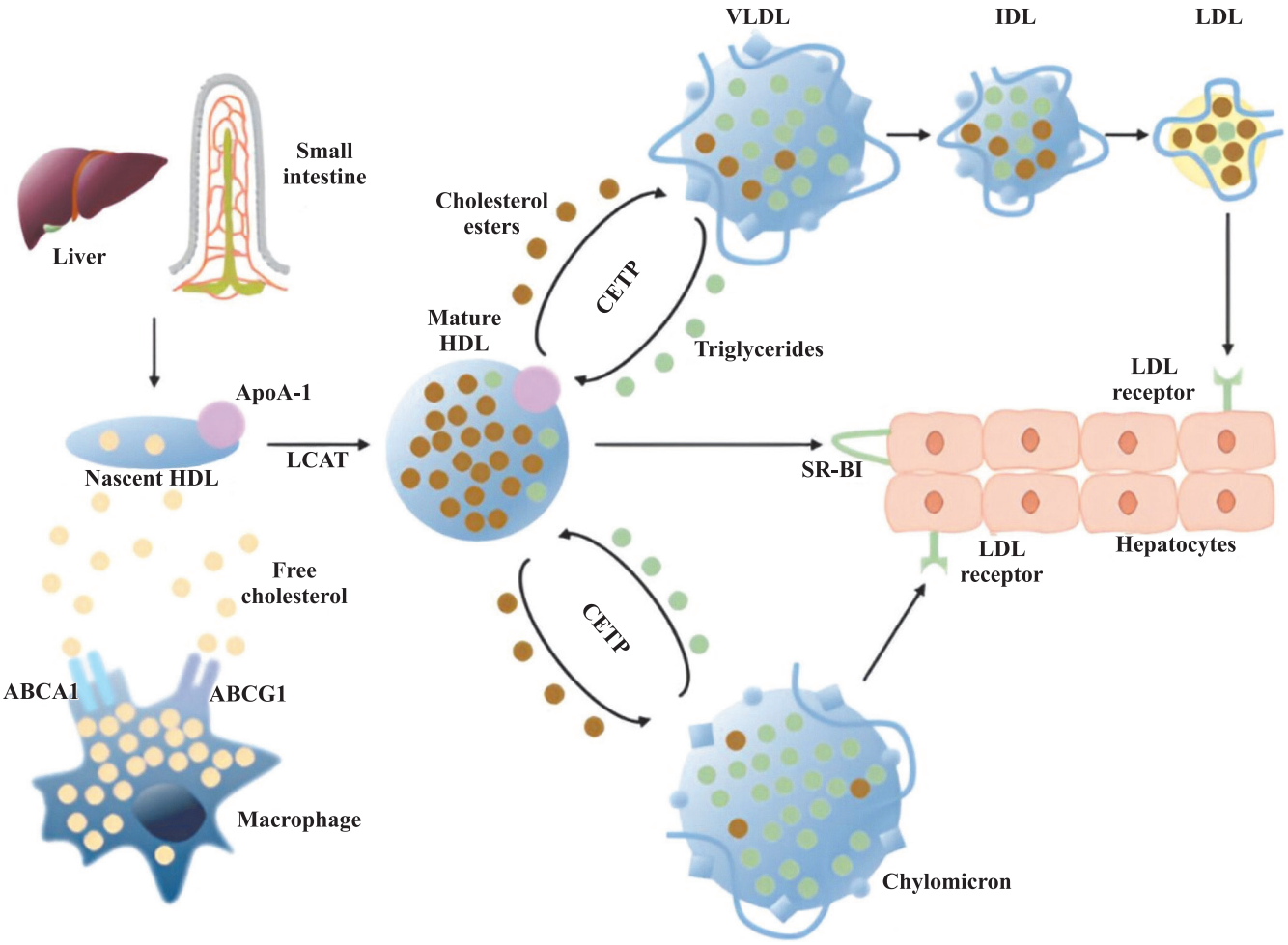

Fig. 2. High-density lipoprotein (HDL) metabolism in reverse cholesterol transport. Apolipoprotein A-I (apoA-I) is secreted by liver and intestine. It interacts with the ATP-binding cassette subfamily member 1 (ABCA1) transporter, which facilitates the transfer of free cholesterol from macrophages to apoA-I, forming nascent, disc-shaped HDL particles. These nascent HDL particles subsequently interact with other transporters, such as ABCG1, to acquire additional free cholesterol. Under the action of lecithin-cholesterol acyltransferase (LCAT), free cholesterol on the HDL surface is esterified into cholesteryl ester (CE) and incorporated into the particle's hydrophobic core, transforming immature HDL into mature, spherical HDL particles rich in CE. Cholesteryl ester transfer protein (CETP) mediates the exchange of CEs from mature HDL for triglycerides (TG) from atherogenic lipoproteins such as very low-density lipoproteins (VLDL), resulting in the formation of low-density lipoproteins (LDL). TG-enriched HDL becomes less mature and more prone to catabolism. LDL receptors on hepatocytes capture LDL particles – enriched in cholesterol after CETP-mediated exchange – providing the primary "direct" route of cholesterol delivery to the liver. In parallel, the scavenger receptor class B type I (SR-BI) receptor on hepatocytes selectively uptakes CEs directly from mature HDL without degrading the entire particle. This process constitutes the central mechanism of reverse cholesterol transport, through which cholesterol collected by HDL from peripheral tissues (notably macrophages) is returned to the liver. IDL, intermediate-density lipoprotein. Adapted from: Suh SH, Kim SW. Dyslipidemia in Patients with Chronic Kidney Disease: An Updated Overview

condition. Uremic toxins – notably indoxyl sulfate and para-cresol – have been shown to suppress LDL receptor expression through activation of the NF-κB and Smad protein signaling pathways. This molecular cascade contributes to renal fibrosis, reduced receptor-mediated uptake of LDL, and ultimately impaired cholesterol clearance [10].

In addition, oxidative stress increases in CKD, leading to oxidation of apolipoproteins (e.g., apoB-100 found in LDL). Carbamylation of apolipoproteins (e.g., ApoB-100 and ApoA-I) is another important process that can impair LDL receptor function and exacerbate dyslipidemia. Oxidation and carbamylation of ApoB-100 can lead to a decrease in LDL receptor activity, which reduces their ability to bind and utilize LDL. In addition, oxidized LDL can be absorbed by macrophages, contributing to the development of atherosclerosis [11].

Patients with CKD are more likely to have small dense LDL (sdLDL), which has a lower affinity for LDL receptors compared to large LDL. This reduces their utilization by cells and increases the duration of their circulation in the blood. In turn, impaired kidney function affects the balance of proteins and electrolytes, which can alter the concentration of apolipoproteins (especially apoB and apoE) necessary for LDL interaction with receptors. This leads to a slowdown in the removal of LDL from the blood [12].

DYSFUNCTION OF HIGH-DENSITY LIPOPROTEINS (HDL) AND LOSS OF THEIR ANTIATHEROGENIC PROPERTIES

Patients with CKD often have reduced plasma levels of HDL, resulting from both impaired synthesis and accelerated catabolism. The decrease in HDL cholesterol levels is paralleled by decreased levels of its major apolipoproteins, ApoA-I and ApoA-II. Notably, the reduction in ApoA-I and ApoA-II levels correlates with the severity of renal dysfunction. Accumulation of uremic toxins in CKD suppresses hepatic ApoA-I synthesis, leading to the formation of dysfunctional HDL particles that have

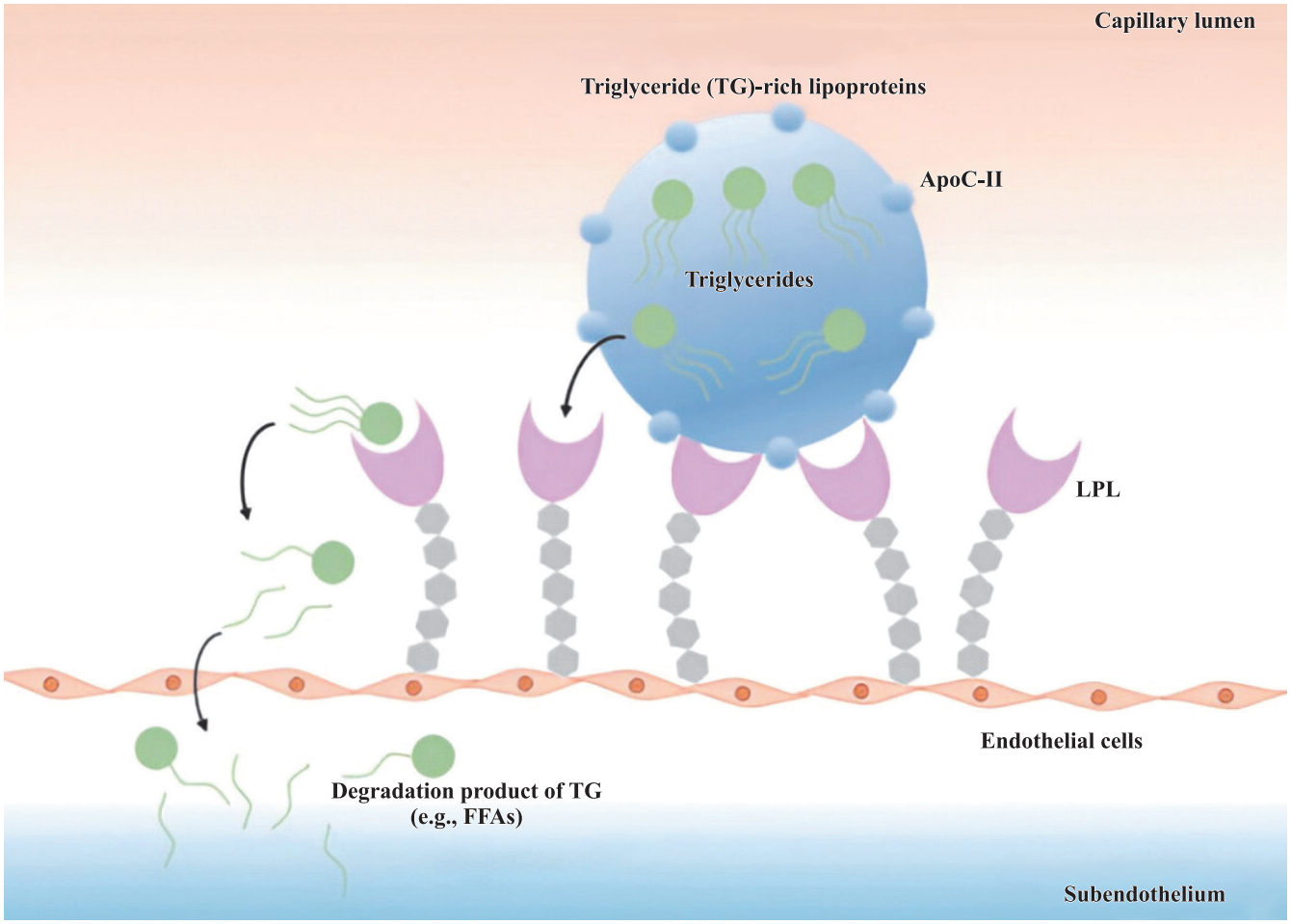

Fig. 3. Mechanism of triglyceride lipolysis. Triglyceride (TG)-rich lipoproteins (i.e., chylomicron and very low-density lipoprotein [VLDL]), enter the capillary lumen. Apolipoprotein C-II (apoC-II) on the surface of these particles activates lipoprotein lipase (LPL), an enzyme anchored on the surface of endothelial cells. LPL degrades TG to release free fatty acids (FFAs) and other degradation products. The liberated FFAs then diffuse across the endothelium into the subendothelial space, where they can be used by tissues for energy needs or stored. Adapted from: Suh SH, Kim SW. Dyslipidemia in Patients with Chronic Kidney Disease: An Updated Overview

diminished capacity for reverse cholesterol transport (RCT) [13].

Under the combined effects of oxidative stress, uremic toxins, and chronic inflammation, the activity of the ATP-binding cassette transporters ABCA1 and ABCG1 – critical mediators of cholesterol efflux from macrophages – is reduced. Impaired function of these transporters limits the removal of cholesterol and disrupts HDL maturation, resulting in an accumulation of immature, discoidal HDL particles. The decreased cholesterol efflux from macrophages promotes foam cell formation within the vascular intima, thereby accelerating atherosclerosis [12].

In addition, HDL lose their ability to remove cholesterol from peripheral tissues due to reduced expression of the scavenger receptor class B type I (SR-BI) in the liver. SR-BI mediates the selective uptake of cholesterol from HDL, and its deficiency results in cholesterol accumulation within the vascular wall, further promoting the formation of atherosclerotic plaques [14].

Oxidative stress, a hallmark of CKD, contributes to the generation of reactive oxygen species that oxidize HDL-associated lipids and proteins. This, along with elevated TG levels, a consequence of decreased LPL activity, these changes substantially impair the cholesterol-transporting capacity of HDL. Oxidized HDL not only loses its antiatherogenic and antioxidative functions, but may also acquire proinflammatory and proatherogenic properties. Moreover, CKD is associated with accelerated clearance of HDL particles from circulation due to structural and functional impairements. This reduces the circulation time of HDL in the blood and decreases its overall effectiveness in maintaining lipid metabolism and protecting blood vessels [15].

Patients with CKD also exhibit reduced plasma levels of lecithin-cholesterol acyltransferase (LCAT), an enzyme that plays a central role in lipoprotein metabolism by catalyzing the esterification of free cholesterol. This process is essential for the maturation and stabilization of HDL and for maintaining reverse cholesterol transport. The decrease in LCAT activity in CKD is associated with reduced expression of the LCAT gene in the liver, the principal site of its synthesis [16].

Deficiency or dysfunction of LCAT leads to accumulation of free cholesterol within HDL particles, impairing the formation of cholesterol esters. Consequently, abnormal lipid species, including non-esterified cholesterol and phospholipids, accumulate, disrupting the structural integrity and functional capacity of HDL [17].

Moreover, the accumulation of uremic toxins such as indoxyl sulfate and para-cresol enhances the activity of cholesteryl ester transfer protein (CETP). CETP facilitates the transfer of cholesterol esters from HDL to LDL and triglyceride-rich lipoproteins (e.g., VLDL and VLDL remnants). This process increases the concentration and atherogenic potential of LDL, while simultaneously reducing the size and functional efficiency of HDL, thereby compromising reverse cholesterol transport (Fig. 4) [18].

EFFECT OF CKD ON LIPOPROTEIN (A) [LP(A)] LEVELS

Lp(a) is a complex plasma lipoprotein structurally similar to LDL, distinguished by the presence of apolipoprotein (a) [apo(a)], which is covalently linked to apoB-100 via a disulfide bond. Apo(a) contains repeating domains similar to plasminogen, a protein involved in fibrinolysis. This structural homology allows Lp(a) to compete with plasminogen for binding sites, thereby inhibiting fibrinolysis and increasing thrombogenic potential. Lp(a) is recognized as an independent risk factor for cardiovascular disease (CVD), including atherosclerosis, myocardial infarction, and ischemic stroke [19].

The plasma concentration of Lp(a) is largely determined by the rate of its synthesis in the liver and catabolism, the latter of which appears to involve the kidneys, although this mechanism is not yet fully understood. Elevated Lp(a) levels are frequently observed with declining glomerular filtration rate (GFR), even in the early stages of renal dysfunction [20]. Studies have shown that Lp(a) levels rise with moderate decrease in GFR (60–90 mL/min/1.73 m^2), independent of albuminuria.

A large multinational cohort study demonstrated a weak positive association between reduced GFR and elevated Lp(a) levels, particularly among non-Hispanic blacks, suggesting potential ethnic variability in this relationship. The authors noted that differences in apo(a) isoform size among populations could partially account for the observed heterogeneity [21].

A detailed study involving 227 white patients without nephrotic syndrome and with varying degrees of renal dysfunction showed that Lp(a) levels were significantly higher in patients with CKD compared with controls without renal impairment. Moreover, an inverse correlation was observed between renal function and plasma Lp(a) levels – the highest concentrations were detected in patients with the most severe renal dysfunction, irrespective of the underlying kidney disease. Interestingly, this relationship was evident only in the subgroup with large apo(a) isoforms and without nephrotic syndrome, suggesting that isoform size may modulate the effect of renal impairment on Lp(a) metabolism [22].

In patients with CKD, the elevation of Lp(a) is likely related to an acquired impairment of its catabolism. This hypothesis is supported by an *in vivo* metabolic study in hemodialysis patients, which demonstrated a significant reduction in the fractional catabolic rate of both apo(a) and apoB, the major protein components of Lp(a). Consequently, prolonged circulatory residence time of Lp(a) leads to its accumulation in plasma [22].

THE ROLE OF CKD IN THE DEVELOPMENT OF INSULIN RESISTANCE AND ITS EFFECT ON LIPID PROFILE

CKD disrupts the elimination of metabolic by-products and toxins, creating a uremic environment that impairs tissue sensitivity to insulin. Uremic toxins such as indoxyl sulfate and para-cresol not only exacerbate insulin resistance, but also directly damage vascular endothelium, thereby exacerbating atherosclerosis in the context of existing dyslipidemia. Furthermore, chronic inflammation and oxidative stress, both hallmarks of CKD, inhibit insulin signaling pathways and disturb the regulation of lipid metabolism [23].

Insulin resistance, being a key link in metabolic disorders, has a significant impact on the development of dyslipidemia among CKD patients, particularly those on RRT. Impaired cellular responsiveness to insulin leads to compensatory hyperinsulinemia, increased lipolysis, and elevated plasma free fatty acid (FFA) levels. These FFAs are taken up by the liver, where they stimulate triglyceride (TG) and VLDL synthesis. In CKD, this mechanism is further aggravated by reduced LPL activity. His contributes to the accumulation of atherogenic particles and the formation of a pattern characteristic of dyslipidemia: high triglyceride levels, low HDL levels, and an increase in the number of LDL particles [24].

FEATURES OF THE MECHANISMS OF DYSLIPIDEMIA DEVELOPMENT IN PATIENTS ON HEMODIALYSIS

During maintenance HD sessions, heparin is routinely administered to prevent blood clotting in the extracorporeal circuit. Although heparin transiently activates LPL, repeated HD procedures eventually lead to LPL depletion, thereby reducing its enzymatic activity between dialysis sessions. This disrupts triglyceride catabolism, resulting in hypertriglyceridemia and elevated levels of VLDL and chylomicrons [25].

During HD procedures, low molecular weight substances are lost through the semipermeable dialysis mem-

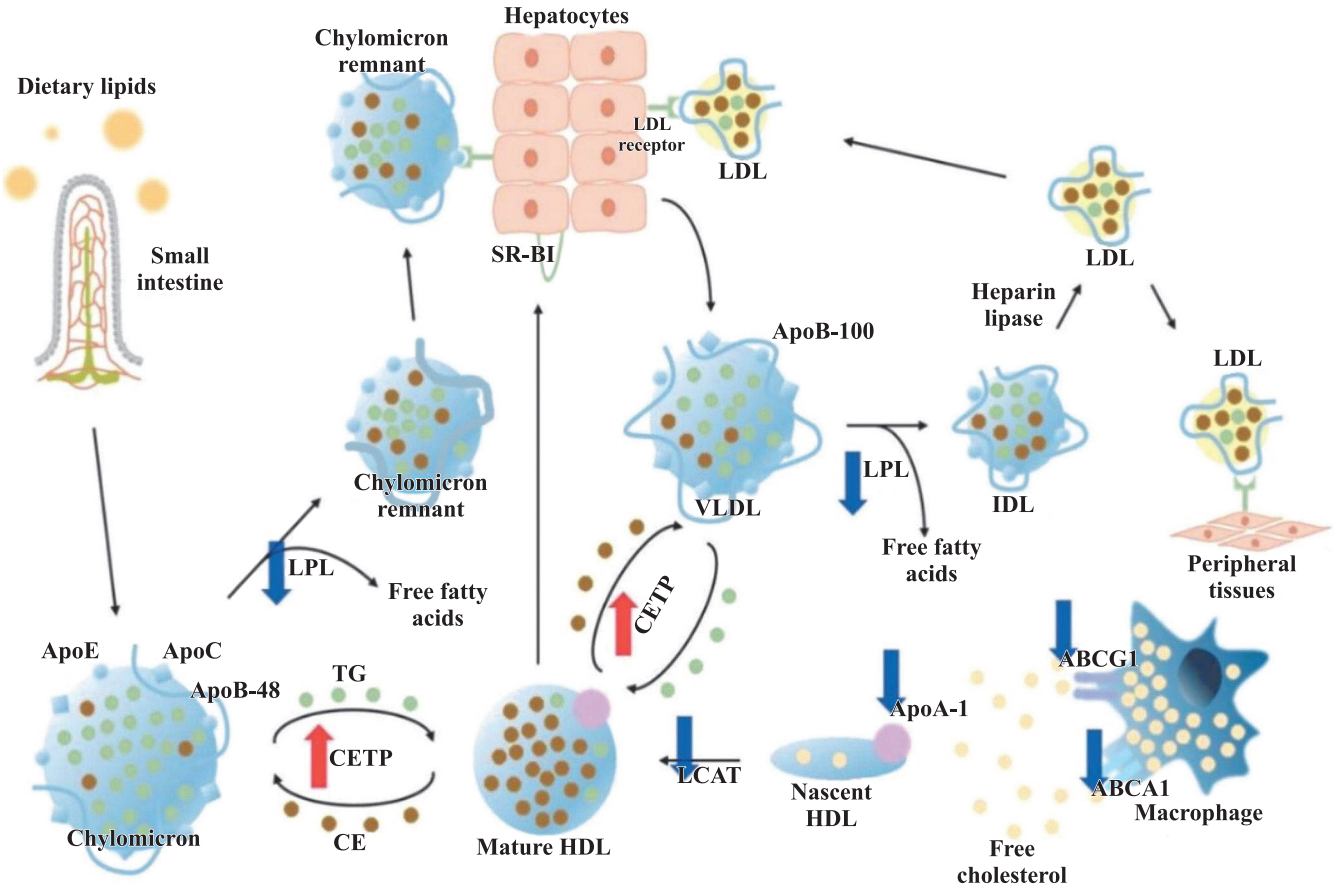

Fig. 4. Schematic representation of defective lipoprotein metabolism in chronic kidney disease (CKD). In CKD, reduced lipoprotein lipase (LPL) activity results in the accumulation of triglyceride (TG)-rich lipoproteins. Simultaneously, decreased synthesis of apolipoprotein A-I (ApoA-I) and reduced activity of lecithin-cholesterol acyltransferase (LCAT), as well as the cholesterol transporters ATP-binding cassette subfamily member 1 (ABCA1) and ATP-binding cassette subfamily G member 1 (ABCG1), lead to the formation of dysfunctional high-density lipoprotein (HDL) particles incapable of effective reverse cholesterol transport. Increased activity of cholesterol ester transfer protein (CETP) raises LDL levels and enhances their proatherogenic potential. CE, cholesteryl ester; IDL, intermediate-density lipoprotein. Adapted from: Suh SH, Kim SW. Dyslipidemia in Patients with Chronic Kidney Disease: An Updated Overview

brane. Carnitine, which is necessary for the transport of fatty acids into the mitochondria, is removed during HD. Carnitine deficiency leads to impaired beta-oxidation of fatty acids fatty acid oxidation and accumulation of triglycerides (TG) and FFAs in plasma [26].

Also, scheduled hemodialysis leads to increased oxidative stress due to a bunch of factors. One of them is blood contact with membranes, which activates leukocytes, platelets, and the complement system. Contact with the dialyser membrane increases the activity of neutrophils and monocytes, which increases the production of pro-inflammatory cytokines (IL-6, TNF-α) and releases reactive oxygen species (ROS) via NADPH oxidase and myeloperoxidase. Moreover, the use of bioincompatible membranes (e.g., cellulose-based) can stimulate the complement cascade (C3a, C5a), further amplifying inflammation and ROS production. Concurrently, there is a loss of antioxidants such as vitamins C and E and glutathione, while recurrent ischemia–reperfusion cycles inherent to HD sessions intensify ROS production [27].

Dyslipidemia is more common in patients undergoing peritoneal dialysis (PD) than in those on HD. This is largely due to the specific features of PD therapy, which relies on dialysates with high glucose content serving as an osmotic agent. Continuous exposure to glucose during PD leads to its systemic absorption, resulting in metabolic disorders. Excess glucose absorption stimulates hepatic VLDL synthesis, promoting hypertriglyceridemia. Furthermore, prolonged hyperglycemia contributes to the development of insulin resistance, which aggravates existing lipid imbalance [28].

It is also important to emphasize that patients with end-stage chronic kidney disease receiving HD almost always have a significant increase in Lp(a) levels, averaging 5–10 times higher than in patients with mild or moderate renal impairment [29]. Interestingly, among HD patients, the degree of Lp(a) elevation correlates with the size of apo(a) isoforms: a significant increase in plasma Lp(a) levels compared with healthy controls is observed only in individuals with large apo(a) isoforms. In contrast, patients on PD show high Lp(a) levels regardless of apo(a) isoform size [22].

DYSLIPIDEMIA IN KIDNEY TRANSPLANT RECIPIENTS

Dyslipidemia in kidney transplant recipients is an important clinical problem that requires special attention. It occurs in approximately 60% of patients. This metabolic disorder substantially increases the risk of cardiovascular disease, which remains the leading cause of mortality in this population. Moreover, lipid metabolism disorders can negatively affect allograft function, accelerating the progression of transplant nephropathy [30].

Following kidney transplantation, plasma Lp(a) levels typically decrease, reflecting the restored metabolic and catabolic role of the kidney in Lp(a) clearance. This supports the concept that changes in Lp(a) in CKD primarily results from loss of renal tissue function [22].

The primary etiological factor underlying post-transplant dyslipidemia in such patients is immunosuppressive therapy. Long-term use of corticosteroids (e.g., prednisolone) disrupts lipid homeostasis. Glucocorticoids enhance insulin resistance, which promotes lipolysis in adipose tissue and increases the plasma FFA levels. This stimulates the synthesis of TG and VLDL in the liver. In addition, corticosteroids suppress LPL activity, further exacerbating hypertriglyceridemia [31].

Calcineurin inhibitors (CNIs) – cyclosporine A (CsA) and tacrolimus (Tac) – play a key role in preventing transplant rejection; however, their impact on lipid metabolism remains clinically significant. Studies have shown that CsA exerts a dose-dependent effect on lipid parameters, increasing total cholesterol, triglycerides (TG), and LDL levels. Moreover, it tends to reduce HDL levels, likely due to suppression of apolipoprotein A-I synthesis. CsA also promotes LDL oxidation, converting these particles into a more atherogenic form.

Although Tac belongs to the same class of CNIs, it exerts a comparatively milder influence on the lipid profile. It is less frequently associated with hypercholesterolemia and reduces HDL to a lesser extent compared to CsA. Nonetheless, Tac may elevate TG levels in certain cases, particularly when administered concurrently with corticosteroids. Evidence regarding its effect on LDL oxidation remains inconclusive [32].

mTOR inhibitors, such as rapamycin and its derivatives (rapalogs), exert complex effects on lipid metabolism that often lead to dyslipidemia. These effects are primarily mediated through their influence on mTOR complexes (mTORC1 and mTORC2), which are central regulators of lipid metabolism. Inhibition of mTORC1 reduces lipogenesis and suppresses adipogenesis by limiting adipocyte proliferation, thereby decreasing adipose tissue accumulation. However, despite reduction in lipogenesis, mTORC1 inhibition enhances lipolysis by activating lipases such as hormone-sensitive lipase and adiponutrin triglyceride lipase, and by stimulating lipophagy (degradation of lipid droplets). Consequently, FFA release and plasma lipid levels increase.

Another important consequence of mTORC1 inhibition is the downregulation of hepatic LDL receptor expression, resulting in impaired LDL clearance and development of hypercholesterolemia [33]. Although the role of mTORC2 in lipid metabolism is less well defined, it is known to regulate lipogenesis and lipolysis through activation of protein kinase AKT1. Chronic use of rapalogs may also inhibit mTORC2, further aggravating dyslipidemia.

Despite their adverse effects on lipid profile, mTOR inhibitors exhibit notable anti-atherosclerotic properties. They reduce macrophage accumulation within atheros-

clerotic plaques, promote autophagy, and enhance cholesterol efflux from macrophages, thereby reducing foam cell formation. These mechanisms may partly offset the negative impact of dyslipidemia on progression of atherosclerosis [34].

METHODS OF PHARMACOLOGICAL MANAGEMENT FOR DYSLIPIDEMIA AND ITS POTENTIAL USE IN PATIENTS ON RENAL REPLACEMENT THERAPY

HMG-CoA reductase inhibitors (statins)

Statins play a central role in the pharmacological management of dyslipidemia owing to their proven efficacy in reducing cardiovascular risk. They are considered the first-line drugs for the treatment of lipid disorders. Their primary mechanism of action involves the competitive inhibition of 3-hydroxy-3-methylglutaryl coenzyme A (HMG-CoA) reductase, the key rate-limiting enzyme in cholesterol synthesis in the liver. This leads to reduced intracellular cholesterol levels in hepatocytes, which in turn triggers a compensatory upregulation of LDL receptors on the surface of hepatocytes. This process enhances the clearance of atherogenic lipoproteins from circulation, particularly the small, dense LDL particles, which are the most atherogenic.

Beyond their lipid-lowering effect, statins have pleiotropic effects. These include attenuation of vascular inflammation, improvement of endothelial function, stabilization of atherosclerotic plaques, and reduction of blood thrombogenicity. Statins demonstrate dose-dependent efficacy: low doses typically reduce LDL cholesterol levels by 20–30%, whereas maximal doses can achieve reductions of up to 50–55%.

However, the use of statins requires careful monitoring due to potential adverse effects. The most clinically relevant are myopathies, which occur in approximately 0.1–0.5% of patients, and elevations in hepatic transaminases, observed in about 2–3% of cases. The risk of these complications increases when statins are co-administered with fibrates, macrolide antibiotics, or antiarrhythmic drugs metabolized via the CYP3A4 enzymatic pathway [35].

The use of statins in dialysis patients remains one of the most debated topics in modern nephrology and cardiology. It is important to recognize that dyslipidemia in this population has distinctive characteristics: normal or even reduced LDL cholesterol levels are frequently observed in conjunction with elevated triglycerides, oxidized lipoproteins, and lipoprotein (a). This atypical lipid profile complicates the use of standard therapy.

However, the key question – whether statins effectively reduce cardiovascular events in dialysis patients – remains unresolved. Large-scale randomized clinical trials, including AURORA and 4D, have shown that although statins modestly lowered LDL cholesterol levels, it did not significantly reduce overall mortality among hemodialysis patients. Nonetheless, subgroup analyses have suggested that certain patients, particularly those with diabetes mellitus or severe hypercholesterolemia (LDL-C >3.76 mmol/L), may benefit from statin therapy with agents such as rosuvastatin or atorvastatin, which were associated with a reduced incidence of myocardial infarction.

It is essential to consider dose adjustments in dialysis patients due to their increased risk of adverse effects. The Kidney Disease: Improving Global Outcomes (KDIGO) working group does not recommend initiating statin therapy in patients on dialysis, unless treatment had been started prior to the initiation of the dialysis [36].

The use of statins in kidney transplant (KT) recipients presents a complex clinical challenge that requires careful consideration of both efficacy and safety. This patient population is classified as high cardiovascular risk, and their dyslipidemia has a distinct profile, largely influenced by immunosuppressive therapy. Traditional immunosuppressants – CNIs (cyclosporine, tacrolimus) and mTOR inhibitors (everolimus, sirolimus) – interfere with statin metabolism, thereby increasing the risk of side effects [37].

According to the KDIGO guidelines, statins are recommended as first-line therapy for the management of dyslipidemia in KT recipients. However, this recommendation is rated as “weak” [36].

Cholesterol absorption inhibitor

Currently, the only drug used in this group is ezetimibe. Unlike statins, ezetimibe acts by selectively blocking the Niemann–Pick C1-like 1 (NPC1L1) transporter protein in the small intestine, thereby inhibiting intestinal cholesterol absorption. This mechanism results in approximately a 54% reduction in hepatic cholesterol influx, leading to a compensatory increase in cholesterol synthesis and a 22.3% reduction in LDL cholesterol levels [38]. When used in combination with statins, ezetimibe produces additive lipid-lowering effects, reducing LDL-C by 24%, ApoB-100 by 14%, triglycerides by 12%, and high-sensitivity C-reactive protein by 13%, while HDL levels typically remain unchanged. However, ezetimibe monotherapy offers only a moderate LDL-C reduction, which may be insufficient for patients with severe hypercholesterolemia [39].

The pharmacokinetics of ezetimibe make it suitable for dialysis patients. Unlike statins, which are primarily eliminated by the liver, ezetimibe is metabolized in the intestine and liver to form an active glucuronide. This metabolite is excreted via both the renal (approximately 10%) and biliary pathways. Importantly, clinical studies (including the SHARP trial) have shown that renal impairment, including end-stage kidney disease requiring dialysis, does not significantly affect the pharmacoki-

netics of ezetimibe, permitting the use of the standard 10 mg/day dose without the need for adjustment.

From a clinical standpoint, ezetimibe provides several key advantages in dialysis patients. It serves as an effective adjunct to statin therapy, allowing the achievement of LDL-C targets without increasing statin doses and the corresponding risk of adverse effects. However, although the SHARP study evaluated the combination of ezetimibe and simvastatin in CKD patients with, it lacked sufficient statistical power to assess cardiovascular outcomes separately in dialysis and non-dialysis subgroups [2]. Based on these findings, the KDIGO working group does not recommend initiating ezetimibe therapy in dialysis patients unless it was started prior to initiation of dialysis [36].

The use of ezetimibe in KT recipients represents an important therapeutic option for managing dyslipidemia, particularly in the context of immunosuppressive therapy. Ezetimibe has minimal pharmacokinetic interaction with immunosuppressants such as tacrolimus or cyclosporine. Unlike many statins, which are metabolized via the CYP3A4 enzyme system and are therefore prone to drug–drug interactions, ezetimibe exerts negligible effects on this metabolic pathway, thereby reducing the likelihood of adverse effects.

Clinically, ezetimibe has demonstrated significant efficacy in KT recipients. In the SHARP study, which included patients with chronic kidney disease (including transplant recipients), the combination of ezetimibe and simvastatin reduced the risk of cardiovascular events by 17% [40]. To avoid the risks associated with high-dose statin therapy, combination therapy with ezetimibe is recommended [37].

Fibrates

Fibrates play an important role in the management of dyslipidemia characterized predominantly by hypertriglyceridemia. Their mechanism of action is based on activation of peroxisome proliferator-activated receptor alpha (PPAR-α), a nuclear receptor that regulates expression of genes involved in lipid metabolism. Activation of PPAR-α enhances the synthesis of lipoprotein lipase, an enzyme responsible for the hydrolysis of triglycerides (TG) in chylomicrons and VLDL, leading to a sharp reduction in circulating TG levels. In addition, fibrates increase HDL levels by upregulating the synthesis of apolipoproteins A-I and A-II, and by stimulating reverse cholesterol transport from peripheral tissues to the liver.

However, the use of fibrates is associated with several adverse effects. The most common include gastrointestinal disorders, liver dysfunction, and liver of gallstone disease. These drugs also sometimes cause pancreatitis. The most serious complication is myopathy, particularly when fibrates are used in combination with statins [41].

The use of fenofibrate is contraindicated or restricted in patients with moderate to severe renal impairment (creatinine clearance <60 mL/min) because of high risk of adverse effects [36].

Currently, there is limited evidence supporting the use of fibrates in KT recipients. Some studies have demonstrated a favorable effect on lipid profiles in this patient cohort [42]. Nevertheless, concerns regarding potential nephrotoxicity have significantly restricted their clinical application KT recipients. Further research is required to establish the safety and efficacy of fibrates in this patient population [43].

Bile acid sequestrants

Bile acid sequestrants represent an older class of lipid-lowering drugs that are now used much less frequently in clinical practice, particularly in patients with CKD, due to several limitations. Their ability to lower LDL levels is only 10–20%, which is significantly inferior to the effectiveness of statins. Moreover, these agents may increase plasma TG levels, making them contraindicated in patients with hypertriglyceridemia. In addition, the use of bile acid sequestrants in CKD remains poorly studied: the lack of convincing data on their safety and efficacy in this group of patients, as well as the risks associated with impaired absorption of nutrients and drugs, significantly limit their use [4].

Niacin

Niacin, which is not excreted by the kidneys, can theoretically be considered safe for use in CKD. However, its clinical application remains limited due to frequent adverse effects and insufficient evidence. Short-term studies have demonstrated the drug's efficacy in lowering lipid levels in CKD patients, confirming its potential role in the correction of dyslipidemia. In recent years, growing interest has focused on niacin and its analogue, niacinamide, particularly in patients with CKD and end-stage renal disease, owing to their ability to reduce serum phosphate levels. According to a meta-analysis of randomized controlled trials, niacin therapy in dialysis patients significantly decreases serum phosphorus concentrations without affecting calcium levels, while also increasing HDL cholesterol. However, no significant effects were observed on LDL cholesterol, TG, or total cholesterol, and the impact on cardiovascular outcomes remains unexplored. Thus, despite its promising dual action in modulating both phosphorus-calcium metabolism and lipid parameters, the widespread use of niacin in CKD and dialysis patients requires further investigation, particularly regarding long-term safety and clinical outcomes [4].

Bempedoic acid

Bempedoic acid is a lipid-lowering drug approved for reducing LDL cholesterol levels in patients who fail to achieve target LDL concentrations with statin therapy or are intolerant to statins. Its mechanism of action in-

volves the inhibition of ATP citrate lyase, a key enzyme in hepatic cholesterol biosynthesis, acting at an earlier stage of the metabolic pathway than statins. In CKD patients, the use of bempedoic acid is currently approved without the need for dosage adjustment in individuals with a glomerular filtration rate (GFR) above 30 mL/min/1.73 m^2 [44].

Findings from the large-scale CLEAR Outcomes (2023) clinical trial demonstrated that bempedoic acid reduces LDL cholesterol by 15–25% as monotherapy and by up to 35–40% when combined with ezetimibe. Furthermore, it was associated with a 13% reduction in major cardiovascular events, including heart attack and stroke, in statin-intolerant patients. At the same time, bempedoic acid offers several clinical advantages: it does not induce muscle-related adverse effects, can be safely combined with other lipid-lowering agents (such as statins or PCSK9 inhibitors), and is administered once daily at a fixed dose of 180 mg, which enhances treatment adherence. However, its use is not without limitations. The drug can elevate serum uric acid levels by approximately 10–15%, increasing the risk of gout, and in rare cases, has been linked to tendinitis or tendon rupture [45]. The possibility of use in patients receiving RRT requires further study.

Proprotein convertase subtilisin/kexin type 9 (PCSK9) inhibitors

The PCSK9 enzyme binds to LDL receptors on the surface of hepatocytes. By destroying the LDL receptor, PCSK9 prevents their recycling back to the cell membrane, leading to a reduction in receptor density and, consequently, an increase in circulating LDL cholesterol levels [46].

PCSK9 inhibitors, such as alirocumab and evolocumab, are monoclonal antibodies that block the interaction between PCSK9 and LDL receptors. This preservation of receptor function enhances LDL uptake and catabolism, resulting in a 50–60% reduction in plasma LDL cholesterol, even among patients with refractory hypercholesterolemia [47].

Preclinical studies have shown that PCSK9 inhibition can attenuate atherogenesis and vascular inflammation within atherosclerotic plaques. Beyond its lipid-lowering properties, PCSK9 inhibition may exert additional angioprotective effects [48]. Clinically, these drugs not only lower LDL and Lp(a) levels but also significantly reduce the incidence of major cardiovascular events in secondary prevention groups.

PCSK9 inhibitors achieve a more rapid and profound reduction in LDL cholesterol, which may be more effective than the milder reduction achieved with statins in CKD patients [49]. Furthermore, emerging evidence suggests that the extent of LDL reduction achieved with PCSK9 inhibitors may influence coronary artery calcification. In one study of 120 patients, combination therapy with a PCSK9 inhibitor and a statin was associated with a lower annual progression of coronary artery calcification compared with statin monotherapy [50].

An analysis of eight phase III ODYSSEY trials demonstrated changes in apoB, non-HDL cholesterol, Lp(a), and HDL cholesterol, irrespective of CKD severity. No specific safety concerns were identified among patients with CKD compared with the overall study population. However, the efficacy and safety of PCSK9 inhibitors in patients with an eGFR below 30 mL/min/1.73 m^2 remain unestablished [51].

In kidney transplant recipients, PCSK9 inhibitors used as adjunctive therapy to statins have shown safety and efficacy in managing hypercholesterolemia and may contribute to a reduction in post-transplant cardiovascular events. Nevertheless, long-term, large-scale studies are required to confirm their potential benefits on cardiovascular outcomes, patient survival, and graft survival [52].

Inclisiran

Inclisiran also inhibits PCSK9 but acts through a fundamentally different mechanism than alirocumab and evolocumab. It is a small interfering double-stranded modified RNA conjugated to N-acetylgalactosamine (GalNAc), a carbohydrate ligand that binds to asialoglycoprotein receptors on hepatocytes. After cellular uptake, inclisiran induces degradation of PCSK9 mRNA, leading to a sustained reduction in PCSK9 protein synthesis [53].

Evidence from the ORION-7 and ORION-1 trials, which assessed the pharmacokinetics, efficacy, and safety of inclisiran in patients with normal renal function as well as mild, moderate, and severe CKD, indicated that dose adjustment is not necessary across different CKD stages [54].

A clinical case of inclisiran use in a patient who received RRT by kidney transplantation has been reported. The graft GFR was calculated at approximately 20 mL/min. Despite receiving the maximum tolerated lipid-lowering therapy (80 mg of atorvastatin and 10 mg of ezetimibe daily), the patient did not achieve the target LDL level (total cholesterol 5.18 mmol/L, LDL 2.46 mmol/L, HDL 2.12 mmol/L, and TG 1.79 mmol/L). Inclisiran was administered according to the following schedule: first injection, then after 3 months, and then every 6 months. LDL levels decreased to 1.03, 1.14, and 1.32 mmol/L after 6, 9, and 12 months, respectively [55].

The use of inclisiran in patients receiving RRT requires further study.

CONCLUSION

Dyslipidemia in CKD patients, especially those on RRT, represents a complex clinical challenge and a major contributor to cardiovascular morbidity and mortality in this population. The pathogenesis of lipid metabolism

disorders in CKD patients on RRT is multifactorial. Current evidence indicates that pharmacological strategies for managing dyslipidemia in this group remain limited.

Therapeutic approaches should be individualized, taking into account the type of RRT, comorbid conditions, and potential drug interactions. Drug treatment of dyslipidemia in patients receiving RRT requires research to explore ways to improve the prognosis for this group of patients who are at high risk for cardiovascular events.

The authors declare no conflict of interest.

REFERENCES

1. *Del Vecchio L, Baragetti I, Locatelli F*. New agents to reduce cholesterol levels: implications for nephrologists. *Nephrol Dial Transplant*. 2020 Feb 1; 35 (2): 213–218. doi: 10.1093/ndt/gfz013. PMID: 30753594.
2. *Ndumele CE, Rangaswami J, Chow SL, Neeland IJ, Tuttle KR, Khan SS et al.* Cardiovascular-Kidney-Metabolic Health: A Presidential Advisory From the American Heart Association. *Circulation*. 2023 Nov 14; 148 (20): 1606–1635. doi: 10.1161/CIR.0000000000001184. PMID: 37807924.
3. *Shutov EV, Nikolaev AYu, Filatova NN*. Cardiorenal syndrome in patients on renal replacement therapy (A review). *Nephrology and Dialysis*. 2018; 20 (3): 262–273. [In Russ, English abstract]. doi: 10.28996/2618-9801-2018-3-262-273.
4. *Lacount S, Tannock LR, Feingold KR, Ahmed SF, Anawalt B, Blackman MR et al.* Dyslipidemia in Chronic Kidney Disease. 2025. Endotext [Internet]. South Dartmouth (MA): MDText.com, Inc.; 2000. PMID: 26247091.
5. Multiple Risk Factor Intervention Trial. Risk factor changes and mortality results. Multiple Risk Factor Intervention Trial Research Group. *JAMA*. 1997 Feb 19; 277 (7): 582–594. PMID: 9032168.
6. *Dawber TR, Kannel WB, Revotskie N, Kagan A*. The epidemiology of coronary heart disease – the Framingham enquiry. *Proc R Soc Med*. 1962 Apr; 55 (4): 265–271. doi: 10.1177/003591576205500403. PMID: 13884013.
7. *Kannel WB, Castelli WP, Gordon T*. Cholesterol in the prediction of atherosclerotic disease. New perspectives based on the Framingham study. *Ann Intern Med*. 1979 Jan; 90 (1): 85–91. doi: 10.7326/0003-4819-90-1-85. PMID: 217290.
8. *Mach F, Baigent C, Catapano AL, Koskinas KC, Casula M, Badimon L et al*. ESC Scientific Document Group. 2019 ESC/EAS Guidelines for the management of dyslipidaemias: lipid modification to reduce cardiovascular risk. *Eur Heart J*. 2020 Jan 1; 41 (1): 111–188. doi: 10.1093/eurheartj/ehz455. Erratum in: *Eur Heart J*. 2020 Nov 21; 41 (44): 4255. doi: 10.1093/eurheartj/ehz826. PMID: 31504418.
9. *Noels H, Lehrke M, Vanholder R, Jankowski J*. Lipoproteins and fatty acids in chronic kidney disease: molecular and metabolic alterations. *Nat Rev Nephrol*. 2021 Aug; 17 (8): 528–542. doi: 10.1038/s41581-021-00423-5. PMID: 33972752.
10. *Harlacher E, Wollenhaupt J, Baaten CCFMJ, Noels H*. Impact of Uremic Toxins on Endothelial Dysfunction in Chronic Kidney Disease: A Systematic Review. *Int J Mol Sci*. 2022 Jan 4; 23 (1): 531. doi: 10.3390/ijms23010531. PMID: 35008960.
11. *Rysz J, Franczyk B, Ławiński J, Gluba-Brzózka A*. Oxidative Stress in ESRD Patients on Dialysis and the Risk of Cardiovascular Diseases. *Antioxidants (Basel)*. 2020 Nov 3; 9 (11): 1079. doi: 10.3390/antiox9111079. PMID: 33153174.
12. *Suh SH, Kim SW*. Dyslipidemia in Patients with Chronic Kidney Disease: An Updated Overview. *Diabetes Metab J*. 2023 Sep; 47 (5): 612–629. doi: 10.4093/dmj.2023.0067. Epub 2023 Jul 24. PMID: 37482655.
13. *Cao H, Meng X*. HDL and Kidney Diseases. *Adv Exp Med Biol*. 2022; 1377: 163–170. doi: 10.1007/978-981-19-1592-5_13. PMID: 35575929.
14. *Gusev E, Sarapultsev A*. Atherosclerosis and Inflammation: Insights from the Theory of General Pathological Processes. *Int J Mol Sci*. 2023 Apr 26; 24 (9): 7910. doi: 10.3390/ijms24097910. PMID: 37175617.
15. *Marsche G, Heine GH, Stadler JT, Holzer M*. Current Understanding of the Relationship of HDL Composition, Structure and Function to Their Cardioprotective Properties in Chronic Kidney Disease. *Biomolecules*. 2020 Sep 21; 10 (9): 1348. doi: 10.3390/biom10091348. PMID: 32967334.
16. *Speer T, Ridker PM, von Eckardstein A, Schunk SJ, Fliser D*. Lipoproteins in chronic kidney disease: from bench to bedside. *Eur Heart J*. 2021 Jun 7; 42 (22): 2170–2185. doi: 10.1093/eurheartj/ehaa1050. PMID: 33393990.
17. *Carty JR, Anastasopoulou C*. Lecithin-Cholesterol Acyltransferase Deficiency. 2024. In: StatPearls [Internet]. Treasure Island (FL): StatPearls. PMID: 38753926.
18. *Ferro CJ, Mark PB, Kanbay M, Sarafidis P, Heine GH, Rossignol P et al*. Lipid management in patients with chronic kidney disease. *Nat Rev Nephrol*. 2018 Dec; 14 (12): 727–749. doi: 10.1038/s41581-018-0072-9. PMID: 30361677.
19. *Lampsas S, Xenou M, Oikonomou E, Pantelidis P, Lysandrou A, Sarantos S et al.* Lipoprotein(a) in Atherosclerotic Diseases: From Pathophysiology to Diagnosis and Treatment. *Molecules*. 2023 Jan 18; 28 (3): 969. doi: 10.3390/molecules28030969. PMID: 36770634.
20. *Ma Z, Zhong J, Tu W, Li S, Chen J*. The functions of apolipoproteins and lipoproteins in health and disease. *Mol Biomed*. 2024 Oct 28; 5 (1): 53. doi: 10.1186/s43556-024-00218-7. PMID: 39465476.
21. *Ren X, Zhang Z, Yan Z*. Association Between Lipoprotein (A) and Diabetic Nephropathy in Patients With Type 2 Diabetes Mellitus: A Meta-Analysis. *Front Endocrinol (Lausanne)*. 2021 Mar 24; 12: 633529. doi: 10.3389/fendo.2021.633529. PMID: 33841331.
22. *Enkhmaa B, Berglund L*. Non-genetic influences on lipoprotein(a) concentrations. *Atherosclerosis*. 2022 May; 349: 53–62. doi: 10.1016/j.atherosclerosis.2022.04.006. PMID: 35606076.
23. *Guarnieri G, Zanetti M, Vinci P, Cattin MR, Barazzoni R*. Insulin resistance in chronic uremia. *J Ren Nutr*.

2009 Jan; 19 (1): 20–24. doi: 10.1053/j.jrn.2008.11.014. PMID: 19121765.
24. *Freeman AM, Acevedo LA, Pennings N*. Insulin Resistance. 2023 Aug 17. In: StatPearls [Internet]. Treasure Island (FL): StatPearls Publishing; 2023 Jan. PMID: 29939616.
25. *Stegmayr B, Zuo L, Zadora W*. Lipid and Bone Effects of Heparin Use During Hemodialysis. *Semin Nephrol*. 2023 Nov; 43 (6): 151480. doi: 10.1016/j.semnephrol.2023.151480. PMID: 38195305.
26. *Zhu S, Zhang F, Shen AW, Sun B, Xia TY, Chen WS et al.* Metabolomics Evaluation of Patients With Stage 5 Chronic Kidney Disease Before Dialysis, Maintenance Hemodialysis, and Peritoneal Dialysis. *Front Physiol*. 2021 Jan 20; 11: 630646. doi: 10.3389/fphys.2020.630646. PMID: 33551851.
27. *Liakopoulos V, Roumeliotis S, Zarogiannis S, Eleftheriadis T, Mertens PR.* Oxidative stress in hemodialysis: Causative mechanisms, clinical implications, and possible therapeutic interventions. *Semin Dial*. 2019 Jan; 32 (1): 58–71. doi: 10.1111/sdi.12745. PMID: 30288786.
28. *Cheng XBJ, Bargman J*. Complications of Peritoneal Dialysis Part II: Nonmechanical Complications. *Clin J Am Soc Nephrol*. 2024 Jun 1; 19 (6): 791–799. doi: 10.2215/CJN.0000000000000418. PMID: 38190143.
29. *Aggarwal HK, Jain D, Lathar M, Yadav RK, Sawhney A*. Lipoprotein-A and carotid intima media thickness as cardiovascular risk factors in patients of chronic kidney disease. *Ren Fail*. 2010 Jul; 32 (6): 647–652. doi: 10.3109/0886022X.2010.486097. PMID: 20540630.
30. *Chmielnicka K, Heleniak Z, Dębska-Ślizień A*. Dyslipidemia in Renal Transplant Recipients. *Transplantology*. 2022 May 23; 3 (2): 188–199. doi: 10.3390/transplantology3020020.
31. *Rahimi L, Rajpal A, Ismail-Beigi F*. Glucocorticoid-Induced Fatty Liver Disease. *Diabetes Metab Syndr Obes*. 2020 Apr 16; 13: 1133–1145. doi: 10.2147/DMSO.S247379. PMID: 32368109.
32. *Rostaing L, Jouve T, Terrec F, Malvezzi P, Noble J.* Adverse Drug Events after Kidney Transplantation. *J Pers Med*. 2023 Dec 14; 13 (12): 1706. doi: 10.3390/jpm13121706. PMID: 38138933.
33. *Iannuzzo G, Cuomo G, Di Lorenzo A, Tripaldella M, Mallardo V, Iaccarino Idelson P et al.* Dyslipidemia in Transplant Patients: Which Therapy? *J Clin Med*. 2022 Jul 14; 11 (14): 4080. doi: 10.3390/jcm11144080. PMID: 35887846.
34. *Al-Kuraishy HM, Sulaiman GM, Mohsin MH, Mohammed HA, Dawood RA, Albuhadily AK et al*. Targeting of AMPK/MTOR signaling in the management of atherosclerosis: Outmost leveraging. *Int J Biol Macromol*. 2025 May; 309 (Pt 2): 142933. doi: 10.1016/j.ijbiomac.2025.142933. PMID: 40203916.
35. *Arvanitis M, Lowenstein CJ.* Dyslipidemia. *Ann Intern Med*. 2023 Jun; 176 (6): ITC81–ITC96. doi: 10.7326/AITC202306200. PMID: 37307585.
36. *Wanner C, Tonelli M.* Kidney Disease: Improving Global Outcomes Lipid Guideline Development Work Group Members. KDIGO Clinical Practice Guideline for Lipid Management in CKD: summary of recommendation statements and clinical approach to the patient. *Kidney Int*. 2014 Jun; 85 (6): 1303–1309. doi: 10.1038/ki.2014.31. PMID: 24552851.
37. *Ponticelli C, Arnaboldi L, Moroni G, Corsini A*. Treatment of dyslipidemia in kidney transplantation. *Expert Opin Drug Saf*. 2020 Mar; 19 (3): 257–267. doi: 10.1080/14740338.2020.1732921. PMID: 32073914.
38. *Kim BK, Hong SJ, Lee YJ, Hong SJ, Yun KH, Hong BK et al.* RACING investigators. Long-term efficacy and safety of moderate-intensity statin with ezetimibe combination therapy versus high-intensity statin monotherapy in patients with atherosclerotic cardiovascular disease (RACING): a randomised, open-label, non-inferiority trial. *Lancet*. 2022 Jul 30; 400 (10349): 380–390. doi: 10.1016/S0140-6736(22)00916-3. PMID: 35863366.
39. *Michaeli DT, Michaeli JC, Albers S, Boch T, Michaeli T.* Established and Emerging Lipid-Lowering Drugs for Primary and Secondary Cardiovascular Prevention. *Am J Cardiovasc Drugs*. 2023 Sep; 23 (5): 477–495. doi: 10.1007/s40256-023-00594-5. PMID: 37486464.
40. *Luo B, Zhong S, Wang X, Guo P, Hou Y, Di W*. Management of blood lipids in post-kidney transplant patients: a systematic review and network meta-analysis. *Front Pharmacol*. 2024 Oct 8; 15: 1440875. doi: 10.3389/fphar.2024.1440875. PMID: 39439889.
41. *Canfora I, Pierno S.* Hypertriglyceridemia Therapy: Past, Present and Future Perspectives. *Int J Mol Sci*. 2024 Sep 8; 25 (17): 9727. doi: 10.3390/ijms25179727. PMID: 39273674.
42. *Pontremoli R, Bellizzi V, Bianchi S, Bigazzi R, Cernaro V, Del Vecchio L et al.* Management of dyslipidaemia in patients with chronic kidney disease: a position paper endorsed by the Italian Society of Nephrology. *J Nephrol*. 2020 Jun; 33 (3): 417–430. doi: 10.1007/s40620-020-00707-2. PMID: 32065354.
43. *Tramontano D, Bini S, Maiorca C, Di Costanzo A, Carosi M, Castellese J et al.* Renal Safety Assessment of Lipid-Lowering Drugs: Between Old Certainties and New Questions. *Drugs*. 2025 Jun; 85 (6): 755–775. doi: 10.1007/s40265-025-02158-0. PMID: 40106181.
44. *Ray KK, Bays HE, Catapano AL, Lalwani ND, Bloedon LT, Sterling LR et al.* CLEAR Harmony Trial. Safety and Efficacy of Bempedoic Acid to Reduce LDL Cholesterol. *N Engl J Med*. 2019 Mar 14; 380 (11): 1022–1032. doi: 10.1056/NEJMoa1803917. PMID: 30865796.
45. *Nissen SE, Lincoff AM, Brennan D, Ray KK, Mason D, Kastelein JJP et al.* CLEAR Outcomes Investigators. Bempedoic Acid and Cardiovascular Outcomes in Statin-Intolerant Patients. *N Engl J Med*. 2023 Apr 13; 388 (15): 1353–1364. doi: 10.1056/NEJMoa2215024. PMID: 36876740.
46. *Barale C, Melchionda E, Morotti A, Russo I*. PCSK9 Biology and Its Role in Atherothrombosis. *Int J Mol Sci*. 2021 May 30; 22 (11): 5880. doi: 10.3390/ijms22115880. PMID: 34070931.
47. *Grzesk G, Dorota B, Wołowiec Ł, Wołowiec A, Osiak J, Kozakiewicz M, Banach J.* Safety of PCSK9 inhibitors. *Biomed Pharmacother*. 2022 Dec; 156: 113957. doi: 10.1016/j.biopha.2022.113957. PMID: 36411665.

48. *Xu S, Ilyas I, Little PJ, Li H, Kamato D, Zheng X et al.* Endothelial Dysfunction in Atherosclerotic Cardiovascular Diseases and Beyond: From Mechanism to Pharmacotherapies. *Pharmacol Rev*. 2021 Jul; 73 (3): 924–967. doi: 10.1124/pharmrev.120.000096. PMID: 34088867.
49. *Mayer G, Dobrev D, Kaski JC, Semb AG, Huber K, Zirlik A et al.* Management of dyslipidaemia in patients with comorbidities: facing the challenge. *Eur Heart J Cardiovasc Pharmacother*. 2024 Nov 6; 10 (7): 608–613. doi: 10.1093/ehjcvp/pvae058. PMID: 39153964.
50. *Ikegami Y, Inoue I, Inoue K, Shinoda Y, Iida S, Goto S et al.* The annual rate of coronary artery calcification with combination therapy with a PCSK9 inhibitor and a statin is lower than that with statin monotherapy. *NPJ Aging Mech Dis*. 2018 Jun 22; 4: 7. doi: 10.1038/s41514-018-0026-2. Erratum in: *NPJ Aging*. 2025 Mar 19; 11 (1): 19. doi: 10.1038/s41514-025-00208-1. PMID: 29951223.
51. *Toth PP, Dwyer JP, Cannon CP, Colhoun HM, Rader DJ, Upadhyay A et al.* Efficacy and safety of lipid lowering by alirocumab in chronic kidney disease. *Kidney Int*. 2018 Jun; 93 (6): 1397–1408. doi: 10.1016/j.kint.2017.12.011. Epub 2018 Mar 8. PMID: 29526502.
52. *Alotaibi T, Nagib AM, Denewar A, Aboateya H, Halim MA, Mahmoud T et al.* Inhibition of Proprotein Convertase Subtilisin/Kexin-9 After Kidney Transplant: Single-Center Experience Among Patients With High Cardiovascular Risk. *Exp Clin Transplant*. 2024 Jan; 22 (Suppl 1): 315–322. doi: 10.6002/ect.MESOT2023.P111. PMID: 38385418.
53. *Voevoda MI, Gurevich VS, Ezhov MV, Sergienko IV*. Inclisiran – a new era in lipid-lowering therapy. *Kardiologiia*. 2022 Jun 30; 62 (6): 57–62. [In Russ, English abstract]. doi: 10.18087/cardio.2022.6.n2115.
54. *Wright RS, Collins MG, Stoekenbroek RM, Robson R, Wijngaard PLJ, Landmesser U et al*. Effects of Renal Impairment on the Pharmacokinetics, Efficacy, and Safety of Inclisiran: An Analysis of the ORION-7 and ORION-1 Studies. *Mayo Clin Proc*. 2020 Jan; 95 (1): 77–89. doi: 10.1016/j.mayocp.2019.08.021. PMID: 31630870.
55. *Ueberdiek L, Jehn U, Pavenstädt H, Gebauer K, Reuter S*. Novel Therapeutic Strategies for Dyslipidemia: First Report of Inclisiran Therapy in a Kidney Transplanted Patient. *Transpl Int*. 2023 Jan 26; 36: 11104. doi: 10.3389/ti.2023.11104. Erratum in: *Transpl Int*. 2023 Mar 23; 36: 11313. doi: 10.3389/ti.2023.11313. PMID: 36776901.

The article was submitted to the journal on 22.05.2025

DOI: 10.15825/1995-1191-2025-4-173-182

COMPARATIVE STUDY OF LUNG PRECONDITIONING PROTOCOLS IN DONORS AFTER CIRCULATORY ARREST: AN EXPERIMENTAL RABBIT MODEL

I.V. Pashkov, Ya.S. Yakunin, K.S. Smirnov, V.K. Bogdanov, N.P. Mozheiko, L.A. Kirsanova, M.V. Olkhovskaya, N.V. Grudinin

Shumakov National Medical Research Center of Transplantology and Artificial Organs, Moscow, Russian Federation

Objective: to perform a comparative analysis of donor lung preconditioning protocols in donors after circulatory arrest, followed by normothermic *ex vivo* lung perfusion (EVLP), using two approaches: topical lung cooling and continued artificial ventilation after circulatory arrest. **Materials and methods.** The study was conducted on male Grey Giant rabbits weighing 4.5–5.0 kg (n = 20). Group 1: Donor lung preconditioning after circulatory arrest using topical cooling (n = 10). Group 2: Donor lung preconditioning after circulatory arrest with continued artificial ventilation in protective modes (n = 10). To evaluate the viability and functional state of donor lungs following preconditioning and cold preservation, both groups underwent normothermic EVLP. Assessments included lactate concentration, perfusate gas composition, endoscopic evaluation of the tracheobronchial tree, and subsequent morphological examination. **Results.** After 60 minutes of cold preservation, all grafts demonstrated satisfactory gas exchange function during normothermic EVLP. In Group 1 (topical cooling), the oxygenation index (OI) at 60 minutes was 552 (461–599) and increased to 558 (462–603) at 120 minutes. In Group 2 (continuous artificial ventilation), OI was 358 (343–368) at 60 minutes, with a tendency to increase to 374 (349–395) at 120 minutes. The difference between the groups was statistically significant (p = 0.000). Lactate levels in both groups showed an upward trend, with a mean value of 6.99 ± 0.81, and no statistically significant intergroup differences were observed (p > 0.05). **Conclusion.** The study demonstrates the potential advantages of using topical cooling as part of the donor lung preconditioning protocol after cessation of effective circulation, employing a dextran-40-based preservation solution at all stages. This approach may increase the number of donor lungs suitable for transplantation.

Keywords: lung transplantation, normothermic ex vivo perfusion, organ donation, organ preservation, dextran-40.

INTRODUCTION

Donation after circulatory death (DCD) represents one of the most promising areas in modern transplantology, offering a viable solution to the persistent shortage of donor organs. Traditionally, lung transplantation has relied on donation after brain death (DBD); however, increasing attention is now being directed toward the use of lungs from DCD donors. This shift is driven by the growing need for donor lungs, improvements in organ preservation techniques, and the introduction of perfusion technologies.

In recent years, the use of lungs from DCD donors has increased markedly. According to 2018 data from the United States, lungs from DCD donors accounted for approximately 20% of all lung transplants. In Europe, this figure varies between countries, from 5% to 40%, yet overall shows a clear upward trend in the adoption of donors after circulatory death [1].

Clinical evidence indicates that outcomes of lung transplantation from DCD donors are comparable to those from DBD donors. International studies show that long-term recipient survival and graft function following DCD lung transplantation are not inferior to traditional lung transplants. Moreover, in some centers, DCD lungs constitute a substantial proportion of all transplanted organs, underscoring the effectiveness of this approach.

In the United States, the 1-year survival rate after lung transplantation from DCD donors is approximately 75–80%, which is slightly lower than the outcomes reported for DBD donors [2, 3]. In Europe, 1-year survival rates following DCD lung transplantation range from 65% to 90%, depending on the country, with results comparable to DBD transplantation observed in the Netherlands, Belgium, Spain, and Italy [3–5]. The 3-year survival rate after DCD lung transplantation is around 70%, which is close to the rates seen with DBD donors.

Corresponding author: Vladimir Bogdanov. Address: 1, Shchukinskaya str., Moscow, 123182, Russian Federation. Phone: (900) 110-42-41. E-mail: bogdanovv@bk.ru

However, DCD lung transplantation is associated with a higher incidence of primary graft dysfunction, largely due to ischemic injury resulting from the absence of lung perfusion after cardiac arrest. Unlike DBD donor lungs – where circulation is maintained until explantation – DCD lungs undergo a period of warm ischemia, which may impair graft quality [6].

Advances such as *ex vivo* lung perfusion (EVLP) have enabled functional assessment, recruitment, and more thorough perfusion of the pulmonary microvasculature prior to transplantation, thereby increasing the number of organs deemed suitable for transplantation [3, 7, 8].

This experimental study compares two protocols for lung explantation from DCD donors, followed by normothermic *ex vivo* perfusion. The first protocol involves topical cooling of the lungs in the pleural cavity using a preservative solution [9–11], while the second protocol utilizes continued mechanical ventilation after cardiac arrest [12, 13]. For both approaches, an original dextran-40–based solution was employed for lung preservation and perfusion [14, 15].

DESIGN OF THE EXPERIMENTAL WORK

The study was conducted on 20 male Grey Giant rabbits weighing 4.5–5.0 kg. All procedures complied with the requirements of the European Convention for the Protection of Vertebrate Animals Used for Experimental and Other Scientific Purposes and Directive 2010/63/EU. The animals were housed in laboratory cages under standardized conditions: controlled temperature (22 ± 2 °C), relative humidity (65%), a 12-hour light–dark cycle, regulated feeding, and ad libitum access to sterilized water. A two-week quarantine period was observed prior to experimentation. All procedures were reviewed and approved by the institutional Committee on Biological Safety and Bioethics.

The study was conducted in two experimental groups:

Group 1. DCD model with topical cooling of the donor lungs and without mechanical ventilation (MV). The lung graft was removed 40 minutes after circulatory arrest, followed by 6-hour cold storage preservation and 2-hour EVLP (N = 10).

Group 2. DCD model with continued MV. The lung graft was removed 40 minutes after circulatory arrest, followed by 6-hour cold storage preservation and 2-hour EVLP (N = 10).

After completing the EVLP procedure, a fragment of each graft was collected for histological examination.

MATERIALS AND METHODS

Donor lung procurement procedure

After preparing the donor animal according to aseptic and antiseptic standards, the surgical field was treated and isolated using sterile drapes. Surgical access was achieved via median sternotomy. Following hemostasis and mobilization of the major vessels, DCD was simulated. In Group 1, MV was continued, while in group 2, MV was discontinued and 50 ml of a dextran-40–based preservation solution was instilled into each pleural cavity, as shown in Fig. 1.

After a 30-minute exposure period, 30 ml of blood was withdrawn from the left ventricle, after which a cannula was inserted into the pulmonary artery. Antegrade perfusion with a dextran-40–based solution (OCS Lung Solution) cooled to 4 °C was initiated. A total of 60 ml of solution was administered using a syringe pump at a rate of 500 ml/hour with an exposure time of 7 minutes. This was followed by mobilization of the lungs. After mobilization, at the height of inspiration and below the distal tip of the endotracheal tube, the trachea was securely ligated and transected. The lungs were then immersed in the dextran-40–based solution at 4 °C and stored under cold preservation for 6 hours.

Anesthesia

Six hours prior to surgery, the donor animal was fasted. The rabbit was transported to the preoperative room for preparation, where sedation was initiated with Zoletil 100 (Virbac, France) 50 mg administered subcutaneously. Under aseptic conditions, an intravenous

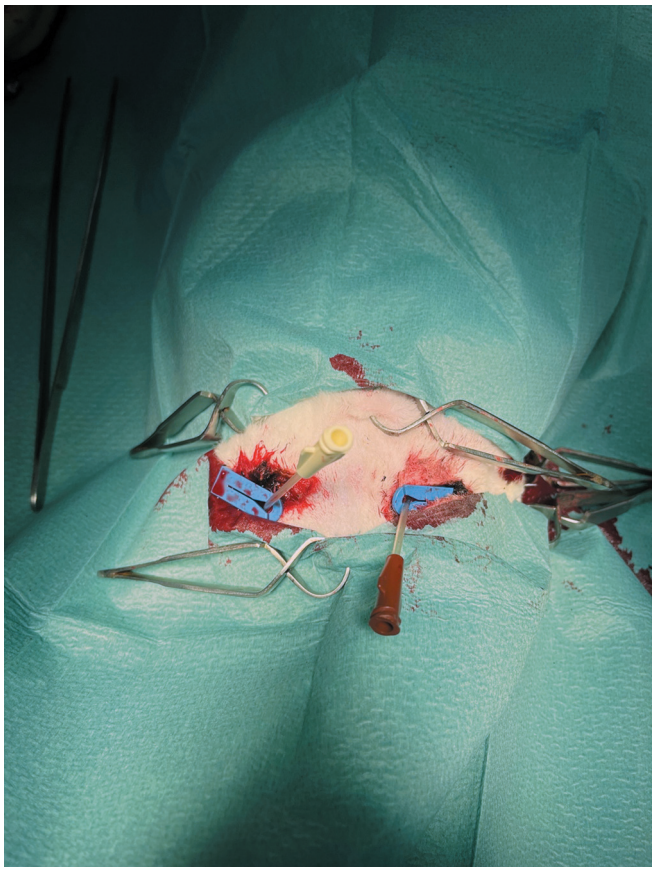

Fig. 1. Topical cooling of the lungs performed through drainage of the right and left pleural cavities using 8 Fr central venous catheters

catheter (Vasofix Certo 22G, BBraun, Germany) was inserted and secured. The animal was positioned in the supine position.

For anesthetic induction, atropine 0.3 mg and dexamethasone 2 mg were administered intravenously, followed by intravenous Zoletil 100 (Virbac, France) 50 mg and propofol (Fresenius Kabi, Germany) 25 mg. Direct laryngoscopy was performed, and tracheal intubation was carried out using a cuffed 3.5 cm endotracheal tube. After confirming correct tube placement, rocuronium (Fresenius Kabi, Germany) 10 mg was administered.

MV was initiated using a WATO EX-65 Pro Vet ventilator (Mindray, China) in VCV mode with the following parameters: tidal volume 50 ml, respiratory rate 35/min, Ppeak 17 cm H_2O, PEEP 3 cm H_2O, I:E ratio 1:1, FiO_2 0.6, and $EtCO_2$ 40 mmHg.

Physiological monitoring was performed using an ePM 12M Vet monitor (Mindray, China). Average values included HR 170/min, SpO_2 98%, and noninvasive arterial pressure of 90/45 mmHg.

Analgesia was maintained with intravenous tramadol (Tramvet, Russia) 25 mg, and sedation was supported with isoflurane (Baxter, USA) at a concentration of 1.5%. Hemodynamic stability was achieved with continuous intravenous infusion of Panangin (Gedeon Richter, Hungary) at 10 ml/hour and norepinephrine at 100 ng/kg.

Prior to inducing circulatory arrest to simulate DCD, heparin 10,000 IU and Vasaprostane (IDT BIOLOGIKA, Germany) 10 µg were administered intravenously. Circulatory arrest was induced using a 20 J electric shock delivered by an electrical fibrillator. An exposure period of 30 minutes followed.

During the exposure, all drug infusions were discontinued. Ventilation parameters were changed: In group 1, MV was discontinued, while in group 2, MV was continued with modified parameters – tidal volume 30 ml, respiratory rate 15/min, Ppeak 10 cm H_2O, PEEP 5 cm H_2O, I:E 1:1, and FiO_2 1.0.

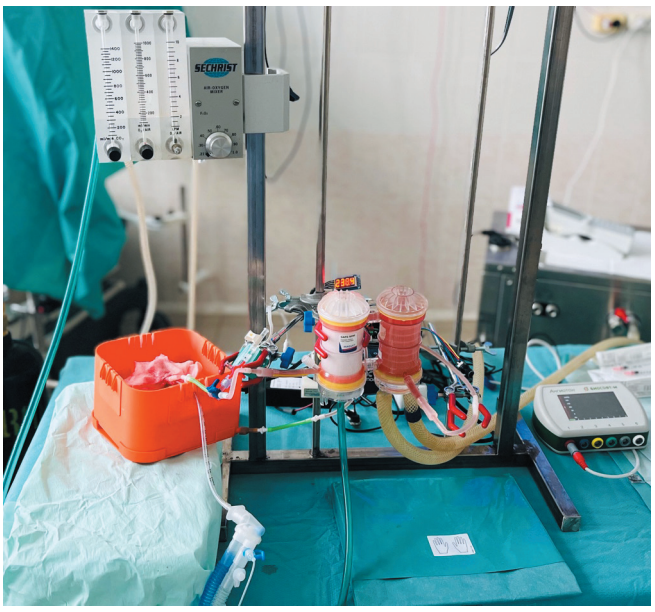

Fig. 2. Perfusion circuit setup for normothermic EVLP

After the 30-minute exposure period, a recruitment maneuver was performed, and the lung procurement procedure was initiated, followed by cold storage preservation.

Ex vivo perfusion procedure

To initiate normothermic perfusion of donor lungs, the stroke volume (SV) of the donor's left ventricle was measured using a GE Logiq V2 ultrasound system in M-mode and Doppler echocardiography with the animal positioned in the right lateral decubitus position. The average SV obtained was 2.6 ml. Cardiac output (CO) was subsequently calculated using the formula CO = SV × HR, where HR is the heart rate. The mean cardiac output was 410 ml/min.

For EVLP using 3D modeling techniques, an organ container was fabricated on a Picaso Designer X Pro 3D printer. This biocompatible plastic reservoir functioned both as a cardiotomy chamber and as a platform for securing the donor lungs during perfusion. The container was reusable and was gas sterilized in individual packaging after each procedure.

The extracorporeal circuit included a reservoir for positioning the donor lungs, a roller pump, a heat exchanger, a laboratory oxygenator with a low priming volume, a flow sensor, and a pressure sensor.

All components were assembled under strict aseptic and antiseptic conditions (Fig. 2). The circuit was primed with 20 ml of a dextran-40–based solution (OCS Lung Solution). Through a leukocyte-depleting infusion filter, 25 ml of whole donor blood was added. The perfusate was supplemented with the following: methylprednisolone 50 mg, vasoprostane – 25 mcg, heparin – 1000 mg, calcium chloride 10% – 1 ml, insulin P – 3 units, magnesium sulfate 25% – 0.2 ml, and ceftriaxone – 100 mg. The total perfusate volume was 50 ml. Prior to initiating lung perfusion, the solution was heated to 28 °C and circulated at a rate of 50 ml/min.

After 6 hours of cold storage preservation, surgical preparation of the lung grafts was initiated in both groups. A 2.2–2.4 mm cannula was inserted into the pulmonary artery, and a 3.0-mm uncuffed endotracheal tube was placed into the trachea. The left atrium was opened to ensure unobstructed perfusate outflow. The heart–lung bloc was then positioned inside the perfusion chamber. The pulmonary vascular bed was filled retrogradely, with careful monitoring to maintain the filling pressure below 3 mmHg. Following vascular filling and deaeration, the perfusion line was connected to the pulmonary artery cannula using an airless technique. Bronchoscopy of the lung graft was subsequently performed using an Ambu aScope™ 4 Broncho Slim 3.8/1.2 disposable broncho-

scope. The obtained endoscopic view is presented in Fig. 3.

The EVLP procedure was conducted in accordance with the Lund protocol. The initial perfusion rate was set at 100 ml/min (25–30% of CO), with pulmonary artery pressure maintained below 25 mmHg and perfusate temperature at 28 °C. Warming of the graft and gradual achievement of the target perfusion parameters required 30 minutes. A general view of the donor lungs during normothermic perfusion is shown in Fig. 4.

Artificial lung ventilation was initiated at a perfusate temperature of 34 °C, 15 minutes after the start of EVLP. Initial ventilation parameters were: tidal volume 2–4 ml/kg of donor body weight, respiratory rate 10/min, Ppeak 20 cm H_2O, PEEP 5 cm H_2O, I:E 1:1, and FiO_2 0.21. The target perfusion parameters were a flow rate of 410–420 ml/min (100% of CO), pulmonary artery pressure up to 25 mmHg, and perfusate temperature of 38.5 °C. Target ventilation parameters included tidal volume 6 ml/kg, respiratory rate 17/min, Ppeak 25 cm H_2O, PEEP 5 cm H_2O, I:E 1:1, and FiO_2 0.21. The EVLP procedure lasted for 120 minutes.

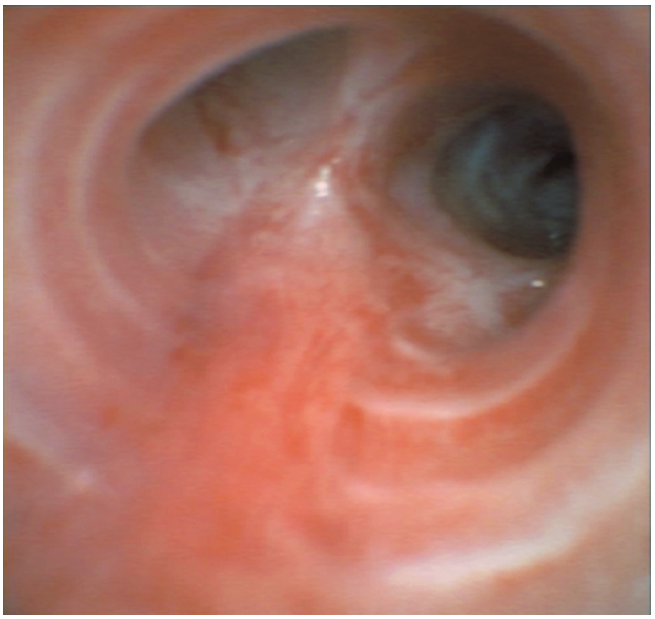

Fig. 3. Endoscopic image during normothermic perfusion

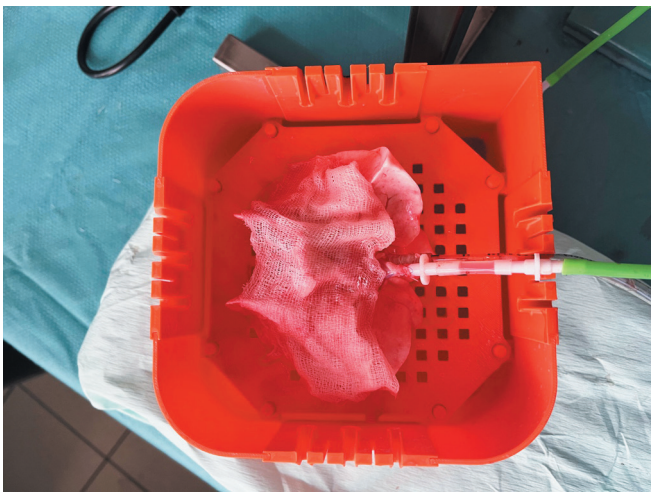

Fig. 4. Lung graft placed in the perfusion reservoir. The pulmonary artery trunk is cannulated, and the trachea is intubated for ventilation

During normothermic perfusion, a base gas mixture of 21% O_2, 5% CO_2, and 74% N_2 was supplied through the oxygenator. Every 30 minutes, the functional status of the donor lungs was assessed, and a deoxygenating mixture consisting of 5% CO_2 and 95% N_2 was administered.

At the end of EVLP, the donor lungs were preserved using 60 ml of a dextran-40–based solution (OCS Lung Solution), infused through the pulmonary artery cannula at a rate of 500 ml/hour. Lung parenchyma samples were then placed in 10% formalin for histological analysis.

Statistical analysis was performed using StatTech v.3.1.10 software (StatTech LLC, Russia). Quantitative variables were tested for normality using the Shapiro–Wilk test (sample size <50). Variables with a normal distribution were summarized as mean (M) and standard deviation (SD), with corresponding 95% confidence intervals (95% CI).

For comparisons of three or more related groups on normally distributed quantitative variables, a one-way repeated-measures analysis of variance (ANOVA) was applied. Differences were considered statistically significant at $p < 0.05$.

RESULTS

Assessment of the functional status of donor lungs during normothermic perfusion

Despite the extensive list of recorded indicators and biochemical analysis results, the oxygenation index (PaO_2/FiO_2) served as the principal criterion for evaluating the gas exchange capacity of the lungs. This calculated ratio reflects the efficiency of oxygen transfer into the pulmonary venous blood relative to the fraction of inspired oxygen. As such, it is considered a key indicator of ischemia–reperfusion injury severity and the preservation of adequate alveolar blood flow. The dynamics of changes in the oxygenation index (OI) in the two experimental groups – used to compare the effectiveness of donor lung preconditioning protocols during normothermic *ex vivo* perfusion – are presented in shown Fig. 5.

Thus, by 60 minutes after initiation of transplant revitalization on the extracorporeal circuit, both groups reached the OI threshold level of approximately 350. However, group 1 showed significantly higher OI values – 552 (461–599) compared with 358 (343–368) in group 2. This difference reflects the more pronounced ischemia–reperfusion injury observed in group 2 during donor lung preconditioning at the DCD stage and subsequent cold storage.

After 120 minutes of EVLP, both groups showed a moderate decline in OI compared with their peaks at 90 minutes – 594 (500–619) in group 1 and 408 (396–418) in group 2 – consistent with the expected increase in interstitial edema. By the end of the 120-minute EVLP period, mean OI remained significantly higher in Group 1 at 558 (462–603) compared with 374 (349–395) in Group 2.

Overall, these results demonstrate the superior effectiveness of topical cooling during DCD lung preconditioning compared with continued protective MV, with statistical significance confirmed at $p = 0.000$.

Lactate levels, assessed as a biochemical marker of ischemia–reperfusion injury, showed a steady increase throughout the perfusion period due to the absence of metabolic clearance mechanisms in the *ex vivo* circuit (Fig. 6).

Baseline lactate levels were recorded 60 minutes after the start of perfusion in both groups, as earlier measurements are not informative for assessing initial reperfusion injury. In group 1, mean lactate level was 0.7 ± 0.6 mmol/L, while in group 2 it was 1.54 ± 0.58 mmol/L. No statistically significant differences were found between the groups at this initial time point ($p > 0.05$), indicating that the two DCD preconditioning protocols did not differ in terms of severity of primary ischemia–reperfusion injury.

Throughout the perfusion period, both groups showed a clear and progressive increase in lactate levels. By the final measurement at 120 minutes, mean lactate levels reached 6.44 ± 1.35 mmol/L in group 1 and 7.02 ± 1.55 mmol/L in group 2. These values remained below the critical threshold of 12 mmol/L. At all time points, intergroup differences remained statistically insignificant ($p > 0.05$). Thus, lactate level did not prove to be a reliable comparative marker for assessing the effectiveness of donor lung preconditioning protocols in the DCD model. The most informative indicators were those reflecting the functional status of the grafts.

Assessment of histological changes in donor lungs

Histological evaluation of lung micro-preparations after preconditioning in the two comparative groups and subsequent EVLP was essential to verify the efficacy and safety of the protocols. Microstructural analysis provided reliable evidence of ischemia-reperfusion injury, its severity, and potential reversibility. In group 1, minimal pathomorphological changes were observed in the lung parenchyma at the final stage of the study (Fig. 7).

Across all samples, the parenchyma exhibited histological signs of functional tissue without significant pathological alterations. Most sections showed well-inflated alveoli, with microatelectatic areas being sparse and unevenly distributed. Moderate interstitial infiltration was present in a few samples. No notable differences in microstructure were observed within group 1 samples: interalveolar septa remained thin, bronchial walls displayed normal histology, and vascular blood filling was moderate.

In group 2, which underwent the artificial ventilation preconditioning protocol, primary graft dysfunction was observed after 120 minutes of EVLP. This corresponded with the reduced OI recorded during functional assess-

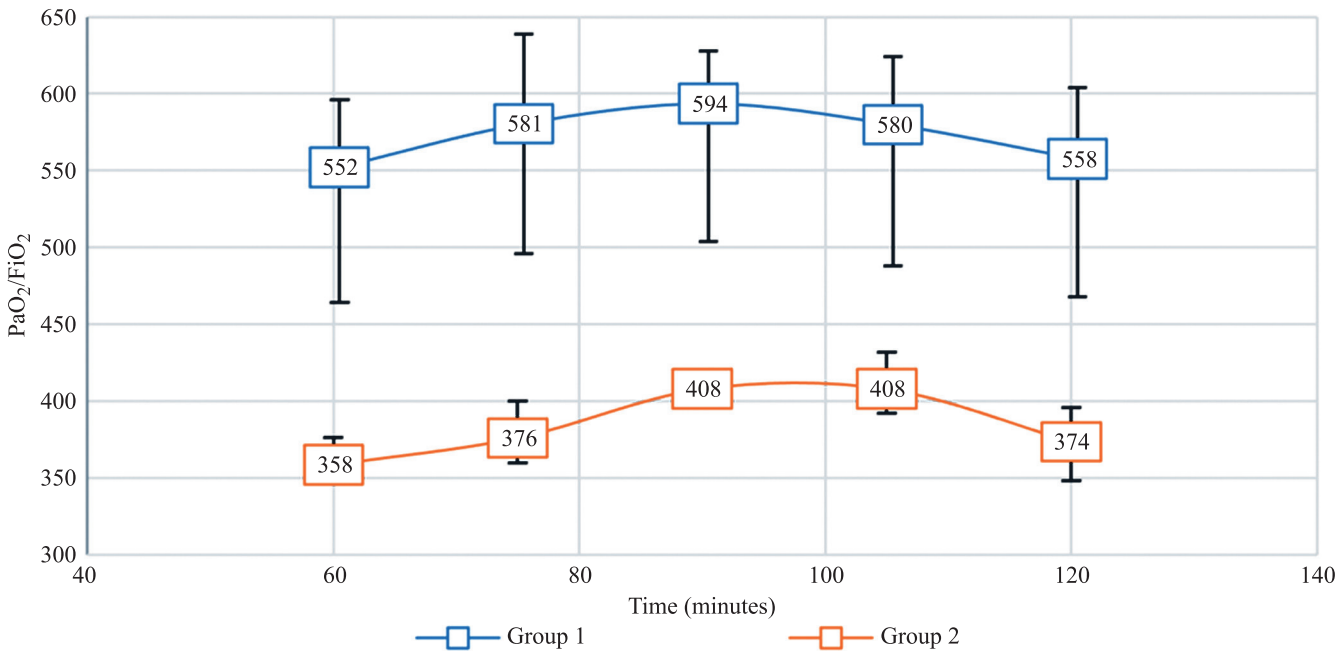

Fig. 5. Dynamics of changes in the PaO_2/FiO_2 ratio. The graph illustrates the mean oxygenation index (PaO_2/FiO_2) during normothermic EVLP. Values are presented as mean, minimum, and maximum. Measurements were taken at 60, 75, 90, 105, and 120 minutes

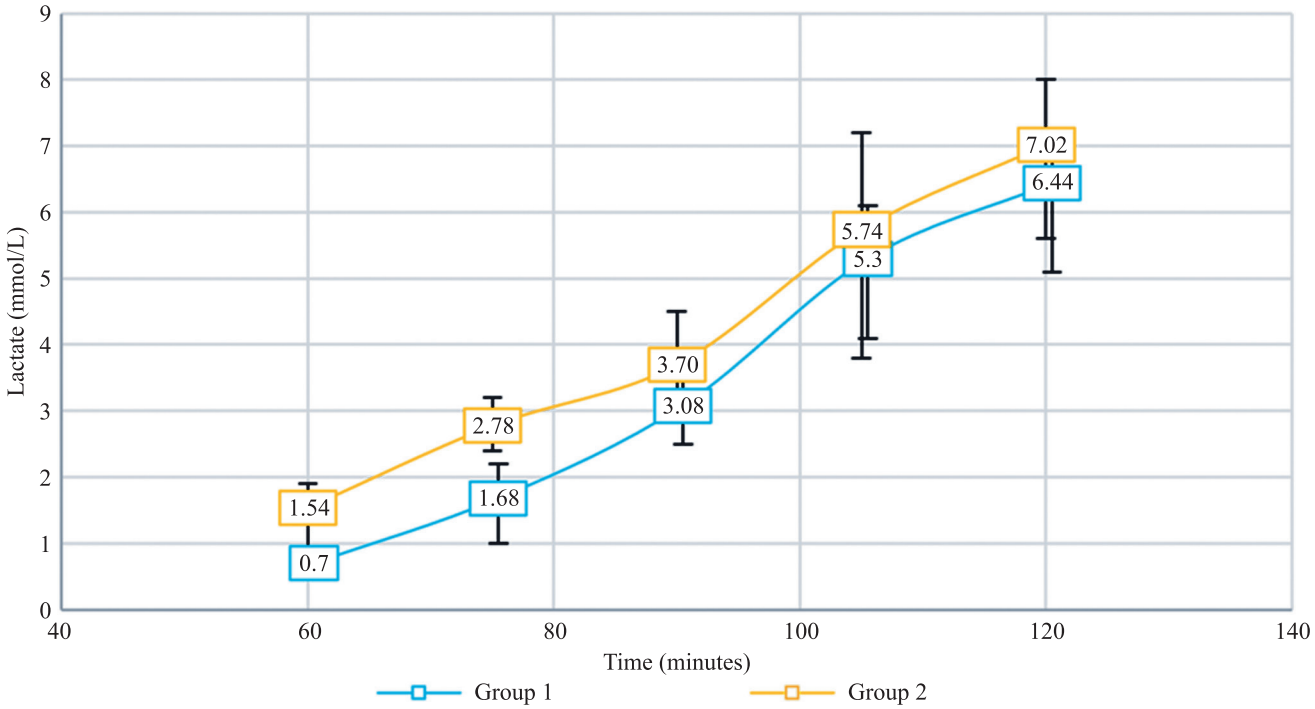

Fig. 6. Dynamics of lactate levels during *ex vivo* perfusion. The graph presents the mean lactate levels measured during normothermic EVLP. Values are shown as mean, minimum, and maximum. Measurements were taken at 60, 75, 90, 105, and 120 minutes

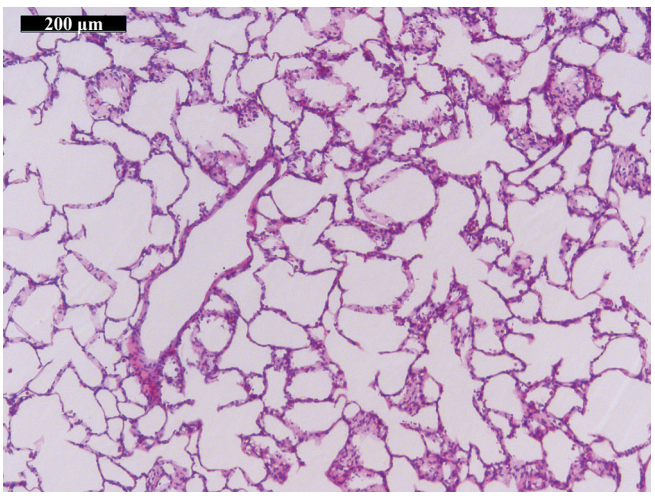

Fig. 7. Histological image of donor lung parenchyma after normothermic EVLP in Group 1 (Spanish protocol). Magnification: 200 µm

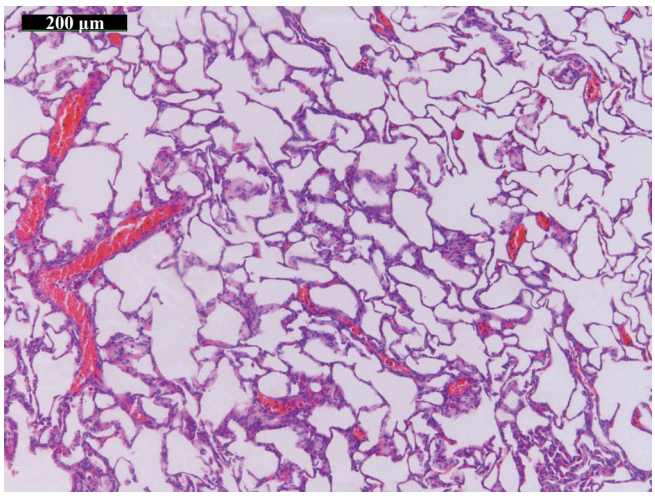

Fig. 8. Histological image of donor lung parenchyma after normothermic EVLP in Group 2 (Italian protocol). Magnification: ×200

ment of the graft. Histological changes were characterized by moderate interstitial edema in the parenchyma and subendothelial edema in the perivascular spaces (Fig. 8).

At 200 µm magnification, lung micro-preparations from group 2 showed fragments of parenchyma with pronounced hyperemia in both macro- and microcirculatory vessels, areas of dystelectasis, intra-alveolar hemorrhages, and desquamation of pneumocytes. Particular importance was attached to the classic signs of dysfunction associated with ischemia-reperfusion injury – edema of the interalveolar septa accompanied by mixed inflammatory infiltration of the interstitium.

DISCUSSION

Data from this experimental study enabled a comparative assessment of two donor lung procurement protocols in DCD donors – topical cooling versus continued MV after cardiac arrest. EVLP outcomes indicate that the topical cooling technique provides more stable gas exchange and metabolic activity of the transplant. Specifically, the OI in group 1 (topical cooling) was consistently

higher at all observation time points compared to group 2 (continued MV), suggesting better preservation of the alveolar-capillary membrane and reduced severity of ischemic injury. Lactate levels in group 1 remained lower, reflecting more efficient tissue metabolism and reduced accumulation of anaerobic glycolysis products. This likely results from faster and more uniform warm protection of the lung parenchyma achieved through topical cooling, whereas continued ventilation after cardiac arrest may offer insufficient protection against reperfusion injury and, in some cases, exacerbate alveolar edema, as confirmed endoscopically in two observations in group 2. Notably, both protocols employed the same dextran-40-based preservative solution, minimizing variability due associated with composition of the perfusate and allowing us to focus on the differences between the procurement methods.

The presented data suggest that the lung procurement technique using topical cooling provides a more pronounced protective effect in the DCD model compared to continuous MV. This finding aligns with previous clinical and experimental studies emphasizing the importance of rapid initiation of cooling and minimization of reperfusion stress as key factors for successful preservation of lungs from DCD donors [16, 17]. Limitations of the present study include the small sample size and the use of a surrogate animal model (rabbits), which warrants caution when extrapolating these results to clinical practice. Nevertheless, the findings provide a solid foundation for further research and optimization of protocols for conditioning lungs from DCD donors.

CONCLUSION

This experimental study confirmed the feasibility of lung donation after cardiac arrest with normothermic normothermic EVLP using an original dextran-40-based preservation and perfusion solution. The use of this solution allowed donor lungs to be preserved without significant alveolar edema in most cases and maintained satisfactory gas exchange function during perfusion. The results indicate that lung procurement with topical cooling provides more effective organ preservation, as reflected by superior oxygenation and metabolic indicators during perfusion. Consistent with published experimental and clinical studies, the clinical implementation of lung donation after circulatory death has the potential to increase the donor pool without substantially raising the risk of primary graft dysfunction, while maintaining long-term survival rates comparable to those observed with lungs from brain-dead donors.

The authors declare no conflict of interest.

REFERENCES

1. *Valapour M, Lehr CJ, Skeans MA, Smith JM, Uccellini K, Lehman R et al.* OPTN/SRTR 2017 Annual Data Report: Lung. *Am J Transplant*. 2019 Feb; 19 Suppl 2: 404–484. doi: 10.1111/ajt.15279.
2. *Cypel M, Sato M, Yildirim E, Karolak W, Chen F, Yeung J et al.* Initial experience with lung donation after cardiocirculatory death in Canada. *J Heart Lung Transplant*. 2009 Aug; 28 (8): 753–758. doi: 10.1016/j.healun.2009.05.009.
3. *Van Raemdonck D, Ceulemans LJ, Neyrinck A, Levvey B, Snell GI*. Donation After Circulatory Death in lung transplantation. *Thorac Surg Clin*. 2022 May; 32 (2): 153–165. doi: 10.1016/j.thorsurg.2021.11.002.
4. *Inci I, Hillinger S, Schneiter D, Opitz I, Schuurmans M, Benden C, Weder W.* Lung Transplantation with Controlled Donation after Circulatory Death Donors. *Ann Thorac Cardiovasc Surg*. 2018 Dec 20; 24 (6): 296–302. doi: 10.5761/atcs.oa.18-00098.
5. *Erasmus ME, Verschuuren EA, Nijkamp DM, Vermeyden JW, van der Bij W.* Lung transplantation from nonheparinized category III non-heart-beating donors. A single-centre report. *Transplantation*. 2010 Feb 27; 89 (4): 452–457. doi: 10.1097/TP.0b013e3181c46a74.
6. *Cypel M, Levvey B, Van Raemdonck D, Erasmus M, Dark J, Love R et al.* International Society for Heart and Lung Transplantation. International Society for Heart and Lung Transplantation Donation After Circulatory Death Registry Report. *J Heart Lung Transplant*. 2015 Oct; 34 (10): 1278–1282. doi: 10.1016/j.healun.2015.08.015.
7. *Cypel M, Yeung JC, Liu M, Anraku M, Chen F, Karolak W et al.* Normothermic *ex vivo* lung perfusion in clinical lung transplantation. *N Engl J Med*. 2011 Apr 14; 364 (15): 1431–1440. doi: 10.1056/NEJMoa1014597.
8. *Spratt JR, Mattison LM, Iaizzo PA, Meyer C, Brown RZ, Iles T et al.* Lung transplant after prolonged *ex vivo* lung perfusion: predictors of allograft function in swine. *Transpl Int*. 2018 Dec; 31 (12): 1405–1417. doi: 10.1111/tri.13315.
9. *Gomez-de-Antonio D, Campo-Cañaveral JL, Crowley S, Valdivia D, Cordoba M, Moradiellos J et al.* Clinical lung transplantation from uncontrolled non-heart-beating donors revisited. *J Heart Lung Transplant*. 2012 Apr; 31 (4): 349–353. doi: 10.1016/j.healun.2011.12.007.
10. *De Antonio DG, Marcos R, Laporta R, Mora G, García-Gallo C, Gámez P et al.* Results of clinical lung transplant from uncontrolled non-heart-beating donors. *J Heart Lung Transplant*. 2007 May; 26 (5): 529–534. doi: 10.1016/j.healun.2007.01.028.
11. *Rodríguez DA, Del Río F, Fuentes ME, Naranjo S, Moradiellos J, Gómez D et al.* Trasplante de pulmón con donantes no controlados a corazón parado. Factores pronósticos dependientes del donante y evolución inmediata postrasplante [Lung transplantation with uncontrolled non-heart-beating donors. Transplantation. Donor prognostic factor and immediate evolution post transplant]. *Arch Bronconeumol*. 2011 Aug; 47 (8): 403–409. Spanish. doi: 10.1016/j.arbres.2011.04.009.
12. *Palleschi A, Zanella A, Citerio G, Musso V, Rosso L, Tosi D et al*. Lung Transplantation From Controlled and Uncontrolled Donation After Circulatory Death (DCD) Donors With Long Ischemic Times Managed by Simple Normothermic Ventilation and *Ex-Vivo* Lung Perfusion

Assessment. *Transpl Int*. 2023 Feb 8; 36: 10690. doi: 10.3389/ti.2023.10690.

13. *Valenza F, Citerio G, Palleschi A, Vargiolu A, Fakhr BS, Confalonieri A et al.* Successful Transplantation of Lungs From an Uncontrolled Donor After Circulatory Death Preserved *In Situ* by Alveolar Recruitment Maneuvers and Assessed by *Ex Vivo* Lung Perfusion. *Am J Transplant*. 2016 Apr; 16 (4): 1312–1318. doi: 10.1111/ajt.13612.
14. *Gautier SV, Pashkov IV, Bogdanov VK, Oleshkevich DO, Bondarenko DM, Mozheiko NP et al*. Normothermic *ex vivo* lung perfusion using a developed solution followed by orthotopic left lung transplantation (experimental study). *Russian Journal of Transplantology and Artificial Organs*. 2023; 25 (2): 158–166. https://doi.org/10.15825/1995-1191-2023-2-158-166.
15. *Gautier SV, Tsirulnikova OM, Pashkov IV, Oleshkevich DO, Filatov IA, Bogdanov VK et al*. Normothermic *ex vivo*perfusion of isolated lungs in an experiment using a russian-made perfusion system. *Russian Journal of Transplantology and Artificial Organs*. 2022; 24 (2): 94–101. https://doi.org/10.15825/1995-1191-2022-2-94-101.
16. *Schroder JN, Patel CB, DeVore AD, Bryner BS, Casalinova S, Shah A et al.* Transplantation outcomes with donor hearts after circulatory death. *N Engl J Med*. 2023 Jun 8; 388 (23): 2121–2131. doi: 10.1056/NEJMoa2212438.
17. *Alzahrani A, Noda K, Chan EG, Ryan JP, Furukawa M, Sanchez PG.* The length of the warm ischemic interval in lung donation after circulatory death does not impact post-transplantation outcomes. *JHLT Open*. 2025 Mar 11; 8: 100244. doi: 10.1016/j.jhlto.2025.100244.

The article was submitted to the journal on 3.08.2025

DOI: 10.15825/1995-1191-2025-4-183-195

IMAGE-BASED CLUSTERING ANALYSIS OF CALCIFICATION PATTERNS IN BIOPROSTHETIC HEART VALVES

E.A. Ovcharenko, K.Yu. Klyshnikov, P.S. Onishchenko, A.E. Kostyunin, A.A. Khromov, A.N. Stasev, T.N. Akentyeva, M.P. Fokeeva, O.L. Barbarash, T.V. Glushkova

Research Institute for Complex Issues of Cardiovascular Diseases, Kemerovo, Russian Federation

Objective: to identify key patterns of calcification in explanted bioprosthetic heart valves (BHVs) using cluster analysis of computed tomography-derived graphical data. **Materials and methods.** The study included 11 UniLine BHVs that were routinely explanted during reoperations for structural valve dysfunction. Computed tomography was used to obtain DICOM images of each sample, followed by generation of maximum intensity projections and segmentation of the valves into individual leaflets (n = 33). The images were pre-processed using binary thresholding to differentiate calcified regions from non-calcified biological tissue. Cluster analysis was performed using various algorithms: Gaussian mixture models, Ordering Points To Identify the Clustering Structure (OPTICS), k-means clustering, agglomerative (hierarchical) clustering, and spectral clustering. A basic quantitative method assessing the proportion of pixels corresponding to calcified areas was used for comparison. The performance of clustering algorithms was evaluated using the silhouette score. The presence of calcium deposits in the valves and the accuracy of binary thresholding were further verified histologically by alizarin red S staining of valve cryosections. **Results.** Data preprocessing based on image binarization yielded a maximum silhouette score of 0.55. Among the clustering algorithms, the highest silhouette scores were achieved with the agglomerative (0.55) and k-means (0.54) methods; however, both demonstrated substantial data imbalance, with up to 85% of samples grouped within a single cluster, limiting their practical applicability. The most balanced clustering was achieved using spectral clustering (silhouette score 0.45) and the basic quantitative approach (0.44). Both methods identified three distinct patterns of bioprosthetic valve leaflet calcification: (1) non-calcified leaflets, (2) partial calcification, and (3) total calcification. **Conclusion.** Three key calcification patterns were identified in explanted BHVs – absence of calcium, partial calcification, and total calcification. Spectral clustering and the basic quantitative method demonstrated the most balanced results, while other algorithms showed pronounced cluster imbalance. Heat map analysis revealed that in partial calcification, mineral deposition typically begins in the commissural and dome regions of the leaflets, near the free edge, and in total calcification, extends across the entire dome and leaflet base.

Keywords: bioprosthetic heart valves; prosthetic valve dysfunction; structural valve degeneration; calcification; cluster analysis.

INTRODUCTION

The introduction of bioprosthetic heart valves (BHVs) has been a major advancement in treating valvular heart disease. Owing to their physiological hemodynamic performance and the absence of a need for long-term anticoagulant therapy, BHVs are widely used in clinical practice. In 2022, 2,526 surgical and 1,633 transcatheter BHVs were implanted in the Russian Federation [1, 2]. However, their long-term durability remains a limitation due to structural valve degeneration, which ultimately leads to hydrodynamic failure. Literature reports indicate that within 10–15 years, up to half of BHVs made from xenopericardial material develop dysfunction [3]. Such cases necessitate repeat valve replacement, a procedure associated with significantly higher risks of serious complications and mortality compared with primary interventions [4–6].

In more than half of cases, calcification of the valve apparatus is the primary cause of BHV dysfunction [7]. Calcium deposition in the leaflets increases their stiffness, leading to characteristic clinical manifestations such as a high transprosthetic gradient, elevated flow velocity, and a reduced effective orifice area [8, 9].

Bioprosthetic tissue mineralization is a multifactorial process driven by the interplay of several mechanisms. These include passive calcium deposition on residual donor cells, chemically cross-linked collagen, and damaged elastic fibers, as well as active biomineralization involving apoptotic immune cells and circulating recipient factors [10]. Cyclic mechanical loading further accelerates calcification by inducing fatigue damage in collagen fibers, thereby creating sites susceptible to mineral deposition [11].

Current research actively investigates the causes and biomechanical consequences of BHV calcification to

Corresponding author: Evgeny Ovcharenko. Address: 6, Akademika Leonida Barbarasha bul'var, Kemerovo, 650002, Russian Federation.
Phone: (3842) 34-53-77. E-mail: ovchea@kemcardio.ru

develop strategies that extend their functional lifespan. One approach to elucidating calcification mechanisms involves analyzing characteristic regions and patterns of mineral deposition within valve structures. Such studies can identify areas most prone to mineralization, their relationship with mechanical stress, and potential directions for improving prosthesis design.

Existing literature presents two contrasting perspectives. Some studies demonstrate distinct and reproducible calcification patterns correlated with regions of high hemodynamic and mechanical stress [12–15] or draw analogies with native valve calcification patterns applicable to BHVs [16, 17]. Others, however, report a random distribution of mineral deposits, focusing solely on the extent and severity of calcification without defining its spatial organization [18, 19]. Both viewpoints are supported by qualitative and quantitative evidence, making it difficult to establish a unified concept of calcification distribution in BHVs.

This study aims to enhance understanding of the characteristic patterns of calcium deposit localization in explanted BHVs treated with ethylene glycol diglycidyl ether, using cluster analysis of computed tomography (CT)-derived graphical data.

MATERIALS AND METHODS

Data acquisition and preparation

The study was based on DICOM images of explanted BHVs obtained using multislice computed tomography (MSCT) on a LightSpeed™ VCT 64 scanner (General Electric, USA). All samples were mounted on a stage and scanned under the following parameters: tube voltage – 120 kV, current – 160 mA, rotation time – 0.9 s, total scan time – 6.8 s, and scan speed – 39.37 mm/rev. Image reconstruction was performed with a slice thickness of 0.625 mm using a standard reconstruction kernel.

Table 1

Clinical characteristics of patients from whom explanted bioprosthetic heart valves were obtained

Parameter	Value
Age at the time of valve replacement, median [Q1; Q2], years	57 [44.75; 65.75]
Gender:	
Male, n (%)	6 (55%)
Female, n (%)	5 (45%)
Reason for valve replacement:	
Structural valve degeneration, n (%)	6 (55%)
Prosthetic endocarditis, n (%)	5 (45%)
Coexisting diseases:	
Hypertensive disease, n (%)	3 (27%)
Dyslipidemia, n (%)	2 (18%)
Diabetes mellitus, n (%)	1 (9%)
Chronic kidney disease, n (%)	7 (64%)
Prosthesis functioning period, median [Q1; Q2], years	2.75 [0.79; 5.90]

A total of 11 Uniline xenopericardial atrioventricular BHVs were analyzed. These prostheses had been routinely explanted and replaced at the Research Institute for Complex Issues of Cardiovascular Diseases in Kemerovo, Russia between 2015 and 2024. A brief clinical description of the patients is provided in Table 1.

The DICOM images obtained were processed as maximum intensity projections (MIP) in a top-view orientation. Each prosthesis image was then manually segmented into three leaflets and aligned into a unified position to achieve an overlay of all leaflets from the 11 samples (Fig. 1).

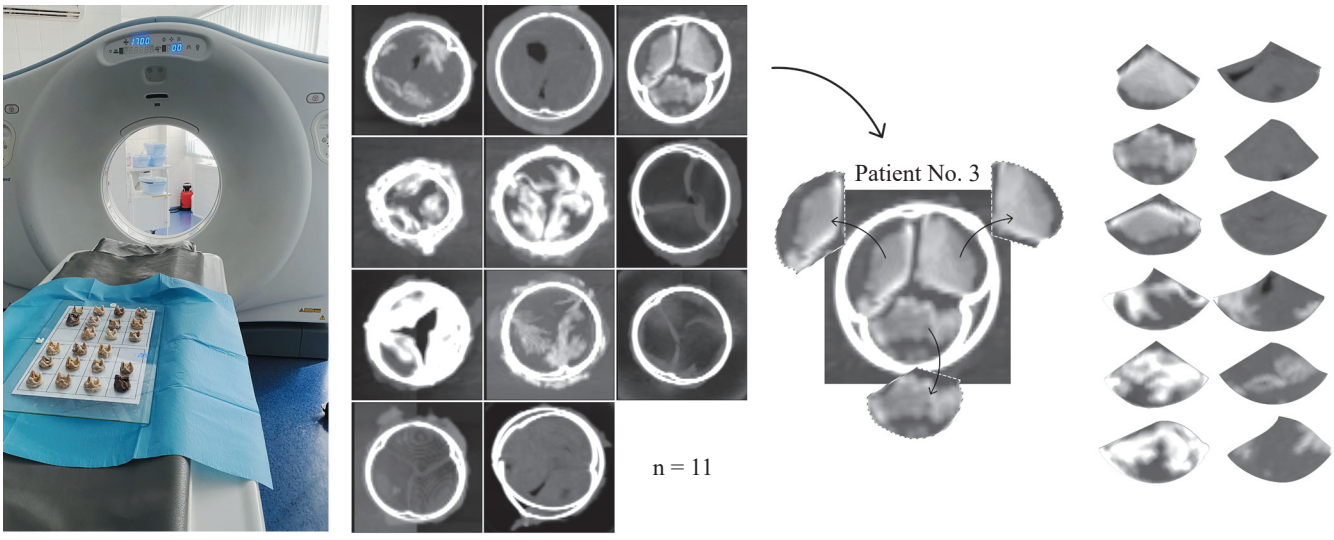

Fig. 1. Workflow for obtaining input data for the segmentation algorithm. An enlarged sequence is presented, from CT scanning of the explanted bioprosthetic heart valves to obtaining images of individual valves used for clustering

The resulting dataset – comprising 33 individual leaflets represented as separate images – was subjected to cluster analysis using various data preprocessing strategies and clustering algorithms.

Data preprocessing strategies

Three preprocessing strategies were applied:

1) **Raw data:** Processing of raw DICOM images without any modifications.
2) **Image binarization to identify calcified regions** (calcified tissue only). A binary thresholding method was applied, where pixels with an intensity range of 193–255 were assigned a value of 255, and all others were set to 0. This approach enabled clear identification of calcified regions, which is clinically relevant for assessing valve degeneration.
3) **Combined representation** (calcified and non-calcified tissue): In this approach, pixels were differentiated in a more detailed way. Pixels with intensities from 193 to 255 were set to 255 (indicating calcification), while those from 1 to 192 were set to 124 (representing non-calcified biomaterial). This strategy allowed for simultaneous highlighting of calcified and soft tissue areas, which facilitated a more detailed analysis of the images obtained.

Clustering algorithms

Basic method. This approach served as a reference (comparison) method. Clustering was performed artificially based on calcium levels. All images were binarized using a threshold of 193/255, after which the number of white pixels – corresponding to areas of valve mineralization – was calculated. The median and quartile values of this parameter were then determined. Based on these statistics, three clusters were defined: low calcification (images with calcium content below the median); medium (images within the third quartile [50–74% of the sample]; high calcification (images within the fourth quartile [75–100% of the sample]).

The following clustering algorithms were applied in the study:

1) **Gaussian Mixture Models (GMM).** This probabilistic model was selected for its ability to represent data as a combination of probability distributions, allowing estimation of intra-cluster variance. GMM is well suited for heterogeneous image datasets, particularly when clusters overlap or have uneven density [20].
2) **Ordering Points to Identify the Clustering Structure (OPTICS).** OPTICS was used to detect clusters of arbitrary shape under conditions of variable data density. Its robustness makes it effective for analyzing fragmented or irregular structures, such as those found in medical images affected by artifacts or low signal-to-noise ratios [21].
3) **k-Means Method.** The k-means algorithm was chosen for its computational efficiency and scalability, which are advantageous in large-scale image segmentation. Although it assumes spherical cluster geometry, its simplicity and established performance in image analysis justify its inclusion in the study [20].
4) **Agglomerative Clustering.** This hierarchical approach was employed to uncover nested structure within the data, enabling a detailed examination of images with multi-scale structural patterns [22].
5) **Spectral Clustering.** This algorithm was applied to identify complex, non-spherical data structures. Its effectiveness in separating non-linearly separable clusters has been confirmed in a number of studies [22].

Indicators analyzed

The study evaluated several quantitative and qualitative indicators to evaluate the performance of the clustering algorithms.

1) **Silhouette score:** This metric, ranging from –1 to +1, was used to assess cluster compactness and separability. Values close to +1 indicate well-defined, cohesive clusters with minimal overlap, while negative values suggest incorrect or ambiguous data partitioning [23].
2) **Clustered image grouping with label display.** Images assigned to each cluster were organized in matrix form with corresponding textual labels. This visualization enabled qualitative assessment of cluster semantic consistency, detection of anomalies, and analysis of object distribution within groups.
3) **Principal component analysis (PCA) visualization.** PCA was employed for linear dimensionality reduction, allowing the data to be represented in a two-dimensional (2D) space. This facilitated assessment of data dispersion and cluster separability.
4) **t-distributed stochastic neighbor embedding (t-SNE) visualization.** Nonlinear dimensionality reduction using t-SNE [24] was applied to visualize clusters with complex, non-linear structures while preserving local relationships between points. The results were compared with PCA visualizations to assess the stability of the identified clustering patterns.
5) **Maximum intensity projections (MIP).** To evaluate the spatial distribution of calcifications, all image slices (frames) were combined into a single 2D projection by selecting the maximum pixel intensity values along the Z-axis.
6) **Heat map of relative cumulative calcium distribution.** Using normalized pixel intensities (range [0–1]), aggregated maps of calcification density were generated for both the overall dataset and individual clusters. This visualization highlighted probabilistic differences in the density and spatial organization of calcifications between groups.

The technical implementation of preliminary data processing, clustering analysis, and data visualization

was carried out in the Python 3.11 programming environment using the OpenCV, NumPy, Pandas, and Scikit-learn libraries. The complete program code is available at: https://github.com/Eugene-Ovcharenko/BHV_leaflet_images_clustering.git.

Visualization of calcium using histological methods

The study results were validated through histological analysis. After MSCT scanning, the valve leaflets were carefully separated from the BHV frame to prepare histological sections. Fragments of the biomaterial were fixed in Neg-50 rapid tissue freezing medium (6502, Thermo Fisher Scientific, USA), and serial cryosections were obtained using an HM525 microtome-cryostat (Thermo Fisher Scientific, USA). The resulting sections, 5 μm thick, were placed on microscope slides.

Calcium deposits were visualized by staining the sections with Alizarin Red S (ab142980, Abcam) according to the manufacturer's instructions. The stained sections were examined under a Meiji Techno MT5300L automated laboratory biological microscope, and subsequent image processing was performed using QuPath 0.4.1 software.

RESULTS

In total, this study produced 325 clustering variants of MSCT data, combining different image preprocessing strategies, clustering algorithms, variable cluster numbers (ranging from 2 to 5), and algorithm-specific hyperparameters. Given the exploratory nature of the analysis, the results were evaluated sequentially according to: data preprocessing strategies, clustering algorithms, and the most effective combinations of both.

Data preprocessing strategies

All preprocessing approaches had a marked impact on the analyzed imaging data (Fig. 2a). Image binarization on calcium intensity threshold, visualized using principal component analysis (Fig. 2b), revealed some distinguishable regions that could be further separated into distinct groups. However, most data points overlapped due to the predominance of empty (non-calcified) areas after binarization.

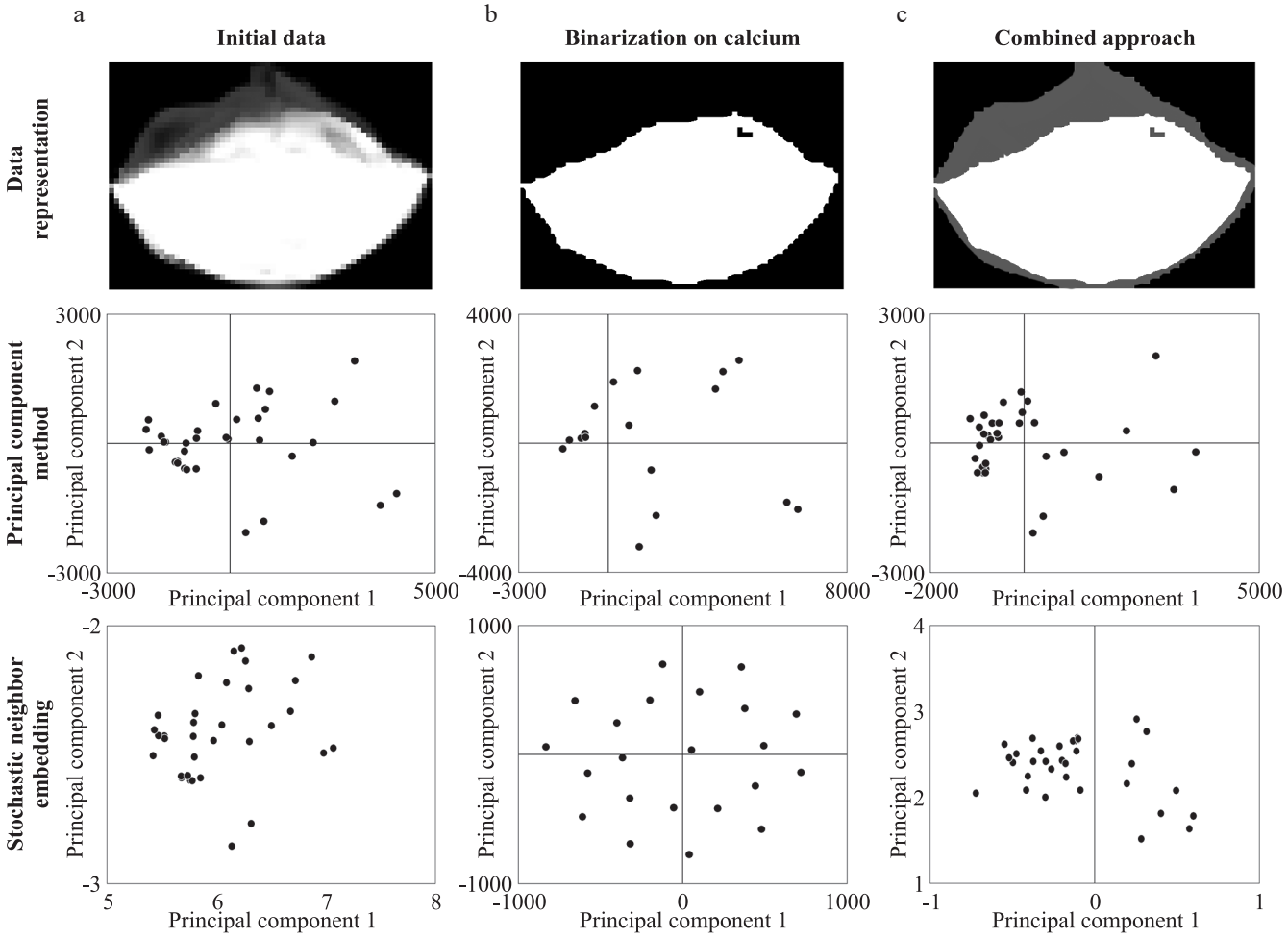

Fig. 2. Visualization of different data preprocessing strategies. Shown are examples of maximum intensity projection (MIP), principal component analysis (PCA) visualization, and t-distributed stochastic neighbor embedding (t-SNE) visualization applied to images of bioprosthetic valve leaflets

The combined option, consisting of a combination of binarized data on calcium threshold and biomaterial threshold, also provided clearer separation and superior visualization when analyzed using t-SNE (Fig. 2c).

Importantly, histological examination of the BHV leaflets confirmed the accuracy of the image binarization results: the locations of macrocalcifications observed in histological sections corresponded closely with the mineralization patterns identified from the processed MSCT images (Fig. 3).

Quantitative analysis of the clustering results across the three preprocessing strategies revealed that only one approach – image binarization based on the calcium threshold – produced satisfactory silhouette scores (Table 2). This method achieved a score of 0.55, which is considered high within the possible range of –1 to +1.

Clustering algorithms

Analysis of the results revealed a marked variation in clustering quality depending on the algorithm used (Table 3). The OPTICS algorithm proved ineffective in this context, showing an extremely low silhouette score close to zero. Other algorithms performed better, achieving silhouette scores in the range of 0.54–0.55 in the best cases. However, in most instances, the resulting clusters were highly unbalanced. Specifically, algorithms with higher silhouette scores consistently produced one dominant cluster (Class I) and two much smaller clusters (Classes II and III), comprising only 3–18% of the dataset. This pronounced imbalance indicates that the observed groupings likely do not reflect distinct patterns of calcification.

Among all the results presented, two configurations stood out: No. 0346 (Basic) and No. 0159 (Spectral) (Table 3). Both demonstrated moderate silhouette scores of 0.44 and 0.45, respectively, with a relatively balanced class distribution. In these cases, the primary class comprised 52% and 64% of the images, respectively, while Classes II and III included 15–24% of the dataset. Overall, these results indicated the presence of distinct

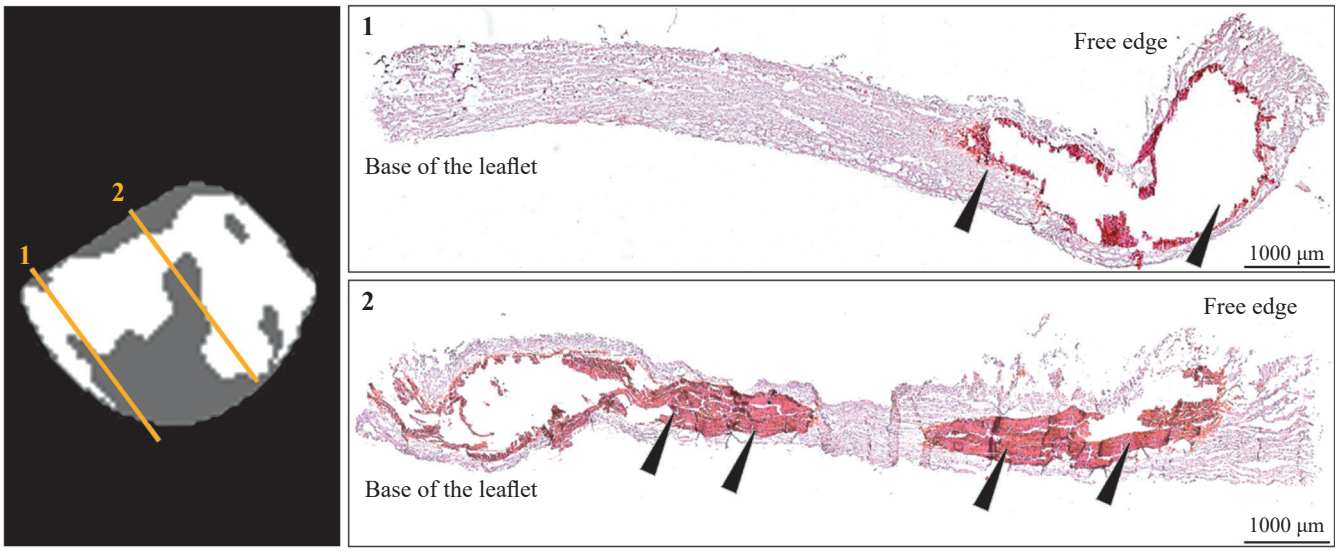

Fig. 3. Comparison between the binarized image of the valve and the corresponding histological section stained with alizarin red S. Arrows indicate areas of calcium deposition

Table 2

Quantitative characteristics of clustering algorithms, grouped by data preprocessing strategy

No.	Strategy	Number of clusters	Silhouette score	Cluster I size, %	Cluster II size, %	Cluster III size, %
0043	Initial data	3	0.37	91	6	3
0042	Initial data	3	0.33	12	82	6
0041	Initial data	3	0.30	58	30	6
0159	Binarization	3	0.55	9	85	6
0346	Binarization	3	0.55	9	85	6
0166	Binarization	4	0.54	85	6	6
0274	Combined	3	0.08	21	58	21
0273	Combined	3	0.07	21	33	45
0271	Combined	3	0.07	21	24	55

Note: For clarity, the table includes only the three preliminary data preprocessing strategies that achieved the best silhouette scores. All other configurations demonstrated significantly lower performance.

calcification classes. The clustering outcomes of these two algorithms (No. 0346 and No. 0159) are illustrated in Fig. 4, showing the division of the dataset into separate classes corresponding to specific calcification patterns. Qualitative analysis revealed that both methods identified three main heterogeneous groups: absence of calcium, partial calcification, and total calcification. It is worth noting that the spectral method misclassified five images exhibiting partial calcification into Cluster I (absence of calcium), which slightly distorted the result.

The next phase of the study involved merging the individual images associated with each cluster to form representative calcification patterns. These patterns were grouped into three categories: no calcification, partial calcification, and total calcification of the valve (Fig. 5).

The next stage of the study involved combining individual images from each cluster into distinct calcification patterns: absence of calcium, partial calcification, and total calcification (Fig. 5). Heat maps generated using two clustering algorithms (basic and spectral) illustrated the probability distribution of mineralization within the leaflet apparatus of the BHVs. Overall, the patterns obtained by both methods were largely consistent; however, the spectral method more distinctly identified certain leaflets with low levels of calcification within cluster I, resulting in qualitative differences between the heat maps. Notably, in cluster II (partial calcification), calcium deposits were predominantly located in the commissural zone and along the valve dome near the free edge, whereas in cluster III (total calcification), they were concentrated in the central portion of the leaflet dome. The PCA diagram (Fig. 6) helps explain this phenomenon: the spectral algorithm tended to assign cluster I (no calcification) to images situated very close to those in cluster II. Thus, the heat map analysis revealed differences between clusters not only in the extent of calcification but also in its spatial distribution.

DISCUSSION

Calcification of BHVs is a multifactorial process driven by a complex interplay of material changes [10]. Research groups have extensively investigated both native heart valves [25] and their bioprosthetic counterparts [12–14] in an effort to identify clinical and metabolic predictors of this condition [26, 27]. An important method for determining the causes and characteristics of bioprosthetic calcification is the analysis of mineral deposit distribution within the valve apparatus.

According to literature reports, investigators have reached two contrasting conclusions when interpreting existing data: some describe a distinct pattern in the localization of calcium deposits, whereas others emphasize their random distribution [12–15, 28, 29]. On one hand, studies correlating calcium accumulation with regions of high mechanical or shear stress have demonstrated well-defined localization patterns [12–15]. The areas of greatest mechanical loading, primarily the valve dome and commissural zones, are therefore regarded as predisposed to mineralization. On the other hand, several authors attribute bioprosthetic calcification to the infiltration of blood-derived molecular components and subsequent immune responses to xenogeneic tissue [28, 29]. Within this framework, the entire volume of the biomaterial becomes a potential target for calcification, and it is not possible to identify a single characteristic pattern [18, 19].

Table 3

Quantitative characteristics of clustering algorithms

No.	Clustering algorithm	Number of clusters	Silhouette score	Cluster I size, %	Cluster II size, %	Cluster III size, %
0346	**Basic**	**3**	**0.44**	**52**	**24**	**24**
0138	Gaussian mixture	3	0.50	76	18	6
0136	Gaussian mixture	3	0.50	79	15	6
0137	Gaussian mixture	3	0.50	79	15	6
0113	OPTICS	3	0.04	24	18	58
0114	OPTICS	2	–0.01	24	76	–
0343	OPTICS	3	–0.08	12	18	70
0120	k-means	3	0.54	82	6	12
0121	k-means	3	0.54	82	6	12
0122	k-means	3	0.54	82	6	12
0198	Agglomerative	3	0.55	85	9	6
0199	Agglomerative	3	0.55	85	9	6
0201	Agglomerative	3	0.53	91	3	6
0159	**Spectral**	**3**	**0.45**	**64**	**15**	**21**
0162	Spectral	3	0.28	27	55	18
0163	Spectral	3	0.28	27	55	18

Note: For clarity, the table includes only the three clustering algorithms that achieved the best silhouette scores. All other algorithms demonstrated significantly lower performance. Minor classes (small cluster sizes) are highlighted in gray.

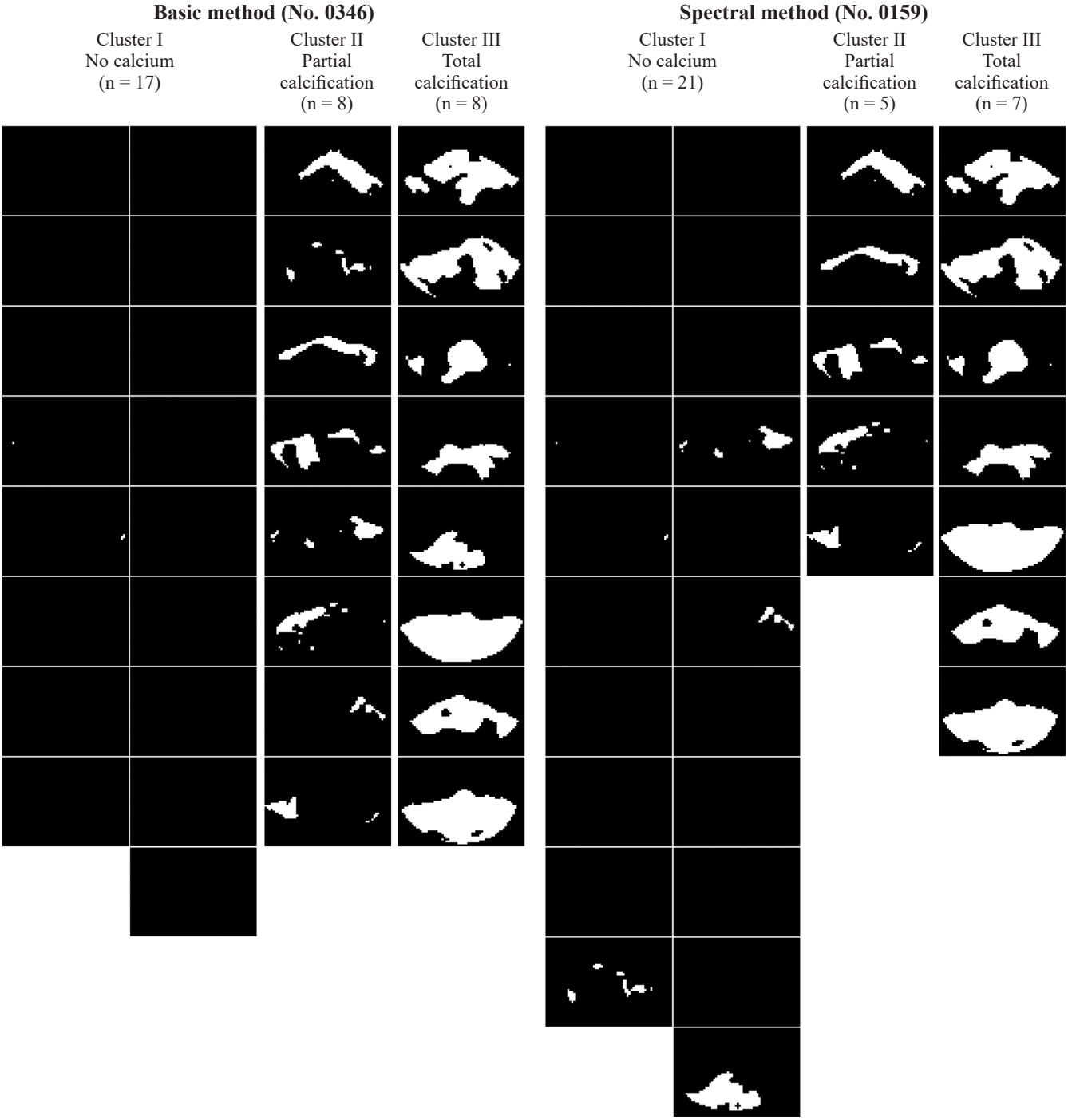

Fig. 4. Visualization of the distribution of valve images after threshold-based calcium detection. The figure illustrates the results obtained using the two most effective clustering algorithms – basic and spectral clustering. Three distinct classes are identified: absence of calcium, partial calcification, and total calcification

Our previous pilot study [30], together with the present investigation, largely supports the former hypothesis – that regions of mineralization tend to colocalize with areas of increased mechanical stress on the valve leaflets. However, the current results provide a more detailed characterization of the extent and spatial distribution of calcium deposits across different degrees of mineralization – we were able to identify the leaflet regions most frequently affected in cases of partial and total calcification.

For cluster II (partial calcification), the predominant areas of mineralization were located in the commissural region and along the valve dome near the free edge, whereas for cluster III (total calcification), calcification was concentrated in the central portion of the dome (Fig. 5). This suggests that the calcification process develops progressively – from initial involvement of the commissures and the line of coaptation to subsequent extension into the dome region.

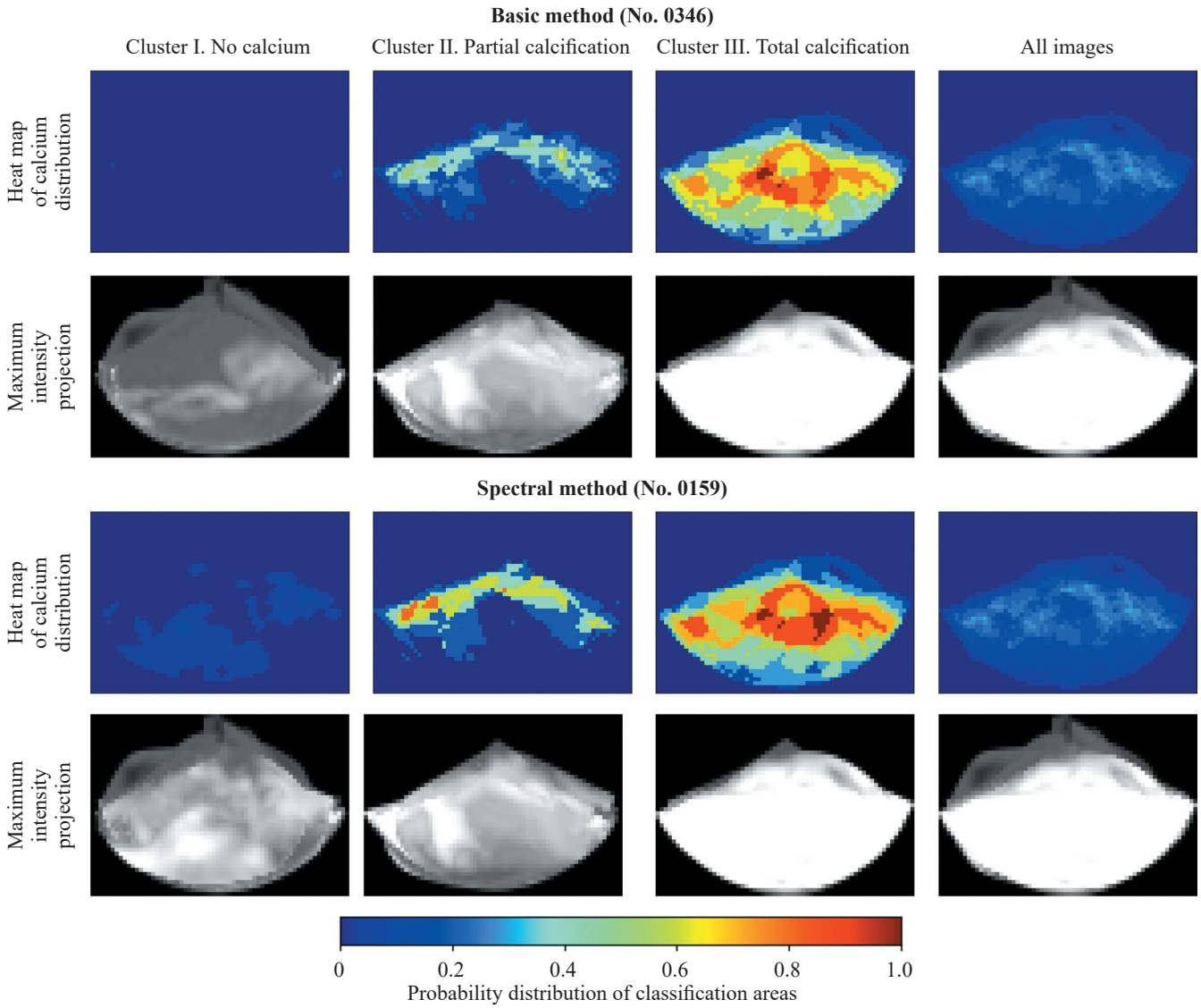

Fig. 5. Final image of calcification clusters obtained using the two most effective approaches – the basic method and the spectral clustering algorithm. The data are presented as a heat map of the relative cumulative distribution of calcium and as an overlay of all the original MSCT images

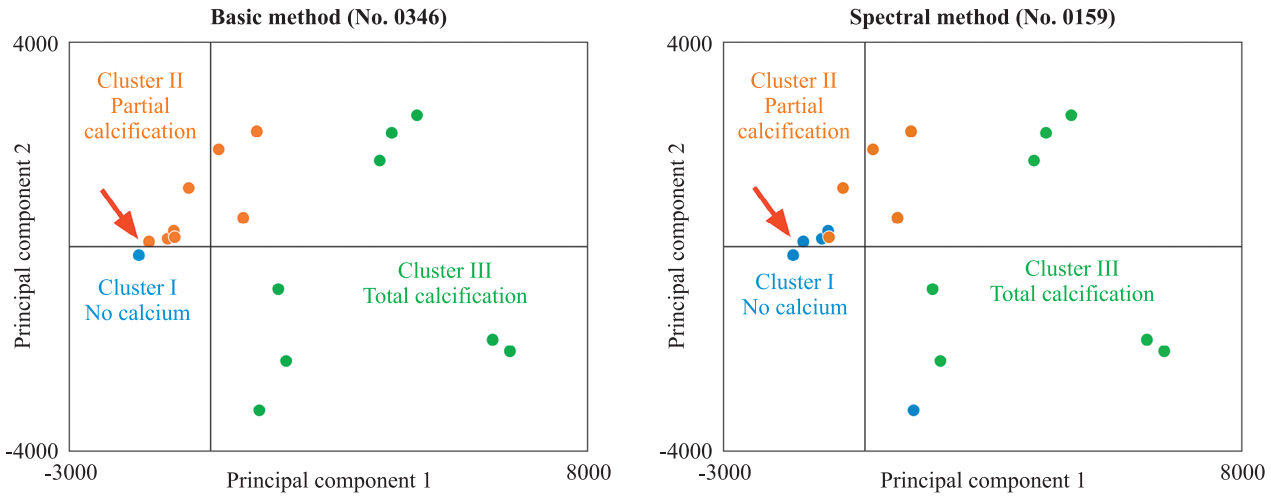

Fig. 6. Principal component analysis (PCA) diagram characterizing the identified clusters of calcification images. Results for both of the most effective algorithms are presented. The arrows indicate key differences between the two algorithms – in clusters I and II. Note: Because of point overlap, cluster I appears as a single point, as all empty images after binarization have the same coordinates within the principal component space

However, the present results do not allow this hypothesis to be confirmed, as further investigation is required.

It is noteworthy that a similar pattern of calcification was observed for both foreign (literature data) and domestic (this study) bioprostheses, despite differences in biomaterial preservation techniques. In a study by Tsolaki et al. (2023) involving Perimount Magna Ease bioprosthetic valves (n = 14) stabilized with glutaraldehyde, the valve dome was identified as the region most susceptible to calcification [12]. In the current study, domestically produced prostheses preserved with ethylene glycol diglycidyl ether exhibited comparable localization of mineralization, primarily within the dome region. This concordance likely reflects the dominant role of mechanical stress as a key factor promoting or accelerating calcification, given that the greatest stress occurs within the dome of the valve leaflet [12].

Finally, it is worth briefly highlighting the applied aspect of this study. From a practical standpoint, the identified calcification patterns make it possible to determine the most vulnerable regions of bioprosthetic valves and to outline potential directions for their structural optimization. For example, the predominant localization of calcium deposits in specific areas of the valve leaflets can be considered in the design of new biomaterials or in modifying valve geometry to reduce mechanical stress, one of the key factors contributing to prosthesis dysfunction [10–15].

From a methodological perspective, analyzing the technical component of the work revealed that data preprocessing techniques significantly influenced the quality of clustering. The most effective approach was image binarization based on a calcium intensity threshold, which yielded the highest silhouette score (0.55), reflecting clear structural differentiation among samples. In contrast, a combined preprocessing strategy – smoothing the brightness range while retaining original, non-binarized images – proved less effective. Thus, binary segmentation of pixels into calcified and non-calcified regions enhances both the accuracy of clustering and the identification of structural patterns associated with pathological changes. This result is quite expected, given that MSCT imaging of bioprostheses is primarily intended to visualize calcium deposits, which therefore serve as the principal criterion for cluster formation: the more pronounced the calcified regions, the easier it is to cluster images.

A comparison of the clustering algorithms demonstrated that the most balanced results were obtained using the spectral algorithm and the basic method. Both approaches provided satisfactory grouping of bioprosthetic valve images into three distinct classes: without calcification, with partial calcification, and with total calcification. In contrast, the Gaussian mixture model, k-means, and agglomerative clustering achieved relatively high silhouette scores but exhibited significant class imbalance, with uneven sample distribution across clusters, thereby complicating the interpretation of results.

CONCLUSION

The optimal method for preprocessing MSCT images of BHVs explanted due to dysfunction was image binarization on the threshold of calcium X-ray density, as determined by clustering quality assessment. Among the tested clustering algorithms, the spectral clustering proved to be the most effective, allowing balanced clusters to be identified based on calcium distribution.

Analysis of the calcification characteristics in BHVs explanted due to dysfunction revealed three key calcification patterns, clearly differentiated by the ratio of mineralized to intact biomaterial: non-calcified leaflets, partial calcification, and total calcification. These characteristic patterns correspond to the extent of structural alteration and are presumably localized in regions exposed to the greatest mechanical stress. Heat maps illustrating the probability of calcium localization showed that, in partial calcification, mineralization predominantly affects the commissural areas and the valve dome near the free edge, whereas in total calcification, calcium deposition extends across the entire dome region.

The authors declare no conflict of interest.

REFERENCES

1. *Bokeriya LA, Milievskaya EB, Pryanishnikov VV, Yurlov IA.* Serdechno-sosudistaya khirurgiya – 2022. Bolezni i vrozhdennye anomalii sistemy krovoobrashcheniya. M.: NMITs SSKh im. A.N. Bakuleva, 2023; 344. (In Russ.).
2. *Alekyan BG, Grigor'yan AM, Staferov AV, Karapetyan NG.* Rentgenendovaskulyarnaya diagnostika i lechenie zabolevaniy serdtsa i sosudov v Rossiyskoy Federatsii – 2021 god. *Endovaskulyarnaya khirurgiya.* 2022; 9: 1–254. (In Russ.). doi: 10.24183/2409-4080-2022-9S.
3. *Wang M, Furnary AP, Li H-F, Grunkemeier GL.* Bioprosthetic Aortic Valve Durability: A Meta-Regression of Published Studies. *Ann Thorac Surg*. 2017 Sep; 104 (3): 1080–1087. doi: 10.1016/j.athoracsur.2017.02.011.
4. *Kaneko T, Vassileva CM, Englum B, Kim S, Yammine M, Brennan M et al.* Contemporary outcomes of repeat aortic valve replacement: A benchmark for transcatheter valve-in-valve procedures. *Ann Thorac Surg.* 2015 Oct; 100 (4): 1298–1304. doi: 10.1016/j.athoracsur.2015.04.062.
5. *Klyshnikov KU, Ovcharenko EA, Stasev AN, Scheglova NA, Odarenko YuN, Khalivopulo IK et al. In vitro* study of a biological prosthetic valve for seamless fixation. *Russian Journal of Transplantology and Artificial Organs*. 2017; 19 (4): 61–69. (In Russ, English abstract). doi: 10.15825/1995-1191-2017-4-61-69.
6. *Balsam LB, Grossi EA, Greenhouse DG, Ursomanno P, Deanda A, Ribakove GH et al.* Reoperative valve surgery in the elderly: Predictors of risk and long-term survival. *Ann Thorac Surg*. 2010 Oct; 90 (4): 1195–1200. doi: 10.1016/j.athoracsur.2010.04.057.

7. *Marro M, Kossar AP, Xue Y, Frasca A, Levy RJ, Ferrari G.* Noncalcific Mechanisms of Bioprosthetic Structural Valve Degeneration. *J Am Heart Assoc*. 2021 Feb 2; 10 (3): e018921. doi: 10.1161/JAHA.120.018921.
8. *Capodanno D, Petronio AS, Prendergast B, Eltchaninoff H, Vahanian A, Modine T et al.* Standardized definitions of structural deterioration and valve failure in assessing long-term durability of transcatheter and surgical aortic bioprosthetic valves: a consensus statement from the European Association of Percutaneous Cardiovascular Interventions (EAPCI) endorsed by the European Society of Cardiology (ESC) and the European Association for Cardio-Thoracic Surgery (EACTS). *Eur Heart J*. 2017 Dec 1; 38 (45): 3382–3390. doi: 10.1093/eurheartj/ehx303.
9. *Dvir D, Bourguignon T, Otto CM, Hahn RT, Rosenhek R, Webb JG et al.* Standardized Definition of Structural Valve Degeneration for Surgical and Transcatheter Bioprosthetic Aortic Valves. *Circulation*. 2018 Jan 23; 137 (4): 388–399. doi: 10.1161/CIRCULATIONAHA.117.030729.
10. *Kostyunin AE, Yuzhalin AE, Rezvova MA, Ovcharenko EA, Glushkova TV, Kutikhin AG.* Degeneration of Bioprosthetic Heart Valves: Update 2020. *J Am Heart Assoc*. 2020 Oct 20; 9 (19): e018506. doi: 10.1161/JAHA.120.018506.
11. *Whelan A, Williams E, Fitzpatrick E, Murphy BP, Gunning PS, O'Reilly D, Lally C.* Collagen fibre-mediated mechanical damage increases calcification of bovine pericardium for use in bioprosthetic heart valves. *Acta Biomater*. 2021 Jul 1; 128: 384–392. doi: 10.1016/j.actbio.2021.04.046.
12. *Tsolaki E, Corso P, Zboray R, Avaro J, Appel C, Liebi M et al.* Multiscale multimodal characterization and simulation of structural alterations in failed bioprosthetic heart valves. *Acta Biomater*. 2023 Oct 1; 169: 138–154. doi: 10.1016/j.actbio.2023.07.044.
13. *Kim H, Lu J, Sacks MS, Chandran KB.* Dynamic Simulation of Bioprosthetic Heart Valves Using a Stress Resultant Shell Model. *Ann Biomed Eng*. 2008 Feb; 36 (2): 262–275. doi: 10.1007/s10439-007-9409-4.
14. *Halevi R, Hamdan A, Marom G, Mega M, Raanani E, Haj-Ali R.* Progressive aortic valve calcification: Three-dimensional visualization and biomechanical analysis. *J Biomech*. 2015 Feb 5; 48 (3): 489–497. doi: 10.1016/j.jbiomech.2014.12.004.
15. *Thubrikar MJ, Deck JD, Aouad J, Nolan SP.* Role of mechanical stress in calcification of aortic bioprosthetic valves. *J Thorac Cardiovasc Surg*. 1983 Jul; 86 (1): 115–125. doi: 10.1016/S0022-5223(19)39217-7.
16. *Morany A, Lavon K, Halevi R, Haj-Ali N, Bluestein D, Raanani E et al.* Fragmentation of Different Calcification Growth Patterns in Bicuspid Valves During Balloon Valvuloplasty Procedure. *Ann Biomed Eng*. 2023 May; 51 (5): 1014–1027. doi: 10.1007/s10439-022-03115-8.
17. *Luraghi G, Matas JFR, Beretta M, Chiozzi N, Iannetti L, Migliavacca F.* The impact of calcification patterns in transcatheter aortic valve performance: a fluid-structure interaction analysis. *Comput Methods Biomech Biomed Engin*. 2021 Mar; 24 (4): 375–383. doi: 10.1080/10255842.2020.1817409.
18. *Pestiaux C, Pyka G, Quirynen L, De Azevedo D, Vanoverschelde J-L, Lengelé B et al.* 3D histopathology of stenotic aortic valve cusps using *ex vivo* microfocus computed tomography. *Front Cardiovasc Med*. 2023 Apr 25; 10: 1129990. doi: 10.3389/fcvm.2023.1129990.
19. *Cartlidge TRG, Doris MK, Sellers SL, Pawade TA, White AC, Pessotto R et al.* Detection and Prediction of Bioprosthetic Aortic Valve Degeneration. *J Am Coll Cardiol*. 2019 Mar 19; 73 (10): 1107–1119. doi: 10.1016/j.jacc.2018.12.056.
20. *Bishop C.* Pattern Recognition and Machine Learning. *Journal of Electronic Imaging*. 2006 Jan; 16 (4): 140–155. doi: 10.1117/1.2819119.
21. *Ankerst M, Breunig MM, Kriegel H-P, Sander J.* OPTICS: ordering points to identify the clustering structure. *ACM SIGMOD Rec*. 1999 Jun; 28 (2): 49–60. doi: 10.1145/304181.304187.
22. *Murtagh F, Contreras P.* Algorithms for hierarchical clustering: an overview. *WIREs Data Min Knowl Discov*. 2012 Dec 7; 2 (1): 86–97. doi: 10.1002/widm.53.
23. *Rousseeuw PJ.* Silhouettes: A graphical aid to the interpretation and validation of cluster analysis. *J Comput Appl Math*. 1987 Nov; 20: 53–65. doi: 10.1016/0377-0427(87)90125-7.
24. *Van der Maaten L, Hinton G.* Visualizing High-Dimensional Data Using t-SNE. *J Mach Learn Res*. 2008; 9 (86): 2579–2605.
25. *Leong SW, Soor GS, Butany J, Henry J, Thangaroopan M, Leask RL.* Morphological findings in 192 surgically excised native mitral valves. *Can J Cardiol*. 2006 Oct; 22 (12):1055–1061.doi:10.1016/S0828-282X(06)70321-X.
26. *Rutkovskaya NV, Kagan ES, Kondyukova NV, Kuzmina OK, Barbarash LS.* Prediction of Risk of Calcification of Heart Valve Bioprostheses on the Basis of Comprehensive Assessment of Recipients Clinical Factors and Their Compliance With Therapy. *Kardiologiia*. 2018; 58 (10): 27–33. (In Russ, English abstract). doi: 10.18087/cardio.2018.10.10182.
27. *Mahjoub H, Mathieu P, Larose E, Dahou A, Sénéchal M, Dumesnil J-G et al.* Determinants of aortic bioprosthetic valve calcification assessed by multidetector CT. *Heart*. 2015 Mar; 101 (6): 472–477. doi: 10.1136/heartjnl-2014-306445.
28. *Frasca A, Xue Y, Kossar AP, Keeney S, Rock C, Zakharchenko A et al.* Glycation and Serum Albumin Infiltration Contribute to the Structural Degeneration of Bioprosthetic Heart Valves. *JACC Basic to Transl Sci*. 2020 Aug 5; 5 (8): 755–766. doi: 10.1016/j.jacbts.2020.06.008.
29. *Sakaue T, Koyama T, Nakamura Y, Okamoto K, Kawashima T, Umeno T et al.* Bioprosthetic Valve Deterioration. *JACC Basic to Transl Sci*. 2023 May 10; 8 (7): 862–880. doi: 10.1016/j.jacbts.2023.01.003.
30. *Ovcharenko EA, Klyshnikov KU, Glushkova TV, Batranin AV, Rezvova MA, Kudryavtseva YA, Barbarash LS.* Evaluation of a failed heart valve bioprosthesis using microcomputed tomography. *Sovremennye tehnologii v medicine*. 2017; 9 (3): 15–22. (In Russ.). https://doi.org/10.17691/stm2017.9.3.02.

The article was submitted to the journal on 18.06.2025

DOI: 10.15825/1995-1191-2025-4-196-200

SUCCESSFUL REOPERATION USING HOMOGRAFTS FOR TRICUSPID AND PULMONARY VALVE REGURGITATION AFTER RADICAL DOUBLE OUTLET RIGHT VENTRICLE CORRECTION

K.V. Shatalov[1], I.V. Arnautova[1], S.V. Patsera[1], K.M. Dzhidzhikhiya[1], R.R. Akhtiamov[1], V.A. Bolsunovskii[2], D.V. Zotov[1], Yu.V. Gusarova[1]

[1] Bakulev National Medical Research Center for Cardiovascular Surgery, Moscow, Russian Federation
[2] Pediatric City Multidisciplinary Clinical Specialized Center for Advanced Medical Technologies, St. Petersburg, Russian Federation

Currently, there is a growing number of repeat cardiac interventions in children who have previously undergone surgery for congenital heart defects. This has renewed interest in identifying reconstructive materials that are resistant to the host's defense mechanisms. Among such materials, cryopreserved homografts in various modifications are of particular relevance. Numerous studies have reported on the use of these prostheses in different anatomical positions; however, cases involving simultaneous implantation of multiple homografts in a single patient for correction of congenital heart defects remain rare. To our knowledge, there are no published reports describing the use of a mitral homograft as a tricuspid valve substitute in combination with prosthetic pulmonary valve replacement using an allograft conduit. This report presents the first successful case of double valve replacement in a pediatric patient who had previously undergone radical correction of a double outlet right ventricle.

Keywords: mitral homograft, pulmonary homograft, repeat interventions.

INTRODUCTION

Currently, there has been a noticeable increase in the number of repeat interventions in congenital heart disease (CHD) surgery. This trend is primarily associated with the growing complexity of the defects being operated on, and the improved survival rates of patients following CHD correction. Whereas the early stages of pediatric cardiac surgery were dominated by the search for effective methods of defect correction, one of the main challenges today lies in identifying the ideal reconstructive material – particularly for heart valve replacement – that maintains long-term functionality without degeneration.

The use of homografts in complex CHD surgery dates back nearly 60 years, beginning in 1966 when Donald Ross performed the first aortic valve replacement with a homograft in an 8-year-old child [1]. Today, pulmonary homografts are predominantly employed in pediatric cardiac surgery, while aortic and mitral homografts are more commonly used in adults [2]. Despite the technical difficulties associated with their implantation, homografts generally provide satisfactory long-term clinical outcomes. However, their broader application in children remains limited by the scarcity of small-sized grafts and the tendency of the tissue to calcify as the child grows.

This report presents the first documented case of double valve replacement – of both the pulmonary and tricuspid valves – using homografts in a patient who had previously undergone radical correction of a double outlet right ventricle (DORV).

CASE DESCRIPTION

A 15-year-old female patient weighing 77 kg was admitted to the pediatric cardiovascular surgery ward at Bakulev National Medical Research Center for Cardiovascular Surgery. She had previously undergone radical correction of DORV in 2009, which included reconstruction of the right ventricular outflow tract (RVOT) using a single-leaflet xenopericardial patch.

At the time of admission, the patient presented with signs of heart failure on physical exertion, including shortness of breath and fatigue. She had a history of frequent infections of the ear, nose, and throat (ENT) organs.

Transthoracic echocardiography revealed severe regurgitation of both the pulmonary and tricuspid valves, with marked dilation of the right ventricle (end-diastolic dimension – 5.7 cm) and right atrium (6.5 × 8.5 cm). The tricuspid annulus was enlarged to 42 mm (Fig. 1).

Based on preoperative diagnostic findings, a decision was made to perform RVOT reconstruction using a cryopreserved allogeneic conduit, with possible replacement of the tricuspid valve (TV).

Corresponding author: Sergey Patsera. Address: 135, Rublevskoe Shosse, Moscow, 121552, Russian Federation. Phone: (925) 135-94-13. E-mail: pazera98@mail.ru

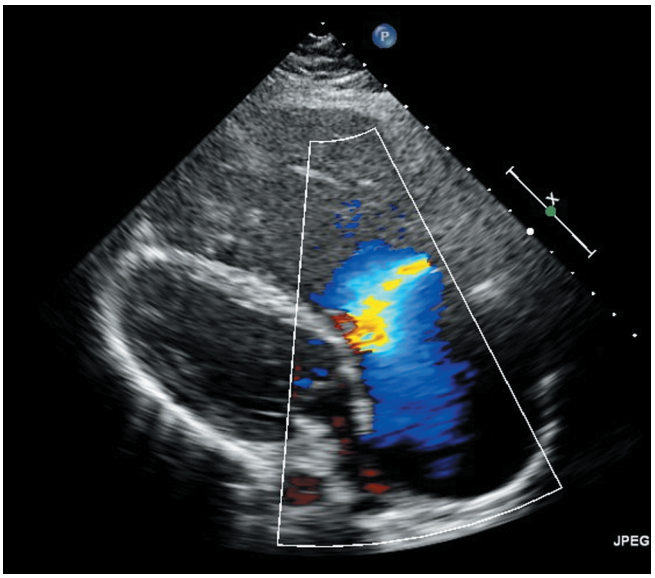

Fig. 1. Transthoracic echocardiography showing grade IV tricuspid valve regurgitation

The operation was carried out under standard cardiopulmonary bypass, hypothermia, and pharmacological cold cardioplegia using Custodiol solution.

Intraoperative examination revealed deformation and severe hypoplasia of all TV leaflets, rendering reconstructive surgery impossible; therefore, valve replacement was indicated.

At the pulmonary trunk level, marked calcification was observed in the previously implanted patch and the preserved native pulmonary valve (PV) leaflets. Complete excision of the calcified patch, native PV leaflets, and altered TV leaflets was performed. Subsequently, prosthetic replacement of the pulmonary trunk was carried out using pulmonary homograft No. 28 (Fig. 2a, Fig. 3a), and the TV was replaced with mitral homograft No. 32 (Fig. 2b, Fig. 3b).

During implantation of mitral homograft, the medial and lateral papillary "legs" were sutured to the interventricular septum, after which the prosthetic annular

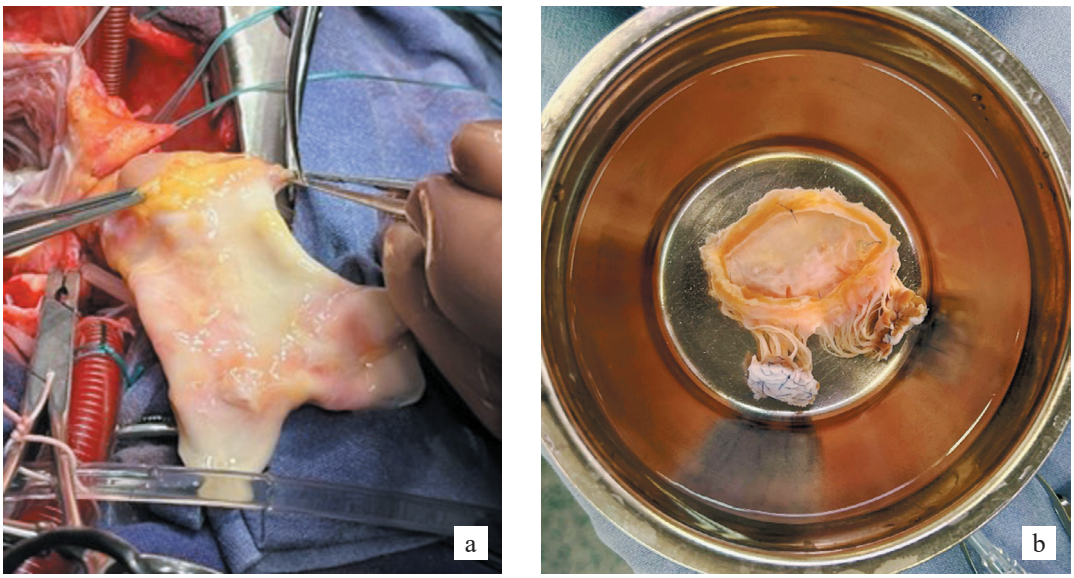

Fig. 2. General view of the homografts used for implantation: a, pulmonary homograft; b, mitral homograft

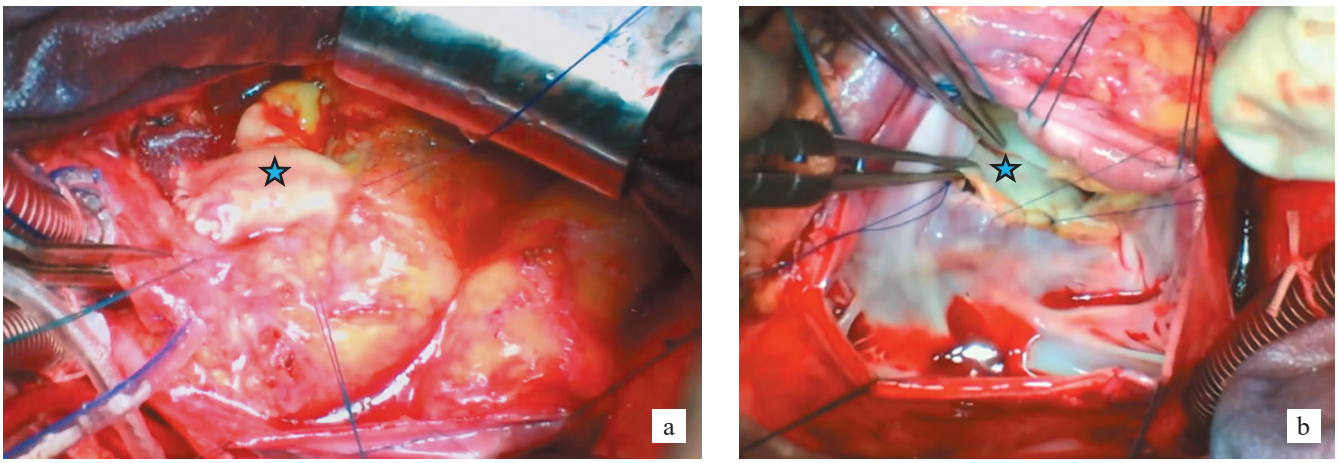

Fig. 3. Intraoperative photographs (patient's head positioned to the left): a, implanted pulmonary homograft (indicated by an asterisk); b, mitral homograft implanted in the tricuspid position (indicated by an asterisk)

rim was secured to the native fibrous ring. The total cardiopulmonary bypass time was 200 minutes, and the aortic cross-clamp time was 130 minutes.

The onset of cardiac activity after cardioplegia was accompanied by complete transverse heart block followed by restoration of sinus rhythm. The immediate postoperative period was uneventful, and the patient was discharged on postoperative day 11.

At the time of discharge, transthoracic echocardiography showed satisfactory function of both prosthetic valves without significant transvalvular gradients (PV prosthesis: systolic gradient 15 mm Hg, grade I regurgitation; TV prosthesis: peak diastolic gradient 4 mm Hg, grade I regurgitation).

At the 8-month follow-up, echocardiographic evaluation revealed no increase in transvalvular gradients or regurgitation.

DISCUSSION

Between 1966 and 1969, Huber and Senning were the first to use mitral homografts for TV replacement in two patients with organic valve disease; however, the outcomes were unsatisfactory [3]. The first series of successful implantations was later reported by Pomar and Mestres in 1993 [4]. In 1996, Hvass et al. described the first successful application of this technique in a six-year-old girl with infective endocarditis [5]. These encouraging results stimulated further development and refinement of surgical techniques for homograft implantation, including improved fixation of papillary muscles and reinforcement of the subvalvular apparatus.

In Russia, the first such operations were performed by Ivan Skopin at Bakulev National Medical Research Center for Cardiovascular Surgery in 1998. Four patients underwent surgery with good immediate and long-term outcomes [6].

The feasibility of using homografts for RVOT reconstruction was first demonstrated by Ross in 1966, when he implanted an aortic homograft into the pulmonary position in an eight-year-old child with pulmonary artery atresia [1]. Subsequently, advances in donor selection, sterilization, cryopreservation, along with increased availability, have firmly established homografts as an essential component of modern cardiac surgery [7–9].

Since the 2000s, alongside homografts, a new generation of biological conduits made from bovine jugular veins has been actively used, demonstrating favorable short-term [10] and long-term outcomes [11, 12]. However, as clinical experience with these conduits accumulated, multiple studies reported a high incidence of infective endocarditis (IE), which remains the principal limitation to their widespread adoption. In a comparative study by Ugaki et al., IE developed in 9.4% of patients with bovine jugular vein conduits, compared with only 0.7% in those with homografts [13]. Moreover, homografts are less prone to stenosis than other biological conduits, thereby significantly reducing the need for repeat interventions [13, 14].

Anticoagulant therapy is mandatory for all synthetic and mechanical prostheses, but it is generally unnecessary when using biological prostheses, including jugular vein and homograft-based conduits [15].

To date, a review of the scientific literature has revealed no published cases describing simultaneous double-valve (tricuspid and pulmonary) replacement using pulmonary and mitral homografts in a single patient. According to a meta-analysis by Van den Eynde et al., pulmonary artery replacement without concomitant correction of tricuspid insufficiency is associated with a higher incidence of significant residual regurgitation compared with simultaneous tricuspid valve repair or replacement [16]. In our case, plastic surgery was limited due to the structural pathology of the tricuspid valve.

Currently, there is a growing trend toward the use of endovascular approaches for reintervention on heart valves after CHD correction [17]. However, this technique remains limited by strict patient selection criteria and the relatively small number of studies confirming its long-term benefits and safety.

CONCLUSION

The presented clinical case demonstrates the feasibility of successful simultaneous implantation of a mitral homograft in the tricuspid position and a pulmonary homograft. Double-valve biological replacement of the pulmonary and tricuspid valves offers several key advantages: the implanted conduits can adapt to somatic growth, unlike frame-based biological or mechanical prostheses, and it eliminates the need for lifelong anticoagulant therapy.

Conflict of interest. *During the procedure, a pulmonary homograft manufactured by the laboratory of allogeneic materials for cardiovascular surgery at Bakulev National Medical Research Center for Cardiovascular Surgery (Moscow), headed by co-author K.M. Dzhidzhikhiya, and a mitral homograft produced by CardioStar (St. Petersburg), whose CEO is co-author V.A. Bolsunovsky, were used.*

REFERENCES

1. *Ross DN, Somerville J.* Correction of pulmonary atresia with a homograft aortic valve. *Lancet*. 1966 Dec 31; 2 (7479): 1446–1447. doi: 10.1016/s0140-6736(66)90600-3.
2. *Rajashekar P, Gupta A, Velayoudam D.* Choice of valve substitutes. *Indian J Thorac Cardiovasc Surg*. 2024 May; 40 (Suppl 1): 78–82. doi: 10.1007/s12055-024-01733-6.
3. *Huber R, Rothlin M, Senning A.* Spätresultate nach Atrioventrikulärklappenersatz mit Mitralallotransplantat.

Thorac Cardiovasc Surg. 1975 Feb; 23 (1): 33–38. doi: 10.1055/s-0028-1096923.

4. *Pomar JL, Mestres CA.* Tricuspid valve replacement using a mitral homograft. Surgical technique and initial results. *J Heart Valve Dis*. 1993 Mar; 2 (2): 125–128. PMID: 8261148.
5. *Hvass U, Lansac E, Chatel D, Henri I.* Mitral homograft for tricuspid valve endocarditis complicating a congenital fistula between the right coronary artery and right ventricle. *J Heart Valve Dis.* 1996 Sep; 5 (5): 564–566. PMID: 8895001.
6. *Shamsiev GA, Muratov RM, Amiragov RI, Babenko SI.* Long-term result of surgical treatment of tricuspid valve infective endocarditis with cryopreserved mitral homograft. *Russian Journal of Thoracic and Cardiovascular Surgery.* 2014; 56 (4): 52–55. (in Russ.).
7. *Shatalov KV, Bolsunovsky VA, Gamisoniya AM, Arnautova IV, Akhtyamov RR.* The first experience of implantation of a mitral homograft in the tricuspid position in children. *Russian Journal of Thoracic and Cardiovascular Surgery.* 2023; 65 (5): 589–594. (in Russ.). doi: 10.24022/0236-2791-2023-65-5-589-594.
8. *Jashari R.* Transplantation of cryopreserved human heart valves in Europe: 30 years of banking in Brussels and future perspectives. *Cell Tissue Bank.* 2021 Dec; 22 (4): 519–537. doi: 10.1007/s10561-021-09902-2.
9. *Brodskiy AG, Bolsunovskiy VA, Kosovskikh EA, Urvantseva IA, Tverdokhlib YaV, Tiltaeva LA, Belyaeva EE.* Correction of truncal insufficiency using a pulmonary homograph in a patient with a common arterial trunk and interrupted aortic arch. *Children's Heart and Vascular Diseases.* 2024; 21 (2): 158–162. (in Russ.). doi: 10.24022/1810-0686-2024-21-2-158-162.
10. *Bové T, Demanet H, Wauthy P, Goldstein JP, Dessy H, Viart P et al.* Early results of valved bovine jugular vein conduit versus bicuspid homograft for right ventricular outflow tract reconstruction. *Ann Thorac Surg.* 2002 Aug; 74 (2): 536–541; discussion 541. doi: 10.1016/s0003-4975(02)03728-1.
11. *Gist KM, Mitchell MB, Jaggers J, Campbell DN, Yu JA, Landeck BF 2nd.* Assessment of the relationship between Contegra conduit size and early valvar insufficiency. *Ann Thorac Surg.* 2012 Mar; 93 (3): 856–861. doi: 10.1016/j.athoracsur.2011.10.057.
12. *Boudjemline Y, Bonnet D, Massih TA, Agnoletti G, Iserin F, Jaubert F et al.* Use of bovine jugular vein to reconstruct the right ventricular outflow tract: early results. *J Thorac Cardiovasc Surg.* 2003 Aug; 126 (2): 490–497. doi: 10.1016/s0022-5223(03)00232-0.
13. *Ugaki S, Rutledge J, Al Aklabi M, Ross DB, Adatia I, Rebeyka IM.* An increased incidence of conduit endocarditis in patients receiving bovine jugular vein grafts compared to cryopreserved homograft for right ventricular outflow reconstruction. *Ann Thorac Surg.* 2015 Jan; 99 (1): 140–146. doi: 10.1016/j.athoracsur.2014.08.034.
14. *Vitanova K, Cleuziou J, Hörer J, Kasnar-Samprec J, Vogt M, Schreiber C, Lange R.* Which type of conduit to choose for right ventricular outflow tract reconstruction in patients below 1 year of age? *Eur J Cardiothorac Surg.* 2014 Dec; 46 (6): 961–966; discussion 966. doi: 10.1093/ejcts/ezu080.
15. *Boethig D, Schreiber C, Hazekamp M, Blanz U, Prêtre R, Asfour B et al.* Risk factors for distal Contegra stenosis: results of a prospective European multicentre study. *Thorac Cardiovasc Surg.* 2012 Apr; 60 (3): 195–204. doi: 10.1055/s-0031-1298062.
16. *Van den Eynde J, Callahan CP, Lo Rito M, Hussein N, Carvajal H, Guariento A et al.* Tricuspid Valve Intervention at the Time of Pulmonary Valve Replacement in Adults With Congenital Heart Disease: A Systematic Review and Meta-Analysis. *J Am Heart Assoc.* 2021 Dec 21; 10 (24): e022909. doi: 10.1161/JAHA.121.022909.
17. *Small AJ, Aksoy O, Levi DS, Salem MM, Yang EH, Aboulhosn JA.* Combined Transcatheter Tricuspid and Pulmonary Valve Replacement. *World J Pediatr Congenit Heart Surg.* 2020 Jul; 11 (4): 432–437. doi: 10.1177/2150135120918777.

The article was submitted to the journal on 21.05.2025

INSTRUCTIONS TO AUTHORS

Articles should contain original information that has not been previously published and is not considered for publication in other editions. Fee for publication of manuscripts will not be charged.

The manuscript should be presented in Microsoft Word format A4, 1.5 spacing, and Times New Roman font size 12. Submit your article to the online submission system in accordance with the instructions on the journal's website https://journal.transpl.ru.

Structure of the article

The Title page should include:

- Initials (first name and patronymic) of the authors of the article should be specified before their respective last names.
- Author names (list the author's initials before listing his or her last name as when registering for ORCID, or Open Researcher and Contributor ID – a non-proprietary alphanumeric code that uniquely identifies scientific authors).
- Full official name of the institution, city and country.
- If authors from different institutions participated in writing of the manuscript, it is necessary to correlate those with the names of the authors by adding a digital index uppercase after last name, and right before the name of the institution.

Information about the authors

For each author fully specify the last and the first name, patronymic and position in the relevant department/institution.

For correspondence

Fully specify the last and the first name, patronymic of the author, who will be holding correspondence, address (including postal code), telephone, fax number, e-mail.

Abstract

Each article must be accompanied by an abstract. The amount of text for the abstract of the original article should be of no more than 300 words, for a literature review, clinical observation – no more than 200 words. The abstract must fully comply with the content of the work. The abstract should not use abbreviations without prior expansion.

Abstract of ***the original article*** should contain the following sections: ***Objective***, ***Materials and methods***, ***Results***, ***Conclusion***. The abstract should present the most important results of the research.

Do not write: "*A comparative analysis of the sensitivity and specificity was conducted …*"

Should write: "*The sensitivity was ... % and ...%, p = , specificity, respectively ...% and ...%, p =* ".

Keywords

At the end of the abstract keywords must be given. To select the keywords a thesaurus of U.S. National Library of Medicine should be used – Medical Subject Headings (MeSH) at https://www.ncbi.nlm.nih.gov/mesh.

Conflict of interest

The author should inform the editor about the factual or potential conflict of interest have included the information about such conflict into the respective section of an article.

If there is no conflict of interest, the author should say so in the form like the following: "Author declares unawareness of the conflict of interest".

This information is supposed to be placed before the article text.

Text of article

Original article should include the following sections:

- Introduction
- Materials and methods
- Results
- Discussion
- Conclusion
- References

Review article should include an analysis of the literature with the presentation of modern sources (mainly in the last 5 years).

Clinical observation should be well illustrated (to reflect the essence of the problem) and include discussion with the use of literature data.

References in the text are indicated by number in square brackets: [1], [2, 5], [14–18] and ***in the references section are presented in order of their appearance in the text.*** All values given in the article should be expressed or duplicated in **SI** units.

References

The author is solely responsible for the accuracy of the data included in the references section of the article. References to unpublished papers or papers in print works are not allowed.

References are presented on a separate page.

The names of journals can be contracted in accordance with an embodiment of reduction adopted by the specific journal.

If the article quoted has DOI (a digital object identifier) or/and PMID (Pub Med identifier) they must be specified after the description of the article. To compile descriptions in References section NLM bibliographic reference citation standard is used – U.S. National Library of Medicine (https://www.nlm.nih.gov/bsd/uniform_requirements.html). If the number of authors does not exceed 6, the bibliographic description includes all the authors. If the number of authors is more, only the first six authors should be indicated and then add et al.

Requirements for tables and figures

Tables should be placed into the text; they should have numbered heading and clearly labeled graphs, convenient and simple to read. Table's data must comply with the numbers in the text, but should not duplicate the information therein. Table references in the text are required.

Illustrations and drawings should be submitted in electronic format (JPEG or TIFF format with a resolution of at least 300 dpi and no smaller than 6 × 9 cm), in a volume of close to 1 MB. Drawings must include all copyright symbols – arrows, numbers, signs, etc. Figure captions should be submitted in a separate file with the extension *.doc. First, the name is given, then all arithmetic and alphabetical symbols (lettering) are explained.

Articles should be addressed
to the Russian Journal of Transplantology and Artificial Organs website:
https://journal.transpl.ru/vtio
E-mail: vestniktranspl@gmail.com

Издание зарегистрировано в Госкомпечати РФ, № 018616 от 23.03.99 г.

Подписано к печати 29.12.25.

Тираж 1000 экз.

ООО «Издательство «Триада».
ИД № 06059 от 16.10.01 г.
170034, г. Тверь, пр. Чайковского, 9, оф. 514,
тел.: +7 (915) 730-10-37, +7 (910) 647-49-85
E-mail: triadatver@yandex.ru
https://www.triada.tver.ru

Заказ 53302